GALACTOFURANOSE BIOSYNTHESIS IS IMPORTANT FOR MAINTAINING NORMAL GROWTH AND CELL WALL PROPERTIES IN *ASPERGILLUS NIDULANS*

A Thesis Submitted to theCollege of
Graduate Studies and Research
In Partial Fulfillment of the Requirements
For the Degree of Doctor of Philosophy
In the Department of Biology
University of Saskatchewan
Saskatoon
Saskatchewan, Canada

By

Md. Kausar Alam

PERMISSION TO USE

In presenting this thesis in partial fulfillment of the requirements for a Postgraduate degree from the University of Saskatchewan, I agree that the Libraries of this University may make it freely available for inspection. I further agree that permission for copying of this thesis/dissertation in any manner, in whole or in part, for scholarly purposes may be granted by the professor or professors who supervised my thesis/dissertation work or, in their absence, by the Head of the Department or the Dean of the College in which my thesis work was done. It is understood that any copying or publication or use of this thesis/dissertation or parts thereof for financial gain shall not be allowed without my written permission. It is also understood that due recognition shall be given to me and to the University of Saskatchewan in any scholarly use which may be made of any material in my thesis.

Requests for permission to copy or to make other uses of materials in this thesis in whole or part should be addressed to:

Head of the Department of Biology
University of Saskatchewan
Saskatoon, Saskatchewan S7N 5E2
Canada

ABSTRACT

The cell wall is essential for fungal survival in natural environments. Galactofuranose (Gal*f*) decorates certain carbohydrates and lipids of *Aspergillus* cell wall, is absent in humans and appears to play a role in fungal cell wall maturation. Previous studies in our lab showed that deletion of any of three sequential-acting genes (*ugeA, ugmA,* and *ugtA*) of Gal*f* pathway caused substantially reduced growth and spore production.

Two genes upstream of the Gal*f* pathway, *galD* and *galE* are essential for galactose metabolism in many systems including the budding yeast, *Saccharomyces cerevisiae*. Interestingly, characterization of *galD* and *galE* in *A. nidulans* using cell and molecular techniques showed that unlike yeast, neither of these genes was essential for growth at physiological pH 7.5. Nevertheless for each case, their expressions were up-regulated by growth on galactose, revealing the relative complexity of galactose metabolism in *A. nidulans*. Our study also showed that repression of the three sequentially acting Gal*f* pathway genes by conditional promoters phenocopied previously characterized deletion morphology. Using anti-Gal*f* (L10) we also showed that deletion and repression of these genes caused no Gal*f* in the hyphal wall. Gene deletion or repression also increased sensitivity to the wall-targeting drug, caspofungin. Related results from qPCR showed that deletion or repression of *ugmA* increased gene expression of α-glucan synthase *agsB* and decreased that of β-glucan synthase *fksA*. Therefore, Gal*f* is non-essential but important for many aspects of *Aspergillus* growth, sporulation, and wall maturation.

Aspergillosis, the most common airborne systemic fungal disease, is typically caused by *Aspergillus fumigatus*. Several *A. fumigatus* UgmA (*Af*UgmA) mutants with altered enzyme activity due to single amino acid changes were used to assess their effect on growth and wall composition in *A. nidulans*. Wild type Af*ugmA* complemented the phenotypic defects in an *A. nidulans ugmA*Δ strain, consistent with these two genes being homologous. The *Af*UgmA crystal structure has been solved, and the *in vitro* enzymatic effects of specific mutations in the enzyme active site have been published. *Af*UgmA mutated strains with reduced activity *in vitro* impaired *A. nidulans* growth in a manner substantially similar to gene deletion and gene down-regulation. Site directed mutagenesis showed that *Af*UgmA residues R182 and R327 were critical for Gal*f* generation both *in vivo* and *in vitro*. This supports

previous results showing that UgmA is essential for Gal*f* biosynthesis. Using fluorescent latex beads, we showed that reduction of wall Gal*f* increased hyphal surface adhesion. Consistent with qPCR studies, immunofluorescence and ELISA results showed that loss or absence of Gal*f* increased wall α-glucan but reduced wall β-glucan. Gal*f* is important for wall surface integrity and for maintaining dynamic co-ordination with other pathways. To begin to assess this dynamic co-ordination, Tandem Affinity Purification (TAP) tagging combined with LC-MS/MS was used to identify the interacting partners of UgmA. Our results showed that UgmA interacted with proteins that are involved in cytoskeleton generation, osmotic adaptation, and cell signalling pathway. Further study will help us to understand the dynamic coordination of Gal*f* biosynthesis pathway with other wall carbohydrate polymers for *Aspergillus* wall formation.

In summary, my thesis results have clearly shown that Gal*f* plays important roles in *Aspergillus* growth, and wall surface integrity. We also showed that Gal*f* deficient strains are hypersensitive to wall-targeting drugs, indicating that Gal*f* biosynthesis pathway could be potential target for combination therapy. The Gal*f* pathway also maintained a dynamic co-ordination with alpha-glucan and beta-glucan carbohydrate pathways. Future study may include developing an inhibitor against UgmA and exploring the relationship of Gal*f* pathway with alpha-glucan and beta-glucan carbohydrate pathways.

ACKNOWLEDGEMENTS

I have been fortunate to have Prof. Susan Kaminskyj as my mentor. I am deeply grateful to her for everything she taught me during the time I spend in her lab, for allowing me to pursue some of my ideas, and for having confidence in my work. Her guidance and support have been integral in the completion of this work.

I owe an immense debt of gratitude to my graduate committee members, Dr. Vikram Misra (Vetenary microbiology), Dr. Yangdou Wei and Dr. Chris Todd (Biology Department) for their valuable suggestions during my research. Also I would like to thank Dr. Margo Moore for serving as my external examiner.

I would also like to thank past/present lab members of Kaminskyj lab, especially Amira El-Ganiny and Sharmin Afroz for their initial help and also for being part of my Galactofuranose gene regulated paper. I extend my sincere thanks to Dr. David Sanders and Dr. van Straaten doing the *in vitro* kinetic study and also for their critical comments on my manuscripts.

I would like to express my sincere thanks to Department of Biology (GTF) and University of Saskatchewan (UGS) for sponsoring my 4-year scholarship. The research in our lab was funded by the Natural Sciences and Engineering Research Council (NSERC), and a Canadian Institutes of Health Research, Research Partnership Program (CIHR-RPP), which is gratefully acknowledged.

During my entire PhD program, I get great help and support from many people from different Departments. I would like to thank Dr. Chad Stewart for helping with qRT-PCR, Guosheng Liu for technical assistance microscopy work. Tom Bonli in Geology Department for SEM, Dr. Pat Krone (Cell and Anatomy Biology) for zebrafish facilities, Dr. Carlos Carvalho for microinjection facility, Dr. Sylvia van den Hurk (VIDO) for ELISA reader.

Finally I would like to express my special thanks to my wife Sharmin Afroz and my parents for their support, co-operation and patience during this work.

TABLE OF CONTENTS

List of Tables

List of Figures

LIST OF ABBREVIATIONS

Af	*Aspergillus fumigatus*
An	*Aspergillus nidulans*
Af*pyrG*	*Aspergillus fumigatus* orotidine 5'-monophosphate decarboxylase
Af*pyroA*	*Aspergillus fumigatus* pyridoxine biosynthesis gene
alcA(p)	alcohol dehydrogenase I promoter
*Af*GlfA/UgmA	*Aspergillus fumigatus* UDP-galactopyranose mutase
*Af*GlfB/Ugt	*Aspergillus fumigatus* UDP-galactofuranose transporter
AFM	atomic force microscopy
BLAST	basic local alignment search tool
Casp	Caspofungincaspofungin
CFW	Calcofluor White
cDNA	complementary DNA
CM	complete medium
CM3G	complete medium with 3% glucose
CMT	complete medium with 100 mM threonine
ELISA	enzyme-linked immunosorbent assay
GalE/GAL1	galactokinase
GalD/GAL7	galactose-1-phosphate uridylyltransferase
Gal*f*	galactofuranose
gDNA	genomic DNA
GFP	green fluorescent protein
GPI	glycophosphatidylinositol
MM-Glu	minimal medium containing 1 % glucose
MM-Gal	minimal medium containing 1 % galactose
MMN	MM-Gal containing 70 mM $NaNO_3$
MMA	MM-Gal containing 70 mM ammonium tartrate
mAb	monoclonal antibody
niiA(p)	nitrite utilization promoter

nkuA	*Aspergillus nidulans* homolog of human KU70
PCR	polymerase chain reaction
qRT-PCR	quantitative real time polymerase chain reaction
SDM	site-directed mutagenesis
SEM	scanning electron microscopy
TEM	transmission electron microscopy
UDP-Gal*f*	uridine diphosphate galactofuranose
UDP-Gal*p*	uridine diphosphate galactopyranose
UgeA	UDP- glucose/galactose 4-epimerase
UgmA	UDP- galactopyranose mutase
UgtA	UDP- Gal*f* transporter
WC	An*ugmA*::wild type Af*ugmA*

CHAPTER 1

Introduction

This thesis consists of six chapters. Chapter 1 includes a general introduction about fungi and the genus *Aspergillus*, galactose metabolism, cell wall composition, *Aspergillus* infection, antifungal drugs, and the galactofuranose (Gal*f*) biosynthesis pathway. Chapter 2 describes the roles of GalD and GalE in *Aspergillus* galactose metabolism. Chapter 3 explains the roles of Gal*f* biosynthesis enzymes in fungal growth, drug sensitivity, and their relationship with major cell wall carbohydrate biosynthesis pathways. Chapter 4 explores how modification of Gal*f* leads to changes in *Aspergillus* cell wall composition and hyphal surface adhesion. Chapter 5 reveals potential interacting partners of *A. nidulans* UDP-galactopyranose mutase using a proteomic approach. Chapter 6 includes a discussion about overall research results in terms of their importance in understanding the complexity of galactose metabolism, contribution of Gal*f* in fungal growth, drug sensitivity, cell wall modification and co-ordination of Gal*f* with other carbohydrate pathways and ends with a discussion about the possibility for anti-Gal*f* drug as a part of a combination therapy and future directions.

1.1 Fungal Biology

Fungi are heterotrophic eukaryotic organisms that are distinct from both plants and animals. Today, fungi are grouped in their own taxonomic kingdom, the Mycota, which is estimated to consist of 3.5 to 5.1 million species (O' Brien et al., 2005; Taylor et al., 2010; Blackwell, 2011), although only ~97,000 have been formally described (Kirk et al., 2008; Blackwell, 2011). Based on recent comprehensive phylogenetic classification, the Mycota contains seven phyla, the Microsporidia, Chytridiomycota, Blastocladiomycota, Neocallimastigomycota, Glomeromycota (includes the traditional phylum Zygomycota), Ascomycota, and Basidiomycota (Hibbett *et al.*, 2007). Together, the Ascomycota and Basidiomycota represent the subkingdom Dikarya (Hibbett *et al.*, 2007).

Like animals, fungi lack chloroplasts and so are heterotrophic organisms, and as such they require organic compounds as energy sources. Unlike plant cell walls that contain cellulose, fungal cell walls contain chitin microfibrils. In general, fungi can propagate in a sexual or asexual way by producing spores. The sexual form of fungi is known as the

teleomorph and the asexual form is the anamorph (Kirk et al 2008). Fungi typically have haploid nuclei. Fungi can be multicellular filamentous (moulds), macroscopic filamentous fungi that form large fruiting bodies (mushroom), or single celled microscopic yeasts. Some fungi are dimorphic, so that they are able to switch between unicellular and multicellular forms at different life cycle stages (e.g. *Candida*) (Osiewacz, 2002).

Fungi are diverse in regard to ecological contribution and biological function. Overall, fungi are abundant worldwide and perform essential roles in ecosystems (Barr and Aust, 1994; Newbound et al., 2010). Many fungi are excellent scavengers in nature, breaking down dead vegetable material (particularly cellulose and lignin) into simpler compounds (Rambold et al., 2013).

Some fungi are used as a source of food, such as mushrooms and truffles, and others including yeasts are used in industrial fermentation processes to produce wine, beer, as well as to produce some useful biochemicals such as antibiotics and enzymes (Bennett, 1998). Some species form symbiotic relationships with plants (Rodriguez and Redman, 2008), which are essential for their survival in terrestrial environments. However, other fungi are detrimental to plants, animals and humans (Monk and Goffeau, 2008; Cannon et al., 2009). Some fungi can cause serious plant diseases (e.g. *Magnaporthe oryzae* causing rice blast disease), that results in the loss of billions of dollars worth of crops each year. Some fungi cause animal diseases and/or human disease (Gould, 2011). They are also used as experimental organisms to study metabolic pathways, growth and development, and cell division because they are eukaryotes, and are relatively closely related to animals (van der Klei and Veenhuis, 2006).

The filamentous fungi (moulds) are different from the unicellular yeasts in their cellular organization and growth (Deacon, 1997). They are composed of long tubular cells called hyphae that exhibit tip localized growth (Kaminskyj and Heath, 1996). Hyphae can be septate (cross walls) or aseptate (no cross walls) depending on their taxonomic group. The hyphae grow and branch until they form a network of threadlike cells called a colony or mycelium. Some of the hyphal branches grow into the air and differentiate to produce asexual spores called conidia. Macroscopic filamentous fungi also grow by producing a mycelium in a nutrient substrate that can be below ground or within a plant. These fungi differ from moulds

(which typically are asexual) because they produce large macroscopic fruiting bodies that hold the sexual spores. Major groups of septate fungi are the Ascomycetes (e.g. *Aspergillus* and *Candida*) and the Basidiomycetes (e.g. *Cryptococcus*). The hyphal cells of septate filamentous fungi can be uninucleate or multinucleate (Todd et al 2007a&b; Wearing et al 2010).

The genus *Aspergillus* is a group of filamentous ascomycetes that include ~250 species. These are typically aerobic, but can be facultative anaerobes. *Aspergillus* species have septate hyphae and characteristic arrangement of conidia on the conidiophore (Fig 1.1). Colonies appear in 1 to 2 d depending on growth temperature; by 5 d they may cover an entire Petri plate. For many filamentous fungi including *Aspergillus,* the predominant life cycle stage is asexual (Fig. 1.1) (Wearing, 2010). *Aspergillus* has a tremendous impact on public health, both beneficially as the workhorse of industrial applications and negatively as plant and human pathogens (Dagenais and Keller, 2009). For example, *A. fumigatus* is a deadly pathogen of immunocompromised patients; *A. flavus* is an agriculturally dangerous toxin producer; *A. niger* and *A. oryzae* are used in industrial processes (Kapoor et al., 1999; Erjavec et al 2009). *A. nidulans* is widely used as a model system to a wide array of biological processes (Todd et al 2007a).

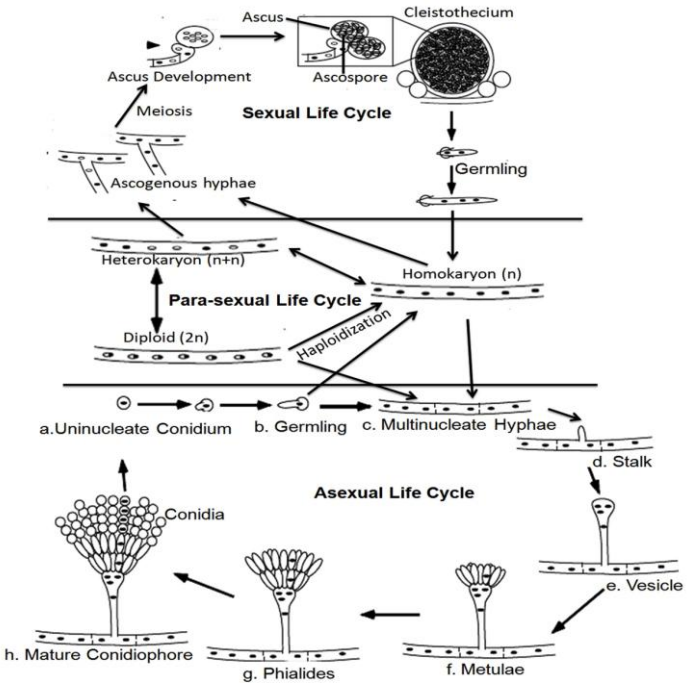

Figure 1.1: Life cycle of *Aspergillus nidulans*, which grows as haploid vegetative filamentous hyphae following germination of uninucleate conidia or binucleate ascospores. **Asexual cycle**: a-c) germination and hyphal growth leads to the formation of a vegetative colony. d) At the onset of spore development, a stalk forms, then e) swells at its tip to form the vesicle. This produces two layers of cells: f) metulae, and g) phialides. In wild type *A. nidulans*, each metula produces a pair of phialides. h) Mature phialides produce chains of uninucleate spores. **Parasexual cycle**: Hyphae from two individuals may fuse to form a heterokaryon, and nuclei in a heterokaryon or a homokaryon may fuse to form a diploid. Hyphae differentiate by asexual development, as above. **Sexual Cycle:** as growth proceeds, sexual development produces nurse cells called Hülle cells and closed fruiting bodies (cleistothecia) containing sexual ascospores within asci. Simplified from Todd et al. (2007b).

1.2 Galactose metabolism in fungi

Galactose metabolism *via* the Leloir pathway (named after the 1970 Nobel laureate Luis Leloir) is conserved from bacteria through humans (Ross et al. 2004). Galactose itself cannot be used directly for glycolysis. Before it can enter the glycolytic pathway, galactose must be converted *via* galactose-1-phosphate into glucose-1-phosphate (Sellick et al. 2008**).** The enzymes of the Leloir pathway are galactokinase (GalE), galactose-1-phosphate uridylyltransferase (GalD), and UDP-glucose/galactose-4-epimerase (UGE) (Christacos et al 2000), which mediate this conversion. Leloir enzymes have attracted significant research attention because of their important metabolic roles. For example, defects in the human enzymes galactokinase or galactose-1-phosphate-uridylyltransferase causes diseases called galactosemias (Holden et al, 2003; Timson 2005). The galactose metabolism and galactofuranose biosynthesis pathways are illustrated together in Fig 2.1 of Chapter 2. In the first step of conversion, galactose is phosphorylated by GalE to produce galactose-1-phosphate. In the next round of the transfer reaction, GalD interconverts glucose- or galactose-1-phosphate to their UDP conjugates and releases glucose-1-phosphate. Once released, glucose-1-phosphate is converted to glucose-6-phosphate and can enter the glycolytic pathway to generate energy. UDP-glucose is a substrate for UGE (UgeA), which

can potentially be processed into UDP-galactofuranose (UDP-Gal*f*) by UDP-galactopyranose mutase (UGM, UgmA) in fungi (El-Ganiny 2008, 2010).

In fungi, galactose can be used for energy generation (catabolism), and for fungal wall glycan synthesis (anabolism) (Fekete et al, 2004). The Leloir pathway has been extensively studied in the yeasts *Saccharomyces cerevisiae* and *Kluyveromyces lactis* (Bhat & Murthy 2001; Rubio-Texeira 2005). All of the Leloir genes are essential for growth on D-galactose in these yeast systems (Slepak et al. 2005, Seiboth et al 2008). Although the Leloir pathway appears to be the main D-galactose degrading route in *Aspergillus*, alternative or additional galactose metabolism pathways via galactitol, sorbitol and fructose (Elorza, 1971) and fructose-6-phosphate and sorbose-6-phosphate have been proposed in *A. nidulans* (Fekete *et al.* 2004). Flipphi *et al.* (2009) hypothesized that galactitol can also be epimerized to D-tagatose via L-sorbose, which might be catabolized via D-sorbitol and D-fructose to D-fructose-6-phosphate. A non-phosphorolytic pathway for D-galactose utilization has been reported for *A. niger* (Elshafei & Abdel-Fatah 2001) but neither the genes nor the proteins have been identified. Similarly, *Hypocrea jecorina* strain with deleted *galE* was able to grow on D-galactose (Seiboth et al. 2004). Therefore, galactose metabolism is more complex in filamentous fungi than in yeast (Slot and Rokas, 2010).

1.3 Fungal cell wall structure

Formation of an outer protective cell wall layer is crucial for the survival and growth of fungi and to establish host-pathogen interaction as well (Latgé, 2007; Cummings and Doering, 2009). In filamentous fungi, wall formation is also an integral part of hyphal extension (Read, 2011). The fungal cell wall also protects cells from mechanical injury, prevents osmotic lysis, and provides passive protection against the ingress of potentially harmful macromolecules. Due to the importance of cell walls for fungal growth and host invasion, and the lack of conservation with animal cell components, the cell wall is a good source of potential antifungal targets (Aimanianda and Latgé, 2010).

Although wall composition varies with fungal species, generally fungal walls are composed of glucans, chitin and/or chitosan, mannans and/or galactomannans, and glycoproteins (Free, 2013). Up to 90 % of wall components are polysaccharides (Latgé 2007).

These can be divided in two groups, depending on their solubility in alkali (Bernard and Latgé, 2001). The alkali-insoluble polysaccharides are thought to be located close to plasma membrane and are primarily composed of β-1,3-glucans, chitin and galactomannan (Latgé 2010). The alkali soluble polysaccharides are present in the entire cell wall; especially in the outer face and are mainly composed of α-(1,3)-glucans with some galactomannan (Bernard and Latgé, 2001; Latgé 2010). In most fungi, two covalently cross-linked polysaccharides, β-(1,3)-glucan and chitin, form the core wall structure that is responsible for structural integrity and shape of the cell (Latgé, 2007). This glucan–chitin complex is covalently bound to other polysaccharides, the composition of which varies among fungi.

β-glucans are ~40% of the mass of the *Aspergillus* wall (Gastebois et al 2009; Free, 2013). A variety of β-glucans, including β-1,3-glucan, β-1,6-glucan, mixed β-1,3-/β-1,4-glucan have been identified in fungal cell walls (Free, 2013). The β-1,3-glucan is the major glucan (Fig 1.2) and is synthesized by β-1,3-glucan synthase, a well-characterized plasma membrane-associated enzyme with multiple transmembrane domains that form a channel through which newly synthesised glucan polymers are extruded into the cell wall space (Klis et al., 2006; Lesage & Bussey, 2006). Each of *A. nidulans*, *A. fumigatus*, *Cryptococcus neoformans*, *Neurospora crassa*, and *C. albicans* have a single β-1,3-glucan synthase, called FKS1 (Thompson et al., 1999; Beauvais et al., 2001) or in *A. nidulans*, FksA. *Saccharomyces cerevisiae* has three glucan synthase genes, but FKS1 functions as a major β-1,3-glucan synthase during vegetative growth in yeast (Klis et al., 2006; Lesage & Bussey, 2006).

Alpha-1,3-glucans (Fig 1.2) are synthesized by plasma membrane-associated alpha glucan synthases (AGS), which extrude newly formed linear glucan polymers through the plasma membrane into the cell wall space. Recent evidence suggested that α-(1,3)-glucan is present in the outermost layer of the fungal hyphal and conidial wall (Claverie-Martin et al 1988; Rappleye et al 2007). Although α-glucan is not essential for most fungi (*Schizosaccharomyces pombe* being the single exception, Hochstenbach et al., 1998), α-glucan can contribute to virulence for some pathogenic fungi (Rappleye et al 2007, Reese et al., 2007; Fujikawa et al., 2012), cell morphology (Reese and Doering, 2003; Cortés et al., 2012), cell wall integrity (Fujioka et al., 2007). *Aspergillus fumigatus* has three α-1,3-glucan synthases (AGS1, AGS2, AGS3), and two of these have been shown to participate in the

synthesis of α-1,3-glucan. Yoshimi *et al.* (2013) and He et al. (2014) recently described *A. nidulans* AgsA and AgsB as α-glucan synthases, with AgsB as the major α-glucan synthase.

Chitin is a relatively minor yet structurally important component of the fungal wall. Yeast species generally have 1–2 % chitin, mostly associated with cytokinesis scars, whereas chitin can comprise up to 15 % of the cell wall mass in filamentous fungi (Free 2013). In both yeasts and filamentous fungi, chitin microfibrils have an enormous tensile strength, covalently bind with β-1,3-glucan, and significantly contribute to the overall integrity of the cell wall (Latgé 2007). Chitin is synthesized by plasma membrane-associated chitin synthases (CHS). All characterized fungi have CHS and most have multiple genes encoding CHS. *Saccharomyces cerevisiae* has three genes that encode CHS (Cabib et al 2001), *C. albicans* has four (Munro et al., 2003). Both *A. nidulans and A. fumigatus* have seven CHS, which contribute to hyphal wall integrity, differentiation and tip growth (Horiuchi, 2009).

Galactomannan is a polysaccharide composed of a mannan core structure with galactose (galactopyranose or galactofuranose; Fig 1.2) side chains, is also commonly found in the wall of *Aspergillus* and some other species, but not in *Candida* (Fontaine et al. 2000). In *A. fumigatus*, the galactomannan is either covalently attached to β-1,3-glucans of the cell wall (Fig. 1.2) or linked to the plasma membrane via a GPI anchor (Costachel et al. 2005). Galactofuranose, a minor cell wall component, has been reported to be present in the wall of many pathogenic fungi and comprise around 5 % of the dry weight of *A. fumigatus* (Lamarre 2009). Typically, Gal*f* has been described to occur in galactomannan as side chains with repeating β-1,5-Gal*f* units that are β-3,6 linked to the mannose backbone (Fig. 1.2) (Latgé *et al.* 1994).

Fungal cell walls also contain glycoproteins, some of which are covalently linked into the cell wall matrix (Cheng 2011; Free 2013). Cell wall glycoproteins are synthesized by ER-associated ribosomes and extruded into the lumen of the ER. Glycoproteins can be attached to the cell membrane either *via* transmembrane domains or *via* a glycosylphosphatidylinositol (GPI) anchor (Cheng, 2011; Free, 2013). As the cell wall proteins are processed within the ER and Golgi apparatus, O-linked glycosylation occurs (addition of mannans or galactomannan) and the N-linked oligosaccharides are further

processed to generate high-mannan outer chain structures (in *S. cerevisiae, C. albicans*) or N-linked galactomannans (*S. pombe, A. fumigatus, N. crassa*) (Free, 2013).

In summary, the details of fungal cell wall composition and structure are still a very complicated puzzle; each element plays a role on its own as well as in concert with the others in the functioning of this structure. Loss of any of these cell wall components (glucans, chitin, mannans, galactomannans, and glycoproteins) can dramatically affect the growth, morphology, and viability of the fungus, demonstrating that all of these components are needed for the formation of a normally functional cell wall.

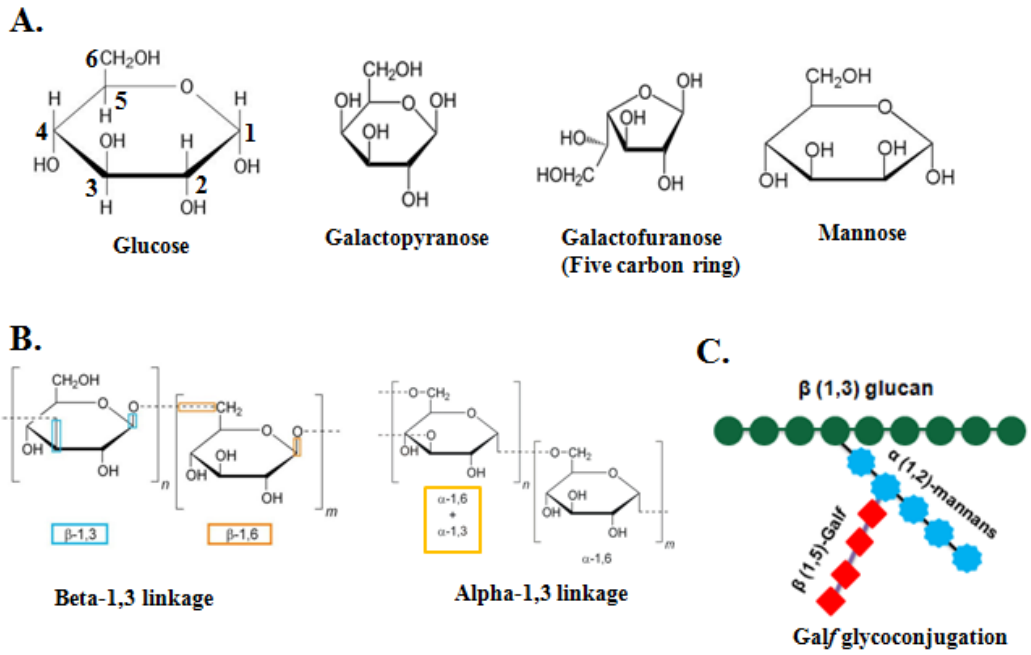

Figure 1.2: Cartoon showing the chemical structures of some fungal wall sugars, linkage of β-1,3 glucan, alpha-1, 3 glucan and glycoconjugation of Gal*f*.

A. chemical structures of glucose, galactopyranose, galactofuranose, mannose.

B. Beta-1,3-linkages in β-glucan and alpha-1,3-linkages in α-glucan.

C. Glyconjugation of Gal*f* with galactomannans.

1.4 Galactofunaose in fungal cell walls:

Despite decades of effort to characterize the composition and architecture of fungal cell walls (Bartnicki-Garcia, 1968; Bowman et al 2006; de Groot et al 2009) many details still

remain poorly understood. For example, recent evidence has shown that cell wall composition can be remodeled following environmental change, and altering certain minor wall components can cause major phenotype effects (Levin, 2005; Fujioka et al 2007; Levin, 2011) (Chapter 3 and references therein). Galactofuranose (Gal*f*) decorates certain wall carbohydrates and lipids (Lamarre et al., 2009). The six-member ring form, galactopyranose (Gal*p*) (Fig 1.2) is abundant in mammals (Pedersen et al 2003; Richards et al 2009). In contrast, the five-member ring form galactofuranose (Gal*f*) (Fig 1.2), detected in many pathogenic microorganisms is absent in higher eukaryotes including humans (Pedersen et al 2003; Richards et al 2009; Lamarre et al., 2009). Gal*f* is important for survival or virulence of many pathogenic microorganisms including bacteria, protozoa and some fungi (Beverley et al 2005; Kleczka et al 2007; Schmalhorst et al 2008; Lamarre et al., 2009). Since Gal*f* is absent from higher eukaryotes and is involved in growth or virulence of many bacteria and fungi, the enzymes involved in the biosynthesis of Gal*f* are considered to be an attractive drug targets (Pan et al 2001, Pedersen 2003).

Interestingly, the presence of Gal*f* is restricted to bacteria (Köplin et al 1997; Leone et al 2010), protozoa (Oppenheimer et al 2011), fungi (El-Ganiny et al., 2008; Latgé, 2009; Tefsen et al., 2012) as well as certain algae (Cordeiro et al 2008), archaea (Eichler and Adams, 2005), and invertebrates (Ma et al 2010). Gal*f* is essential in *Mycobacterium tuberculosis*, making Gal*f* biosynthesis a drug target against mycobacteria (Scherman et al 2003). Gal*f* is also found as glycoconjugates on the cell surface of *Leishmania* and *Trypanosoma* and shown to be important in parasite-cell interaction (MacRae et al., 2006; Kleczka et al., 2007).

In fungi, Gal*f* has been found in pathogenic *Penicillium, Histoplasma, Cryptococcus* and *Aspergillus* species (Barr et al, 1984; Latgé, 1994; Vaishnav et al 1998) and is considered to be an important component of a variety of cell surface glycoconjugates and glycans (Barr et al. 1984; El-Ganiny 2008; Lamarre 2009; Shibata and Okawa 2011). In contrast, yeast-like fungi belonging to the *Taphrinomycotina* and *Saccharomycotina* subphyla within the Ascomycota such as *Saccharomyces cerevisiae, Schizosaccharomyces pombe, Candida albicans, Pichia pastoris* do not have wall Gal*f* (Tefsen et al 2012).

In *A. fumigatus* walls (Fig. 1.3), Gal*f* is said to account for about 5 % of the total wall dry weight (Lamarre et al., 2009; Free et al 2013) and is reported to be part of galactomannans (Fig 1.3), glycoproteins, sphingolipids and lipophosphogalactomannans (Latgé, 2009). The presence of Gal*f* in *A. fumigatus* improves cell integrity and reduces adhesion to mammalian epithelial and endothelial surfaces by masking underlying mannan structures (Lamarre et al., 2009). In *A. nidulans*, deletion of Gal*f* results in severe defects: 500-fold reduction in hyphal growth rate and colony sporulation; aberrant cell shape; soft walls with abnormally sticky surfaces (El-Ganiny et al, 2008, 2010; Afroz et al. 2011). Gal*f* is also important for normal adherent properties of cell wall in *A. nidulans* (Paul et al. 2011).

Nevertheless, Gal*f* is not essential for any fungi studied to date. However, its presence is important for cell wall growth, maturation and integrity. Although the effects of Gal*f* are observed to vary with the organism, generally Gal*f* deficient strains are hypersensitive to wall-targeting drugs and exhibit a constitutive osmotic stress phenotype that could be partially remediated by growing on 1 M sucrose (El-Ganiny et al. 2008). Gauwerky et al. (2009) and Aimanianda & Latgé (2010) suggest that these non-essential wall components have the potential to be useful anti-fungal drug targets.

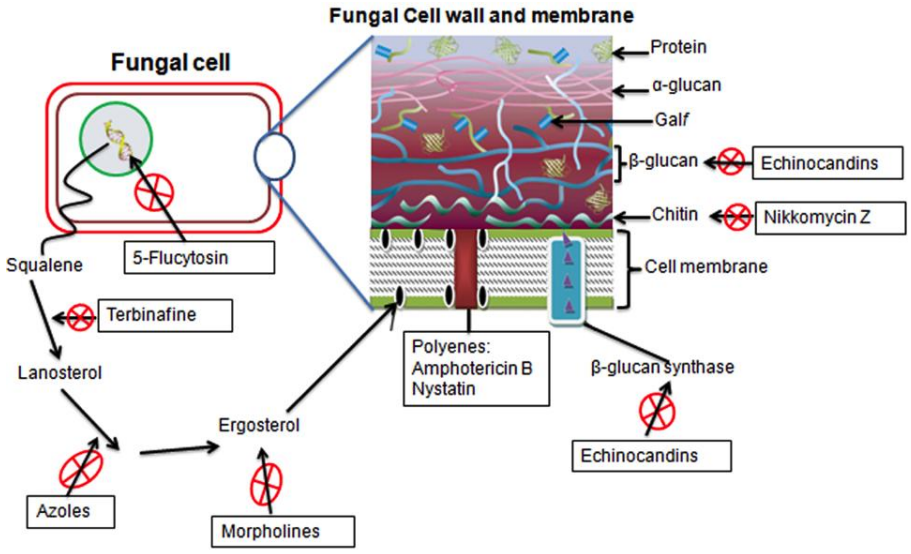

Figure 1.3: Fungal cell wall organization and targets for antifungal therapy. Some parts of this image were modified from Gastebois et al. 2009.

1.5 *Aspergillus nidulans* as a model system

Aspergillus species have both positive and negative impacts on humanity. *Aspergillus nidulans* is one of the most thoroughly characterized fungi with respect to genetics and cell biology. *Aspergillus* hyphae are septate and their cells are haploid and multinucleate. However, *A. nidulans* asexual spores are uninucleate (Todd et al 2007). *Aspergillus nidulans* is important because it is closely related to a large number of other *Aspergillus* species of industrial and medical significance *e.g*., *A. niger*, *A. oryzae*, *A. flavus*, and *A. fumigatus* and serves as a model for their biology (Todd et al 2007). Research on *A. nidulans* has made many contributions to the understanding of spore development, cell cycle regulation, cell polarity generation and maintenance, gene regulation, secondary metabolism, and signalling (Osmani et al., 1988; Timberlake, 1990; Momany, 2002; Yu & Keller, 2005).

There are several advantages that make *A. nidulans* an excellent experimental model system. *Aspergillus nidulans* has a well-characterized, conventional genetic system unlike most *Aspergillus* species, which are asexual or have cryptic sexual cycles (Fig 1.1) (Todd et al., 2007 a&b). The *A. nidulans* sexual cycle is readily induced so this species is easily manipulated using classical and molecular genetics (Todd et al., 2007a). It undergoes DNA-mediated transformation, and genes from other *Aspergillus* species typically function in *A. nidulans*. It grows rapidly as a filamentous fungus on solid or in liquid media under a variety of nutritional conditions (Todd et al, 2007a). *Aspergillus nidulans* is homothallic, which means that any two strains can be mated directly. *Aspergillus* species are normally haploid, but can also be induced to grow as a heterokaryon or a vegetative diploid (Fig. 1.1). *Aspergillus* produces both asexual spores (conidia) and sexual spores (ascospores) (Todd et al 2007b). *Aspergillus nidulans* is relatively safer [less infective to humans] than *A. fumigatus* and most other *Aspergillus* species (de Aguirre et al., 2004). Analysis of cell wall sugars of *A. fumigatus* and *A. nidulans* showed that both fungi have overall similar wall sugar composition (Guest and Momany, 2000).

The genomes of *A. nidulans*, *A. fumigatus*, and several other *Aspergillus* species have been sequenced (Galagan et al., 2005; Wortman et al., 2009). The size of the *A. nidulans* genome is relatively small, about 31 Mb (available on the Broad Institute: http://www.broadinstitute.org/scientific-community/science/projects/fungal-genome-

initiative/fungal-genome-initiative). It has eight well-marked chromosomes containing an estimated 11,000–12,000 genes. Approximately 900 genes have been identified in *A. nidulans* by conventional matings; 432 have been mapped to locus, and 254 are cloned and sequenced (according to Broad Institute data). There are several extensively curated comparative databases of many *Aspergillus* species and easy-to-use web-based tools for accessing, analyzing and exploring these data which accelerate *Aspergillus* research (Rokas et al., 2007; Arnaud et al., 2010). Altogether, studies in *A. nidulans* contribute significantly to understanding fundamental biological principles and are relevant for biotechnology and industrial applications, as well as human, animal and plant fungal pathogenesis.

1.6 *Aspergillus* infection

Fungi cause a wide range of illnesses in humans, from minor skin conditions to life-threatening invasive disease. Generally, fungal infections can be categorized into groups such as superficial and systemic. Superficial infections affect the surface of the body, the skin, mucous membrane, the nails, and the hair. These include ringworm, athlete's foot, and yeast infections (Ho and Cheng, 2010). A systemic fungal infection is caused either by an opportunistic organism that attacks a person with a weakened immune system (opportunistic infection), or by an invasive organism that is common in a specific geographic area, such as *Coccidioides immitus* and *Histoplasma capsulatum* (Bradsher, 1996; Erjavec et al., 2009; Welsh et al., 2012). Unlike superficial infections, human systemic fungal infections are an increasing threat (Fisher et al., 2012), particularly due to improved medical technology leading to larger populations of immune-compromised people. The most common opportunistic fungal infections that affect people are candidiasis, aspergillosis, and cryptococcosis. Clinically, candidiasis and aspergillosis account for between 80-90 % of systemic fungal infections in immunocompromised and hospitalized patients (Onnis et al 2009).

Aspergillus is second to *Candida* as a cause of invasive or systemic fungal infections (Erjavec et al., 2009). *Aspergillus* is usually acquired in hospital, mainly by intensive care patients (Heinemann et al 2004). Mortality is 50-100 % even with treatment (van der Woude et al 2004). Although there is a great number of *Aspergillus* species, *Aspergillus fumigatus* is

the primary causative agent of human infections followed by *A. flavus*, *A. terreus*, *A. niger*, and the model organism, *A. nidulans* (Dagenais and Keller, 2009). *Aspergillus fumigatus* is one of the most common airborne spore-producing fungi in the world (Perfect and Casadevall, 2006**)**. Its conidia production is prolific, and so human respiratory tract exposure is almost constant, (Perfect and Casadevall, 2006) because their concentration in the air is high, approximately 1- 100 conidia per m^3 (Latgé, 2001). Depending on the immune status of the host, *A. fumigatus* can cause a spectrum of diseases ranging from the infection in the sinus, airway, or lung tissues in immunocompetent persons to acute invasive aspergillosis in immunocompromised patients (Latgé, 1999).

The exact mechanism for *A. fumigatus* pathogenicity is not yet identified. However, it has been speculated that *A. fumigatus* virulence is directly correlated with its specific biological characteristics: the small size of the conidia (2–3 μm), rapid mycelial growth at 37 °C, and minimum nutritional requirements (Latgé, 1999). In addition, production of secondary metabolites and toxins and the presence of 'pathogenicity islands' in genome that contain genes that code for one or more virulence factors, such as adhesins and toxins are also considered as pathogenic determinants of *A. fumigatus* (Fedorova et al. 2008).

The frequent use of anti-fungal drugs (particularly use of azoles in agriculture), immunosuppressive agents after organ transplantation, cancer chemotherapy, hematological malignancies, chronic granulomatous disease, advanced AIDS, and advances in surgery have caused a dramatic increase in the number of immunocompromised individuals who are more susceptible to *Aspergillus* infections (Perfect and Casadevall, 2006). The primary route of human infection is by inhalation of airborne conidia, followed by conidial deposition in the bronchioles or alveolar spaces. The lungs are the most common site of *Aspergillus* infection (Latgé, 1999). If the conidia can overcome the immune defence mechanisms in the lung, they germinate and produce a compact vegetative mycelium that invades the lung tissues (Latgé, 1999, 2001). The virulence of *A. fumigatus* can then be caused either by the production of fungal proteins that promote mycelial growth into the lung parenchyma or by structural features of the conidia that confer resistance to the host's antifungal mechanisms (Latgé, 2001).

In immunocompromised individuals, the incidence of invasive infection can easily be 50 % of patients, with a morbidity rate of ≥50 % (Denning, 1998). Late diagnosis and relatively poor knowledge about fungal pathogenicity and virulence factors result in 60-90 % mortality rate in humans (Tekaia and Latgé, 2005). In sum, the number of immunocompromised individuals is increasing which lead to increase in *Aspergillus* infection. However, as described below, very few antifungal drugs are available to treat these infections.

1.7 Antifungal drugs and fungal resistance:

Effective treatment for fungal infection has become an increasing concern as the frequency of fungal infection increases due to increased numbers of immuocompromised patients (Sheppard et al 2004). Fortunately, over the last few decades, a few potent antifungals and the increasing use of combination therapy have improved our ability to fight life-threatening fungal disease. However, the number of available antifungal drugs is very limited. Moreover, few drugs meet the criteria of an ideal antifungal agent such as broad spectrum of activity, low host toxicity, flexible routes of administration, and reasonable cost (Chapman et al., 2008). Finding such an ideal target is always complicated due to the underlying biochemical similarities between humans and fungi (Aimanianda and Latgé, 2010). In addition, resistance to antifungal treatment can occur. A general schematic diagram of fungal cell and its drug targets is given in Fig. 1.3.

Existing antifungal drugs are grouped into classes according to their targets. The newest class of antifungals (~2005) is the echinocandins that target fungal wall biosynthesis (Fig 1.3). Echinocandins bind non-competitively to the catalytic subunit of β-1,3-glucan synthases (Fks). Fks are membrane protein complexes that are responsible for the synthesis of cell wall β-1,3-glucans (Walker et al., 2010). Inhibition of Fks leads to disruption of the structure of the growing cell wall, resulting in osmotic instability and death in susceptible fungal species (Bowman et al., 2002). Among the numerous semisynthetic echinocandins developed in the last decades, caspofungin (trade name: Cancidas, Merck and Co.), micafungin (trade name: Mycamine, Astellas Pharmaceuticals) and anidulafungin (trade name: Eraxis, Pfizer Pharmaceuticals) are Food and Drug Administration (FDA)-approved (Goswami et al., 2012). As they show good fungicidal (*Candida spp.)* or fungistatic

(*Aspergillus spp.*) activity against the most important human pathogenic fungi including azole-resistant strains, they are an important addition to the antifungal armamentarium (Bowman, 2002). However, echinocandins are not effective against *C. neoformans* or non-*Aspergillus* moulds. Because β-1,3-glucan synthases do not exist in mammalian cells, human toxicity associated with echinocandins is limited (Gauwerky et al., 2009). However they must be administered by injection (Kauffman and Carver, 2008). Evidence of acquired resistance against echinocandins has already been reported in *Candida* (Lee et al. 2012). All the echinocandin-resistant *Candida* isolates tested to date harbored Fks mutations and had increased chitin content (Lee et al. 2012). In the case of *A. fumigatus*, the introduction of point mutations within the *fks1* gene caused elevated MEC values (Gardiner et al. 2005; Rocha et al. 2007). In addition, over-expression of the *fks* gene as well as increases in chitin synthesis (Gardiner et al. 2005; Arendrup et al 2008) might also be responsible for the emerging resistance in these filamentous fungus pathogens.

Cell membrane targeting antifungals either bind directly to ergosterol (polyenes) or inhibit ergosterol biosynthesis (azoles, allylamines) (Fig 1.4). Ergosterol is the main sterol component of the fungal cell membrane. Ergosterol is chemically similar to human cholesterol, and this similarity may result in toxicity in human treatment.

The polyenes bind irreversibly to ergosterol and disrupt the fungal plasma membrane that results in increased membrane permeability, the leakage of the cytoplasmic ion contents and ultimately death of the fungal cell (Bolard, 1986; reviewed by Sanglad 2011). Thus, the polyenes are fungicidal. Nystatin was the first polyene drug to be used clinically. It is active against *Candida* and *Aspergillus*. However, nystatin can only be used topically due to problems with its solubilisation in injectable solvents, as well as its human toxicity (Carrillo-Munoz et al., 1999). Amphotericin B is a polyene that was developed shortly after nystatin (~1956). It has a broad spectrum of activity, and is used successfully to treat various yeasts and mould infections (Gallis et al., 1990). Acquired resistance to amphotericin B is often associated with alteration of membrane lipids, especially sterols. Recently, *C. albicans* clinical isolates resistant to amphotericin B were described that lacked ergosterol and accumulated other sterols (Chau et al 2005; Martel et al., 2010).

Azoles are the best-studied class of antifungal drugs (Sheehan et al., 1999). In addition, azoles are widely used as agricultural fungicides to control plant fungal diseases (Verweij et al., 2009). Azoles are generally recognized as fungistatic agents at clinically achievable concentrations. However, recent *in vitro* studies with itraconazole and voriconazole demonstrated fungicidal activity against conidial suspensions of *A. fumigatus* and several other *Aspergillus* species at concentrations below those attained with recommended dosages (Manavathu et al., 1998). Azole antifungal agents used in medicine are categorized as imidazoles (ketoconazole, miconazole, clotrimazole) or triazoles (fluconazole, itraconazole, posaconazole, voriconazole, and ravuconazole). Azoles target a cytochrome P_{450} enzyme, lanosterol 14α-demethylase, (referred to as Erg11p in yeast). This is the product of the *ERG11* gene as a common cellular target in yeast or moulds (Zhang et al., 2007). The use of imidazoles is limited to treating superficial mycoses due to their human toxicity (Zhang et al., 2007)**.** In general, the triazoles are relatively safe, even when used for prolonged periods, although they can cause liver toxicity (Spanakis et al., 2006). Yeasts or filamentous fungi can use several mechanisms to become resistant to azole antifungal agents such as up-regulation of ABC-transporter genes, multidrug transporter genes, alterations in cellular target (Erg11/Cyp41), and biofilm formation (reviewed by Sanglad, 2011). In general azoles are relatively safer than the drugs that target DNA synthesis (see below), however, host toxicity and evolving resistance limit their application in humans.

The allylamines inhibit an early stage of ergosterol biosynthesis by binding the enzyme squalene epoxidase (Fig 1.3). Terbinafine is the only allylamine in clinical use for subcutaneous infections. Terbinafine has good *in vitro* activity against *Aspergillus spp*., *Fusarium spp.* and other filamentous fungi but has variable activity against yeasts (Petranyi et al., 1987). Terbinafine may cause gastrointestinal upset and transient elevation of liver enzymes (Gauwerky et al., 2009).

Other agents, including flucytosine (5-fluorocytosine; 5-FC) and griseofulvin target nucleic acid biosynthesis and mitosis respectively (Carrillo-Muñoz et al., 2006; Cannon et al., 2009). In the cell, 5-FC belongs to the class of pyrimidine analogues. It is converted into the metabolically active nucleoside analogue 5-fluorouracil, which inhibits RNA and DNA synthesis. 5-FC is not usually administered as a single agent because of rapid development of

resistance (Barchiesi et al., 2000). It is therefore used mainly in combination with other agents, particularly amphotericin B for treatment of *Candida* species and *C. neoformans* infections (Barchiesi et al., 2000). Resistance may occur due to the deficiency or lack of enzymes implicated in the metabolism of 5-FC, or resistance may be due to the deregulation of the pyrimidine biosynthetic pathway, in which products can compete with the fluorinated metabolites of 5-FC (Bossche et al., 1994).

Overall, although the arsenal of antifungals has expanded, currently available drugs do not meet the increasing requirements of managing infection in complex patient populations. In addition, no single class of antifungal is effective against all invasive mycoses, and some are highly selective. Besides emerging resistance, there are other problems associated with current antifungal therapies such as host toxicity and narrow activity spectra. The problems associated with current antifungal drugs require the development of new antifungals for clinical therapy.

1.8 The Gal*f* biosynthesis pathway and its possibility to be a drug target in *Aspergillus*

Biosynthesis of Gal*f*-containing glycoconjugates requires enzymes for the synthesis of activated sugar donors and transporters that ensure substrate availability in the proper cellular compartment(s). Enzymes in the Gal*f* pathway have been well studied in prokaryotes (Weston et al., 1998; Mikusova et al., 2006). These include UDP-galactopyranose mutase (UGM) that catalyzes the inter-conversion between UDP-Gal*p* and UDP-Gal*f* (Weston et al., 1998) and galactofuranosyl transferase(s) that transfer Gal*f* moieties from UDP-Gal*f* to glycoconjugate molecules (Belanova et al., 2008).

In eukaryotes including fungi, Gal*f* biosynthesis and incorporation in the cell wall is a multistep process that is summarized in Fig 1.4. In *Aspergillus*, it starts with the synthesis of nucleotide-sugar donor UDP-Gal*p* (Fig 1.4). UDP-Gal*p* is generated by the epimerization of UDP-glucose by UDP-glucose-4-epimerase (UGE), as well as by the salvage of galactose (Fig 2.1 in Chapter 2). In many organisms, galactose salvage occurs via the Leloir pathway, which includes GalE and GalD and provides a unique means for cells to use galactose as a carbon and energy source (Fekete et al, 2004). UDP-Gal*f* is produced directly from UDP-Gal*p* by UDP-galactopyranose mutase (UgmA) (El-Ganiny et al 2008). UDP-Gal*f* is then transported

into the lumen of the Golgi by UgtA (Afroz et al 2011). Finally, the enzyme Gal*f* transferase is responsible for transferring Gal*f* from transported UDP-galactofuranose (Gal*f*) to the respective glycoconjugate molecules (Fig 1.4).

In *A. fumigatus* walls, Gal*f* is reported to be part of four different molecules including galactomannans, glycoproteins, several sphingolipids, and lipophosphogalactomannan (Latgé, 2009). Based on the likely Gal*f*-containing structures (Latgé, 2009), it is expected that multiple putative galactofuranosyl (Gal*f*) transferases contribute to the synthesis of the different glycoconjugates. Finally, all glycoconjugates are transported to the cell surface from where they are eventually transferred to the cell wall, or released into the extracellular space. Gal*f* transferases that incorporate Gal*f* into glycoconjugates have been identified in bacteria and protozoa, and most recently in fungi (Komachi et al., 2013).

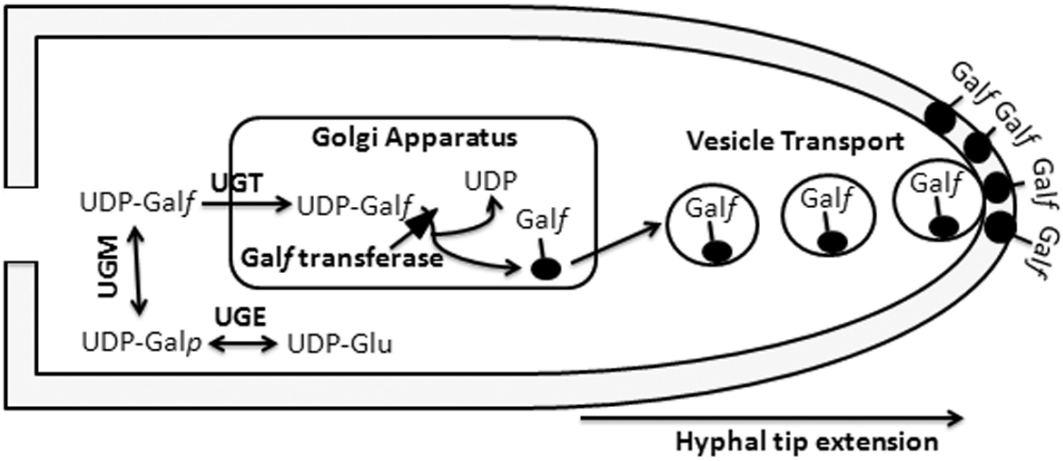

Figure 1.4**: Predicted model for Gal*f* biosynthesis and its deposition to cell wall.** UDP-Glu; uridine diphosphate-glucose, UGE; UDP-glucose-4-epimerase, UDP-Gal*p*; UDP-Galactopyranose, UGM; UDP-galactopyranose mutase; UDP-Gal*f*; UDP-galactofuranose, UGT; UDP-galactofuranose transporter, Gal*f*-Transferase; galactofuranose transferase, Gal*f*; galactofuranose.

1.8.1 Galactokinase (GalE) and galactose-1-phosphate uridylyltransferase (GalD)

Galactose is transported and phosphorylated by GalE to form galactose-1-phosphate. In the next round of the transfer reaction, GalD interconverts glucose- or galactose-1-phosphate to their UDP conjugates. Both of these steps are highly conserved in species ranging from bacteria to humans (Holden et al., 2003). In addition, both use the Leloir

pathway for D-galactose metabolism and therefore, all genes are essential for growth on D-galactose (Slepak et al. 2005, reviewed in Seiboth et al 2007).

GalE is essential for galactose metabolism in *S. cerevisiae* (Slepak et al. 2005). GalD is also essential for *S. cerevisiae* growth on galactose (Slepak et al. 2005) and for galactose metabolism in *Kluyveromyces lactis* (Dickson and Riley 1989). Although GalD and GalE appear to be the main D-galactose degrading enzymes in *Aspergillus*, alternative or additional galactose metabolism pathways via galactitol, sorbitol and fructose have been proposed in *A. nidulans* (Elorza, 1971; Fekete *et al.* 2004).

1.8.2 UDP-glucose-4-epimerase (Uge):

The catalytic conversion of UDP-galactopyranose from UDP-glucose by UDP-glucose/galactose 4-epimerase (*UGE*/*Gal10*) is a step in the Leloir pathway of galactose metabolism. This step is highly conserved in species ranging from bacteria to humans (Holden et al., 2003)**.** Loss of Uge (called GalE in humans) activity causes a metabolic disorder called galactosemia (Openo et al., 2006). In some species, this step may be the only mechanism for providing galactose to the cell in the absence of an external source (Singh et al., 2007). Some fungi including *C. neoformans, S. pombe* and some *Aspergillus* species have two genes that both encode functional UDP-glucose/galactose epimerases (Moyrand, 2008; Suzuki et al., 2009), whereas some other fungi (e.g. *C. albicans*) have only one (Singh et al., 2007). *C. albicans* glucose/galactose-4-epimerase was found to be essential for growth on galactose. In *C. neoformans,* Uge1 is essential for capsule formation and virulence, whereas Uge2 is necessary for the cells to utilize galactose as a carbon source at 30 ºC but is not required for virulence (Moyrand et al., 2008). Mutations of Uge (*GalE*) in *S. cerevisiae* cause galactose sensitivity: the mutants cease growth in response to trace quantities of galactose, even in the presence of other carbon sources (Wasilenko and Fridovich-Keil, 2006). In *A. nidulans*, the ugeA deleted strain is viable on glucose but has reduced growth and sporulation (El-Ganiny 2010). In the protozoan, *Trypanosoma brucei,* galactose metabolism mediated by Uge (called GalE) is essential for parasite growth and survival (Roper et al., 2002).

Trypanosoma brucei Uge is a validated drug target for African sleeping sickness. Some inhibitors of *T. brucei* Uge were identified by screening a small library of natural

products and commercially available compounds. Unfortunately, these inhibitors showed a small degree of selectivity between human and *Trypanosoma* enzymes (Urbaniak et al., 2006). Although Uge is highly conserved amongst diverse organisms, it may be possible to find compounds that selectively inhibit its function in specific organisms. However, UgeA is not essential in any *Aspergillus* species, unlike *Trypanosoma* (Roper et al., 2002), so selection pressures to overcome a future potential therapeutic compound might be reduced.

1.8.3 UDP-galactopyranose mutase (Ugm)

The cytosolic enzyme Ugm is the key enzyme in the Gal*f* biosynthesis pathway. Ugm is responsible for interconversion of UDP-Gal*p* and UDP-Gal*f*. The gene encoding Ugm (also called GlfA in *A. fumigatus*) has been identified and characterized in several eukaryotes, including *L. major*, *T. cruzi*, *Caenorhabaditis elegans, A. fumigatus, A. nidulans,* and *A. niger* (Beverley et al. 2005; Kleczka et al. 2007; Damveld et al. 2008; El-Ganiny et al. 2008; Schmalhorst et al. 2008; Novelli et al. 2009). Ugm in different systems has been shown to be important for survival, growth, and/or pathogenicity. Deletion of *ugm* from *Mycobacterium tuberculosis* showed that it was essential for growth and survival (Pan et al., 2001). Targeted replacement of *glf* in *L. major* (the causative agent of leishmaniasis) caused attenuation of virulence (Kleczka et al., 2007). Deletion of *glf-1* from the nematode *C. elegans* caused a significant late embryonic and larval lethality due to defective surface coat formation (Novelli et al., 2009). Deletion of *ugmA* in *A. fumigatus, A. nidulans,* and *A. niger* revealed the corresponding knock-out strains were all completely lacking in Gal*f* and exhibited marked alterations to their cell wall and growth (Damveld et al. 2008; Lamarre et al 2009). Additionally, infection of mice by Ugm deletion strains of either *L. major* or *A. fumigatus* showed significant attenuation to virulence (Kleczka et al 2007; Schmalhorst et al 2008). *A. niger* has two genes that encode putative UDP-galactopyranose mutase (*ugmA* & *ugmB*). Damveld et al. (2008) had shown that *A. niger* strains with defective *ugmA* homologues had impaired colony growth and increased wall α-glucan content.

The crystal structure of *Escherichia coli* Ugm was described in 2001 (Sanders et al., 2001), followed by the crystal structures of UGM from *M. tuberculosis* and *K. pneumoniae* (Beis et al., 2005). Although the sequence conservation between prokaryotic and eukaryotic

Ugms is low (15–20 %), a number of features are conserved, including the presence of FAD (van Straaten et al, 2011). Recently, the crystal structure of *A. fumigatus* Ugm has been solved (van Straaten et al, 2011). Despite low sequence identity with known prokaryotic Ugms, the overall fold is largely conserved. Fungal Ugms function as homotetramers (van Straaten et al, 2011), whereas *L. major* Ugm functions as a monomer (Oppenheimer et al. 2011) and hence both differ from the dimeric bacterial Ugms.

Considering the fact that Ugm is critical for microbial growth and virulence and is not found in humans, Ugm is an attractive target for drug discovery (Oppenheimer et al 2011). Several inhibitors of bacterial UGM have been reported (Dykhuizen et al., 2008), but no inhibitor has been developed that is effective against fungal Ugm. Notably, UgmA is not essential in either of these *Aspergillus* species, unlike several pathogenic bacteria, so selection pressure to overcome a future potential therapeutic compound might be reduced.

1.8.4 UDP-Gal*f* transporter

Many nucleotide sugars are synthesized in the cytosol and then translocated to the lumen of Golgi or ER by the action of the nucleotide-sugar transporters (NSTs) (Handford et al., 2006). NSTs are integral proteins typically with six to ten transmembrane domains (Handford et al., 2006). They occur in all eukaryotes and frequently are located in the membrane of the Golgi apparatus, an organelle in the endomembrane system where the biosynthesis of glycoconjugates and polysaccharides occurs. Glycosylation requires a sugar donor that typically is a nucleoside diphosphate sugar (NDP-sugar) or nucleoside monophosphate sugar (Reyes and Orellana, 2008).

UDP-Gal*f* is a nucleotide diphosphate sugar, which is synthesized in the cytosol and so must be translocated into a membrane-bound organelle prior to incorporation into glycoconjugates. Interestingly, an UDP-Galf transporter (GlfB/UgtA) seems to be presented in all filamentous fungi of the subphylum Pezizomycotina and is directly adjacent or in close proximity to the GlfA/UgmA gene, which encodes the UGM (Tefsen et al 2012). However, until now UDP-Galf transporter (GlfB) has only been characterized in *A. fumigatus* and *A. nidulans*. In both species, *ugtA*/*glfB* is adjacent to the *glfA*/*ugmA* and both transporters localized to the Golgi equivalent (Engel et al. 2009; Afroz et al 2011). Analysis of

glycoproteins, glycolipids and galactomannans of the *A. fumigatus glfB* knockout strain revealed that none of these compounds contain Gal*f* moieties. The deletion or repression of the UDP-Gal*f* transporter (UgtA) in *A. nidulans* impaired growth and sporulation and increased drug sensitivity (Afroz et al 2011). Af*glfB* restored wild type growth in the An*ugtA*Δ strain, showing that these genes have homologous function (Afroz et al 2011).

In summary, the UDP-Gal*f* transporter actively translocates the nucleotide sugar UDP-Gal*f* from cytosol into Golgi equivalent in fungi. To our knowledge UDP-Gal*f* transporter has only been studied in *A. fumigatus* and *A. nidulans*. Moreover, UDP-Gal*f* specific transporter is absent in animals. Notably, the *ugtA*Δ strain showed significantly more sensitive to Caspofungin (Afroz et al., 2011), suggesting that drugs that could be developed to target the Gal*f* biosynthesis pathway have potential for combination therapy.

1.8.5 Galactofuranosyl transferases

Gal*f* exists as glycoconjugates in microbial cell wall. The enzyme galactofuranosyl transferase (Gal*f* transferase) is responsible for transferring Gal*f* from UDP-Gal*f* to the respective glycoconjugate molecules (Chen and Okayama, 1988). These glycosylation steps take place in one or more compartments of the endomembrane system. Generally it involves in transferring monosacchararides to proteins, lipids or carbohydrates to produce glycoconjugates. To better understand the role of individual Gal*f*-containing glycoconjugates in cell wall biosynthesis or pathogenesis, it is necessary to identify and characterize the Gal*f* transferases that catalyze the addition of Gal*f* from UDP-Gal*f* to the respective acceptor substrates.

Several Gal*f* transferases have been identified in prokaryotes, such as WbbI in *E. coli* that performs β-1,6-coupling of Gal*f* to α-glucose (Wing et al. 2006) and WbbO in *K. pneumoniae* that couples Gal*f* in a β-1,3-linkage to Gal*p* (Guan et al. 2001). Two galactofuranosyl transferases were identified in *Mycobacterium*, GlfT1 (Rv3782) and GlfT2 (Rv3808c) (Belanova et al., 2008). GlfT1 initiates the first step of galactan synthesis, whereas GlfT2 is a bifunctional enzyme responsible for the majority of galactan polymerization (Szczepina et al., 2010). LPG1 is the only putative Gal*f* transferase described in *L. major*, (Novozhilova and Bovin, 2010). Many glycosyltransferases have been identified in fungi

including glucan synthases, chitin synthases, and mannosyltransferases (Klutts et al., 2006). However, until now only one putative Gal*f* specific transferase (GfsA) has been reported in *Aspergillus nidulans* and *Aspergillus fumigatus* (Komachi et al, 2013). Disruption of *gfsA* reduced binding of β-Gal*f*-specific antibody EB-A2 to galactomannoproteins (Komachi et al, 2013). Gal*f* transferases are considered as a potential anti-microbial drug target. Some inhibitors have already been synthesized against Gal*f* transferases and proven to be potent drugs against *Mycobacterium* (Peltier et al., 2010).

In sum, all the enzymes in the Gal*f* pathway are important but not essential for fungal for normal growth, sporulation and wall maturation. Therefore, none of these enzymes in Gal*f* biosynthesis pathway itself have the potential to be an antifungal drug target. However, considering Gal*f*-lacking strains had substantially reduced growth and hypersensitivity to caspofungin, anti-Gal*f* drugs (once created) may be useful in combination with existing antifungal drugs. Combination therapy is already in use to combat fungal infection. For example, it has been shown that toxicity of amphotericin B can be reduced in combination with echinocandins (Mihu et al., 2010). Use of flucytosine in combination with many other drugs helps in preventing the rapid development of resistance (Johnson et al., 2004). Altogether, considering the emergence of resistance against antifungal drugs and the high rate of mortality from fungal infections, there is a pressing need for new therapeutic options. Use of combination therapy, especially anti-Gal*f* drugs in combination with echinocandins may overcome both emergence resistance and infection problems.

1. 9. Summary

Systemic fungal infection is life threatening, especially for immunocompromised patients. Treatment of fungal infections is challenging because fungi share many metabolic pathways with mammals. In addition, due to emerging drug resistance, current antifungals are losing effectiveness. Therefore, new therapeutic approaches, including antifungal agents with novel mechanisms of action, are urgently needed. The cell wall is essential for fungal survival in natural environments. Polysaccharides and glycoconjugates are significant components of fungal walls. They form an interface between cells or organisms and their environment, enabling cell–cell interactions and signaling events. Due to the importance of cell walls for

fungal growth and host invasion, and the lack of conservation with animal cell components, the cell wall is expected to be a good source of potential antifungal targets.

Gal*f* decorates certain carbohydrates and lipids, comprises about 5 % of the *Aspergillus fumigatus* cell wall, and may play a role in systemic aspergillosis. In the filamentous fungus, *A. nidulans*, galactokinase (GalE) mediates galactose phosphorylation to galactose-1-phosphate. Galactose-1-phosphate uridylyltransferase (GalD) interconverts glucose- or galactose-1-phosphate to their UDP conjugates. UDP-glucose is a substrate for UDP-galactose-4-epimerase (UgeA) to create UDP-galactopyranose, which can potentially be processed into UDP-Gal*f* by UDP-galactopyranose mutase (UgmA). Gal*f* is transported into the Golgi by the UDP-Gal*f* transporter (UgtA) and eventually deposited as galactofuranose (Gal*f*) in the cell wall as a Gal*f* glycoconjugate.

During my research, I characterized the function of enzymes that involve in galactose metabolism and Gal*f* biosynthesis using gene deletion strategy, and by controlling gene expression with regulatable promoters to compare the effects of gene repression and induction. Phenotype characterization of the deleted strains in comparison to the wild type strain used fluorescence microscopy, scanning electron microscopy (SEM), and transmission electron microscopy (TEM). Gene product localization used green fluorescent protein (GFP) tagging, and Gal*f* localization used immunofluorescence microscopy. To assess whether Gal*f*-targeting compounds (once created) might be useful for combination therapy, I assessed the sensitivity of the Gal*f*-defective strains to commercially available antifungal drugs. I also studied how modification of *A. nidulans* Gal*f* leads to changes in cell wall α-glucan and β-glucan content, hyphal surface adhesion using immunofluorescence, ELISA, and a fluorescence bead assay. Interacting partners of UgmA were revealed using tandem affinity purification and LC-MS analysis.

1.10. Outline and objectives

My thesis consists of six Chapters. The first chapter is the general introduction. Chapters 2-5 contain four manuscripts that discuss the roles of GalD and GalE in galactose metabolism (Chapter 2), roles of enzymes (UgmA, UgeA, UgtA) of Gal*f* biosynthesis pathway in fungal growth, drug sensitivity, and relationship with other major carbohydrate

biosynthesis pathways (Chapter 3), how modification of Gal*f* leads to changes in cell wall composition, hyphal surface adhesion and response to antifungal drugs (Chapter 4), and revealing the interacting partner of *A. nidulans* UgmA using a proteomic approach (Chapter 5). My roles in these manuscripts are described on the first page of each chapter. In the final chapter of my thesis (Chapter 6), I discuss my overall research results in terms of their importance in understanding the complexity of galactose metabolism in *Aspergillus* spp., contribution of Gal*f* in fungal growth, development, drug sensitivity, cell wall modification and co-ordination Gal*f* with other carbohydrate pathways. The final section of Chapter 6 discusses the possibility for anti-Gal*f* drug as a part of a combination therapy and future directions.

My thesis work is based on following objectives,

1. Exploring the biological roles of galactose metabolism enzymes in the model filamentous fungi *Aspergillus nidulans.*

   Hypothesis: The *A. nidulans* strains that lack galactose metabolism enzymes will be unable to grow when galactose is the sole carbon source.

2. Exploring the roles of Gal*f*-defective strains in wall maturation and sensitivity to available antifungal drugs.

   Hypothesis: Gal*f* deletion/repressed *A. nidulans* strains will have a wall defect that will make them more sensitive to wall-targeting agents.

3. Assessing how modification of UDP-galactopyranose mutase activity leads to changes in *A. nidulans* cell wall α-glucan and β-glucan content, hyphal surface adhesion and response to antifungal drugs.

   Hypothesis: *Aspergillus nidulans* strains lacking UgmA or hosting mutated UgmA will have significantly altered carbohydrate content in their cell wall compared to the wild type strain. These UgmA defective strains will also have less or no Gal*f* in their cell wall.

4. Revealing the interacting partner of *Aspergillus nidulans* UgmA using tandem affinity purification (TAP).

   Hypothesis: UgmA is part of a protein complex in *A. nidulans* that likely includes UgeA, UgtA, and members of α-glucan and beta-glucan metabolism.

CHAPTER 2

Aspergillus galactose metabolism is more complex than that of *Saccharomyces*: the story of GalD^{GAL7} and GalE^{GAL1}

This Chapter studies the biological roles of two enzymes in galactose metabolism pathway, GalD^{GAL7} and GalE^{GAL1}. The manuscript has been published as "***Aspergillus* galactose metabolism is more complex than that of *Saccharomyces*: the story of GalD^{GAL7} and GalE^{GAL1}**," in Botany 91(7): 467-477 by Md. Kausar Alam and Susan Kaminskyj, 2013.

This Chapter was based on our hypothesis "the strains that lack galactose metabolism enzymes will be unable to grow when galactose is the sole carbon source". The objectives of the research in this Chapter were

1. To identify putative GalD and GalE in *A. nidulans*
2. To explore the biological roles of galactose metabolism enzymes in *A. nidulans*
3. To investigate the effects of *galD* and *galE* deletion on colony growth, hyphal morphogenesis, drug senstivity and cell wall ultrastructure.
4. To determine the subcellular localization of *A. nidulans* GalD and GalE

My contribution in this Paper: This project was the first project of my program. I started with identification of *Aspergillus nidulans* GalD^{GAL7} and GalE^{GAL1}. I performed all the experiments including: designing primers for gene deletion, confirming the deletion, GFP tagging, characterization of GalD^{GAL7} and GalE^{GAL1} strains using confocal, SEM and TEM, Immunolocalization of Gal*f* in wild type and GalD^{GAL7} and GalE^{GAL1} strains, complementing GalD^{GAL7} and GalE^{GAL1} strain defects using *S. cerevisiae GAL7 and GAL1,* drug sensitivity study. I did the statistical analysis of the data and the editing of the final figures. I wrote the first draft of the manuscript. Professor Susan Kaminskyj and I worked together to revise this draft prior to submission. We also worked together on the revision.

Full title: ***Aspergillus*** **galactose metabolism is more complex than that of** ***Saccharomyces*****: the story of GalD^{GAL7} and GalE^{GAL1}**

Authors, in order of appearance: Md. Kausar Alam and Susan G. W. Kaminskyj [a]

Md. Kausar Alam, Department of Biology, University of Saskatchewan, 112 Science Place, Saskatoon, SK S7N5E2. Email: kausar.alam@usask.ca

Susan G. W. Kaminskyj, Department of Biology, University of Saskatchewan, 112 Science Place, Saskatoon, SK S7N5E2. Email: susan.kaminskyj@usask.ca

Author for correspondence: Susan Kaminskyj; tel +1 306 966 4422, fax +1 306 966 4461. Email susan.kaminskyj@usask.ca

Abstract

Saccharomyces cerevisiae GAL1 (galactokinase) generates galactose-1-phosphate; GAL7 (galactose-1-phosphate uridylyltransferase) transfers UDP between galactose and glucose and their respective sugar-1-phosphate conjugates; each is essential on galactose. *Aspergillus nidulans* ANID_04957 has 41% amino acid sequence identity with GAL1; ANID_06182 has 50% sequence identity with GAL7. *Aspergillus nidulans* GalE (galactokinase) and GalD (galactose-1-phosphate uridylyltransferase) names are consistent with prior studies. The galDΔ and galD5 strains did not grow on minimal medium galactose (MM-Gal) at pH4.5, but did on MM glucose; both grew on MM-Gal at pH7.5. The galEΔ and galE9 strains grew on MM-Gal at both pH levels. Complemented galDΔ:ScGAL7 and galEΔ:ScGAL1 strains demonstrated functional homology. Both galD5 and galE9 alleles were truncated. Both galDΔ and galEΔ produced wild type conidiophores on MM-Glu, but few spores; sporulation was lower on MM-Gal pH7.5. GalD-GFP and GalE-GFP were cytosolic, and more intense on MM-Gal than MM-Glu, consistent with qRT-PCR. Galactofuranose immunolocalization in galDΔ walls was wildtype on MM-Glu, low on MM-Gal pH7.5, and absent on MM-Gal pH4.5. The galDΔ and galEΔ strains were more sensitive to Caspofungin and to Itraconazole on MM-Gal pH7.5. GalD and GalE are functionally homologous to *S. cerevisiae* GAL7 and GAL1, respectively, supporting their being other routes for galactose metabolism in *Aspergillus. A. nidulans* galactose metabolism is more complex than S. cerevisiae

Key words: *Aspergillus nidulans*, galactose, galactose-1-phosphate uridylyltransferase, galactokinase, GAL7, GAL1.

Abbreviations: MM-Glu, Minimal medium containing 1 % glucose; MM-Gal, minimal medium containing 1 % galactose; GalD, galactose-1-phosphate uridylyltransferase; GalE, galactokinase;

2. 1. Introduction

Galactose metabolism is conserved from bacteria through humans (Christacos et al. 2000; Ross et al. 2004). Galactose itself cannot be used directly for glycolysis. Before it can enter the Embden-Meyerhof glycolytic pathway, galactose must be converted *via* galactose-1-phosphate into glucose-1-phosphate (Sellick et al. 2008**)**. The enzymes of the Leloir pathway are responsible for this conversion. The Leloir pathway enzymes for galactose metabolism are galactokinase, galactose-1-phosphate uridylyltransferase, and UDP-glucose/galactose-4-epimerase (Holden et al. 2003). These enzymes are named differently in different systems. To avoid confusion, names for orthologous genes in *Aspergillus*, *Saccharomyces*, *Escherichia* and Human are included in Figure 2.1. The Leloir pathway is also summarized in Figure 2.1.

In humans, mutations in any Leloir enzyme can produce clinical deficiencies in galactose metabolism known as galactosemias (Holden *et al.* 2003; Timson et al. 2005). Mutations in human galactokinase and galactose-1-phosphate uridylyltransferase produce galactosemia types I & II respectively (Holden et al. 2003; Timson et al. 2005). Symptoms begin within a few days of birth, and progress to poor growth and mental retardation, cataracts, and potentially fatal accumulations of galactose in tissues. Treatment requires a diet free of lactose and high-galactose foods such as celery and stone fruits. More than 130 different mutations in human galactose-1-phosphate uridylyltransferase have been mapped to the *E. coli* GALT crystal structure (Wedekind et al. 2004) and correlated with their clinical outcomes (Elsas and Lai, 1998).

Saccharomyces cerevisiae galactose-1-phosphate uridylyltransferase (GAL7) and galactokinase (GAL1) were characterized by Slepak et al. (2005), who described them as having pivotal roles in *S. cerevisiae* growth and metabolism. An *S. cerevisiae* strain deleted for *GAL7* (*gal7*Δ) ceased growth after 0.2 % galactose was added to the yeast extract-glycerol broth in which it had been growing exponentially. The full effect of growth inhibition by galactose in *gal7*Δ cells required ~4 h, during which they accumulated galactose-1-phosphate (Slepak et al. 2005). Using RT-PCR and gene expression profiling, they also showed that during 'galactose intoxication' RNA and ribosome biogenesis were down-regulated and inositol biosynthesis was up-regulated, suggesting that galactose-1-phosphate accumulation had multiple adverse effects. Slepak et al. (2005) also showed that unlike *gal7*Δ*,* in *gal1*Δ the

addition of 0.2 % galactose did not prevent growth. Both the presence of galactose and the absence of glucose are required for induction of galactose metabolism enzymes (Timson, 2007).

The biological function of galactokinase (GalE) and galactose-1-phosphate uridylyltransferase (GalD) have not been fully characterized in *Aspergillus.* Roberts (1963, 1970) described some roles of mutant alleles of these enzymes in galactose metabolism, and Fekete et al. (2004) explored the enzymatic role of galactokinase in *Aspergillus nidulans*.

The *Aspergillus nidulans* Leloir pathway enzymes UDP-glucose/galactose-4-epimerase (ugeA) (El-Ganiny et al. 2010) and UDP-galactopyranose mutase (ugmA) (El-Ganiny et al. 2008) are required for wild type hyphal morphogenesis and spore development, and have similar deletion phenotypes. Consistent with their role in generating galactofuranose (Gal*f*) residues for the cell wall, strains without UgeA or UgmA both lack wall Gal*f* and have similar defects in hyphal wall architecture (Paul et al. 2011). Deletion of the UDP- Gal*f* transporter, UgtA that acted downstream of UgmA has a similar effect (Afroz et al. 2011). Here, we characterize deletion strains for *A. nidulans* galactokinase and glucose-1-phosphate uridylyltransferase, which function immediately upstream of UgeA, and compare them to partially described mutant alleles of these enzymes from earlier studies (Roberts, 1970).

2. 2. Methods

2. 2.1. Cultures and growth conditions

Strains, plasmids and primers used in this study are listed in Table S1. *Aspergillus nidulans* strains were grown as described in El-Ganiny et al. (2008) using media described in Kaminskyj (2001), and supplemented for nutritional markers as required. Minimal medium contained 1 % glucose or 1 % galactose (MM-Glu or MM-Gal, respectively), plus nitrate salts and trace elements. MM-Gal containing 70 mM $NaNO_3$ was called MMN. MM-Gal containing 70 mM ammonium tartrate as the N-source was called MMA. Complete medium (CM) was MM amended with 0.4 % peptides (0.2 % peptone, 0.1 % casamino acids, 0.1 % yeast extract) and vitamin solution. The morphometric analysis, expression, and drug studies used MM-Gal containing nitrate at pH 7.5.

2. 2.2. Strain construction and validation

Protoplasting followed procedures in Osmani et al. (2006). Protoplast storage is described in El-Ganiny *et al.* (2010). Gene knockout, complementation, GFP-tagging, and cDNA construction is described in El-Ganiny et al. (2008, 2010), and Afroz et al. (2011). Confirmation of gene manipulation used genomic DNA from putative transformant strains as a template for PCR with combinations of primers as shown Suppl Table S1 and Figs. S1-S6. Spore genomic DNA was extracted using the microwave procedure described in Alam et al. (*in press*). cDNAs were cloned into pCR4-TOPO, and sequenced using a Genetic Analyzer (Applied Biosystems).

2. 2.3. Complementation of *galDΔ* with *S. cerevisiae GAL7* and *galEΔ* with *S. cerevisiae GAL1*

GAL7 and GAL1 were amplified from *S. cerevisiae* genomic DNA. A construct consisting of GAL7, the selectable marker Af*pyroA*, and 1 kb flanking regions of the galD coding sequence, was created using fusion PCR and introduced into the galDΔ strain. ScGAL1 was introduced in the *galEΔ* strain as described for GAL7. Strains were validated using PCR (described above) and morphometry on MM-Gal (described below).

2. 2.4. Strain morphometry

Colony and hyphal characteristics of the *galD*Δ, *galD5*, *galE*Δ, and *galE9* strains were quantified using procedures described in El-Ganiny *et al*. (2008). Colony growth was compared for strains inoculated as 5 µL drops containing 5000 spores, and incubated for 2 d at 28 ºC. For fluorescence microscopy, freshly harvested conidia were grown on coverslips for 16 h at 28 ºC in liquid MM-Glu or MM-Gal (with nitrate, pH 7.5), fixed in formalin, stained with 0.4 µg/mL Hoechst 33258 (for nuclei) and 0.2 µg/mL Calcofluor (for cell walls). Samples were imaged by confocal fluorescence microscopy using a Zeiss META510 and a 63×, N.A. 1.2 multi-immersion objective, and 405 nm excitation.

Hyphal width (at septa) and basal cell length (distance between adjacent septa) were measured for 30 cells per strain, and nuclei were counted in those cells. Morphometry data

(Table 2.1) are mean ± standard error of the mean. The number of branches in the apical 100 μm was counted for hyphae grown on MM-Glu and MM-Gal.

Spores harvested from colonies that appeared to have developed from single spores after 3 d at 28 °C were used to estimate number produced per colony, as previously described by El-Ganiny *et al.* (2008). Sporulation rate for strain and media combinations are expressed with respect to wild type on MM-Glu (100 %), which was 5 x 10^8 spores per colony. Spore germination counted germlings produced by defined numbers of conidia inoculated on three replicate plates after 24 h at 28 ºC; for *galD*Δ on galactose, germination was assessed after 48 h at 28 ºC.

Cell wall thickness was measured on TEM cross-sections of hyphae where the cell membrane was crisply in focus (10 hyphae, 2 or 3 measurements each) as described in Afroz *et al.* 2011. ANOVA tests were used to assess the statistical significance of differences using GraphPad (Prism Software).

2. 2.5. Scanning and transmission electron microscopy

SEM followed procedures in El-Ganiny *et al.* (2010) for colonies grown for 3 d at 28 ºC on dialysis tubing laid on selective media. TEM examined hyphae grown for 16 h on dialysis tubing (Afroz *et al.* 2011) laid on MM agar.

2. 2.6. Galf immunolocalization, GalD and GalE localization

Hyphal wall Gal*f* content was assessed using immunolocalization following procedures in El-Ganiny et al. (2008) and examined using confocal fluorescence microscopy. Monoclonal anti-Gal*f* antibody L10 was a gift of Prof. Frank Ebel (Univ Munich). Primary antisera were used at full strength; TRITC-conjugated goat-antimouse was used at 1:10 dilution. GalD-GFP and GalE-GFP localization, under the control of their wild type promoters, was examined in growing hyphae using confocal fluorescence microscopy. Controls included samples with no primary antibody, or no secondary antibody. These produced no fluorescent signal. Within each fluorescence-based study, imaging parameters were kept constant to permit comparison.

2. 2.7. Quantitative real time PCR (qRT-PCR)

Total RNA was extracted from wild type strain AAE1 that had been grown for 16 h at 37 ºC on MM-Glu or MM-Glycerol, or MM-Gal (nitrate, pH 7.5), using an RNeasy plus mini-kit (Qiagen). One microgram of total RNA was used for cDNA synthesis using a Quantitect Reverse Transcription Kit (Qiagen). To quantify *galD* and *galE* expression, we used 2-step qRT-PCR (QuantiTect® SYBR Green PCR kit; Qiagen) and an iQ5 real-time PCR detection system (Bio-Rad). Conditions: one cycle at 95 ºC for 10 min, 40 cycles of 95 ºC for 30 s, 60 ºC for 1 min and 72 ºC for 1 min. Data were analyzed using the thermocycler-associated software. The *galD* and *galE* expression was normalized using *actA* (Upadhyay & Shaw, 2008). Following amplification, melting curves for the products were generated to ensure that each represented homogenous species.

2. 2.8. Antifungal susceptibility testing

Drug sensitivity of *galD*Δ, *galE*Δ and wild type strains was compared using a disc diffusion assay (Afroz *et al.* 2011). Strains were grown for two rounds on the test media before being used for drug sensitivity studies, to compensate for potential spore dowry effects. For this test, 1 x 10^7 spores were mixed into 20 mL of 50 ºC MM agar and immediately poured in 9 cm Petri plates. After the medium had solidified, sterile 6 mm paper discs were placed on the agar surface. Anti-fungal drug stock solutions were micro-pipetted onto individual disks: 20 mg/mL Caspofungin® in water, 20 mg/mL Itraconazole® in water, or 10 mg/mL Calcofluor White in 25 mM KOH (Hill *et al.* 2006). Solvent control studies with DMSO and 50 % ethanol showed no zone of inhibition. The plates were incubated at 30 ºC and assessed after 48 h (Kiraz et al. 2009).

The radius of the zone of inhibition was calculated as
[diameter with no visible growth (mm) – disk diameter] / 2.

For each biological replicate, two measurements at orthogonal axes were taken for each disk on each plate. Four plates (biological replicates) were assessed for each strain and medium combination, and each experiment was repeated. These data were used for statistical analysis (ANOVA). Data are presented as indexed values for *galD*Δ and *galE*Δ on MM–Glu or MM-Gal with respect to wild type on MM–Glu or MM-Gal. Mean ± SE of two

measurements for each of three biological replicates were used for statistical analysis (not shown).

2. 3. Results

2. 3.1. Identification and characterization of Aspergillus nidulans GalD and GalE

Saccharomyces cerevisiae GAL7 and *GAL1* encode galactose-1-phosphate uridylyltransferase and galactokinase, respectively (Broach, 1979). BLAST analysis of the primary amino acid sequences of *S. cerevisiae* GAL7 and GAL1 using http://www.broadinstitute.org/annotation/genome/aspergillus_group/Blast.html showed that *A. nidulans* ANID_06182.1 had 50 % sequence identity with GAL7 and *A. nidulans* ANID_04957.1 had 41 % sequence identity with GAL1. These had been annotated as a galactose-1-phosphate uridylyltransferase and a galactokinase, respectively. We named ANID_06182 as GalD and ANID_04957 as GalE, to be consistent with Roberts (1963, 1970). Reactions mediated by *A. nidulans* GalD and GalE (this paper), UgeA (El-Ganiny et al. 2010), and UgmA (El-Ganiny et al. 2008) are shown in Fig. 2.1 *Aspergillus nidulans* GalD had 80-85 % amino acid sequence identity with *A. clavatus, A. flavus, A. fumigatus, A. niger, A. oryzae* and *A. terreus* orthologues, 43 % with *Homo sapiens* GALT, and 46 % with *Escherichia coli* GALT. *Aspergillus nidulans* GalE had 80-85 % amino acid sequence identity with *A. clavatus, A. flavus, A. fumigatus, A. oryzae* and *A. terreus* orthologues, and 38 % with *Homo sapiens* GALK.

We replaced the ANID_06182 coding sequence in the *nkuA*Δ strain A1149 with *A. fumigatus pyroA,* creating strain *galD*Δ. We replaced ANID_04957, also in A1149, with *A. fumigatus pyrG* creating strain *galE*Δ. Conidia produced by each type of primary transformant were able to form colonies on MM-Glu that lacked pyridoxine or pyrimidine, respectively (Osmani et al. 2006). Thus, neither GalD nor GalE was essential for growth on glucose.

2. 3.2. *Aspergillus nidulans* galDΔ, galD5, galEΔ and galE9 phenotypes

Hyphal morphometry, sporulation, and germination data for wild type and deletion strains grown on glucose and galactose are provided in 2. 1. The *galD*Δ and galD5 strains strain did not form colonies on MMN-Gal or MMA-Gal at pH4.5, but did at pH7.5 (Fig. 2.2). Roberts (1970) suggested that Leloir pathway enzymes have optimal function at pH 4-6.5, and

that alternative pathways are available at higher pH, that is, >7. We compared the growth of all the deleted and mutant strains at pH 4.5 and pH 7.5 to determine whether our *galD* and *galE* deletion strains would phenocopy the *galD* and *galE* mutants that were described in Roberts (1970). Phenotypes of *galD5* strains, A212 and A213 were similar to *galD*Δ (Fig. 2.2).

Unlike the *S. cerevisiae GAL7*Δ strain, galactose was not toxic for *A. nidulans galD*Δ. The *galE*Δ strain grew and sporulated on both MMN-Gal and MMA-Gal at both pH4.5 and pH7.5. The colony size of *galE9* strain was similar to *galE*Δ on MM-Gal (nitrate) at pH7.5 and pH4.5. We compared the ability of wild type, *galD*Δ, and *galE*Δ strains to grow on a variety of substrates (Fig. 2.3). The wild type, *galD*Δ and *galE*Δ strains all grew on MM containing glucose, galactose, or glycerol as sole carbon sources (Fig. 2.3A), but their colony phenotypes differed. On glucose and glycerol, *galD*Δ and *galE*Δ strains gave wild type colonies (Fig. 2.3A). We have also grown deleted strains on MM containing both glucose and galactose (data not shown). On MM-Glu+Gal, both deleted strains grew like wild type, which means glucose is able to repress the galactose-associated phenotype.

Sporulation of the *galD*Δ and *galE*Δ strains were reduced about 10-fold on MM-Glu and 100-fold on MM-Gal compared to the wild type strain (Table 2.1, Fig. 2.2). The hyphae of *galD*Δ and *galE*Δ strains grown on MM-Gal were slightly wider than on MM-Glu, and their near-apical regions were highly branched (Table 2.1; Fig. 2.3B). The *galD*Δ strain was unable to form colonies on galactose at pH 4.5 which indicates that GalD is extremely important for *A. nidulans* growth at that pH. In contrast, the *galE*Δ strain formed sparse colonies on MMN-Gal and MMA-Gal at both pH 4.5 and pH 7.5, as did the *galE9* strain, A214 (Fig 2.2) which indicates that GalE plays a less important role than GalD in *A. nidulans* galactose metabolism.

We generated a [*ugeA*Δ*, galD*Δ] double deletion strain since these enzymes were expected to share substrate pools. [*galD*Δ*, ugeA*Δ] strain grown on MM-Glu had compact colonies that resembled those of *ugeA*Δ strain grown on MM-Glu (El-Ganiny *et al.* 2010). However, on MM-Gal, the [*galD*Δ*, ugeA*Δ] strain failed to grow (Fig. 2.3A). Previously, El-Ganiny *et al.* (2010) showed that *ugeA*Δ germination and growth was negligible on

galactose. Therefore, we did not find any significant difference between *ugeAΔ* single mutant and [*galD*Δ*, ugeA*Δ] double mutant.

SEM of wild type (Figs. 2.4A, B), *galD*Δ (Figs. 2.4C-F), and *galE*Δ (Figs. 2.4G, H) strains showed that all of them sporulated better on MM-Glu (Figs. 2.4A, C, E, G) than MM-Gal (Figs. B, D, F, H) consistent with results in Table 2.1. For *galD*Δ on glucose there were both small wild type conidiophores (Fig. 2.4C) as well as structures that appeared to be swollen conidiophore vesicles that failed to produce metulae (arrows in Fig. 2.4E). The inset in Fig. 2.4E (Fig 2.4e) shows these naked conidiophore vesicles at higher magnification. On galactose, the *galD*Δ strain produced some metulae and phialides, but these were misshapen and produced few spores (Fig. 2.4 D). The *galE*Δ strain grown on glucose produced small conidiophores with metulae and some phialides (Fig. 2.4G), whereas on galactose the *galE*Δ strain typically arrested with metulae (Fig. 2.4 H). The *galD*Δ arrest stage corresponds to stage D and the *galE*Δ arrest to stage E according to Martinelli and Clutterbuck (1971).

Germination of wild type spores was similar on glucose and galactose, as expected, but this was not the case for *galD*Δ and *galE*Δ strains. Germination of *galD*Δ and *galE*Δ spores was somewhat lower than wild type on glucose, but on galactose it was reduced (15 %; *galE*Δ) or highly reduced (1 %; *galD*Δ) (Table 2.1).

El-Ganiny *et al*. (2010) showed that hyphal walls of the *ugeA*Δ strain grown on glucose were twice as thick as wild type and had a poorly consolidated outer layer. Using TEM we found that *galD*Δ hyphal walls had a poorly consolidated outer layer reminiscent of *ugeA*Δ, and had a wall thickness similar to *ugeA*Δ (Table 2.1; Fig. S9; El-Ganiny et al. 2010). The *galE*Δ hyphal walls also resembled those of *galD*Δ on both galactose and glucose (Table 2.1, Fig. S9).

Together, these analyses showed that both *galD*Δ and *galE*Δ strains had defects at multiple stages. The most severe were for *galD*Δ on galactose at pH 4.5, but defects were also notable on galactose at pH 7.5. In contrast, we did not any find severe growth defects for *galE*Δ strain on galactose at either pH 4.5 or pH 7.5.

2. 3.3. *Aspergillus nidulans* galD *and* galE *complementation with* Saccharomyces cerevisiae GAL7 *and* GAL1

We generated *galD*Δ:*GAL7* and *galE*Δ:*GAL1* strains to test for functional complementation of the *A. nidulans* and *S. cerevisiae* uridylyl transferase and galactokinase orthologues respectively. The wild type, *galD*Δ:*GAL7* and *galE*Δ:*GAL1* strains all produced wild type colonies on galactose, glucose, and glycerol (Fig. 2.3A), and as well the complemented strains had a wild type hyphal phenotype (Fig. 2.3C). Thus, *S. cerevisiae GAL7* and *GAL1* were able to restore the loss of *A. nidulans galD* and *galE* at the colony and cellular level, respectively, showing that they are functionally homologous. We refer to them as $GalD^{GAL7}$ and $GalE^{GAL1}$.

2. 3.4. Comparison of wild type, galD, *and* galE cDNA with galD5 and galE9

The ANID_04957 (*galE*) coding sequence was predicted to contain three introns and ANID_06182 (*galD*) to contain two introns. We confirmed the length and position of these introns by comparison with the genomic sequence on the Broad Institute. The *galD5* mutation had a single nucleotide change at base 628 in A212 and A213 (both G → T) that inserted a stop codon at amino acid 210 of this 384-residue protein (Fig. S10). The *galE9* mutation had conservative mutation, D69E, and near the 3' end had a single base pair insertion at position 1477. This frame shift altered the residues beginning at 480 from …LTEEYYL… to …RRRSAIstop at residue 493 of this 524-residue protein (Fig. S11).

2. 3.5. Localization of GalD and GalE *in Aspergillus nidulans*

GalD and GalE were each C-terminal tagged with green fluorescent protein (GFP) under the control of their endogenous promoters. Both strains were morphologically wild type, suggesting that these constructs were fully functional. Both GalD-GFP and GalE-GFP confocal fluorescence patterns were cytosolic and did not show obvious longitudinal gradients (Fig. 2.5 A-D). Both the GalD-GFP and GalE-GFP fluorescence intensities were noticeably higher in germlings following overnight growth on MM-Gal (Fig. 2.5B, D) compared to MM-Glu (Fig. 2.5A, C). We quantified the relative fluorescence intensity using Zeiss LSM 510 region of interest (ROI) software. Increased fluorescence intensity in cells grown on MM-Gal (Fig. 2.5E) suggested there should be a comparable increase in *galD* and *galE* expression assessed by qRT-PCR when grown on MM-Gal.

Wild type colonies were grown for 16 h in liquid MM-Glu, MM-Glycerol and MM-Gal. RNA was extracted from them so that the relative *galD* and *galE* expression could be quantified using qRT-PCR in comparison to actin (*actA*). Compared to *actA*, expression of *galD* on MM-Gal was 10.6-fold more than on MM-Glu (Fig. 2.5F); expression of *galE* on MM-Gal was 6.5-fold more than on MM-Glu (Fig. 2.5F). We did not find any significant change in *galD* and *galE* expression on MM-glycerol compared to MM-Glu. This suggests that the expression of GalD-GFP and GalE-GFP is 6 to 10 times lower when glucose or glycerol is the carbon than when galactose is the carbon source

2. 3.6. Galactofuranose immunolocalization

Gal*f* was immunolocalized in hyphal walls of wild type, *galD*Δ and *galE*Δ hyphae grown on MM-Glu and MM-Gal at pH 7.5 and at pH 4.5. Gal*f* levels were similar in wild type hyphae grown on MM-Glu, MM-Gal pH 4.5 and MM-Gal pH 7.5 (Fig. 2.6A- C). The *galD*Δ hyphal walls on MM-Glu (Fig. 2.6D) had a more intense Gal*f* signal than on MM-Gal at pH 7.5 (Fig. 2.6E). A clump of spores without visible signal was observed in the *galD*Δ strain germlings on MM-Gal at pH 4.5 (Fig. 2.6F). Gal*f* immunolocalization in *galE*Δ hyphal walls was similar to wildtype on MM-Glu and MM-Gal at pH 4.5 and pH 7.5. Thus, GalD appears to contribute to Gal*f* biosynthesis, but onlywhen galactose is sole carbon source. In contrast, *galE*Δ does not appear to contribute to Gal*f* biosynthesis at either pH.

2. 3.7 Sensitivity to antifungal compounds

The sensitivity of wild type, *galD*Δ and *galE*Δ strains to antifungal compounds used a disc-diffusion assay. The radius of the zone of inhibition provided quantitative visual information. We compared Calcofluor White that binds to fungal walls, Caspofungin that inhibits beta-glucan synthase, and Itraconazole that inhibits ergosterol synthesis. Sensitivity is presented as an index compared to wild type on the same medium, so that values greater than 1.0 indicate drug hypersensitivity. Statistical analysis of the raw data and comparison to sensitivity indices showed that a difference of >0.2 in index value correlated with statistical significance. Representative plates from this study are shown in Fig. 2.7, with quantitative results presented in Table 2.1B.

The wild type strain had similar sensitivity to Caspofungin and Itraconazole on MM-Glu and MM-Gal (Fig. 2.7), but was more sensitive to Calcofluor White on MM-Gal. The *galD*Δ and *galE*Δ strains were significantly more sensitive to all three drugs when grown on MM-Gal than MM-Glu (Table 2.1B).

2. 4. Discussion

Aspergillus nidulans GalD (galactose-6-phosphate uridylyltransferase) and GalE (galactokinase) are functionally homologous to *S. cerevisiae* GAL7 and GAL1, respectively. The *galD*Δ:*GAL7* and *galE*Δ:*GAL1* complemented strains had wild type colony and hyphal phenotype when grown on MM-Gal.

GAL7 is essential for *S. cerevisiae* growth on galactose (Slepak et al. 2005) and for galactose metabolism in *Kluyveromyces lactis* (Dickson & Riley, 1989). However, $GalD^{GAL7}$ is only essential for *A. nidulans* when grown on MM-Gal at pH 4.5. At pH 4.5 the *galD*Δ strain grown on galactose was severely impaired at all stages from germination to colony development. In contrast, there was limited growth and sporulation at pH 7.5.

GAL1 is essential for galactose metabolism in yeast (Dickson & Riley, 1989). Unlike GAL1, $GalE^{GAL1}$ was not essential for *A. nidulans* growth on MM-Gal. For *A. nidulans galD*Δ and *galE*Δ strains, galactose adversely affected germination, conidiophore initiation, and metulae, phialide, and spore formation. Taken together, the *A. nidulans* Leloir enzymes $GalD^{GAL7}$ and $GalE^{GAL1}$ play multiple but not essential roles in *A. nidulans* growth and development. The *galD*Δ and *galE*Δ strains provide insights into their function that would not be possible in a species where they were essential. Identifying products that interact with GalD and GalE will help clarify their roles in galactose fungal metabolism.

Aspergillus nidulans galD5 and *galE9* mutant strains were unable to grow on MM galactose containing nitrate below pH 6, but could grow on complete medium (CM) with galactose (Roberts, 1970); CM has peptides as well as nitrate. Fekete et al. (2004) reported that an *A. nidulans galE*Δ strain they called EFES2 could grow on galactose in the presence of ammonium tartrate. We confirmed these observations and showed that GalD was all-but-essential for germination and growth on MM-Gal at pH 4.5, but not at pH 7.5, whereas GalE was important but not essential under any condition in this study. Ammonium tartrate (we used 70 mM) is also a carbon source, but likely an insignificant level. galD5 and galE9

encode C-terminal truncations of the transferase and kinase, respectively and in addition the C-terminus of the *galE9* product had altered polarity and charge. Our data are consistent with previous results, and point to the C-termini of GalD^{GAL7} and GalE^{GAL1} being important for function. Roberts (1963) also reported that galactose auxotrophs were more common than those of fructose, maltose, or sorbitol, which suggests that galactose-derived compounds such as Gal*f* are relatively more important. Gal*f* is a cell wall component that is important for growth and wall maturation in *A. nidulans* (El-Ganiny et al. 2010, Afroz et al. 2011).

The Leloir pathway appears to be the main D-galactose degrading route in *Aspergillus*, but alternative or additional galactose metabolism pathways have been reported. *Aspergillus nidulans* galactose metabolism pathways via galactitol, sorbitol and fructose (Elorza & Arst, 1971) and fructose-6-phosphate and sorbose-6-phosphate (Fekete *et al.* 2004) have been proposed. Flipphi *et al.* (2009) hypothesized that galactitol can also be epimerized to D-tagatose via L-sorbose, with subsequent cleavage into two glycolytic triose-phosphates. None of these pathways describe the fate of D-sorbose, but perhaps L-sorbose is catabolized via D-sorbitol and D-fructose to D-fructose-6-phosphate (Flipphi et al. 2009). In *Saccharomyces*, d-fructose-6-phosphate can be converted to N-acetyl glucosamine, which is a substrate for chitin synthesis (Milewski et al. 2006). This alternative pathway is led by formation of galactitol by aldose reductase. Aldose reductase requires NADPH. Therefore, it is possible that aldose reductase is inactive when nitrite is the sole N source because both nitrate and nitrite reductases require NADPH and have high affinity (Bhushan et al. 2002).

GalD-GFP and GalE-GFP are cytosolic, did not show obvious longitudinal gradients. GalD-GFP and GalE-GFP fluorescence was significantly higher for cells germinated on MM-Gal than MM-Glu consistent with qRT-PCR showing ten-fold higher *galD* and six-fold higher *galE* expression on MM-Gal than MM-Glu. GalD-GFP and GalE-GFP fluorescence levels are similarly consistent with results from *S. cerevisiae* where the Leloir pathway genes showed higher levels of expression induced by galactose (Lohr et al. 1995). Higher *galD* and *galE* expression on galactose correlated with lower germination, growth, and sporulation, consistent with but less severe than the galactose effect on *S. cerevisiae*.

GalE-GFP fluorescence distribution was even, whereas in *S. cerevisiae* GAL7-GFP localization is clumped (Christacos et al. 2000). The *S. cerevisiae* Leloir pathway enzymes

have been proposed to form multi-enzyme complexes (Abadjieva et al. 2001; Kindzelskii et al. 2004). Unlike in *Saccharomyces*, pronounced galactose toxicity has not been reported in *Aspergillus* and their Leloir pathways genes are not clustered. Slot and Rokas (2010) suggest that gene clustering may correlate with Leloir pathway defects that produce toxic intermediates.

Gal*f* was immunodetectable when the wild type and *galE*Δ strains were grown on MM-Glu or MM-Gal. Gal*f* was also detectable when the *galD*Δ strain was grown on MM-Glu. The Gal*f* content of *galD*Δ grown on MM-Gal pH 7.5 was low, and Gal*f* was undetectable on MM-Gal at pH 4.5. Taken together, this suggests that GalD but not GalE has a direct role in Gal*f* biosynthesis. Deletion of UgeA and UgmA led to loss of hyphal wall Gal*f* (El-Ganiny et al. 2008 & 2010). The [*galD*Δ, *ugeA*Δ] strain was able to germinate on MM-Gal, and grew on MM-Glu and MM-glycerol, again suggesting that *A. nidulans* has additional metabolic pathways leading to energy generation and wall glycan biosynthesis. Growth on MM-Glu or MM-Gal resulted in hyphal walls of the galDΔ and galEΔ mutants 50% thicker than the cells walls of the wild type, comparable to *ugeA*Δ strains (El-Ganiny et al. 2010; Paul et al. 2011). Also like the *ugeA*Δ strain, the *galD*Δ hyphal walls accumulated extraneous material when grown in liquid culture, which has been seen previously (El-Ganiny et al. 2008; Lamarre et al. 2009; El-Ganiny et al. 2010; Afroz et al. 2011; Paul et al. 2011). Gal*f* residues are found in galactomannans, glycoproteins, lipophosphogalactomannans and sphingolipids (Lamarre et al. 2009), where they may have multiple roles in cell wall structure and cell wall surface adhesion. High spatial resolution chemical analysis of fungal cell walls (Gough & Kaminskyj, 2010; Prusinkiewicz et al. 2012) and atomic force microscopy (Paul et al. 2011) may be able to detect differences in composition consistent with these changes.

The *galD*Δ and *galE*Δ strains were more sensitive than wild type to Calcofluor White when grown on galactose than glucose, suggesting their walls were somehow different (maybe weaker) than those of wild type. The *galD*Δ and *galE*Δ strains were also more sensitive to Caspofungin and to Itraconazole when grown on galactose, both of which act in the cytoplasm and must transit the cell wall. We had comparable results on CM (*not shown*), showing that GalD-related drug sensitivity was also repeatable in complex medium. It may be possible to find compounds that would inhibit GalD function without affecting human GALT.

However, these would not be useful by themselves given the diversity of nutrients available in a host organism.

In conclusion, we have shown that *A. nidulans* GalD^{GAL7} and GalE^{GAL1} play several roles in *A. nidulans* growth and sporulation. GalD^{GAL7} is essential for growth on galactose medium at pH 4.5, whereas GalE^{GAL1} appears to be dispensable. The *galD*Δ and *galE*Δ sporulation phenotypes arrest at different stages, so likely their products have additional metabolic functions. GalD and GalE expression are upregulated by growth on galactose, but germination and sporulation of *galD*Δ and *galE*Δ was suppressed on galactose. The *galD*Δ and *galE*Δ strains were significantly more sensitive than wild type to antifungal agents on galactose-containing media. Characterization of phenotypes related to the roles of GalD^{GAL7} and GalE^{GAL1} reveals the complexity of galactose metabolism in *A. nidulans*, and that functional homology does not ensure homologous function in different systems.

Acknowledgements

We are pleased to acknowledge support from the Natural Science and Engineering Council of Canada Discovery Grant program (SGWK), the NSERC Research Tools and Instruments program (SGWK), the Canadian Institutes of Health Research Regional Partnership Program (SGWK) and the Univ Saskatchewan (MKA). We thank the Bonham-Smith lab (Department of Biology, UofS) for use of their qRT-PCR, the Andrès lab (Dept. Biology, UofS) for DNA sequencing, Tom Bonli (Geological Sciences, UofS) for scanning electron microscopy, and Prof. Frank Ebel (Univ Munich) for the anti-Galf mAbs. Finally, we thank Amira El-Ganiny and several anonymous reviewers for comments.

Table 2.1. Characteristics of *Aspergillus nidulans* wild type, *galD*Δ and *galE*Δ strains on minimal medium supplemented with nitrate at pH 7.5, containing 1 % glucose or 1 % galactose.

A. Fungal morphometry [a]

Strain:	**Wild type**		***galD*Δ**		***galE*Δ**	
Growth medium:	**Glucose**	**Galactose**	**Glucose**	**Galactose**	**Glucose**	**Galactose**
Hyphal width (µm)	2.4 ± 0.0	2.2 ± 0.3	2.3 ± 0.1	2.6 ± 0.3	2.3 ± 0.0	2.5±0.0
Basal cell length (µm)	26 ± 1.0 [c]	24 ± 2.3 [c]	19 ± 1.8 [d]	15.5 ± 4.8 [e]	22±0.17 [c]	15±0.11 [e]
Nuclei per basal cell	4.2 ± 1.1 [c]	3.9 ± 0.7 [c]	3.3 ± 0.3 [cd]	2.5 ± 0.5 [d]	2.5±0.03 [d]	1.8±0.04 [e]
Branches/apical 100 µm	0.6 ± 0.1 [c]	0.6 ± 0.1 [c]	0.8 ± 0.1 [d]	5.6 ± 0.4 [e]	0.7 ± 0.1 [cd]	3.4 ± 0.4 [e]
Spores per colony	100 %	21 %	10 %	0.4 %	12 %	1.3 %
Germination rate	97 %	97 %	78 %	1 %	60 %	15 %
Cell wall thickness (nm)	56 ± 3 [c]	67 ± 2 [c]	102 ± 3 [d]	107 ± 1 [d]	100 ± 2 [d]	120 ± 2 [e]

B. Antifungal drug sensitivity index [b]

Strain:	**Wild type**		***galD*Δ**		***galE*Δ**	
Growth medium:	**Glucose**	**Galactose**	**Glucose**	**Galactose**	**Glucose**	**Galactose**
Calcofluor White	1.0	1.5	1.2	2.2	1.1	1.9
Caspofungin	1.0	1.0	1.1	1.5	1.0	1.4
Itraconazole	1.0	1.1	1.1	1.5	1.1	1.3

[a] Measurement details are described in Methods. Mean ± SE of two measurements for each of four biological replicates were used for statistical analysis (*not shown*). Values in individual rows that are followed by different letters (c-e) are significantly different at $P < 0.05$ (ANOVA).

[b] Drug sensitivity was measured using a disc diffusion assay (see Fig. 2.7). For Caspofungin, sensitivity was the radius (mm) of the clear zone with no visible growth. Mean ± SE of two measurements for each of three biological replicates were used for statistical analysis (data are presented in supplemental Table S3). Sensitivity index values are for each drug/strain combination compared to wild type on that medium. Values > 1.0 are more sensitive than wild type. Index values that differed by > 0.2 were based on data that were significantly different.

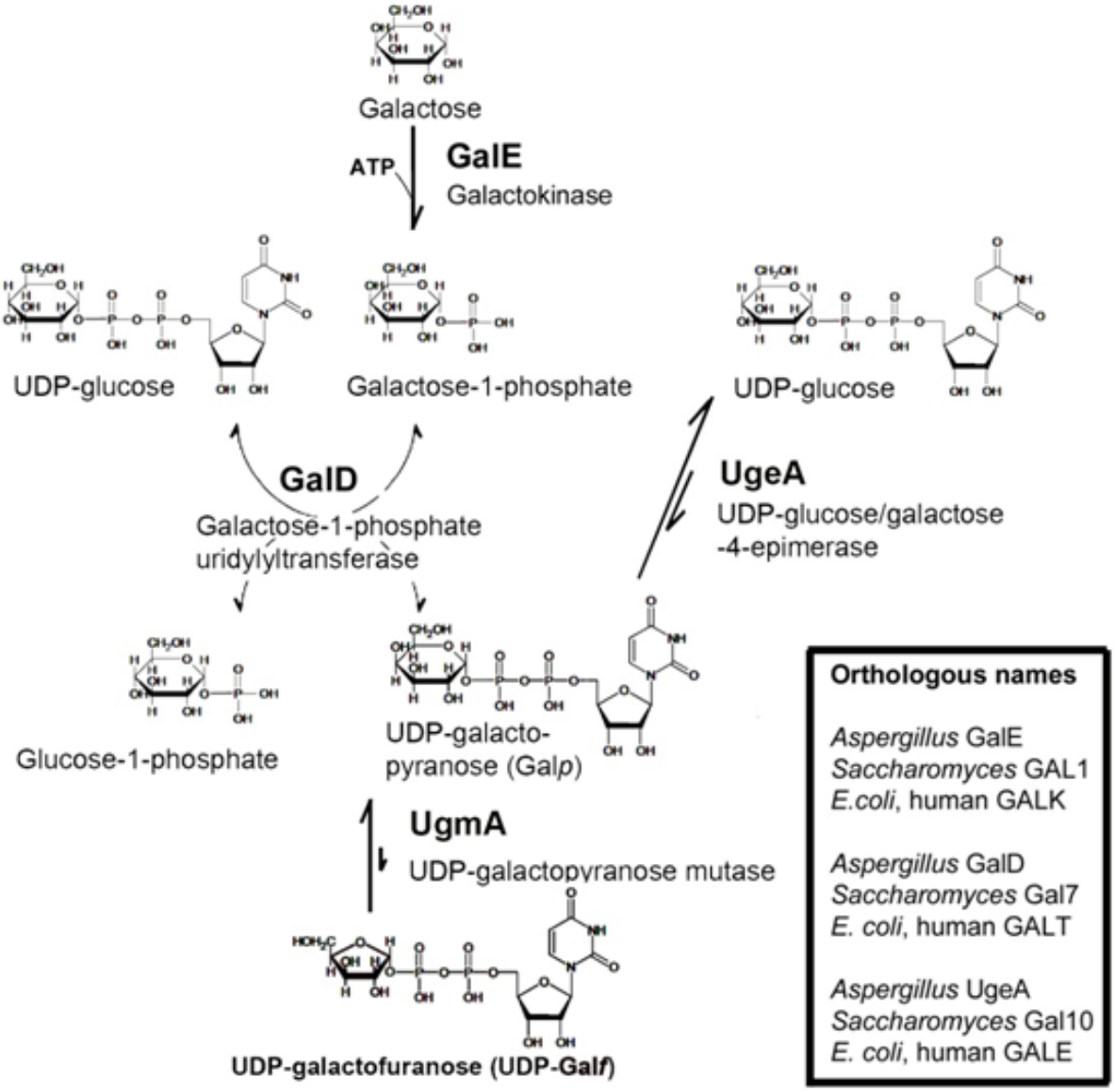

Fig. 2.1 *Aspergillus nidulans* galactose metabolic reactions discussed in this paper.

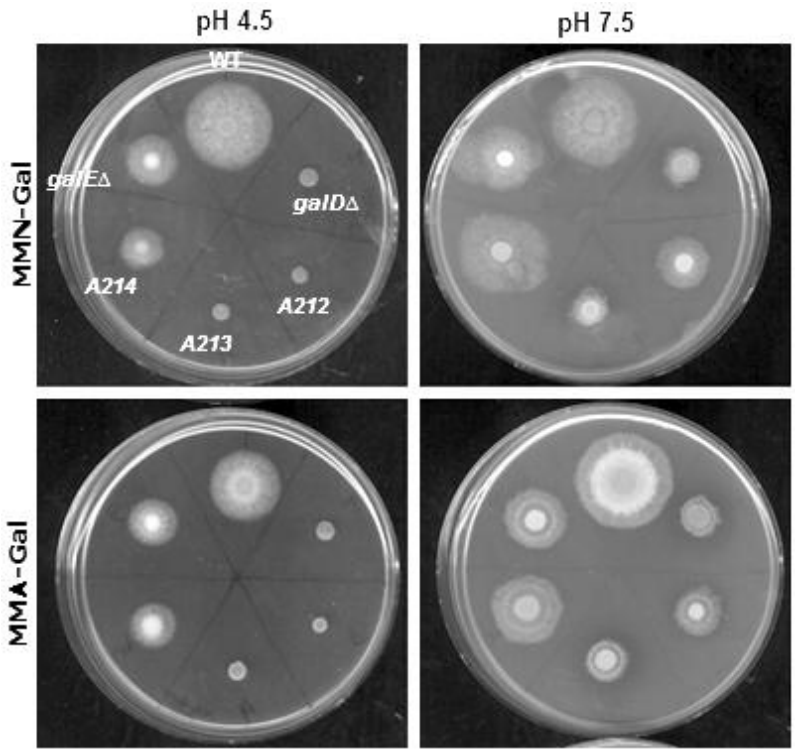

Fig.2.2. Colony phenotype of *Aspergillus nidulans* wild type (AAE1), galactose-1-phosphate uridylyltransferase strains *galD*Δ*, galD5* (A212, A213), and galactokinase strains *galE*Δ and *galE9* (A214) strains on minimal medium containing galactose with two different nitrogen sources and pH levels. Colonies were inoculated from 5 µL droplets containing 5000 conidia, and grown for 3 d at 30 °C. The *galD*Δ, A212, A213 strains did not grow beyond the original droplet size on MM-Gal containing nitrate (MMN-Gal) or ammonium (MMA-Gal) at pH 4.5, but all strains grew and sporulated on these media at pH 7.5.

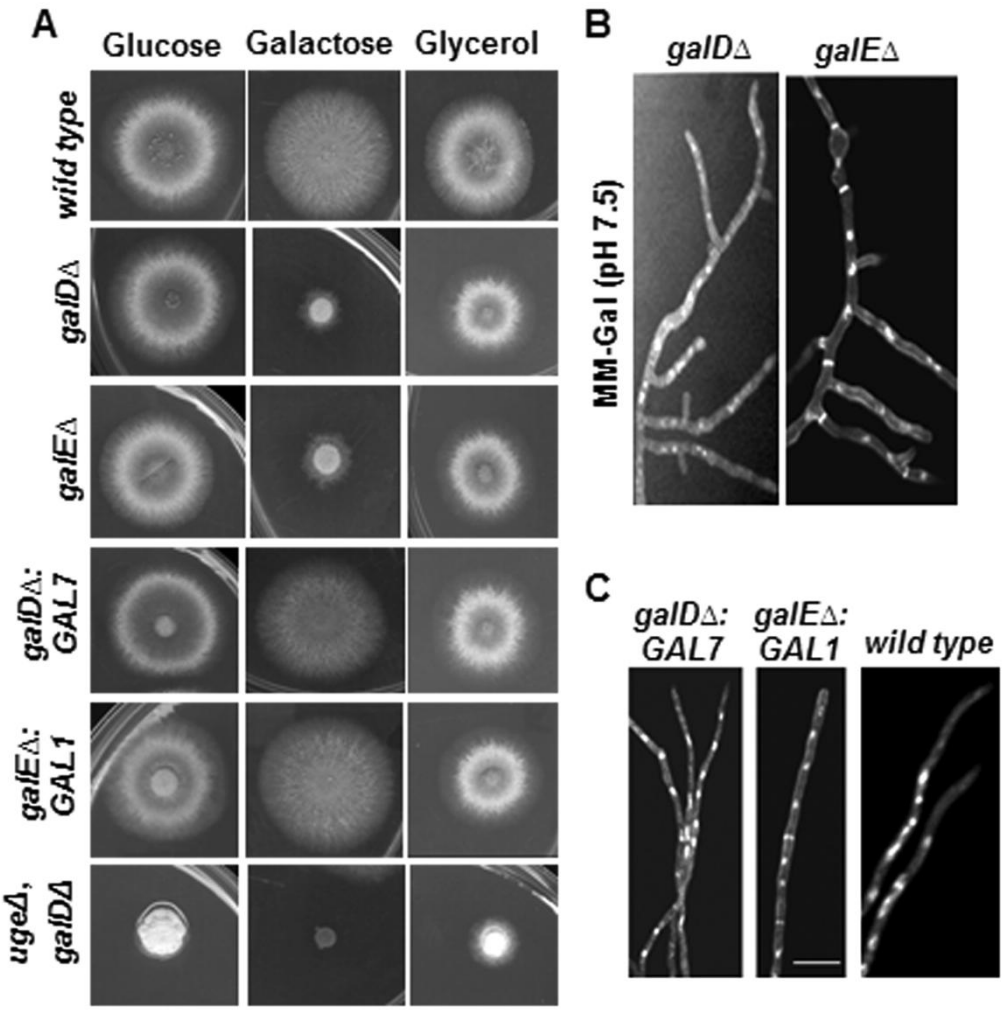

Fig. 2.**3**. *Aspergillus nidulans* colony (A) and hyphal (B&C) phenotypes related to galactose metabolism. A) *Aspergillus nidulans* strains grown on MM-Nitrate containing 1 % glucose, 1 % galactose, or 1 % glycerol at pH 7.5. Wild type (AAE1), deleted (*galD*Δ and *galE*Δ), complemented [*galD*Δ:*GAL7* and *galE*Δ*:GAL1*], and double deletion [*ugeA*Δ*, galD*Δ] strains. B) Hyphal branching phenotypes for deleted (*galD*Δ and *galE*Δ) strains on MM-Gal. C) Hyphal branching phenotypes for complemented [*galD*Δ:*GAL7* and *galE*Δ*:GAL1*] and wild type strains on MM-Gal Bar in the bottom right-hand image in (C) represents 10 µm for B and C.

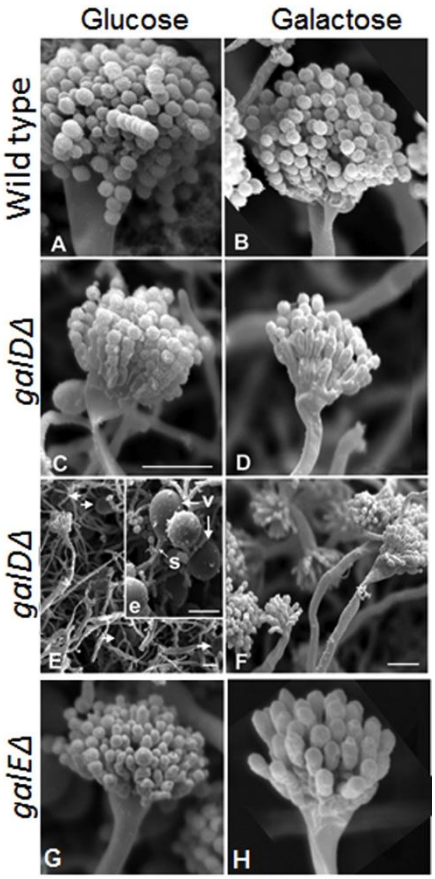

Fig. 2.**4.** Conidiophore development of *Aspergillus nidulans* wild type, *galD*Δ and *galE*Δ strains on medium containing peptides, nitrate and 1 % glucose or 1 % galactose (pH 7.5). Well-developed conidiophores of wild type, *galD*Δ and *galE*Δ grown on glucose (**A, C, G**) and galactose (**B, D, H**). Bar in C = 10 μm for images A-D, G & H. (**E**) On glucose, *galD*Δ colonies formed conidiophore vesicles (arrows in E) that frequently failed to form metulae and became overgrown by aerial hyphae. (**e**) Magnified inset shows abnormal conidiophores (arrows in E) with detail of naked conidiophore vesicles (v) and conidiphore stalks (s). On galactose, *galD*Δ (D) and *galE*Δ (H) produced metulae and phialides, but few spores (see Table 2.1). Bar in F = 100 μm for images E, e & F.

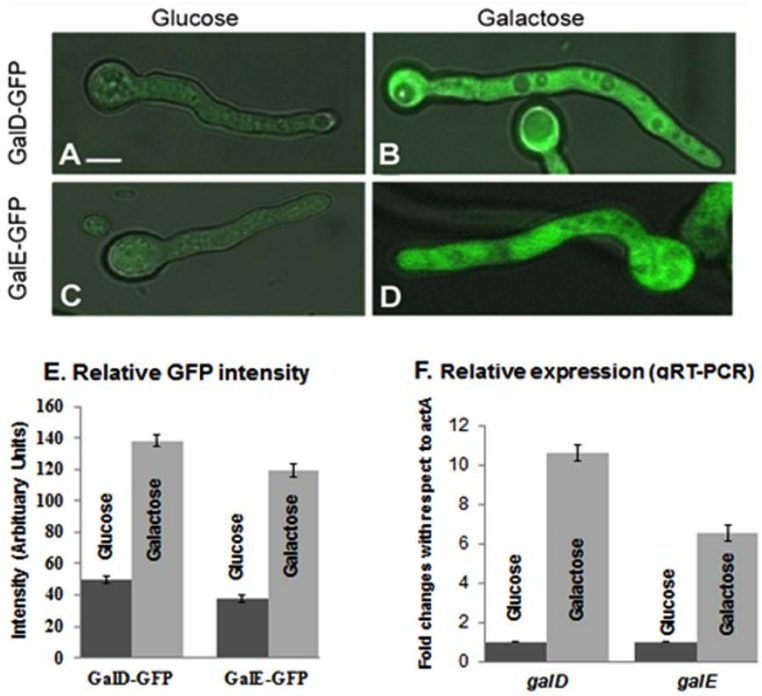

Fig. 2.**5.** *Aspergillus nidulans* galactose-1-phosphate uridylyl transferase (GalD) and galactokinase (GalE) are expressed in the cytoplasm, and their expression is regulated by carbohydrate source. (A-D) Fluorescence intensity for both GalD-GFP and GalE-GFP is higher for cells grown on minimal medium containing nitrate and 1 % galactose, pH 7.5, compared to media containing glucose. These images were collected using identical confocal settings. Bar in A = 5 µm, for A-D. (E) Quantitation of GalD-GFP and GalE-GFP intensity, using intensity at 30 randomly-selected cellular sites per sample, as measured by system software. (F) Relative expression of *galD and galE* using qRT-PCR, expressed as fold changes with respect to *actA.*

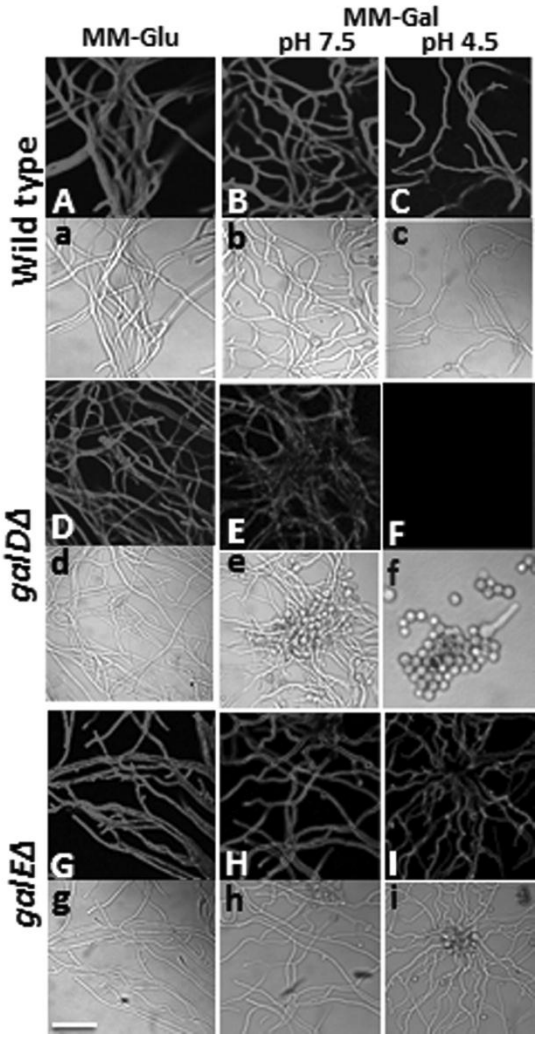

Figure 2.6. Galactofuranose immunolocalization in *Aspergillus nidulans* hyphal walls using the L10 monoclonal anti-Gal*f* antibody. A-C) Wild type grown on A) MM-Glu, B) MM-Gal, pH 7.5, C) MM-Gal, pH 4.5. D-F) *galD*Δ grown on D) MM-Glu, E) MM-Gal, pH 7.5, F) MM-Gal, pH 4.5. G-I) *galE*Δ grown on G) MM-Glu, H) MM-Gal, pH 7.5, I) MM-Gal, pH 4.5. Lower case letters are corresponding transmission images. The fluorescence intensity in E was significantly lower than in A-D; image (e) shows that *galD*Δ spores germinated poorly on MM-Gal. The *galD*Δ strain had even lower germination on MM-Gal pH 4.5 (f), and the spores did not contain galactofuranose (F). Bar in g represents 10 μm for all parts of this image.

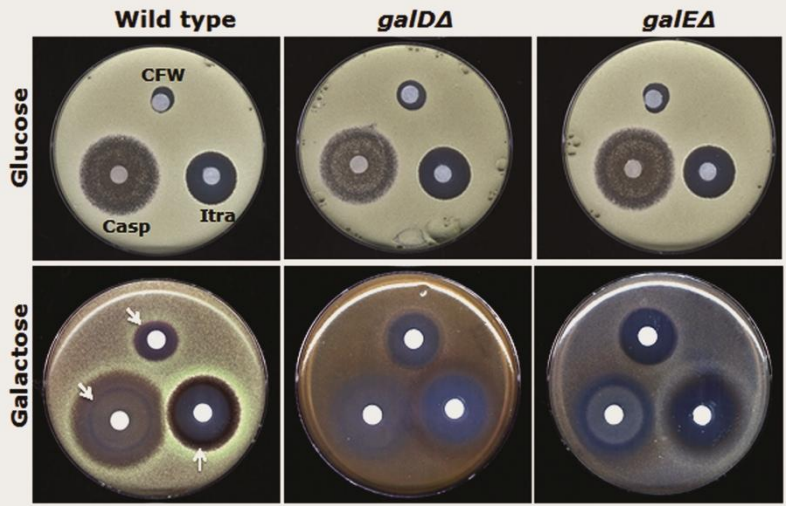

Fig. 2.7. Response of *Aspergillus nidulans* wild type, *galD*Δ and *galE*Δ strains to agents that target cell walls (Calcofluor White, CFW), beta-glucan synthesis (Caspofungin, Casp), and ergosterol synthesis (Itraconazole, Itra). All strains were grown on minimal medium with nitrate at pH 7.5, containing 1 % glucose or 1 % galactose. Quantitative results are provided in Table 2.1. Arrows indicates where measurements were taken.

Supplemental information

Supplemental Table S1: Strains and primers used in this study

Aspergillus nidulans

A1149 [a]	*pyrG89; pyroA4; nkuA::argB*
A212 [a]	*galD5 biA1;wA3 T1(III->VIII)*
A213 [a]	*galD5 biA1;wA3 T1(VI;VIII)*
A214 [a]	*biA1;wA3;galE9*
AAE1 [b]	*pyrG89*::*Ncpyr4+*; *pyroA4*; *nkuA*::*argB*
AKA1 *galD*Δ[c]	AN6182::Af*pyroA*; *pyrG89*; *pyroA4*; *nkuA*::*argB*
AKA2 *galE*Δ[c]	AN4957::Af*pyrG*; *pyrG89*; *pyroA4*; *nkuA*::*argB*
AKA3 GalD-GFP [c]	AN6182-GA_5-GFP-Af*pyrG*; *pyrG89*; *pyroA4*; *nkuA*::*argB*
AKA4 GalE-GFP [c]	AN4957-*GA_5-GFP-AfpyrG; pyrG89; pyroA4; nkuA::argB*
AKA6 [*ugeA*Δ, *galD*Δ] [c]	AN4727::*AfpyrG*; AN6182::Af*pyroA*; *pyrG89*; *pyroA4*; *nkuA*::*argB*

Escherichia coli

BL21-gold (DE3) [d]

Plasmids

AO18 [a]S-TAG,	Af*pyrG*, Kan^R
pCR4-TOPO [e]	Kan^R, amp^R
pFNO3 [a]	GA5-GFP, Af*pyrG*, Kan^R
pTN1 [a]	A*fpyroA*, Amp^R

Primers	**Sequence 5' → 3'**
***galD* deletion**	
PKA1, up galD F [c]	ACTTATCACTAAGGCATGGCGT
PKA2, up galD R [c]	TGGTACCGTTGGAAGCCATATCAAGATACAGTAGGGGAAGAGG
PKA3, dn galD F [c]	TGGCCAAGAGAGGATGGTAAATATCGGAAGAAGTTGGATTCCTA
PKA4, dn galD R [c]	GAATGTCTCGAATACAGCGTG
PKA5, AfPyroA F [b]	ATGGCTTCCAACGGTACCA
PKA6, AfPyroA R[b]	TTACCATCCTCTCTTGGCCA
PKA7, Fusion F [c]	AAAATCAGTTTATAGTCGGTCAACTGT
PKA8, Fusion R [c]	ATCGATTCAACATTTCTTCAACG

***galD* deletion confirmation**

PKA1, up galD F [c]	ACTTATCACTAAGGCATGGCGT
PKA4, dn galD R [c]	GAATGTCTCGAATACAGCGTG
Ame16, MidPyroA R[b]	TCAACAACATCTCCGGTACC

***galE* deletion**

PKA21, up galE F	GCAGGGCGCTTTTTGAT
PKA23, up galE R	TGGTACCGTTGGAAGCCATATCAAGATACAGTAGGGGAAGAGG
PKA24, dn galE F	GAGTATGCGGCAAGTCATGAT GAATATCGCGGCGAGC
PKA22, dn galE R	AGAGGACCACAATGGAATTGAGT
PKA19, galE Fus-F	GCCGGCGAAGGAATAATG
PKA20, galE Fus-R	GCAACTACTTCAAACAGCTCAGTC

***galE* deletion confirmation**

PKA21, up galE F	GCAGGGCGCTTTTTGAT
Ame8, midPyrG R	CACATCCGACTGCACTTCC
PKA22, dn galE R	AGAGGACCACAATGGAATTGAGT

***galD*Δ::*GAL7* complementation**

PKA66, GAL7 F [c]	TGGCTAGCAAAGATATAAAAGCAG
PKA67, GAL7 R [c]	AATTGCGACTTGGACGACATTTACAGTCTTTGTAGATAATG
PKA68, GAL7 Fus F [c]	ATGACTGCTGAAGAATTTGA
PKA69, Up GalD R [c]	TCAAATTCTTCAGCAGTCATATCAAGATACAGTAGGGGAAGAGG
PKA70, Dn galD F [c]	GAGTATGCGGCAAGTCATGAATATCGGAAGAAGTTGGATTCCTA

***galD*Δ::*GAL7* complementation confirmation**

PKA1, up galD F [c]	ACTTATCACTAAGGCATGGCGT
PKA4, dn galD R [c]	GAATGTCTCGAATACAGCGTG
Ame8, midPyrG R[b]	CACATCCGACTGCACTTCC

***galE*Δ::*GAL1* complementation**

PKA87, GAL1 F [c]	ATGACTAAATCTCATTCAGAAGAAGTG
PKA153, GAL1 R [c]	TGGTACCGTTGGAAGCCATTTATAATTCATATAGACAGCTGCCCA
PKA85, Up GalE R [c]	ATGAGATTTAGTCATGGTGGGGTAAACTGAGACTGAC
PKA86, Dn galE F [c]	TGGCCAAGAGAGGATGGTAATGAATATCGCGGCGAGC

***galE*Δ::*GAL1* complementation confirmation**

PKA21, Up-galE F [c]	GCAGGGCGCTTTTTGAT
PKA22, galE dnR [c]	AGAGGACCACAATGGAATTGAGT

Ame8, midPyrG R[b]	CACATCCGACTGCACTTCC
***galD-gfp* tagging**	
PKA9, galD F [c]	ACCACAACCCCAAATACGAA
PKA10, galD R [c]	GCCTGCACCAGCTCCGGAATCCAACTTCTTCCGAT
PKA11, galD dnF [c]	AGTATGCGGCAAGTCATGAGGACATCCCATGTAGACGTGT
PKA12, galD dnR [c]	AAGATTGGCCTCAAATTGCA
PKA13, GFP-FusF [c]	GCGGTCAAGGAGGAACAA
PKA14, GFP-FusR [c]	CCTATACTTTGAATCTCGAAATCGA
Ame 27 5GA-GFPF[b]	GGAGCTGGTGCAGGC
Ame 28 5GA-GFPR[b]	TCATGACTTGCCGCATACT
***galD-gfp* tagging confirmation**	
PKA9, galD F [c]	ACCACAACCCCAAATACGAA
PKA12, galD dnR [c]	AAGATTGGCCTCAAATTGCA
Ame8, midPyrG R[b]	CACATCCGACTGCACTTCC
***galE–gfp* tagging**	
Ame27 5GA-GFP F	GGAGCTGGTGCAGGC
Ame28 5GA-GFP-R	TCATGACTTGCCGCATACT
PKA25, galE F	TCTGTTCAGCACGTTGCC
PKA43, galE R	GCCTGCACCAGCTCCAACATCAACCTGAGAAATTGCAG
PKA44, galE dnF	AGTATGCGGCAAGTCATGAAATATCGCGGCGAGC GGAA
PKA26, galE dnR	CGCAATCTACATCGGCAACTAC
PKA45, GFP-Fus-F	ATCACTTTCCTCATGGCCC
PKA46, GFP Fus-R	AGCTGAGTCAGCCCCAA
***galE-gfp* tagging confirmation**	
PKA25, galEA F	TCTGTTCAGCACGTTGCC
PKA26, galE dnR	CGCAATCTACATCGGCAACTAC
Ame8, midPyrG R[b]	CACATCCGACTGCACTTCC
***galD*Δ*:: ugeA*Δ construction**	
ame41, up ugeA-F	CTCCTATGGTATGTCTCTTCCAACTT
ame43, up ugeA-R	AATTGCGACTTGGACGACATGGTGAATGTGAATTGAATGCAG
ame44, dn ugeA-F	GAGTATGCGGCAAGTCATGAATGGAAATCTTGAATGGATT
ame46, dn ugeA-R	AACTCGACTTTTCGCAGCTC
ame42, uge fusion-F	TCCTAACTTTTGTTACTTTAGGCCC

ame42, uge fusion-R	GGGTACAAAACCGCTACGC
cDNA cloning	
PKA15, galD cDNA F [c]	ATGGTTGAAAGCGTCCTCG
PKA16, galD cDNA R [c]	CTAGGAATCCAACTTCTTCCGA
PKA29, galE F [c]	ATGGCGACCCCGCAG
PKA30, galE R [c]	TCAAACATCAACCTGAGAAATTGC
qRT-PCR	
PKA17 GalD qPCR F [c]	AGCAGGAACGCGTAGTCTTTGAGA
PKA18 GalD qPCR R [c]	CACGCTTGTGCGTCTTGCTAATGA
PKA27 GalE F [c]	AGCAGTGAGCGTCGACGTGATTAT
PKA28 GalE R [c]	TAAGTGCACCAACTAACCCAGCCT

a Fungal Genetics Stock Center, www.fgsc.net

b El-Ganiny et al. (2008)

c This study

d Novagen (www.emdchemicals.com)

e Invitrogen (www.invitrogen.com)

Supplemental Table S2: Raw data that were used to generate qRT-PCR graph

Gene set	Sample	Average C_t	C_t for Actin	DC_t	DDC_t (DC_tsample-DC_t control)	Fold change
galE	Glu	19.18	23.411	-4.231		1
	Gala	16.47	23.41	-6.94	-2.709	6.538
	Gly	18.38	23	-4.62	-0.389	1.3
galD	Glu	19.65	22.21	-2.56		1
	Gala	16.24	22.2	-5.96	-3.4	10.55
	Gly	19.3	22.5	-3.2	-0.64	1.55

Supplemental Table S3: Antifungal drug sensitivity[1] of *Aspergillus nidulans* wild type, *galD*Δ and *galE*Δ strains on minimal medium supplemented with nitrate at pH 7.5, containing 1 % glucose or 1 % galactose.

Strain:	**Wild type**		***galD*Δ**		***galE*Δ**	
Growth medium:	**Glucose**	**Galactose**	**Glucose**	**Galactose**	**Glucose**	**Galactose**
Calcofluor White	1.0 ± 0.03^{a}	1.5 ± 0.06^{b}	1.1 ± 0.02^{a}	2.1 ± 0.03^{c}	1.0 ± 0.02^{a}	1.9 ± 0.06^{c}
Caspofungin	2.5 ± 0.03^{a}	2.6 ± 0.03^{a}	2.7 ± 0.03^{a}	3.7 ± 0.02^{b}	2.6 ± 0.03^{a}	3.4 ± 0.06^{b}
Itraconazole	1.9 ± 0.02^{a}	2.1 ± 0.03^{a}	2.0 ± 0.03^{a}	2.7 ± 0.02^{b}	2.1 ± 0.03^{a}	2.4 ± 0.06^{b}

[1] Drug sensitivity was measured using a disc diffusion assay (see Fig. 2.7). For Caspofungin, sensitivity was the radius (mm) of the clear zone with no visible growth. Mean ± SE of two measurements for each of three biological replicates were used for statistical analysis. Values in individual rows that are followed by different letters (a-d) are significantly different at $P < 0.05$ (ANOVA). These data were presented as drug sensitivity index values in Table 2.1.

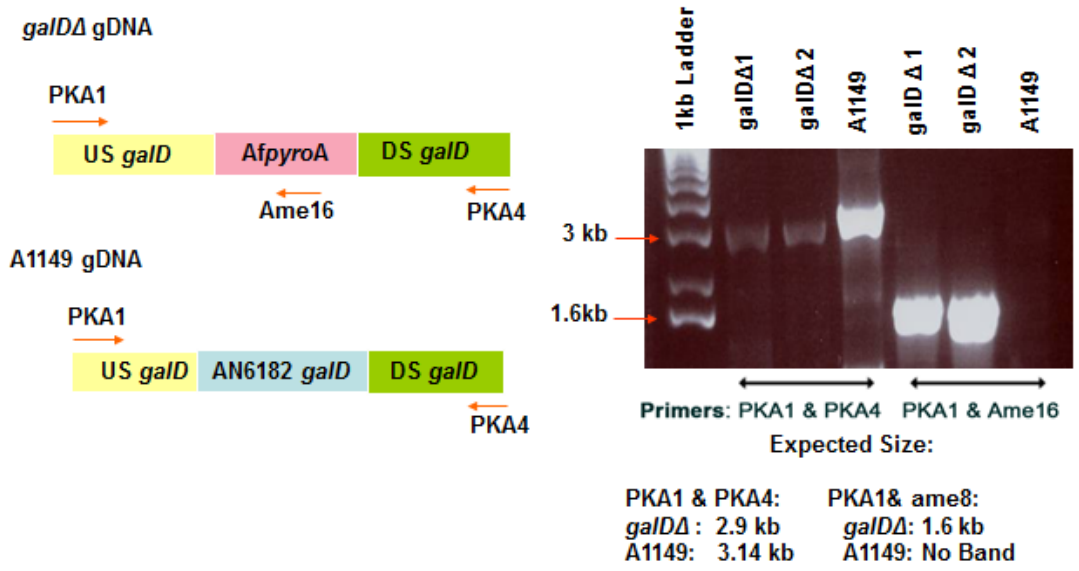

Supplemental Figure S1. Confirmatory PCR for *galD* deletion. US: up stream; DS: downstream. gDNA; genomic DNA. Af*pyroA galD*

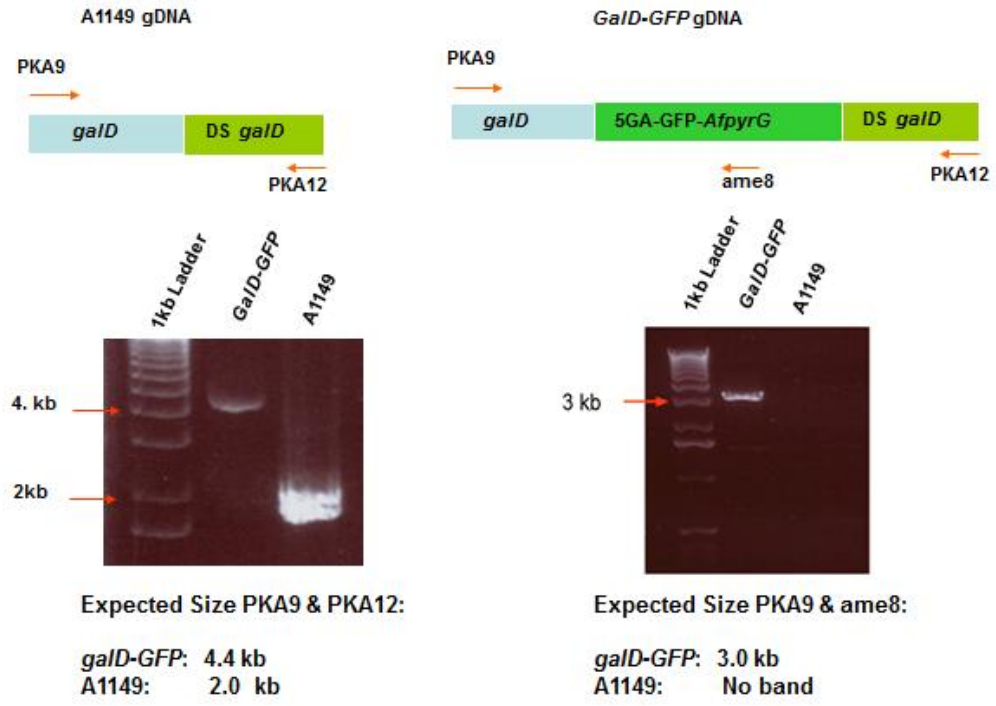

Supplemental Figure S2. Confirmatory PCR for GalD-GFP tagging.

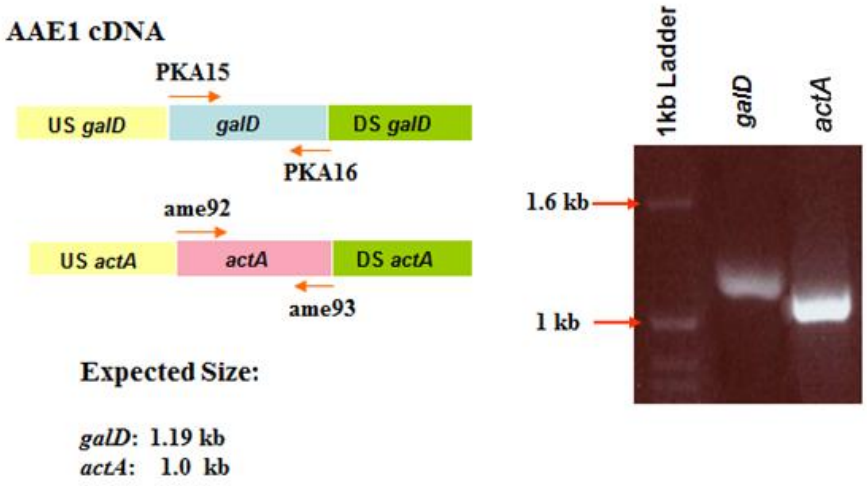

Supplemental Figure S3: PCR showing *galD* and *actA* amplified from AAE1 cDNA. *actA* is used as a control.

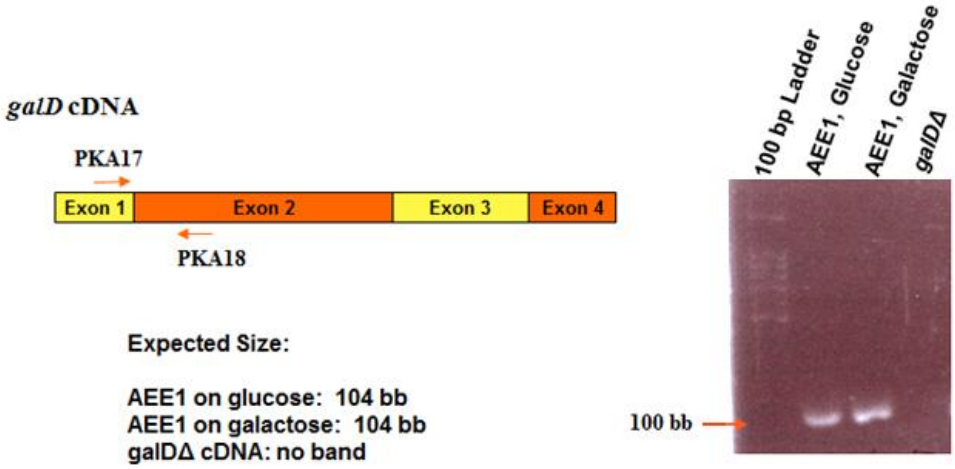

Supplemental Figure S4: qPCR Confirmation using primers that span on Exon 1&2.

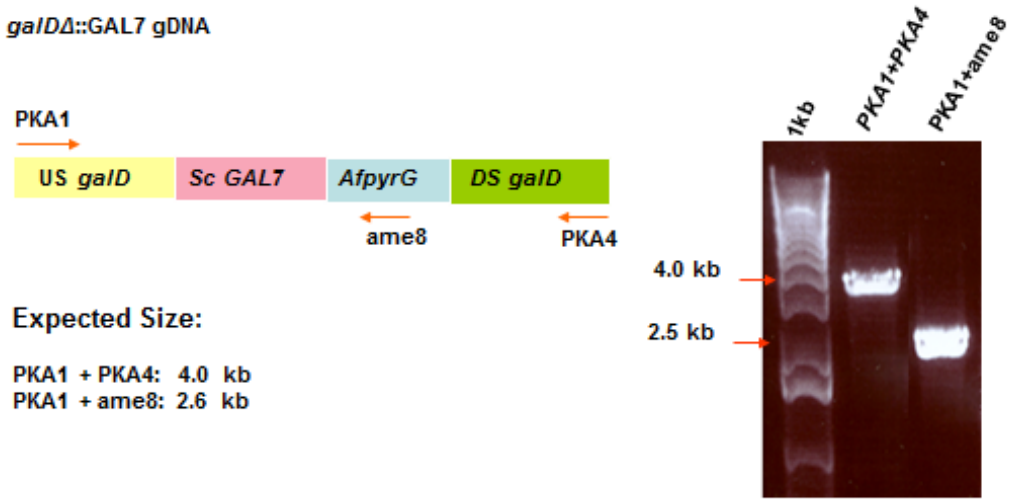

Supplemental Figure S5: Confirmation PCR for *galD::GAL7 strain*

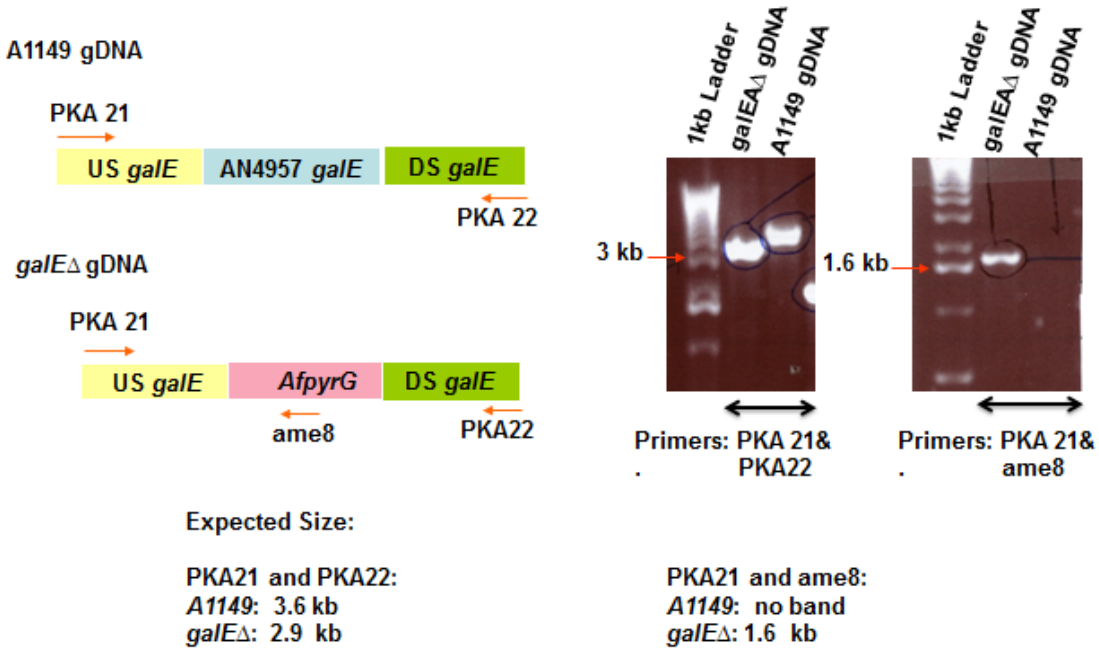

Supplemental Figure S6: Confirmation PCR for *galE* deletion

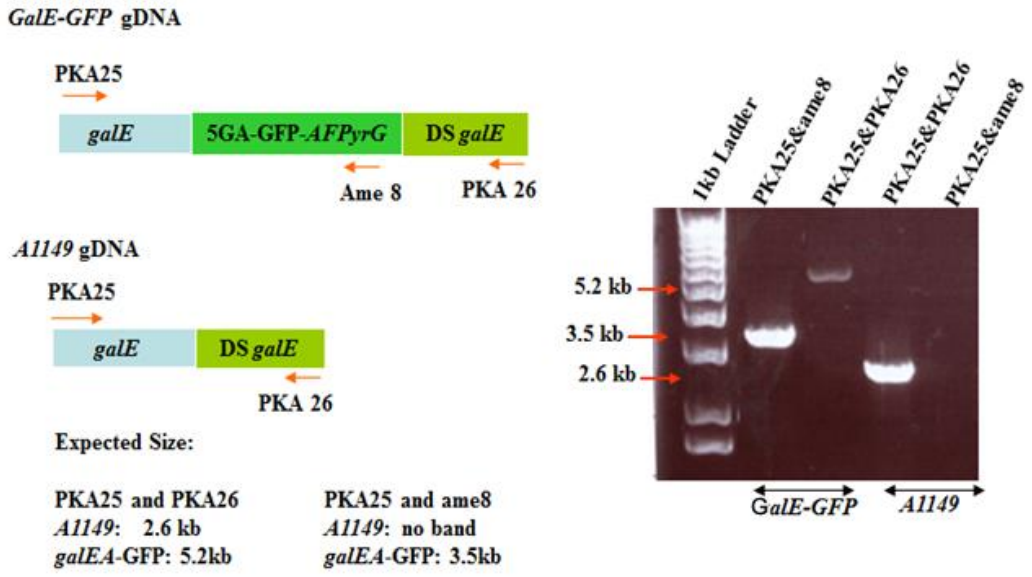

Supplemental Figure S7: Confirmation of GalE-GFP tagging

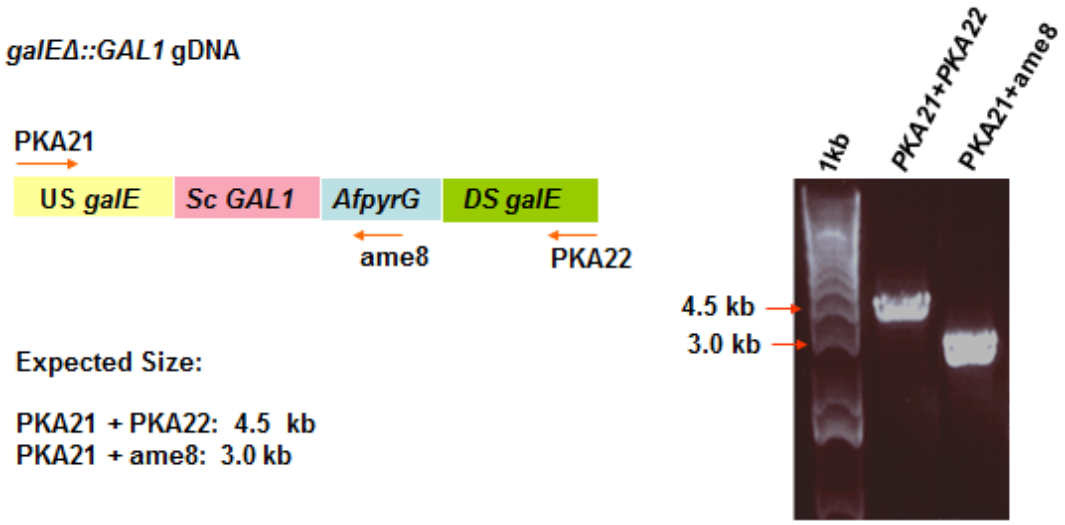

Supplemental Figure S8: Confirmation PCR for *galE::GAL1 strain*

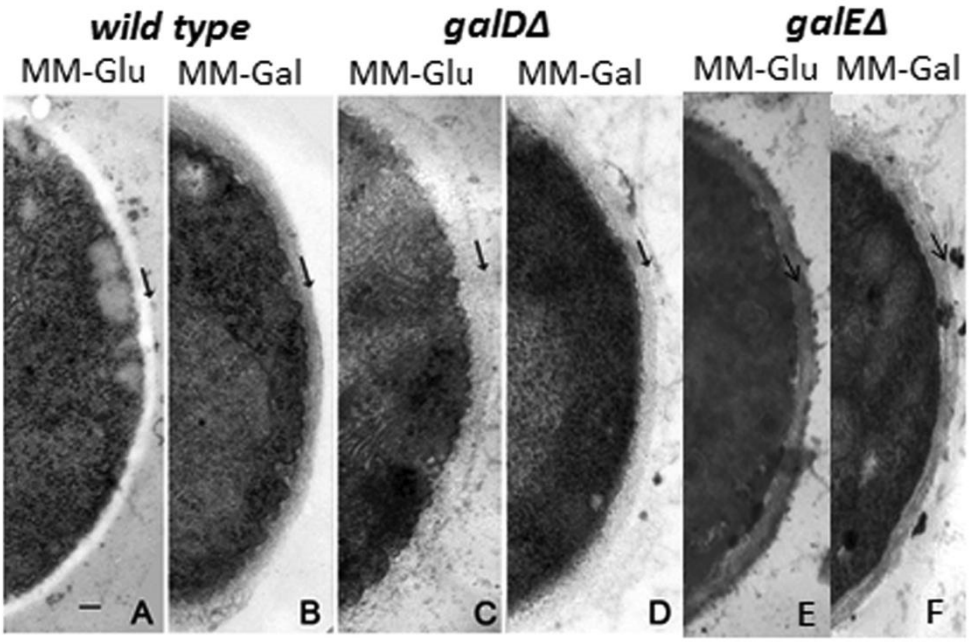

Supplemental Figure S9. Transmission electron micrographs of cross sections of wild type (A, B), *galD*Δ (C, D) and *galE*Δ hyphae (E, F). Hyphae were grown on dialysis tubing overlying MM-Glu (A, C, E) or MM-Gal (nitrate, pH 7.5) (B, D, F). These images were contrast adjusted for comparison of walls; hence the cytoplasm appears relatively dark. Arrows indicate the outer surface of the hyphal wall. Bar in A = 100 nm, for A-F.

Supplemental Figure 10: ClustalW comparison of amino acid sequences for GalD from A1149, A212, and A213. We have sequenced *galD* from A1149 (WT), *galD* mutants (A212 & A213) and compared with *galD* sequence at BI (Broad Institute).

```
BI          MVESVLDDISHRRYNPLRGAYVLVSPHRTKRPWQGAQETPSKTTLPDYDATCYLCPGNKR 60
A1149       MVESVLDDISHRRYNPLRGAYVLVSPHRTKRPWQGAQETPSKTTLPDYDATCYLCPGNKR 60
A212        MVESVLDDISHRRYNPLRGAYVLVSPHRTKRPWQGAQETPSKTTLPDYDATCYLCPGNKR 60
A213        MVESVLDDISHRRYNPLRGAYVLVSPHRTKRPWQGAQETPSKTTLPDYDATCYLCPGNKR 60
            ************************************************************

BI          AQGDHNPKYEKTFIFVNDYSAVKEEQAPYHPEAGTETESFFLRADPVTGKCYVLTFSAAH 120
A1149       AQGDHNPKYEKTFIFVNDYSAVKEEQAPYHPEAGTETESFFLRADPVTGKCYVLTFSAAH 120
A212        AQGDHNPKYEKTFIFVNDYSAVKEEQAPYHPEAGTETESFFLRADPVTGKCYVLTFSAAH 120
A213        AQGDHNPKYEKTFIFVNDYSAVKEEQAPYHPEAGTETESFFLRADPVTGKCYVLTFSAAH 120
            ************************************************************

BI          NLTLADLSPVEIVPVINAWTDVYIAHLSPSSPLAAAASKLTISSGSPAASLAKPNEQYRY 180
A1149       NLTLADLSPVEIVPVINAWTDVYIAHLSPSSPLAAAASKLTISSGSPAASLAKPNEQYRY 180
A212        NLTLADLSPVEIVPVINAWTDVYIAHLSPSSPLAAAASKLTISSGSPAASLAKPNEQYRY 180
A213        NLTLADLSPVEIVPVINAWTDVYIAHLSPSSPLAAAASKLTISSGSPAASLAKPNEQYRY 180
            ************************************************************

BI          MQIFENKGAAMGCSNPHPHGQIWTTSSLPEELAAELEQMKKYRREHNGGHMLADYAALES 240
A1149       MQIFENKGAAMGCSNPHPHGQIWTTSSLPEELAAELEQMKKYRREHNGGHMLADYAALES 240
A212        MQIFENKGAAMGCSNPHPHGQIWTTSSLP-                               239
A213        MQIFENKGAAMGCSNPHPHGQIWTTSSLP-                               239
            ****************************

BI          KKQERVVFENDAFLVVCPWWAIWPFETMIISKTHKRALVDLDDNEKAQLAEAIAEVTRRY 300
A1149       KKQERVVFENDAFLVVCPWWAIWPFETMIISKTHKRALVDLDDNEKAQLAEAIAEVTRRY 300
A212        KKQERVVFENDAFLVVCPWWAIWPFETMIISKTHKRALVDLDDNEKAQLAEAIAEVTRRY 299
A213        KKQERVVFENDAFLVVCPWWAIWPFETMIISKTHKRALVDLDDNEKAQLAEEIAEVTRRY 299
            ************************************************ ********

BI          DNLFETHFPYSMGIHQAPLEGSEEEIEASYLHLHFYPPLLRSATVRKFLVGYELMAEPQR 360
A1149       DNLFETHFPYSMGIHQAPLEGSEEEIEASYLHLHFYPPLLRSATVRKFLVGYELMAEPQR 360
A212                                                                     359
A213                                                                     359

BI          DITPEQAAARLRGCGGELYRKKLDS 385
A1149       DITPEQAAARLRGCGGELYRKKLDS 385
A212
A213
```

Supplemental Figure S11: ClustalW comparison of amino acid sequences for GalE from A1149 and A214. We have sequenced *galE* from A1149 (WT), *galE* mutant (A214) and compared with *galE* sequence at BI (Broad Institute).

```
BI          MATPQELVPRTESIAEVYATDNASATTASPEHVKRFNNLVSHFHKQYNHSPDFVARSPGR 60
A1149       MATPQELVPRTESIAEVYATDNASATTASPEHVKRFNNLVSHFHKQYNHSPDFVARSPGR 60
A214        MATPQELVPRTESIAEVYATDNASATTASPEHVKRFNNLVSHFHKQYNHSPDFVARSPGR 60
            ************************************************************

BI          VNIIGEHIDYNLYDVLPTAVSVDVIIAVKVVPTESSESAVKIANVLPDKFPTREFSVPKD 120
A1149       VNIIGEHIDYNLYDVLPTAVSVDVIIAVKVVPTESSESAVKIANVLPDKFPTREFSVPKD 120
A214        VNIIGEHIEYNLYDVLPTAVSVDVIIAVKVVPTESSESAVKIANVLPDKFPTREFSVPKD 120
            ********:***************************************************

BI          SDVEIDPKKHEWVNYFKAGLVGALKVLRKGAADGSFAPASMEVLVDGNVPPGGGISSSAA 180
A1149       SDVEIDPKKHEWVNYFKAGLVGALKVLRKGAADGSFAPASMEVLVDGNVPPGGGISSSAA 180
A214        SDVEIDPKKHEWVNYFKAGLVGALKVLRKGAADGSFAPASMEVLVDGNVPPGGGISSSAA 180
            ************************************************************

BI          FVCSSALAVMKANNHDVSKQDLLDLAVVSERAVGVYSGGMDQAASIFSRRGYLLYTQFFP 240
A1149       FVCSSALAVMKANNHDVSKQDLLDLAVVSERAVGVYSGGMDQAASIFSRRGYLLYTQFFP 240
A214        FVCSSALAVMKANNHDVSKQDLLDLAVVSERAVGVYSGGMDQAASIFSRRGYLLYTQFFP 240
            ************************************************************

BI          NFSVQHVAIPKAAEEITFLMAQSFVTSNKAETAPRHYNLRVAECTLASVVLAKANGLTLP 300
A1149       NFSVQHVAIPKAAEEITFLMAQSFVTSNKAETAPRHYNLRVAECTLASVVLAKANGLTLP 300
A214        NFSVQHVAIPKAAEEITFLMAQSFVTSNKAETAPRHYNLRVAECTLASVVLAKANGLTLP 300
            ************************************************************

BI          KDNSSLGYSLRTFHNELMRKEGRLGDPLEYQIDSVIQATLDILTQEQGYTREEIAQLLSI 360
A1149       KDNSSLGYSLRTFHNELMRKEGRLGDPLEYQIDSVIQATLDILTQEQGYTREEIAQLLSI 360
A214        KDNSSLGYSLRTFHNELMRKEGRLGDPLEYQIDSVIQATLDILTQEQGYTREEIAQLLSI 360
            ************************************************************

BI          SVPELETTYLSSFPVQAERFLLRQRALHCFKEARRVLDFKACLANASTLDDKRIHYLGQL 420
A1149       SVPELETTYLSSFPVQAERFLLRQRALHCFKEARRVLDFKACLANASTLDDKRIHYLGQL 420
A214        SVPELETTYLSSFPVQAERFLLRQRALHCFKEARRVLDFKACLANASTLDDKRIHYLGQL 420
            ************************************************************

BI          LNESQDSCRDVYECSAPQVDEICNIARKAGTWGSRLTGAGWGGCTVHMLPQSKVEAVTKA 480
A1149       LNESQDSCRDVYECSAPQVDEICNIARKAGTWGSRLTGAGWGGCTVHMLPQSKVEAVTKA 480
A214        LNESQDSCRDVYECSAPQVDEICNIARKAGTWGSRLTGAGWGGCTVHMLPQSKVEAVTKA 480
            ************************************************************

BI          LTEEYYLKYFPDISEEKLKEAMVISKPSNGSFLITGAAISQVDV 524
A1149       LTEEYYLKYFPDISEEKLKEAMVISKPSNGSFLITGAAISQVDV 524
A214        RRRSAI-
```

CHAPTER 3

Aspergillus nidulans galactofuranose biosynthesis affects antifungal drug sensitivity

This Chapter explored the roles of Gal*f* in hyphal growth, drug sensitivity and the relation of Gal*f* with other cell wall carbohydrate pathways. The manuscript has been published as *Aspergillus nidulans* galactofuranose biosynthesis affects antifungal drug sensitivity (2012) in Fungal Genetics and Biology 49: 1033-1043 by **Md Kausar Alam**, Amira El-Ganiny, Sharmin Afroz, David A. R. Sanders, Juxin Liu and Susan GW Kaminskyj, 2012.

This Chapter was based on our hypothesis ``Gal*f* deletion/repressed strains will have a wall defect that will make them more sensitive to wall-targeting agents``. The objectives of the research in this Chapter were

1. Roles of Gal*f* biosynthesis pathway enzymes (UgmA, UgeA, UgtA) in fungal growth, wall maturation, drug sensitivity
2. Relationship Gal*f* biosynthesis pathway enzymes with other major carbohydrate biosynthesis pathways

My contribution in this Paper: My contribution was to generate conditional strains and to confirm drug sensitivity with respect to deletion, repression, and over-expression of these Gal*f* biosynthesis genes. I established the immunofluorescence experiment for which we got the cover page image. I also showed the relationship of Gal*f* with α-glucan and β-glucan using qRT-PCR. I wrote and updated the literature review for the main draft of the submitted manuscript, based on an unpublished Chapter in El-Ganiny's Ph. D. thesis. I completed the study, which required generation and analysis of the *niiA*(p) regulated strains, additional drug studies, and integration of several data sets. I generated the first complete draft of the submitted manuscript. Professor Susan Kaminskyj and I worked together to revise this draft prior to submission. We also worked together on the revision.

***Aspergillus nidulans* galactofuranose biosynthesis affects antifungal drug sensitivity.**

Md Kausar Alam [a*], Amira M. El-Ganiny [a b*], Sharmin Afroz [a], David A. R. Sanders [c], Juxin Liu [d], and Susan G. W. Kaminskyj [a e]

[a] Department of Biology, University of Saskatchewan, 112 Science Place, Saskatoon SK S7N 5E2, Canada.

[b] Department of Microbiology, Faculty of Pharmacy, Zagazig University, Egypt.

[c] Department of Chemistry, University of Saskatchewan, 110 Science Place, Saskatoon SK S7N 5C9, Canada

[d] Department of Mathematics and Statistics, University of Saskatchewan, 106 Wiggins Road, Saskatoon SK S7N 5E6, Canada

[e] Author for correspondence: susan.kaminskyj@usask.ca; Telephone: 1 (306) 966 4422

* contributed equally to the manuscript

Running head: *Aspergillus* Gal*f* influences echinocandin sensitivity

Key words: *Aspergillus nidulans*; galactofuranose; UDP-galactopyranose mutase; UDP-glucose/galactose-4-epimerase; UDP-galactofuranose transporter; *alcA* promoter; *niiA* promoter; immunofluorescence; sporulation; hyphal morphometry; drug sensitivity.

Abbreviations: Af, *Aspergillus fumigatus*; *alcA*(p), alcohol dehydrogenase I promoter; CM, complete medium; CM3G, complete medium with 3% glucose; CMT, complete medium with 100 mM threonine; Gal*f*, galactofuranose; gDNA, genomic DNA; mAb, monoclonal antibody; *niiA*(p), nitrite utilization promoter; MM, minimal medium; MMA, minimal medium ammonium; MMN, minimal medium nitrate; qPCR, quantitative real time PCR; UDP, uridine diphosphate, UGE; UDP-glucose/galactose-4-epimerase, UGM; UDP-galactopyranose mutase, UGT; UDP-galactofuranose transporter

Abstract

The cell wall is essential for fungal survival in natural environments. Many fungal wall carbohydrates are absent from humans, so they are a promising source of antifungal drug targets. Galactofuranose (Gal*f*) is a sugar that decorates certain carbohydrates and lipids. It comprises about 5 % of the *Aspergillus fumigatus* cell wall, and may play a role in systemic aspergillosis. We are studying *Aspergillus* wall formation in the tractable model system, *A. nidulans*. Previously we showed single-gene deletions of three sequential *A. nidulans* Gal*f* biosynthesis proteins each caused similar hyphal morphogenesis defects and 500-fold reduced colony growth and sporulation. Here, we generated *ugeA*, *ugmA* and *ugtA* strains controlled by the *alcA*(p) or *niiA*(p) regulatable promoters. For repression and expression, *alcA*(p)-regulated strains were grown on complete medium with glucose or threonine, whereas *niiA*(p)-regulated strains were grown on minimal medium with ammonium or nitrate. Expression was assessed by qPCR and colony phenotype. The *alcA*(p) and *niiA*(p) strains produced similar effects: colonies resembling wild type for gene expression, and resembling deletion strains for gene repression. Gal*f* immunolocalization using the L10 monoclonal antibody showed that *ugmA* deletion and repression phenotypes correlated with loss of hyphal wall Gal*f*. None of the gene manipulations affected itraconazole sensitivity, as expected, but deletion of any of *ugmA*, *ugeA* or *ugtA*, as well as their repression by *alcA*(p) or *niiA*(p), increased sensitivity to caspofungin. Strains with *alcA*(p)-mediated overexpression of *ugeA* and *ugtA* had lower caspofungin sensitivity. Gal*f* appears to play an important role in *A. nidulans* growth and vigor.

3. 1. Introduction

Human systemic fungal infections are an increasing threat (Fisher et al., 2012), particularly due to improved medical technology leading to larger populations of immune-compromised people. Systemic infections from a dozen or more fungi lead to morbidity despite aggressive anti-fungal drug treatment (Lass-Florl, 2009). Overall, *Aspergillus* is second only to *Candida* as a cause of invasive fungal infections (Erjavec et al., 2009). Humans have few anti-fungal drug options because fungi share many biochemical pathways with animals. A major difference between organisms in these kingdoms is that fungal cells have a carbohydrate wall. This wall protects the fungal cell from damage, and mediates the interaction between the fungus and its environment. If the wall is removed or weakened, the fungus cannot survive in natural environments (Bennett et al., 1985). About 90 % of the fungal wall is composed of polysaccharides that are not found in human hosts (Latgé, 2007). Echinocandins are the only antifungal drugs in clinical use that block aspect component of fungal wall synthesis, i.e. the formation of β-1,3-glucans that comprise about half of fungal cell wall polysaccharides in some species (Espinel-Ingroff, 2009). However, echinocandins are clinically effective only against *Candida* and *Aspergillus*. They must be used intravenously (Denning, 2003); and drug-resistant strains have already been identified (Walker et al., 2010). There is a pressing need to develop additional antifungal drugs (Mircus et al., 2009) particularly against novel aspects of fungal physiology. Gauwerky et al. (2009) suggest that minor wall components as well as virulence factors have the potential to be useful anti-fungal drug targets.

We are exploring an aspect of wall biosynthesis in *Aspergillus nidulans*, the galactofuranose (Gal*f*) biosynthesis pathway. Gal*f* is the five-membered ring form of galactose found in the cell wall of many microorganisms including fungi, but only the six-member ring form called galactopyranose is found in mammals. In microorganisms, Gal*f* residues form the side chains of glycoconjugates including galactomannan. Gal*f* biosynthesis genes encode UDP-glucose/galactose-4-epimerase (UgeA) (El-Ganiny et al., 2010), UDP-galactopyranose mutase (UgmA) (El-Ganiny et al., 2008), and the UDP-galactofuranose transporter (UgtA) (Afroz et al., 2011). Although none of these genes was essential for *A.*

nidulans in culture, deletion strains had aberrant wall maturation (Paul et al., 2011) and 500-fold reduced hyphal growth and sporulation rate.

Gal*f* residues in human serum can be used to track a patient's response to therapy for systemic *Aspergillus* infections (Bennett et al., 1985; Stynen et al., 1992; Shibata et al., 2009). Gal*f* has been shown to be essential for the virulence of the pathogenic protozoan, *Leishmania* (Kleckza et al., 2007). Gal*f* could be a virulence determinant in *A. fumigatus* based on studies with a UgmA (also known as GlfA) deletion strain in a murine model (Schmalhorst et al., 2008). Recent evidence to the contrary (Heesemann et al., 2011) showed that *A. fumigatus* hyphae pretreated with monoclonal antibodies (mAbs) specific to hyphal Gal*f* residues had similar virulence to untreated hyphae. Nevertheless, Gal*f* metabolism could still be a useful target for anti-fungal drug development (Pederson and Turco, 2003) because it plays important although not fully-understood roles in fungal growth.

Regulated promoters can be used to explore the role (Waring et al., 1989) and requirement (Hu et al., 2007) for *Aspergillus* genes, typically using the *alcA* (Waring et al., 1989; Monteiro and De Lucas, 2010) and *niiA* (Monteiro and De Lucas, 2010) promoters whose expression is controlled by carbon source or nitrogen source, respectively. For example, repression of *A. nidulans* chitin synthase *chsB* in an *alcA*(p)-*chsB* strain caused slow growth and highly branched hyphae (Ichinomiya et al., 2002). Repression of *alcA*(p)-regulated *A. fumigatus* O-mannosyltransferase 2 (Af*pmt2*) caused growth retardation, abnormal cell polarity, defective cell wall integrity, and reduced conidiation (Fang et al., 2010). Repression of *alcA*(p)-regulated protein kinase C (*pkcA*) reduced germination rate, hyphal growth and conidiation, as well as increasing hyphal wall thickness and sensitivity to wall-selective agents: Caspofungin, Calcofluor White, and Congo Red (Ronen et al., 2007). As expected, this strain was also more sensitive to the protein kinase inhibitor staurosporine although it responded like wild type to amphotericin B and voriconazole (Ronen et al., 2007). Binder et al. (2010) showed that an *alcA*(p)-*pkaA* strain grown on repression medium was hypersensitive to PAF, an antifungal protein. Taken together, expression-regulated strains have been used successfully to study cell wall formation in *Aspergillus* species.

Expression-regulated strains have also been used to identify new cell wall destabilizing compounds (Mircus et al., 2009) and to study cell wall integrity in the presence of anti-fungal

agents. Fortwendel et al. (2009) used *alcA*(p)-regulated *A. fumigatus* strains defective in cell wall integrity pathway genes (*rasA*, *cnaA* and *crzA* strains) to show that low cell wall integrity correlated with echinocandin sensitivity. Jiang et al. (2008) created *A. fumigatus* strains conditionally expressing *alcA*(p)-regulated GDP-mannose pyrophosphorylase. These strains had defective cell walls, impaired polarity maintenance, reduced conidiation, and increased sensitivity to wall targeting chemicals. Regulating gene expression is a powerful adjunct to deletion analysis for exploring gene function.

Here, we describe studies on the function of Gal*f* biosynthesis genes using strains whose endogenous promoter was replaced by the alcohol dehydrogenase promoter *alcA*(p) (Ichinomiya et al., 2002; Waring et al., 1989) which is highly induced by alcohols, especially threonine, and is repressed by glucose (Romero et al., 2003, Tribus et al., 2010). As a precaution against potential complications from using a sugar-repressed promoter to study the carbohydrate-rich wall, we repeated key experiments with these genes regulated by *niiA*(p), which is regulated by nitrogen source (Monteiro et al., 2010). Under gene repression conditions with both promoters, the regulated strain colonies phenocopied their respective deletion strains. Notably, all the deletion strains were significantly more sensitive to the wall-targeting drug Caspofungin, as were the repressed strains. Our results suggest that the role of Gal*f* biosynthesis plays multiple roles in fungal growth, wall architecture, and drug sensitivity, and as such may be a useful drug target.

3.2. Materials and methods

3.2.1. Strains, plasmids and culture conditions

Strains, primers and plasmids are listed in Suppl Table A. *Aspergillus nidulans* strains were maintained on complete medium (CM) with supplements for nutritional markers as described in Kaminskyj (2001). To manipulate *alcA*(p)-regulated gene expression, CM that otherwise contained 1 % glucose was modified as follows: maximum repression used CM containing 3 % glucose (CM3G); overexpression used CM lacking glucose but containing 100 mM threonine (CMT). For *niiA*(p)-regulated gene expression, minimal medium (MM) containing 70 mM $NaNO_3$ (MMN) was used for induction, and MM containing 10 mM ammonium tartrate (MMA) was used for repression. Media used for *niiA*(p)-regulation were

supplemented with vitamin solution and pyridoxine. We were not able to find a medium for overexpressing *niiA*(p)-regulated genes.

3.2.2. Construction of regulatable promoter strains

A promoter exchange module consisting of Af*pyrG* and *alcA*(p) was amplified from the plasmid, p*alcA*(p) (a gift of Loretta Jackson-Hayes, Rhodes College). This module was inserted immediately upstream of each Gal*f* biosynthesis gene to create *alcA*(p)-regulated strains. A 1.2-kb DNA fragment containing Af*niiA*(p) was amplified by PCR from genomic DNA of wild type *A. fumigatus*. This was used to create a *niiA*(p)-regulatable promoter module, also with Af*pyrG* as the selectable marker. This construct was inserted immediately upstream of the coding sequence for each Gal*f* biosynthesis gene to create *niiA*(p)-regulated strains (Suppl Fig. A).

3.2.3. Transformation

Constructs were transformed into A1149 protoplasts. Protoplasting and transformation followed procedures in Osmani et al., (2006) and Szewczyk et al., (2007). Long-term storage of competent protoplasts is described in El-Ganiny et al. (2010). Primary transformants were grown on selective medium containing 1 M sorbitol or 1 M sucrose as osmostabilizer. Spores from these colonies were streaked three times on selective medium prior to gDNA extraction. Genomic DNA from transformant spores (see below) was used as template for PCR to confirm the each manipulation (Suppl Fig. A).

3.2.4. Isolation of genomic DNA from *Aspergillus nidulans* spores

Approximately 1×10^7 spores from individual 2 d old colonies were harvested in sterile distilled water, pelleted in 1.5 mL microfuge tubes, and aspirated to dampness. Tubes containing damp spore samples were sealed with lid-locks, floated in 100 mL water, and microwaved at full power for 6 min. Then 35 µL of TE buffer (10 mM Tris-Cl, 1 mM EDTA, pH 8) was added to each tube. Tubes were vortexed briefly and put on wet ice for 5 min. The spore-DNA suspension was centrifuged at 16,000 x *g* for 5 min to pellet debris. One microliter of supernatant was used as PCR template for amplicons up to 4 kb long.

3.2.5. RT-PCR and qPCR

Gene expression studies compared levels of Gal*f* biosynthesis genes in wild type, deleted, and *alcA*(p)-, and *niiA*(p)-regulated *ugeA*, *ugmA* and *ugtA* strains. Spores were inoculated in CM or induction or repression liquid media, and incubated at 28 °C with shaking at 250 rpm for 16 h. Mycelia were collected by centrifugation, frozen in liquid nitrogen, and lyophilized. Total RNA was extracted using an RNeasy plant kit (Qiagen) following manufacturer's instructions. RNA concentration was measured using a Nanodrop®, then diluted to 400 ng/µL. Genomic DNA elimination and reverse transcription used a QuaniTect reverse transcription kit (Qiagen) following the manufacturer instructions (Cuero et al., 2003).

Quantitative real time PCR (qPCR) was performed in 96-well optical plates in an iQ5 real-time PCR detection system (Bio-Rad). Gene expression was assayed in triplicate in total volume 20 µL reactions containing cDNA at an appropriate dilution and SYBR green fluorescein (Qiagen). A no-template control was used for each gene. Actin was used as a reference gene (Bohle et al., 2007). Primers actF and actR (Suppl Table A) were designed to amplify regions that included an intron in the *actA* genomic sequence. These primers generated a ~200 bp band from cDNA and ~400 bp band from gDNA, to detect genomic DNA contamination in the template. The qPCR amplification used the following conditions: 95 °C/15 min for one cycle, 95 °C/15 s, 55 °C/40 s and 72 °C/30 s for 40 cycles and final extension cycle of 72 °C/2 min. Melting curve analysis was done using the following cycle: 15 s at 65 °C with an increase of 0.5 °C each cycle to 95 °C. For *FKS* and *ags1* gene expression analysis, we used wild type (AAE1), *ugmA*Δ, and Af*niiA*(p)-*ugmA* strains. The relative expression was normalized to *actA* (Upadhyay and Shaw, 2008) and calculated using the ΔΔCt method (Livak and Schmittgen, 2001). Three independent biological replicates were performed for each strain/culture condition.

3.2.6. Colony growth and sporulation

Colony characters were examined as described in El-Ganiny et al. (2008). Strains were grown for two generations on inducing or repressing media to control for possible dowry effects, then spores of wild type and regulated strains were streaked on induction or repression

media and incubated for 3 d at 28 °C to give isolated colonies. The diameter of ten colonies/strain was measured to the nearest millimeter using a dissection microscope. The number of spores produced per colony was counted for four colonies/strain. Isolated colonies were vortexed in a microfuge tube containing 1 mL water, then samples of spores were counted with a hemocytometer.

3.2.7. Microscopy

Samples were prepared for confocal microscopy as described in El-Ganiny et al. (2008). Freshly harvested spores were grown on coverslips at 28 ºC for 16 h in induction or repression media. Hyphae were fixed and stained with Hoechst 33258 (for nuclei) and Calcofluor (for cell walls). Samples were imaged using a Zeiss META510 as described previously (El-Ganiny et al., 2008). LSM image browser software was used for measurements of hyphal width (at septa) and basal cell length (distance between adjacent septa).

Gal*f* content of wild type, *ugmA*-GFP, *ugmA*Δ, and *niiA*(p)-*ugmA* hyphae was assessed using immunolocalization. Monoclonal anti-Gal*f* antibodies L10 and L99 were a generous gift of Prof. Frank Ebel (Univ Munich). Primary antibodies were used at full strength; TRITC-conjugated goat-anti-mouse was used at 1:10 dilution. Immunofluorescence procedures followed El-Ganiny et al. (2008) and samples were examined using confocal epifluorescence microscopy.

Transmission electron microscopy was used to measure hyphal wall thickness for *alcA*(p)-regulated colonies grown on dialysis tubing overlying CMT or CM3G. Samples were prepared as described in Kaminskyj (2000). Hyphal wall thickness was measured where the cell membrane bilayer was crisply in focus. Typically three sites were measured for each of ten hyphae per strain/medium combination.

Scanning electron microscopy was used to examine conidiating wild type and *alcA*(p)-regulated colonies following the procedure in El-Ganiny et al. (2008). Strains were grown on dialysis tubing laid on CMT and CM3G for 3 d at 28 ºC. Colonies were fixed by immersion in 1 % glutaraldehyde, dehydrated in acetone, critical point dried (Polaron E3000, Series II), and gold sputter coated (Edwards model S150B). Samples were imaged with a JEOL 840A scanning electron microscope.

3.2.8. Drug sensitivity testing.

Antifungal agents and solvents were obtained from the following manufacturers: amphotericin B, terbinafine, itraconazole, dimethyl sulphoxide (DMSO) (Sigma Chemicals); ethanol (VWR); caspofungin (a gift from Schering-Plough, now Merck). Stock solutions were prepared as follows: amphotericin B (20 mg/mL in DMSO), itraconazole (1.6 mg/mL in DMSO), terbinafine (1.6 mg/mL in 50 % ethanol), and caspofungin (20 mg/mL in sterile water). Aliquots of stock solutions were stored at -80 ºC.

Wild type and Gal*f*-biosynthesis gene deletion strains were grown on CM; gene-regulated strains were grown on repression and expression media. Spore suspensions collected from 4 d old colonies were filtered through VWR 413 filter paper (average pore size 5 μm) to remove hyphae and conidiophores. Spores in the filtered suspension were counted using a hemocytometer and adjusted to 50,000 spores/μL.

Antifungal drug sensitivity testing used a disc-diffusion method modified from (Kontoyiannis et al, 2003; Lass-Florl, 2009), as described in Afroz at al. (2011). Strains were grown for two rounds on the test media before being used for drug sensitivity studies, to compensate for potential spore dowry effects. For the drug sensitivity test, 1×10^7 spores were mixed into 20 mL of 50 ºC expression or repression agar and immediately poured in 9 cm diameter Petri plates. After the medium had solidified, sterile 6 mm paper discs were placed on the agar surface. Anti-fungal drug stock solutions (described above) were micro-pipetted onto individual disks: 10 μL of terbinafine and itraconazole, and 20 μL of amphotericin B and caspofungin. Solvent control studies with DMSO and 50 % ethanol showed no zone of inhibition. The plates were incubated at 28 ºC and assessed after 48 h (Kiraz et al., 2009).

The radius of the zone of inhibition was calculated as

[diameter (mm) with no visible growth – disk diameter (mm)] / 2

Two measurements at orthogonal axes were taken for each disk on each plate; four plates were assessed for each strain and medium combination, and each experiment was repeated. These data were used for statistical analysis. Data are presented as indexed values with respect to wild type on CM (for deletion strains) and with respect to wild type on the test medium (for regulated strains).

3.2.9. Data processing and analysis

Confocal images were processed using LSM examiner. Images are presented using Adobe Photoshop 7.1. Statistical analysis used Kruskal-Wallis and associated *post hoc* tests with R software: R 2.13 for kruskal.test, and R 2.9 for kruskalmc.test.

3.3. Results

We examined the roles of Gal*f*-biosynthesis gene products for anti-fungal drug sensitivity using conditional strains whose gene expression was under the control of the regulatable promoter, *alcA*(p) (Romero et al., 2003; Tribus et al., 2010). Previously we had deleted each of these genes: *ugmA* (El-Ganiny et al., 2008); *ugeA* (El-Ganiny et al., 2010); *ugtA* (Afroz et al., 2011), to study the effects on *A. nidulans* morphogensis, conidiation, and wall ultrastructure. We expected that gene repression would have similar effects to gene deletion, and that over-expression would have little effect. We used these strains to assess the role of Gal*f* biosynthesis in sensitivity to anti-fungal drugs, especially Caspofungin that targets cell wall synthesis. For each section, we present *ugmA* results in detail, followed by comparison with results for *ugeA* and *ugtA*. The *alcA*(p) data were confirmed using *niiA*(p)-regulation (Gauwerky et al., 2009; Monteiro and De Lucas, 2010).

3.3.1. Construction and validation of regulated strains.

We replaced each endogenous Gal*f* biosynthesis gene promoter with the *alcA*(p) and with the *niiA*(p) conditional promoters, using Af*pyrG* as the selectable marker (Szewczyk et al., 2007). Primary transformants were grown on CM or MM, respectively, containing 1 M sorbitol or 1 M sucrose as an osmotic stabilizer. Strain construction and confirmation is shown in Suppl Fig. A.

To select media appropriate for regulation of Gal*f* biosynthesis genes in *A. nidulans*, the *alcA*(p)-*ugmA* strain was grown on CM containing a variety of carbon sources, and the colony morphologies were compared qualitatively. Media included CM with 100 mM threonine (CMT), 1 % fructose plus 100 mM threonine, 1 % ethanol, 1 % glycerol, 1 % glucose (CM), or 3 % glucose (CM3G), as well as YEPD (1 % yeast extract, 2 % peptone, 2 % dextrose [=glucose]) that was previously used in Zarrin et al. (2005). Growth of the *alcA*(p)-*ugmA* strain on YEPD resembled the *ugmA*Δ strain, however the sporulation of the wild type strain

on YEPD was greatly reduced (*not shown*) so it was deemed unsuitable for our purposes. In comparison, growing the wild type strain on CM *vs* CM3G *vs* CMT caused substantially less variation in wild type colony characteristics (Table 3.1).

Growth of the *niiA*(p)-regulated *ugmA* strain was compared on MM containing nitrate salts (MMN), nitrite salts, ammonium tartrate (MMA), and ammonium nitrate as nitrogen sources. Colony growth of the *niiA*(p)-*ugmA* strain resembled wild type on MM containing nitrate, nitrite, and ammonium nitrate, but resembled the deletion strain on MMA.

The expression level of *ugeA*, *ugmA* and *ugtA* were assessed in wild type and respective regulated strains using qRT-PCR, with *actA* expression as the comparator. Expression of *ugmA* and *actA* in the wild type transformation parent of the regulated strains was comparable on all media used (upper panels in Fig. 3.1A, B). For *alcA*(p)-*ugmA* regulation, growth on CMT showed roughly comparable *ugmA* and *actA* expression levels, whereas growth on CM3G caused a dramatic decrease on *ugmA* but not *actA* expression (lower panels in Fig. 3.2A). We found substantially similar results with *niiA*(p)-*ugmA* expression levels (with respect to *actA*) when grown on inducting MMN vs repressing MMA media (Fig. 3.1B). We also found that regulation of *ugeA* (upper panel in Fig. 3.1C) and *ugtA* (lower panel in Fig. 3.1C) by these promoters was comparable to *ugmA*. The effect of *alc*(p)-*ugeA*, *alc*(p)-*ugmA*, and *alc*(p)-*ugtA* regulation with respect to the wild type strain were also compared using qPCR, again with *actA* as the comparator (Fig. 3.1D). Consistent with our RT-PCR results for *alcA*(p)-regulation, overexpression was associated with 8, 4, and 6-fold increase in *ugeA*, *ugmA* and *ugtA* expressions respectively, and repression with 100-150-fold decrease in all the *alcA*(p)-regulated strains (Fig. 3.1D).

3.3.2. Repression of Galf biosynthesis genes causes compact colony growth and reduced sporulation

Growing the *alcA*(p)-*ugmA* strain on CM3G to repress *ugmA* produced growth and sporulation phenotypes similar to the *ugmA*Δ strain, regarding colony diameter, spores per isolated colony, hyphal width, and basal cell length (Table 3.1; Fig. 3.2). Scanning electron micrographs showed reduced sporulation was due to a decrease in conidiophore number as well as aberrant conidiophore formation (Fig. 3.3). For the *alcA*(p)-*ugeA* and *alcA*(p)-*ugtA*

strains, growth on CM3G resulted in compact colonies with wide, branched hyphae that had substantially reduced sporulation. Strains grown on CMT resembled wild type (Table 3.1; Figs. 3.2, 3.3).

The *ugmA*Δ and *alcA*(p)-*ugmA* repressed strains differed in hyphal wall thickness (Table 3.1). The walls of the *alcA*(p)-*ugmA* strain on CM3G were twice as thick as wild type on the same medium, but only half as thick as the *ugmA*Δ strain on CM (Table 3.1; El-Ganiny et al., 2008). We repeated the *alcA*(p)-*ugmA* CM3G fixation on two separate occasions with similar results. The *alcA*(p)-*ugeA* and *alcA*(p)-*ugtA* wall thicknesses when grown on CM3G were also thinner than the comparable deletion strains (Table 3.1). Thus, deletion and *alcA*(p)-repression phenotypes for Gal*f* biosynthesis genes differed in some quantitative aspects.

We expected that over-expression of Gal*f* biosynthesis genes would be benign, since their product activity should depend on substrate availability. The *alcA*(p)-*ugmA* strain grown on CMT produced wild type colonies that sporulated more abundantly than on CM3G (Table 3.1). In addition, the *alcA*(p)-*ugmA* hyphae on CMT were wider than wild type and had shorter basal cells (Table 3.1), whereas the *alcA*(p)-*ugeA* and *alcA*(p)-*ugtA* hyphae more closely resembled the wild type strain (Table 3.1).

3.3.3. Deletion and repression of ugmA cause hyphal morphogenesis defects that correlate with loss of immunolocalizable wall Galf

We expected repression of Gal*f* biosynthesis would reduce wall Gal*f* content, as we had previously shown for *ugmA*Δ (El-Ganiny et al., 2008). Prof. Frank Ebel's group (Univ. Munich) recently generated the L10 and L99 anti-Galf mAbs, (Heesemann et al., 2011) that have high affinity for hyphal wall Gal*f*. They generously provided us with samples of each mAb. We had strong Gal*f* immunolocalization in wild type phenotype *A. nidulans* hyphal walls using L10 (Fig. 3.4A, B, D), but less intense signal with L99 (*not shown*). In addition to wall staining, the cytoplasm also contained L10-reactive material, consistent with UgmA-GFP localization being cytoplasmic (Fig. 3.4B' and B") and UDP-Gal*f* being synthesized in the cytoplasm prior to Gal*f* incorporation into wall compounds (El-Ganiny et al., 2010). Both *ugmA*Δ (Fig. 3.4C), and *niiA*(p)-*ugmA* strains grown on MMA repression medium (Fig. 3.4

E), had wide, highly-branched hyphae. As expected, the *ugmA* deletion and repression strain hyphal walls lacked detectable wall Gal*f* (Fig. 3.4C, E), as did their cytoplasm.

3.3.4 Galf biosynthesis affects α-glucan synthase and β-glucan synthase expression

Both deletion and repression of Gal*f* biosynthesis in *A. nidulans* are associated with increased hyphal wall thickness (Table 3.1; El-Ganiny et al. 2008), albeit to different levels. Damveld et al., (2008) had previously shown that *A. niger* strains with defective *ugmA* homologues had increased wall α-glucan content. We compared the expression level of α-glucan synthase (*ags1*) in wild type, *ugmA*Δ, and Af*niiA*(p)-*ugmA* strains growing on MMN and MMA (Fig. 3.5A). As expected, Af*niiA*(p)-*ugmA* grown on MMN (induction) had similar expression to wild type. Compared to the wild type parental strain, *ags1* expression was more than 4-fold higher in a *ugmA*Δ strain, or in the Af*niiA*(p)-*ugmA* on MMA (repression). We also compared the expression level of *β*-glucan synthase (FKS) in wild type, *ugmA*Δ, and Af*niiA*(p)-*ugmA* strains growing on MMN and MMA (Fig. 3.5B). Af*niiA*(p)-*ugmA* grown on MMN (induction) had almost similar expression to wild type. Compared to the wild type parental strain, FKS expression was about 2.5-fold decreased in a *ugmA*Δ strain, or in the Af*niiA*(p)-*ugmA* on MMA (repression).

3.3.5 Repression of Galf biosynthesis increases sensitivity to Caspofungin

Sensitivity to anti-fungal drugs of wild type and gene deletion strains on CM, *alcA*(p)-regulated strains on CMT and CM3G, and *niiA*(p)-regulated strains on MMN and MMA, was tested using a disc-diffusion drug-sensitivity assay. We compared Caspofungin (blocks wall β-1,3-glucan synthesis) with drugs that target ergosterol (Amphotericin B) and ergosterol biosynthesis (Itraconazole and Terbinafine). In addition, both 5-fluocytosine and Nikkomycin Z were assessed for their effect on wild type and Gal*f*-biosynthesis gene deletion strains. Neither of these latter drugs inhibited colony growth, but Nikkomycin Z delayed germination by several hours, causing spores to swell considerably before germ tube establishment (*data not shown*).

For clarity, Table 3.2 shows drug sensitivity values for Itraconazole and Caspofungin only, since in this assay Amphotericin B and Terbinafine results were comparable to

Itraconazole. Sensitivities of deletion and regulated expression strains are presented as an index compared to wild type on the same medium. Values greater than 1.0 indicate strains and conditions associated with drug hypersensitivity. Statistical analysis of the raw data and comparison to sensitivity indices showed that an index difference of >0.2 correlated with statistical significance. Fig. 3.6 shows representative results related to those in Table 3.2, where gene transcription level was controlled by *alcA*(p).

Expression levels of the Gal*f* biosynthesis genes did not significantly affect sensitivity to Itraconazole. Caspofungin sensitivity was increased for all three Gal*f* biosynthesis gene-deletion strains compared to wild type. Similarly, the *alcA*(p)- and *niiA*(p)-regulated strains were hypersensitive to Caspofungin when grown on their respective repression media (Table 3.2, Fig. 3.6). When these genes were over-expressed on CMT, the *alcA*(p)-*ugmA* strain was more sensitive to Caspofungin, but the regulated *ugeA* and *ugtA* strains were less sensitive. Growth of these strains on MMN (expression, but not overexpression) did not affect drug sensitivity. Taken together, the hyphal wall Gal*f* content (Fig. 3.4) was consistent with our expectations for the Caspofungin sensitivity (Table 3.2) of *ugmA* deleted and repressed strains.

3.4. Discussion

Deletion of any of three sequential-acting genes in the Gal*f* biosynthesis pathway causes similar defects in *A. nidulans* hyphal morphogenesis and colony development (El-Ganiny et al., 2008; El-Ganiny et al., 2010; Afroz et al., 2011) and in wall surface structure, force compliance, and adhesion (Paul et al., 2011). Gal*f* forms the side chains of many glycoconjugates (Latgé, 2007; Latgé, 2009) but its role(s) in wall formation and maturation are still far from understood. We expected that wild type levels of Gal*f* biosynthesis would be important for Caspofungin resistance because we had previously found that the walls Gal*f* deletion strains were structurally compromised (Paul et al., 2011). To test this we compared the drug sensitivity of gene deletion and wild type with regulated Gal*f*-biosynthesis strains. This is the first study to explore the roles of Gal*f* biosynthesis proteins on drug sensitivity of *A. nidulans* strains using the *alcA* and *niiA* promoters, and the first to examine the effect of regulating genes in the Gal*f* biosynthesis pathway. We expected that the products of these

genes would have similar effects on sensitivity to antifungal compounds that targeted cell walls but not to those that targeted other aspects of fungal physiology. Consistent with this, we found increased echinocandin sensitivity for the deletion strains and repressed strains, but no significant change for compounds affecting ergosterol or its biosynthesis.

3.4.1. Altering Galf biosynthesis gene expression level affects wall formation, colony growth, and development

The phenotypes of strains deleted or repressed for Gal*f* biosynthesis pathway genes were generally comparable. Repression of *alcA*(p)-*ugmA* with 3 % glucose (CM3G) and of *niiA*(p)-*ugmA* with ammonium (MMA) both caused colony and hyphal defects comparable to the *ugmA*Δ strain (El-Ganiny et al., 2008). Consistent with our RT-PCR and qPCR results, this is strong evidence that our regulatable promoter strains were functioning as expected. Similar results have been found for regulated histone deacetylase (*rpdA*) controlled by *alcA*(p) and *xylP*(p) (Tribus et al., 2010), and repression of protein kinase C (*pkcA*) on hyphal growth, wall thickness, and antifungal compound sensitivity (Ronen et al., 2007).

Gene-deletion and gene-repression phenotypes were qualitatively similar in most respects. However, for each of the Gal*f* biosynthesis genes considered in this study, *alcA*(p)-repressed strains sporulated better than the comparable deletion strains, and their hyphal walls were half the thickness of the respective deletion strains. These anomalies prompted us to repeat our studies on all three genes using *niiA*(p)-regulation which is repressed by ammonium. Results for colony growth and development regulated by the *niiA*(p) were comparable to those for *alcA*(p), consistent with the phenotypes were caused by changes in gene expression level. Overexpression of *alcA*(p)-*ugmA* on CMT also caused a hyper-branching phenotype that slightly reduced colony growth rate. Taken together, repression *vs* deletion morphology, and (over)expression *vs* wild type phenotypes were generally similar.

In *A. niger*, mutation of *ugm1* is associated with an increase in wall alpha-glucan content (Damveld et al. 2008). We tested whether there was a comparable relationship between Gal*f* and alpha-glucan in *A. nidulans* using qPCR to compare alpha-glucan synthase (*ags1*) levels. Both the *ugmA*Δ and *alcA*(p)-*ugmA* strain grown on repression medium had about four-fold increases in *ags1* expression. The MOPC104E mAb has previously been used

for an α-glucan dot blot assay, however to date we have been unable to replicate these results at least with immunofluorescence. The function of *Aspergillus* wall α-glucan is not yet well understood (He and Kaminskyj, *in preparation).* Notably, a triple *AGS* mutant in *A. fumigatus* was found to lack α-1,3-glucans (Henry et al., 2011). This triple deletion strain had a wild type phenotype on solid medium, suggesting that α-1,3-glucans may be dispensable for *A. fumigatus* vegetative growth (Henry et al., 2011) at least under these conditions.

3.4.2. Altering Galf biosynthesis-gene expression level affects Caspofungin sensitivity

We compared sensitivity of wild type, Gal*f* biosynthesis-gene deletion strains, and Gal*f* biosynthesis-regulated strains for their sensitivity to Caspofungin compared to drugs that target fungal membranes via ergosterol or ergosterol-biosynthesis. In this study, sensitivity to Itraconazole was typical of other membrane-targeting drugs, and was not related to Gal*f* biosynthesis gene presence or function. Therapeutically, *Aspergillus* species are reported to be resistant to Itraconazole (Erjavec et al., 2009), making it a useful control treatment. Statistical analysis compared average radii of growth inhibition, presented as an index of sensitivity with respect to wild type.

All of the gene deletion strains were significantly more sensitive than wild type to Caspofungin, consistent with our previous AFM studies on the deletion strains that showed defects in wall architecture and strength (Paul et al., 2011). For *ugmA* strains regulated by *alcA*(p) and *niiA*(p), colonies grown in repression conditions were at least as Caspofungin-sensitive as the knockout strains. Since we showed that deletion or repression of *ugmA* decreased *fksA* expression, this might contribute to Caspofugin sensitivity. Unexpectedly, colonies with over-expressed *alcA*(p)-*ugmA* were also significantly more sensitive to Caspofungin than wild type. This is consistent with the abnormal width and branching of overexpressed *alcA*(p)-*ugmA* hyphae, but the cause is not known.

Unlike *ugmA*, although both *ugeA* and *ugtA*, *alcA*(p)- and *niiA*(p)-repression caused Caspofungin hypersensitivity, the *alcA*(p)-overexpressed *ugeA* and *ugtA* strains were significantly less sensitive to Caspofungin. Consistent wit this, increasing *Mycobacterium ugmA* expression was reported to increase resistance to isoniazid (Richards et al., 2009). Gal*f* biosynthesis genes have both shared and divergent functions in cell wall metabolism.

3.4.3 Effect of gene deletion versus gene repression

We had expected that gene deletion and repression phenotypes would be similar for most aspects of colony and cell morphometry, since net UgmA and UgtA activity should be substrate-limited and to our current knowledge the only role of Gal*f* is in the cell wall. Contrast enhancement of the RT-PCR results in Fig. 3.1 showed that transcription was not abolished on gene repression media. Similarly gene over-expression was expected to have little effect due to substrate limitations, but found that Caspofungin sensitivity decreased for *alcA*(p)-overexpression of *ugeA* and *ugtA*. Transcript stability and translation of *ugmA* mRNA has not been explored in this study.

Galactose metabolism genes are clustered in *Saccharomyces cerevisiae* (Slot and Rokas, 2010). In *A. nidulans* the *ugmA* and *ugtA* coding sequences are AN3112 and AN3113, respectively, but the other genes in its Leloir pathway are not clustered. Gene product interaction is important for many pathways, e.g. signal transduction, reviewed in Keshet and Seger (2010). Surface topography and charge mediate protein-protein interactions. The surface of a selectable marker product will be unlike the gene product it replaces, so it cannot participate in wild type pathway interactions. In contrast, suppression of gene expression, even to 1 % of wild type level as estimated for *alcA*(p)- and *niiA*(p)-*ugmA* repression in this study, could lead to a small amount of wild type protein. Consistent with this, some aspects of the repression morphometry phenotypes were less severe than the deletion strains. The *alcA*(p)-overexpression drug sensitivity phenotypes also suggest that modulating wild type gene product abundance might have subtle effects.

In sum we have shown that the *alcA*(p)- and *niiA*(p)-regulated control of Gal*f* biosynthesis provides novel information about the role of this pathway in *A. nidulans*. In general, the gene repression and gene deletion phenotypes were comparable for colony growth and morphology, and overexpressed strains resembled wild type. That this was not always so, suggests possible interactions with other aspects of cell wall synthesis or maintenance. Notably, deletion and repression phenotypes were significantly more sensitive to Caspofungin, suggesting that as proposed in Paul et al. (2011), their walls are significantly less robust. We remain hopeful that an inhibitor of this pathway may be therapeutically beneficial.

Acknowledgements

SGWK and DARS are pleased to acknowledge shared funding from the Canadian Institutes of Health Research Regional Partnership Program and individual funding from the Natural Sciences and Engineering Research Council (NSERC) of Canada Discovery Grant program. AME thanks the Egyptian Ministry of Higher Education for her Fellowship. KA thanks the University of Saskatchewan (UofS) for a UGS postgraduate scholarship. SA thanks the UofS for a Graduate Equity scholarship and a UGS. We thank Merck for their gift of Caspofungin. Fungal Genetics Stock Center archives fungal strains and related resources. , for the gift of L10 and L99 monoclonal anti-Gal*f* antibodies were a gift of Prof. Frank Ebel, University of Munich. The *alcA*(p) plasmid was a gift from Dr. Loretta Jackson-Hayes, Rhodes College, Memphis TN. We thank University of Saskatchewan Department of Biology Dr. Peta Bonham-Smith and Chad Stewart for assistance with the qPCR. Tom Bonli, Department of Geological Sciences, University of Saskatchewan provided excellent SEM technical assistance.

Table 3.1: Colony and hyphal characteristics [a] of wild type and deletion strains grown on CM, and wild type and *alcA*(p)-regulated *Aspergillus nidulans* galactofuranose biosynthesis strains grown on over-expression (CMT) and repression (CM3G) media.

Character	Expression (medium)	Wild type	*ugmA*	*ugeA*	*ugtA*
Colony	Neutral (CM; wild type, Δ)	17 ± 0.4^{f}	4 ± 0.2^{g}	5 ± 0.2^{g}	4 ± 0.2^{g}
diameter	Overexpression (CMT)	22 ± 0.5^{f}	17 ± 0.6^{g}	21 ± 0.5^{f}	16 ± 0.2^{g}
(mm)[b]	Repression (CM3G)	16 ± 0.4^{f}	4 ± 0.2^{g}	5 ± 0.2^{g}	4 ± 0.1^{g}
Spores	Neutral (CM; wild type, Δ)	107 ± 15^{f}	0.2 ± 0.1^{g}	0.4 ± 0.1^{g}	1.3 ± 0.2^{g}
/colony	Overexpression (CMT)	12.4 ± 1^{f}	8.2 ± 1^{g}	10.8 ± 1^{fg}	13.8 ± 4^{f}
(x 10^{6})[c]	Repression (CM3G)	38 ± 11^{f}	0.6 ± 0.1^{g}	3.0 ± 0.6^{g}	3.8 ± 0.1^{g}
Hyphal	Neutral (CM; wild type, Δ)	2.7 ± 0.4^{f}	3.6 ± 0.6^{g}	3.6 ± 0.1^{g}	3.5 ± 0.1^{g}
width	Overexpression (CMT)	2.1 ± 0.03^{f}	3.0 ± 0.0^{g}	2.2 ± 0.04^{f}	1.9 ± 0.05^{h}
(µm)[d]	Repression (CM3G)	3.1 ± 0.05^{f}	3.7 ± 0.1^{g}	3.6 ± 0.1^{g}	3.4 ± 0.0^{g}
Basal cell	Neutral (CM; wild type, Δ)	26 ± 1^{f}	15 ± 1^{g}	14 ± 1^{g}	16 ± 1^{g}
length	Overexpression (CMT)	27 ± 1.2^{f}	14 ± 0.6^{g}	22 ± 1.2^{h}	25 ± 0.5^{h}
(µm)[d]	Repression (CM3G)	30 ± 1.7^{f}	17 ± 1.0^{g}	24 ± 1.1^{f}	16 ± 0.5^{g}
Cell wall	Neutral (CM; wild type, Δ)	54 ± 2^{f}	204 ± 10^{g}	123 ± 4^{h}	183 ± 1^{i}
thickness	Overexpression (CMT)	36 ± 2^{f}	42 ± 1^{g}	30 ± 1^{h}	40 ± 1^{g}
(nm) [e]	Repression (CM3G)	50 ± 2^{f}	82 ± 3^{g}	59 ± 2^{g}	83 ± 5^{g}

a Values are presented as mean ± standard error. For colonies grown on CM, values for wild type and *ugmA*Δ hyphae were taken from El-Ganiny et al. (2008); for *ugeA*Δ hyphae from El-Ganiny et al. (2010); for *ugtA*Δ hyphae from Afroz et al. (2011). Cellular characteristics were compared using a Kruskal-Wallis test, and shown for each characteristic to be significantly different at $P<0.05$. Differences for strains grown on CMT or CM3G were compared using a Kruskal-Wallis multiple comparison test. For each row, values followed by different letters (f-i) are significantly different at $P<0.05$.

b 10 colonies per strain/medium combination

c At least 3 colonies per strain/medium combination.

d 50 measurements per strain/medium combination. Hyphal width was measured at septa. Basal cell length was between adjacent septa.

e Measured from transmission electron micrographs for at least seven cross-sectioned hyphae per strain/medium combination, typically at three places per hypha where the cell membrane bilayer was crisply in focus.

Table 3.2: Antifungal drug sensitivity[a] index[b] comparing wild type, deletion, and *alcA*(p)-regulated Gal*f* biosynthesis strains.

Itraconazole[c]

Expression (medium)	Wild type	*ugmA*	*ugeA*	*ugtA*
Neutral (CM); wild type and Δ strains	1.0	1.1	1.1	1.1
alcA(p) Overexpression (CMT)	0.8	1.1	0.9	1.1
Repression (CM3G)	0.8	1.1	1.0	1.1
niiA(p) Expression (MMN)	1.0	1.0	1.1	1.0
Repression (MMA)	1.0	1.2	1.2	1.2

Caspofungin[c]

Expression (medium)	Wild type	*ugmA*	*ugeA*	*ugtA*
Neutral (CM); wild type and Δ strains	1.0	1.8	1.3	1.7
alcA(p) Overexpression (CMT)	1.0	1.3	0.5	0.7
Repression (CM3G)	1.0	1.9	1.5	1.8
niiA(p) Expression (MMN)	1.0	1.0	0.9	1.0
Repression (MMA)	1.0	1.9	1.6	1.7

a Drug sensitivity was measured using a disc diffusion assay (see Fig. 3.6). For Caspofungin, sensitivity was the radius (mm) of the clear zone with no visible growth (see arrows on Fig. 3.6B). Mean ± SE of two measurements for each of four biological replicates were used for statistical analysis (Kruskal-Wallis multiple comparison test). Data that used for statistical analysis were presented in supplemental Table B.

b Index sensitivity values are for each drug/strain combination compared to wild type on that medium. Wild type values are compared to CM with 1 % glucose. Gene deletion strains are compared to wild type on CM. Regulated strains are compared to wild type on the same medium. Index values > 1.0 are more sensitive than wild type. Index values that differed by > 0.2 were based on data that were significantly different.

c See Materials and Methods for details regarding drug dosage and medium formulation.

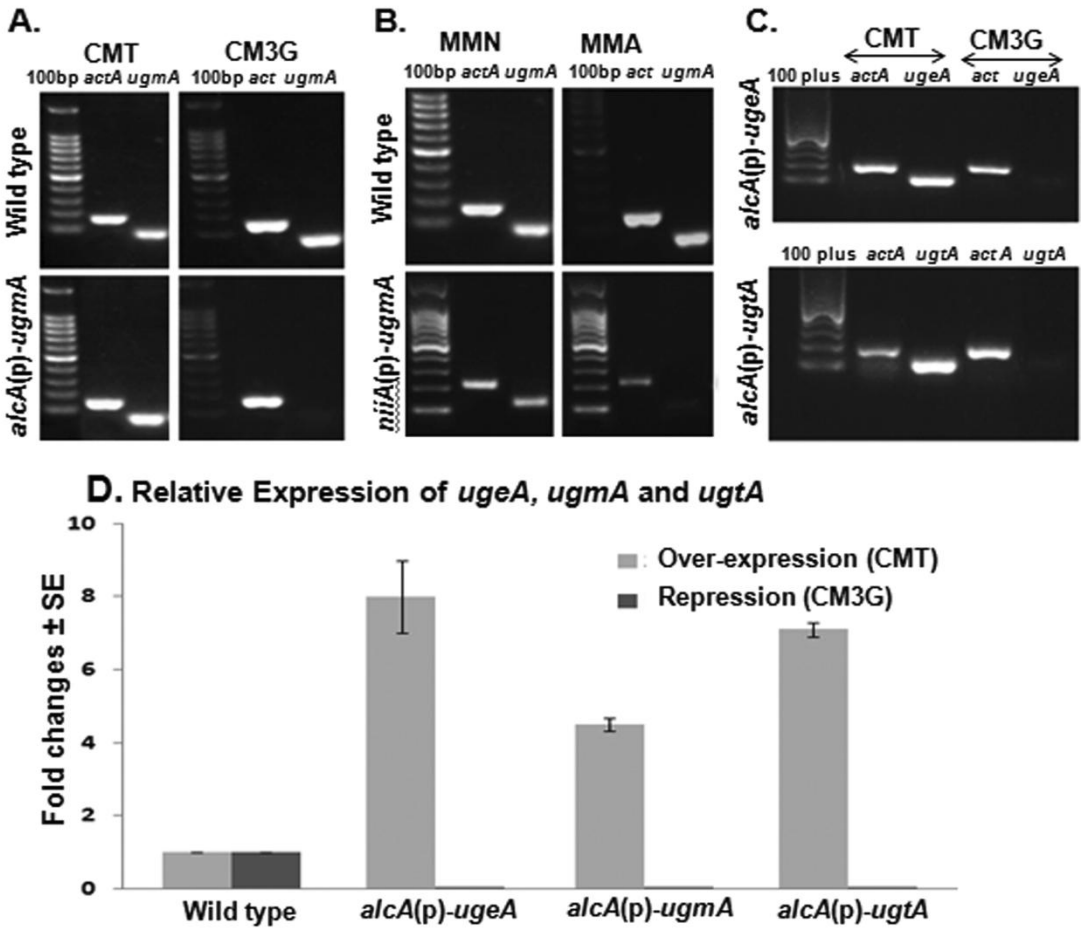

Fig. 3.1. Expression of *ugmA*, *ugeA*, and *ugtA* in wild type and regulated strains. A, B) RT-PCR showing *actA* and *ugmA* expression in wild type and *ugmA*-regulated strains. A) *alcA*(p)-*ugmA* grown on overexpression medium CMT, and repression medium CM3G. B) *niiA*(p)-*ugmA* grown on expression medium MMN, and repression medium MMA**.** C) RT-PCR showing the *ugeA* (upper panel) and *ugtA* (lower panel) expression in regulated strains grown on overexpression medium CMT, and repression medium CM3G. D) Relative expression using qPCR of *ugeA*, *ugmA*, and *ugtA* with respect to *actA* for wild type grown on CM, and *alcA*(p)-regulated strains grown on CM3G (repression) and CMT (over-expression).

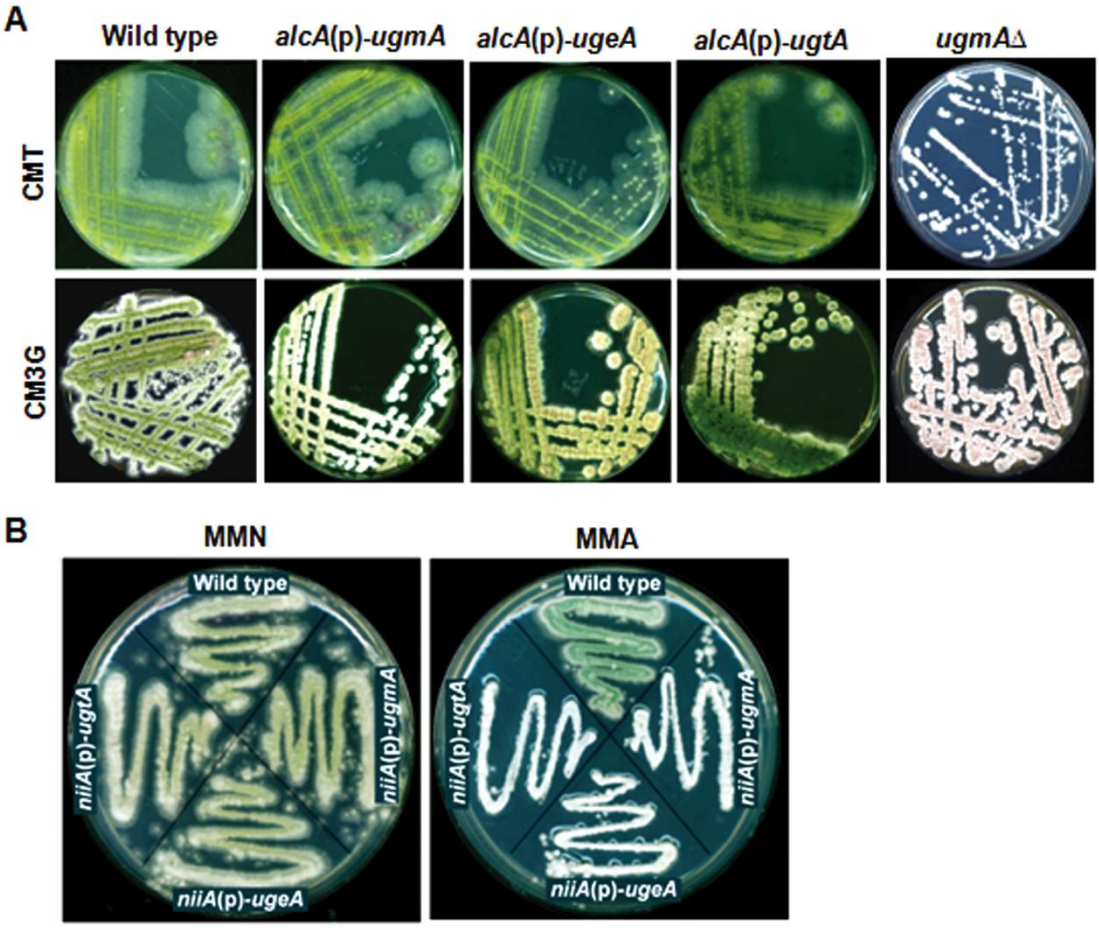

Fig. 3.2. Colony morphology of wild type and conditional promoter-regulated strains of *ugmA, ugeA, ugtA*. In each of A and B, the colonies are the same age. A) Wild type and *alcA*(p)-regulated strains grown on complete medium containing 100 mM threonine (CMT) or 3 % glucose (CM3G) as sole carbon sources, for gene over-expression or repression, respectively. B) Wild type and *niiA*(p)-regulated strains grown on minimal medium containing nitrate (MMN) or ammonium (MMA) for gene expression or repression, respectively.

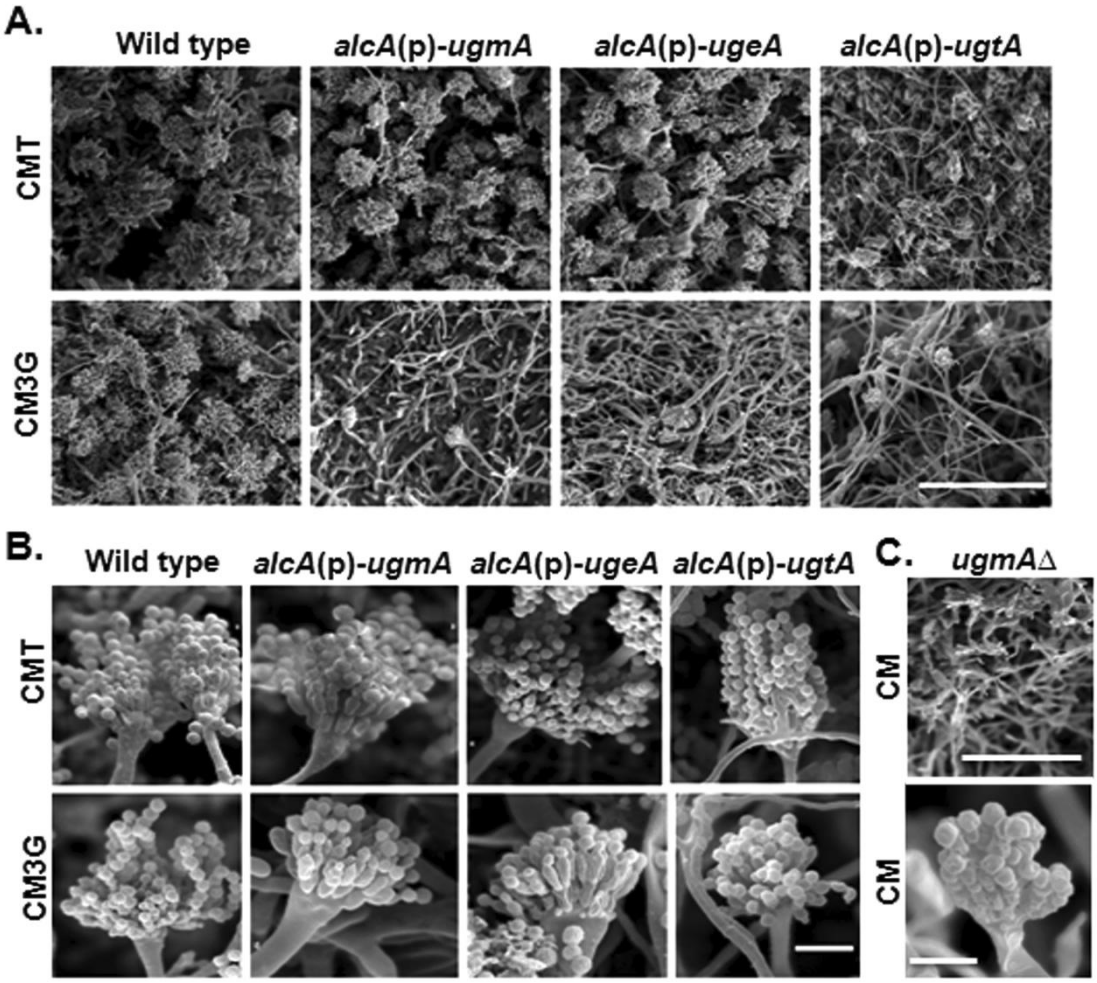

Fig. 3.3. Scanning electron micrographs showing: colony (A), and conidiophore (B) phenotype for wild type and *alcA*(p)-regulated *ugmA*, *ugeA*, and *ugtA* strains grown on CMT for overexpression and CM3G for repression. C) Colony and conidiophores of *ugmA*Δ on CM. On CMT media, the *alcA*(p) strains have abundant conidiophores with long chains of spores similar to wild type strain. On CM3G media, *alcA*(p)-*ugmA*, *alcA*(p)-*ugeA*, *alcA*(p)-*ugtA* produced many fewer conidiophores similar to *ugmA*Δ strain. Scale bar is 100µm for A & C (upper panel) and 10 µm for B & C (lower panel).

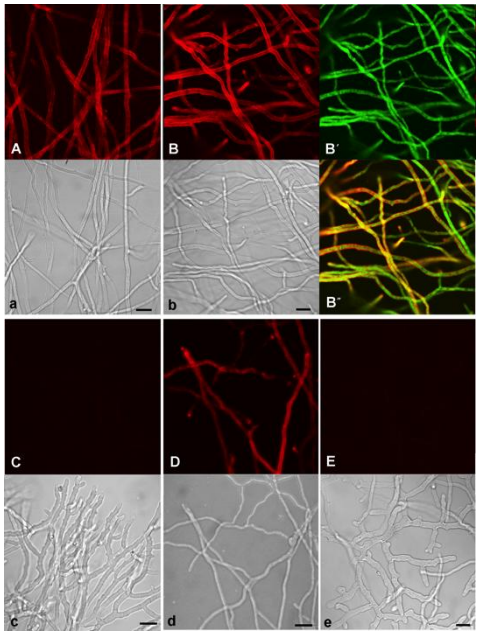

Fig. 3.4. Galactofuranose immunolocalization in *Aspergillus nidulans* hyphae using the L10 monoclonal antibody. (A) wild type, B) UgmA-GFP, C) *ugmA*Δ, D) *niiA*(p)-*ugmA* grown on induction medium, E) *niiA*(p)-*ugmA* grown on repression medium. Lower case letters are corresponding brightfield images. B' shows UgmA-GFP distribution, which is cytoplasmic, as expected. B" shows a merge of B and B'. Bars = 10 μm.

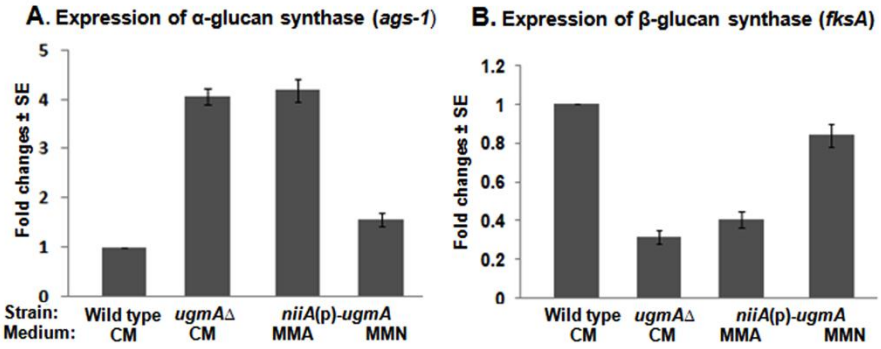

Fig. 3.5. The expression of α-glucan synthase (*ags1*) and β-glucan synthase (*fksA*) is affected by galactofuranose biosynthesis. Quantitative PCR results for *ags1* (A) and *fksA* (B) expression (as fold changes with respect to *actA* ± SE) for wild type, *ugmA* deletion, and *ugmA*-regulated strains.

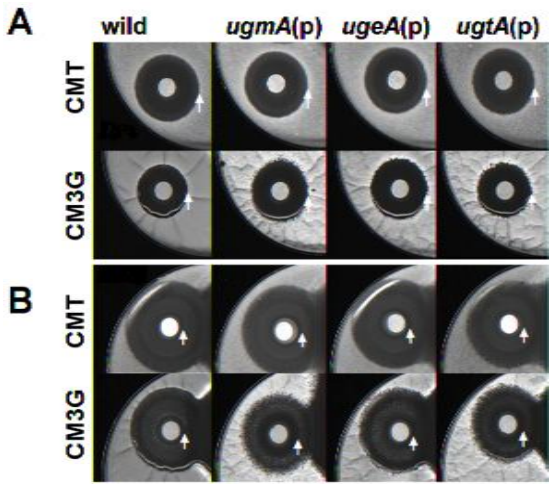

Fig. 3.6. Response of wild type and *alcA*(p)-regulated *ugmA, ugeA, and ugtA* strains to A) Itraconazole and B) Caspofungin. The *alcA*(p)-regulated genes were overexpressed by growth complete medium containing 100 mM threonine (CMT), and repressed by growth on complete medium containing 3% glucose (CM3G). Arrows indicate the edge of the zone with no visible growth, from where diameter was measured. On Caspofungin, sensitivity is measured at the innermost clear zone.

Supplemental Table A: Strains, primers and plasmids used in this study

Strains

Name	Description	Genotype
A1100[a]	Wild type	*A. fumigatus* AF293
A1149[a]	*A. nidulans*	*pyrG89; pyroA4; nkuA::argB*
AAE1[b]	*A. nidulans*	*pyrG89:N. crassa pyr4+; pyroA4; nkuA::argB*
AAE2[b]	*A. nidulans ugmAΔ*	AN3112*::AfpyrG; pyrG89; pyroA4; nkuA::argB*
AAE5[c]	*A. nidulans ugeAΔ*	AN4727::*AfpyrG*; *pyrG89; pyroA4*, *nkuA::argB*
ASA1[d]	*A. nidulans ugtAΔ*	AN3113::Af*pyrG*; *pyrG89*; *pyroA4*; *nkuA* :: *argB*
AAE12[e]	*A.nidulans alcA*(p)-*ugmA*	*ugmA*p*::pyrG:alcA*p:*ugmA*; *pyrG89; pyroA4; nkuA::argB*
AAE13[e]	*A. nidulans alcA*(p)-*ugeA*	*ugeA*p*::pyrG:alcA*p:*ugeA*; *pyrG89; pyroA4; nkuA::argB*
ASA4[e]	*A. nidulans alcA*(p)-*ugtA*	*ugtA*p*::pyrG:alcA*p:*ugeA*; *pyrG89; pyroA4; nkuA::argB*
AKA10[e]	*A. nidulans niiA*(p)-*ugmA*	*ugmA*p*::pyrG:niiA*p:*ugmA*; *pyrG89; pyroA4; nkuA::argB*
AKA11[e]	*A. nidulans niiA*(p)-*ugeA*	*ugeA*p*::pyrG:niiA*p:*ugeA*; *pyrG89; pyroA4; nkuA::argB*
AKA12[e]	*A. nidulans niiA*(p)-*ugtA*	*ugtA*p*::pyrG:niiA*p:*ugeA*; *pyrG89; pyroA4; nkuA::argB*

Primers Sequence 5`→3`

Promoter exchange *alcA*(p)

Ame115[e]	*ugmA*F	TCCTATCACCTCGCCTCAAAATGCTTAGTCTAGCTCGCAAGAC
Ame 23[b]	*ugmA* R	GCCTGCACCAGCTCCCTGCGCCTTATTCTTAGCAAA
Ame 1[b]	UpugmAF	GACTCTTGAGATTTGCTTGGGTCTC
Ame114[e]	UpugmAR	TCAGTGCCTCCTCTCAGACAGAGAAGAGAGCGAAGCTGCAG
Ame118[e]	Promoter F	CTGTCTGAGAGGAGGCACTGA
Ame119[e]	PromoterR	TTTGAGGCGAGGTGATAGGA
Ame116[e]	ugmAFusF	GTAGTTGACAAGCATACGGAGTACTC
Ame117[e]	ugmAFusR	GGACCAGTAGGGACCTTCCT
Ame120[e]	ugeAF	TCCTATCACCTCGCCTCAAAATGCCTTCTGGATCTGTCCT
Ame 48[c]	ugeA R	TTATTTCTTGAGCTGTTCCAGC
Ame 41[c]	UpugeA F	CTCCTATGGTATGTCTCTTCCAACTT
Ame121[e]	UpugeA R	TCAGTGCCTCCTCTCAGACAGGGTGAATGTGAATTGAATGCAG
Ame122[e]	ugeAFus F	TGTTACTTTAGGCCCGCAAG
Ame123[e]	ugeAFus R	GTCCACAGCCACAGATCCTC
SA1[d]	Up ugtA F	AAATAATATCTGCTTCGACCCACA
SA67[e]	UpugtA R	TCAGTGCCTCCTCTCAGACAGTTTGAGAGCGCGAGCTTG
SA71 [e]	ugtAF	TCCTATCACCTCGCCTCAAAATGAGCAGCTCCGAAGAGAA

SA31 [d]	ugtA R	TTAAGCATTGCCAGTACTGGC
SA5 [d]	ugtA Fus F	ATAGTGACAATAATTTTCTCCAGAGAA
SA69 [e]	ugtA Fus R	GGAATCGGGAGCGTAGCT
Ame134 [e]	Midpromoter F	GTGTTTGGTGTTGCCAAAGAC

Promoter exchange *niiA*(p)

KA114[e]	niiAF(PyrGTail)	GAGTATGCGGCAAGTCATGAGTCGGTATCGATTGAAGGAAAC
KA115[e]	niiA R	CCAGTATGGTACCACAGCTCAT
KA117[e]	UgmAF(NiiATail)	ATGAGCTGTGGTACCATACTGGATGCTTAGTCTAGCTCGCAAGA
KA118[e]	UgeA F(NiiATail)	ATGAGCTGTGGTACCATACTGGATGCCTTCTGGATCTGTCCT
KA116[e]	UgtA F(NiiATail)	ATGAGCTGTGGTACCATACTGGATGAGCAGCTCCGAAGAGAA

qRT-PCR

Ame 84[e]	*ugm* F	CGTTCCCAGCTTTCAGGATA
Ame 85[e]	*ugm* R	CTTTGCAGCACCCAATCC
Ame100[e]	*act* F	TTCGGGTATGTGCAAGGC
Ame101[e]	*act* R	TCGTGACAACACCGTGCT
SE11[e]	*FKS* F	GTGTGGTCCGTTTCGCTATT
SE12[e]	*FKS* R	GCTCAAGAAGGATGCCACTC
SE15[e]	*ags1*F	ACGCTCTTCCTCGCACTG
SE16[e]	*ags1*R	GAGGTTATGGCATAGGTTGTG

Plasmids

p*alcA*(p)[f]	pGEM, *alcA*(p), Af*pyrG* ampR

[a] Fungal Genetics Stock Center www.fgsc.net.

[b] El-Ganiny et al. (2008)

[c] El-Ganiny et al. (2010)

[d] Afroz et al. (2011)

[e] This study.

[f] Dr. Loretta Jackson-Hayes, Rhodes College, Memphis TN.

Supplemental Table B: Antifungal drug sensitivity[1] comparing wild type, deletion, and *alcA*(p)-regulated Gal*f* biosynthesis strains.

Itraconazole

Expression (medium)	Wild type	*ugmA*	*ugeA*	*ugtA*
Neutral (CM); wild type and Δ strains	7.0 ± 0.3 [a]	7.8 ± 0.2 [a]	7.5 ± 0.2 [a]	7.4 ± 0.1[a]
alcA(p) Overexpression (CMT)	8.3 ± 0.3 [a]	8 ± 0.2 [a]	6.6 ± 0.2 [b]	7.6 ± 0.1[a]
Repression (CM3G)	7.0 ± 0.1[a]	7.6 ± 0.2 [a]	7.3 ± 0.2 [a]	7.8 ± 0.3[a]
niiA(p) Expression (MMN)	7.0 ± 0.2[a]	7.1 ± 0.1 [a]	7.0 ± 0.2 [a]	7.0 ± 0.1[a]
Repression (MMA)	6.8 ± 0.2[a]	8.0 ± 0.1 [a]	7.8 ± 0.2 [a]	8.0 ± 0.1[a]

Caspofungin

Expression (medium)	Wild type	*ugmA*	*ugeA*	*ugtA*
Neutral (CM); wild type and Δ strains	3.5 ± 0.05[a]	6.3 ± 0.2[b]	4.5 ± 0.6[c]	6 ± 0.2[b]
alcA(p) Overexpression (CMT)	4.3 ± 0.2[a]	4.5 ± 0.1[a]	1.7 ± 0.1[c]	3.4 ± 0.2[d]
Repression (CM3G)	3.4 ± 0.1[a]	6.8 ± 0.2[b]	2.8 ± 0.2[c]	6.2 ± 0.2b[b]
niiA(p) Expression (MMN)	3.4±0.1[a]	3.34±0.1 [a]	3.1±0.2 [a]	3.47±0.1 [a]
Repression (MMA)	3.1±0.1[a]	5.56±0.1[b]	5.21±0.1[c]	5.9±0.1[bc]

1 Drug sensitivity was measured using a disc diffusion assay (see Fig. 3.6). For Caspofungin, sensitivity was the radius (mm) of the clear zone with no visible growth (see arrows on Fig. 3.6B). Mean ± SE of two measurements for each of four biological replicates were used for statistical analysis (Kruskal-Wallis multiple comparison test). For each row, values followed by different letters (a-c) are significantly different at $P<0.05$.

Supplemental information:

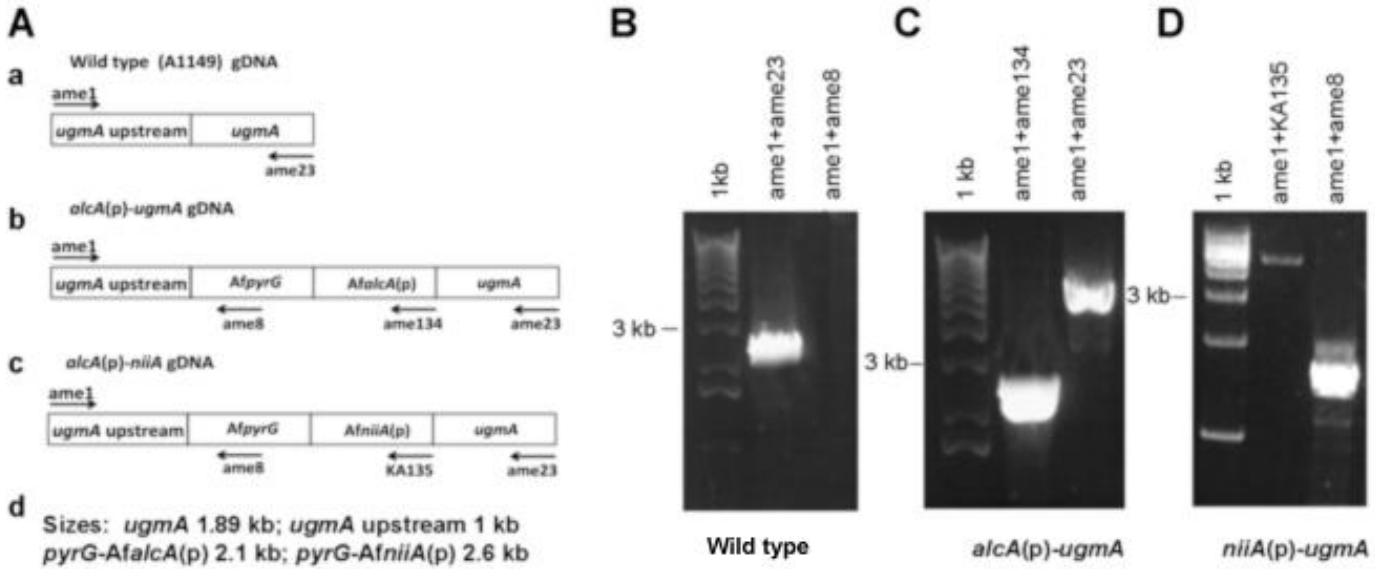

Supplemental Figure A.

Promoter exchange for *ugmA*.

A) Cartoon showing gDNA for a) wild type, b) *alcA*(p), c) *niiA*(p), including position of primers used for confirmation PCR. d) Expected sizes for amplicons using the primer pairs in a-c.

B-D) Confirmatory PCR using gDNA template from B) wild type A1149, C) *alcA*(p)-*ugmA*, and D) *niiA(*p)-*ugmA*.

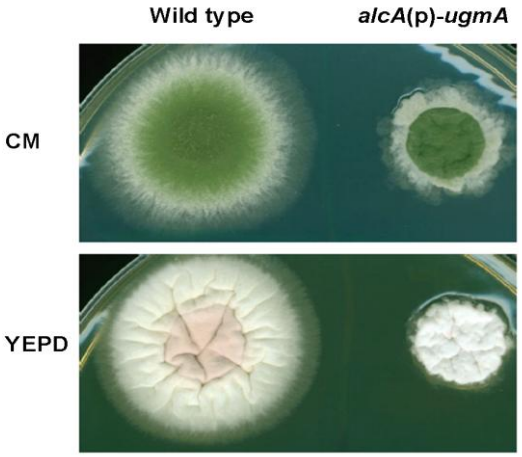

Supplemental Figure B. Growth and conidiation of Wild type and *alcA*(p)---*ugmA* strains on CM and YEPD

CHAPTER 4

Aspergillus nidulans cell wall composition and function change in response to hosting several *Aspergillus fumigatus* UDP-galactopyranose mutase activity mutants.

This Chapter demonstrates how modification of *A. nidulans* UDP-galactopyranose mutase leads to changes in cell wall α-glucan and β-glucan content, hyphal surface adhesion and response to antifungal drugs. The manuscript has been accepted for publication on 2, December, 2013 as ***Aspergillus nidulans* cell wall composition and function respond to hosting several *Aspergillus fumigatus* UDP-galactopyranose mutase activity mutants** in **PLoS One** by **Md Kausar Alam***, Karin E. van Straaten, David A. R. Sanders and Susan GW Kaminskyj, 2013.

*Correcsponding author

This Chapter was based on our hypothesis ``Strains lacking UgmA or hosting mutated UgmA will have significantly altered carbohydrate content in their cell wall compared to the wild type strain. These UgmA defective strains will also have less or no Gal*f* in their cell wall. The objectives of the research in this Chapter were

1. Characterization of structurally important amino acid residues of *Af*UgmA using *A. nidulans* as a host.
2. To explore the role of Gal*f* in *A. nidulans* hyphal surface adhesion and response to antifungal drugs
3. To determine how modification of *A. nidulans* UDP-galactopyranose mutase leads to changes in cell wall α-glucan and β-glucan content
4. To determine the cell wall Gal*f* content in UgmA defective strains.

My contribution in this Paper: I designed and performed all the experiments mentioned in this manuscript except the enzyme kinetic study, which was performed by Dr. Karin van Straaten. I generated all the final figures and wrote the manuscript, which was edited by Dr. Kaminskyj, Dr. David Sanders and Dr. Karin van Straaten prior to submission. I am the corresponding author of this paper.

***Aspergillus nidulans* cell wall composition and function change in response to hosting several *Aspergillus fumigatus* UDP-galactopyranose mutase activity mutants.**

Md Kausar Alam*, Karin E. van Straaten, David A. R. Sanders, and Susan G.W. Kaminskyj

Department of Biology, University of Saskatchewan, 112 Science Place, Saskatoon, SK S7N 5E2, Canada.

*author for correspondence. Email: kausar.alam@usask.ca

Abstract

Deletion or repression of *Aspergillus nidulans ugmA* (An*ugmA*), involved in galactofuranose (Gal*f*) biosynthesis, impairs growth and increases sensitivity to Caspofungin, a β-1,3-glucan synthesis antagonist. The *A. fumigatus* UgmA (*Af*UgmA) crystal structure has been determined. From that study, *Af*UgmA mutants with altered enzyme activity were transformed into An*ugmA*Δ to assess their effect on growth and wall composition in *A. nidulans*. The complemented (An*ugmA*::wild type Af*ugmA*) strain had wild type phenotype, indicating these genes had functional homology. Consistent with in vitro studies, *Af*UgmA residues R182 and R327 were important for its function in vivo, with even conservative amino (R→K) substitutions producing An*ugmA*Δ phenotype strains. Similarly, the conserved *Af*UgmA loop III histidine (H63) was important for Gal*f* generation: the H63N strain had a partially rescued phenotype compared to An*ugmA*Δ. Collectively, *A. nidulans* strains that hosted mutated *Af*UgmA constructs with low enzyme activity showed increased hyphal surface adhesion as assessed by binding fluorescent latex beads. Consistent with previous qPCR results, immunofluorescence and ELISA indicated that An*ugmA*Δ and Af*ugmA*-mutated *A. nidulans* strains had increased α-glucan and decreased β-glucan in their cell walls compared to wild type and Af*ugmA*-complemented strains. Like the An*ugmA*Δ strain, *A. nidulans* strains containing mutated Af*ugm*A showed increased sensitivity to antifungal drugs, particularly Caspofungin. Reduced β-glucan content was correlated with increased Caspofungin sensitivity. *Aspergillus nidulans* wall Galf, α-glucan, and β-glucan content was correlated in *A. nidulans* hyphal walls, suggesting dynamic coordination between cell wall synthesis and cell wall integrity.

4.1 Introduction

The cell wall is essential for the survival of fungi in natural environments. In fungi, the cell wall is about one quarter of the average fungal biomass (Gastebois et al., 2009), and about a third of the fungal genome (~4000 genes) is involved in cell wall biosynthesis and maintenance (de Groot et al., 2009). Polysaccharides and glycoconjugates contribute to proper functioning of the cell wall and cell membranes that collectively form the interface between the fungal cell and its environment (Tefsen et al., 2012). Due to the importance of cell walls for fungal growth and host invasion, and the relative lack of conservation with animal cell components, the cell wall is expected to be a good source of potential antifungal targets (Bowman and Free, 2006; Aimanianda and Latgé, 2010)

Aspergillus fumigatus is considered to be the most important airborne, human pathogenic fungus (Latgé, 2001). *Aspergillus nidulans* is a closely related model species with easy molecular genetic manipulation (Todd et al., 2007a). Carbohydrate analysis of *A. fumigatus* and *A. nidulans* walls shows that both species have similar composition (Guest and Momany, 2000), ~40% each of α-glucan and β-glucan (Gastebois et al., 2009; Free, 2013). Despite decades of research characterizing fungal cell wall composition and structure (Bowman and Free, 2006; de Groot et al., 2009), many details remain poorly understood. Notably, recent evidence shows that fungal walls can be rapidly remodeled in response to environmental change (Kovács, 2013), adds another layer of complexity.

Galactofuranose (Gal*f*) has an important role in fungal wall maturation (El-Ganiny et al., 2008 & 2010, Afroz et al., 2011; Alam et al., 2012). Gal*f* is found in glycoconjugates that are important for survival or virulence of microorganisms including some bacteria, protozoa and fungi (; Pan et al., 2001; Beverley et al., 2005; Kleczka et al., 2007; Schmalhorst et al., 2008; Lamarre et al., 2009), but it is lacking in vertebrates. Since Gal*f* is absent from higher eukaryotes and is involved in growth or virulence of some bacteria and fungi, the enzymes involved in its biosynthesis are potential drug targets (Pan et al., 2001; Pedersen and Turco, 2003). Notably, loss of or reduction in wall Gal*f* following gene deletion or repression in *A. nidulans* correlated with increased caspofungin sensitivity *in vitro* (Afroz et al., 2011; Alam et al., 2012). *In vivo* pathogenicity studies related to wall Gal*f* are few, and to date are equivocal (Lamarre et al., 2009; Schmalhorst et al., 2008). We have characterized the Gal*f* biosynthesis

pathway in *A. nidulans* as a model system (El-Ganiny et al., 2008 & 2010, Afroz et al., 2011; Paul et al., 2011; Alam et al., 2012) and are extending this to *A. fumigatus* in preparation for future testing of antifungals.

UDP-galactopyranose mutase is the first committed enzyme in the Gal*f* biosynthesis pathway in both *A. fumigatus* (*Af*GlfA [Schmalhorst et al., 2008] also called *Af*UgmA [Lamarre et al., 2009]) and *A. nidulans* (*An*UgmA [El-Ganiny et al., 2008]). *Aspergillus nidulans* strains deleted for An*ugmA* have 500-fold reduced hyphal growth and spore production (El-Ganiny et al., 2008). UgmA is unique in *A. nidulans* and *A. fumigatus*, but is not essential in either species.

The crystal structure of *Af*UgmA has been determined (van Straaten et al., 2012). *Af*UgmA has conserved arginine residues, R182 and R327 that are important for function *in vitro*. In addition, H63 and F66 are expected to contribute to *Af*UgmA activity because the loop containing them changes position depending on the redox state of the FAD cofactor (van Straaten et al., 2012). Assessing the roles of these amino acids for the *in vivo Aspergillus* phenotype is expected to refine the *in vitro* characterization of UGM (van Straaten et al., 2012), since *in vitro* enzymatic studies might not be precisely comparable to their *in vivo* function (Garcia-Contreras et al., 2012), and because H63N mutant did not express sufficiently for *in vitro* characterization. Here we examined the *in vivo* effects of structurally and functionally important amino acid residues of *Af*UgmA using *A. nidulans* as a host system, comparing cell wall composition, hyphal surface adhesion and response to antifungal drugs.

4.2. Results

We used *A. nidulans* as a host for wild type (WT), wild type complemented (WC), and single amino acid mutants of *Af*UgmA to assess their effect on colony growth, wall composition, wall surface adhesiveness, and drug sensitivity. We hypothesized there would be concordance between *Af*UgmA function *in vitro*, and the *in vivo* phenotype; *in vivo* characterization provided additional information.

4.2.1 Fungal phenotype for mutations affecting *Af*UgmA activity

We generated an [An*ugmA*::wild type Af*ugmA*] complemented (WC) strain in *A. nidulans* to confirm functional homology, and for quantitative characterization that had not been done previously (El-Ganiny et al., 2008). The WC strain phenocopied wild type *A. nidulans* hyphal morphometry and colony development (Figure 4.1, Table 4.1, and Figure S7). Table 2 presents the relative enzyme activity of wild type and mutated UgmA strains, derived from data in Table 3 of (van Straaten et al., 2012). As expected, the R327K and R327A strains phenocopied the An*ugmA*Δ strain for spore formation, colony growth, and hyphal morphometry (Figure 4.1, Table 4.1). Reduced sporulation was due to fewer conidiophores and aberrant conidiophore formation (Figure S2), comparable to the An*ugmA*Δ strain. The R182K *in vivo* phenotype had improved sporulation compared to An*ugmA*Δ but not colony growth. There were no significant differences between the R182A and An*ugmA*Δ phenotypes (Fig. 4.1, Table 4.1). Sporulation in *A. nidulans* appears to have a less stringent requirement for Gal*f* content than does hyphal growth (Table 4.2).

H63 is expected to contribute to *Af*UgmA activity because it is part of the flexible loop (loop III) above the *si*-face of the isoalloxazine ring that changes position due to the redox state of the FAD cofactor (van Straaten et al., 2012). Structural analysis suggests H63N might keep UgmA loop III in the conformation similar to that seen in prokaryotic UGMs (Beis et al., 2005; Partha et al., 2009; Sanders et al., 2011) and the reduced *Af*UgmA structure (van Straaten et al., 2012) by forming an H-bond with Q458. The *in vitro* H63N enzyme activity was not tested because of low protein expression for this construct. Notably, the *in vivo* H63N phenotype was comparable to that of R182K (Table 1, Figures 4.1 and S2), implying that the H63N strain likely would show a similar enzyme activity to R182K. This suggests that the flexibility of loop III plays a role in the catalytic activity of AnUGM. As with R182K, the major improvement compared to An*ugmA*Δ was in sporulation. This is consistent with Gal*f* having multiple roles in the *Aspergillus* phenotype, with sporulation being more responsive to low levels of UgmA activity than hyphal morphology.

F66 is at the end of *Af*UgmA loop III and may control loop III flipping and consequently opening of the mobile loops depending on the redox state of the cofactor (van Straaten et al., 2012). The *Af*UgmA-F66A enzyme activity was almost double that of R182K (Table 2). *In vivo,* the F66A phenotype was relatively comparable to wild type (Table 4.1,

Figure 4.1) regarding sporulation (Figure S2) and hyphal morphometry, but restricted for colony diameter.

Together, these data show that *Af*UgmA R327 is critical for function *in vitro* and *in vivo*. H63, F66, and R182 each contribute to catalytic efficiency but to a much lesser extent. For all mutants, sporulation was less dependent on UgmA activity than hyphal or colony morphometry, consistent with the fact that *ugmA*Δ and R327A strains had limited sporulation. In sum, the *in vivo Af*UgmA mutant phenotypes correlated well with *in vitro* UgmA activity, and for H63N the *in vivo* data extended otherwise unobtainable characterization.

4.2.2 Loss of wall Gal*f* is associated with increased hyphal surface adhesion

We used modified fluorescent polysterne beads visualized with confocal microscopy to assess hyphal surface adhesiveness, as adapted from (Alam et al., 2012). The WT and WC hyphae had relatively fewer fluorescent beads attached compared to An*ugmA*Δ. Bead attachment for the strains with R182K, R182A, R327K, or R327A was similar to An*ugmA*Δ (Figure 4.2). Figure 4.2 used bead adhesion by the R327A strain to represent all of these latter mutant strains. For the F66A and H63N strains, bead attachment was slightly higher than wild type or WC strains but much lower than An*ugmA*Δ or the other mutant strains (Figure 4.2). The bead adhesion assay showed major changes in adhesion, but did not discriminate between subtle differences. It might be due change in surface hydrophobicity or charge. Atomic force microscope (AFM) force mapping might reveal these changes, but this is currently beyond our scope. However, our previous published paper showed using AFM force mapping that *ugmA*Δ strain hyphal wall surfaces had higher adhesion and reduced resilience compared to wild type *A. nidulans* walls (Paul et al., 2011).

4.2.3 *Af*UgmA active site mutations do not affect UgmA-GFP cytoplasmic distribution

El-Ganiny *et al.* showed that *An*UgmA-GFP was cytoplasmic and evenly distributed along hyphae, consistent with UgmA lacking a signal peptide (also suggested in Lamarre et al., 2009). To confirm that expression of wild type and mutated *Af*UgmA did not affect cytoplasmic distribution in *A. nidulans*, strains were C-terminal GFP-tagged under the control of the *ugmA* endogenous promoter (Figure S1). Previously, we had found that N-terminal

*An*UgmA-GFP abolished wild type UgmA function, since an RFP-UgmA strain had a An*ugmA*Δ phenotype (El-Ganiny and Kaminskyj, *unpublished*). The WC-GFP strain had WT hyphal and colony morphology, and abundant conidiation (*data not shown*), indicating that *Af*UgmA-GFP did not interfere with *A. nidulans* growth. The *A. nidulans* strains containing GFP-tagged R182A, R327A or H63N had compact colony growth, phenotypically similar to the respective untagged strains. GFP distribution in each strain was cytosolic, excluded from membrane-bounded organelles, and lacked a pronounced longitudinal gradient (Figure 4.3), consistent with wild type distribution of *An*UgmA in *A. nidulans* (El-Ganiny et al., 2010).

To confirm that the even GFP distribution was not due to cleavage of the GFP tag, we extracted total proteins from the wild-type and mutated GFP-tagged strains (WT, R182A-GFP, R327A-GFP, H63N-GFP and *Af*UgmA-GFP) strains, followed by separation of proteins using 10 % SDS-PAGE and western blotting with anti-GFP (Figure 4.3B). Notably, the great preponderance of signal was at 87 kDa, consistent with GFP-tagged UgmA, and essentially none was at 27 kDa, which would be consistent with cleaved GFP. The anti-GFP western blotted protein preparations from GFP-tagged mutant strains were consistent with wild type AnUgmA-GFP distribution (El-Ganiny 2010) and with *Af*UgmA-GFP distribution (Figure S6). This suggested that the phenotype effects of mutated *Af*UgmA constructs did not relate to alterations in sub-cellular distribution. We do not have an anti-UgmA, so we were unable to perform the complementary experiments to directly measure the intracellular UgmA levels *in vivo* in order to confirm the stability of *Af*UgmA.

4.2.4 Alteration in Gal*f* affects wall glucan composition in *A. nidulans*

Alam *et al.* 2012 showed using qPCR that gene expression of α-glucan synthase, *agsB* and β-glucan synthase, *fksA* were influenced by the level of An*ugmA* activity. However, synthase gene expression is not necessarily directly related to wall glucan content. We quantified cell wall α-glucan, β-glucan, and Gal*f* using ELISA (Table 4.2) and immunofluorescence (Figures 4.4-4.6) in WT, WC, mutated and An*ugmA*Δ strains.

Aspergillus nidulans WT and WC strains had strong Gal*f* immunolocalization in hyphal walls (Figure 4.4). The F66A strain had the highest level of hyphal wall Gal*f* immunofluorescence of any of the mutants, consistent with ELISA quantification (Table 4.2)

and with its relatively high *in vitro* UgmA activity (Table 4.2). The R182K and H63N strain hyphal wall Gal*f* immunofluorescence quantitation was half that of F66A (Figure 4.4), comparable to ELISA results (Table 4.2) showing Gal*f* content in these strains is 35-45 % of F66A. Low hyphal wall Gal*f* was consistent with phenotypic differences, showing concordance between wall composition and hyphal morphology (Figure 4.1, Tables 4.1, 4.2). WT, WC and F66A cell wall Gal*f* content in (Table 2) was correlated with sporulation (Table 4.1, Figs. 4.1, S2). The R327K, R327A, R182A strains lacked immunolocalizable Gal*f* and all aspects of their phenotype resembled the An*ugmA*Δ strain. Taken together, wall Gal*f* content was consistent with *in vitro Af*UgmA activity and with other aspects of hyphal and colony development phenotype.

Aspergilllus nidulans wild type and WC hyphal walls had relatively low α-glucan content (Table 4.2, Figure 4.5) compared to mutant and An*ugmA*Δ strains. This is consistent with our previous qPCR studies on gene expression (Alam et al., 2012), but was more nuanced regarding cellular distribution. Alpha-glucan staining was most pronounced in the older hyphal regions, and was undetectable at wild type and WC hyphal tips. The α-glucan immunofluorescence intensities were stronger in the R327K, R327A, R182K, R182A and An*ugmA*Δ strains (Figure 4.5), but again were substantially lower at hyphal tips (*not shown*). ELISA results for α-glucan (Table 4.2) were comparable to immunofluorescence quantification in older regions of the hyphae. In sum, wall α-glucan content of all the mutants and An*ugmA*Δ strains was influenced by alteration in Gal*f* and it was inversely correlated with UgmA enzyme activity levels (Table 4.2).

Aspergillus nidulans wild type and WC hyphal walls had relatively higher β-glucan levels than the mutants and An*ugmA*Δ strains (Figure 4.6, Table 4.2). The quantitative difference in β-glucan level between WT, WC, F66A and all other strains was more pronounced than for α-glucan or Gal*f*. ELISA results for β-glucan were consistent with immunofluorescence quantification, showing a decline in wall β-glucan content with decrease in UgmA enzyme activity levels (Table 4.2).

These data show the relative importance of *Af*Ugm amino acid residues in and near the active site is R327 > R182 ~ H63 >> F66. Clearly, *in vitro* enzyme and *in vivo* phenotype

analysis have strong complementarity. We plan to use phenotype analysis as part of our strategy to assess the efficacy of potential UgmA-inhibitor compounds.

4.2.5 Loss of *Af*UgmA activity leads to increased sensitivity to some antifungal compounds

If Gal*f* biosynthesis is to achieve its promise as an antifungal drug development target, most likely as a part of a combination therapy, strains with reduced *Af*UgmA should be expected to be more sensitive to antifungal compounds. We compared Caspofungin (β-glucan synthesis), Itraconazole (ergosterol synthesis), and Calcofluor White (chitin crystallization) sensitivity on all the strains (Table 4.2). Analysis of the raw drug sensitivity data showed that index values that differed by 0.2 were significantly different, as it had been seen in our previous studies (Alam et al., 2012). None of the mutations notably affected sensitivity to Calcofluor White. Strains with substantially reduced Gal*f* (R182 and R327 mutants) were significantly more sensitive to Itraconazole. Furthermore, Caspofungin sensitivity was significantly increased for all of the mutant strains compared to wild type, almost 2-fold for R327K and *AnugmA*Δ. Even F66A, which still had a substantially wild type hyphal and colony phenotype, and wall composition was significantly more sensitive to Caspofungin (Table 4.2).

4.3. Discussion

We used quantitative methods to correlate *in vitro* UgmA enzymatic function and *in vivo* fungal cell and developmental phenotype related to site-directed changes to conserved amino acid residues in the *Af*UgmA catalytic site. We were able to assess residues for which there was structural and *in vitro* enzymatic function information (van Straaten et al., 2012), as well as residues where enzymatic activity had not yet been assessed. These analyses provide a coherent picture of changes in *A. nidulans* related to the efficacy of an enzyme involved in an early step in Gal*f* biosynthesis in *Aspergillus* that affects wall composition-structure-function.

Previously we showed qualitatively that *A. fumigatus* Af*ugmA* restored wild type hyphal morphology in the *A. nidulans ugmA*Δ strain (El-Ganiny et al., 2008). We have extended that preliminary observation with quantitative assessment of colony phenotype and wall composition for *A. nidulans* whose native *An*UgmA had been replaced with wild type

*Af*UgmA or with *Af*UgmA constructs mutated in or near the enzyme active site. This approach provided a way to correlate structure and function of *Af*UgmA, regardless of whether gene products could be analyzed *in vitro*. According to van Straaten *et al.* (van Straaten et al., 2012), for *in vitro* enzymatic studies all the mutants (except H63N) were over-expressed, purified and studied, with no apparent changes in protein stability. There was no evidence of changes to the overall protein structure as the mutants crystallized under similar conditions and resulted in similar crystallographic structures (van Straaten et al., 2012). In addition, none of the mutations affected the cellular *Af*UgmA distribution assessed with GFP-tagging and anti-GFP immuno-blotting. These results are consistent with the effects we observed being due to changes in *Af*UgmA activity or other aspects of cellular interaction. Since all the mutants were expressed under endogenous An*ugmA* promoter to assess phenotype *in vivo*, it is also possible that these effects might be due to the instability of mutant protein. Although western blot showed the same level of fluorescence intensity for GFP tagged mutants and wild type *Af*UgmA against anti-GFP antibody, direct intracellular evaluation of these mutants and wild type *Af*UgmA stability *in vivo* is beyond our scope at this moment because of lacking an antibody directed against *Af*UgmA.

Comparing protein structure analysis and *in vitro* enzymatic activity of wild type *Af*UgmA with conservative (R→K) and non-conservative (R→A) mutants showed that R327 was essential to UgmA function (van Straaten et al., 2012). Structural data in (van Straaten et al., 2012) shows that R327 stabilizes the position of the diphosphates of the nucleotide sugar and facilitates positioning of the galactose for catalysis. The R327K mutation impaired enzyme function whereas the R327A mutation produced a strain with no UgmA activity detectable *in vitro* (Table 4.2, and van Straaten et al., 2012). Consistent with this, *A. nidulans* strains whose wild type *An*UgmA had been replaced with AfUgmA-R327A qualitatively and quantitatively resembled the An*ugmA*Δ strain. The role of R182 was slightly less critical than that of R327 (Table 4.2). R182 is important for sugar orientation related to catalysis, as well as for catalytic efficiency (van Straaten et al., 2012). When *Af*UgmA-R182K replaced the native *An*UgmA, the R182K strain showed significantly better growth and sporulation than An*ugmA*Δ, whereas the R182A strain resembled the An*ugmA*Δ deletion strain.

This is the first time that we have been able to partially rescue the An*ugmA*Δ phenotype by genetic means. Previously we had shown that low levels of Calcofluor White, or 1 M sucrose, partially remediated the An*ugmA*Δ defects, however this was only for morphogenesis of submerged hyphae, and not for sporulation (El-Ganiny et al., 2008). Similarly, the R182K strain showed that sporulation was more effectively remediated by low levels of Gal*f* than was hyphal morphogenesis. Gal*f* immunolocalization using EBA2 (El-Ganiny et al., 2008) vs L10 (Alam et al., 2012) shows substantially different localization patterns. EBA2 preferentially stained conidia, metulae and phialides, whereas L10 stained hyphae. Together these suggest that there are at least two different types of Gal*f*-containing compound in *Aspergillus* walls.

We also examined the roles of two amino acids that could be functionally important because they are part of loop III, which moves upon redox state of the cofactor (van Straaten et al., 2012). H63 is a highly conserved residue for prokaryotic and eukaryotic UGMs. The H63N construct expressed poorly *in vitro* so it had not been studied for *in vitro* enzyme activity. Histidine is positively charged at physiological pH whereas asparagine is polar but not charged. Correlating strain phenotype characteristics with estimates of UgmA activity suggested that the H63N strain UgmA activity would be comparable with the R182K strain. F66 is a highly conserved residue amongst eukaryotic UGMs. The *Af*UgmA F66A strain showed a 6.3-fold decrease in UgmA activity compared to wild type *Af*UgmA *in vitro* (Table 4.2). The *in vivo* F66A phenotype was similar to wild type indicates that *in vivo* function of UgmA does not impair at this level of decrease in *in vitro* activity. Our results further indicate that changes in *Af*UgmA loop III affect catalytic activity and that H63 is important but not critical for UGM activity.

Our previous work showed that deletion or down-regulation of any of three sequential genes in *A. nidulans* Gal*f* biosynthesis was associated with comparable reductions in hyphal growth rate and sporulation (El-Ganiny et al., 2008 & 2010, Afroz et al., 2011; Alam et al., 2012), with increased sensitivity to fungal wall-targeting compounds (Afroz et al., 2011; Alam et al., 2012), with changes in α-glucan and β-glucan synthase gene expression (Alam et al., 2012), and with changes in wall surface adhesion (Paul et al., 2011). Here we have correlated the effect of mutations in *Af*UgmA (transformed into *A. nidulans*) with

morphometry, with quantitative immunofluorescence, with ELISA quantification of wall carbohydrates, with changes in wall adhesiveness, and with sensitivity to anti-fungal compounds.

Notably, reductions in wall Gal*f* content correlated with increased wall α-glucan content (r^2=0.972, P<0.0001) and in decreased wall β-glucan content (r^2= 0.980, P=0.0001) shown in this study were consistent with increased *agsB* and decreased *fksA* expression (Alam et al., 2012). Not surprisingly, *A. nidulans* cell wall α-glucan and β-glucan content were also strongly correlated (r^2=0.993, P<0.0001). Given that in wild type cells α-glucan and β-glucan are each thought to comprise about 40 % of the *A. nidulans* wall (Gastebois et al., 2009; Free, 2013), this strongly suggests that the cell is metabolically constrained as to where it apportions metabolites for wall synthesis, so that increases in abundance of one major polymer must limit the resources available for synthesis of the others. However, this does not directly explain why engineered changes in Gal*f* content (perhaps 5 % of total [Lamarre et al., 2009]) are so strongly related to changes in α-glucan and β-glucan content. We suspect these will be coordinated through the cell wall integrity pathway, which is a focus of current research.

Decreased *fksA* expression and β-glucan content correlated with increased sensitivity to Caspofungin (r^2=0.855, P<0.0005), which is mechanistically satisfying. Notably, an *ugmA* overexpressed strain also showed Caspofungin hypersensitivity (Alam et al., 2012) suggesting that balanced expression of wall components is important for wild type phenotype and drug resistance.

The mutant (except F66A) and deletion strains also showed a smaller but still significant increase in sensitivity to Itraconazole. Previously using AFM force mapping (Paul et al., 2011) we had found that *ugmA*Δ strain wall surfaces were more force-compliant than wild type walls, suggesting that they had reduced resilience. Itraconazole targets ergosterol biosynthesis, and so is expected to affect membrane fluidity. It appears likely that a combination of wall and membrane defects is particularly difficult for a fungal cell to resist. Once UGM inhibitors have been developed, we expect that they will show enhanced efficacy if given in combination with amphotericin B as well as Itraconazole.

Compared to wild type, An*ugmA*Δ *A. nidulans* had higher adhesion to AFM Si_3N_4 probe tips (Paul et al., 2011). In addition, Af*ugmA*Δ strains have been shown to be highly adherent to pulmonary epithelial cells, to glass or plastic surfaces compared to wild type (Lamarre et al., 2009). Consistent with these previous results, An*umgA*Δ and mutant strains have increased hyphal adherence to latex beads compare to wild type strain (Figure 4.2). Higher adhesion (Lamarre et al., 2009) has been correlated with both higher and lower pathogenicity (Schmalhorst et al., 2008; Lamarre et al., 2009) but there are few studies of this type and further research is needed. This disparity could be due to lower growth rates in *Af*UgmA mutants, thus potentially also to lower tissue penetration.

Taken together, we have shown that fungal phenotype can provide useful estimates of functional information on the role of some amino acid residues, even though their mutant gene products were poorly expressed *in vitro* (i.e. H63N). Our results in this study suggest that UgmA activity correlated with hyphal phenotype: a < 7-fold decrease produced a wild type phenotype (wild type *Af*UgmA, F66A), ~20-fold decrease resulted in partial function (H63N and R182K), and a ≥ 70-fold decrease (R182A, R327K, R327A, AnUgmAΔ) was insufficient to synthesize a functional level of wall Gal*f*.

In conclusion, we have shown that reduced AfUgmA activity due to mutation did impair *A. nidulans* growth in a manner substantially similar to gene deletion and gene down-regulation. UgmA distribution was not affected by these manipulations. Loss or absence of Gal*f* increased wall α-glucan but reduced wall β-glucan (which were strongly correlated), and with increased hyphal surface adhesion and Caspofungin sensitivity. Thus, it seems that *A. nidulans* needs a balanced expression of UgmA (not high, not low [Alam et al., 2012]) to generate a resilient wall for normal growth and wall surface integrity. In the future, we anticipate that our approach will also be useful for assessing the effects of UgmA-targeting drugs (under development by the Sanders group).

4.4 Materials and methods

4.4.1 Strains, plasmids, and culture conditions

Strains, primers and plasmids are listed in Table S1. The *A. nidulans* strains were maintained on complete medium (CM) supplemented for nutritional markers as described in

(Kaminskyj, 2001). Bacterial strains were grown on LB with antibiotics as required (Table S1). All water was freshly prepared by 18 MegOhm ultrapure (Barnstead NanoDiamond).

4.4.2 Site-directed mutagenesis and overexpression of F66A-*Af*UGM

Site-directed mutagenesis of the F66A *Af*UGM mutant was performed using the QuikChange™ site-directed mutagenesis kit (Stratagene, Inc.) according to the manufacturer's protocol. Comparable methods were used for creating the other SDM strains (van Straaten et al., 2012). Over-expression vector pET22b harboring the Af*UGM* gene was used as the template DNA. The PCR mixture contained 50 ng of template DNA and 15 pmole of each primer. PCR amplification was carried out in a GeneAmp PCR PTC100 System. The original methylated plasmid was digested with *Dpn*I, then 2 µL of the reaction was used to transform competent *E. coli* Dh5α cells (Novagen). Ampicillin-resistant colonies were selected from the LB plates, and the specific mutation was verified by DNA sequencing. The mutant enzyme was overexpressed and purified as previously described (van Straaten et al., 2012).

4.4.3 Enzyme kinetics

Kinetic constants for F66A *Af*UGM mutant were determined as previously described (van Straaten et al., 2012a). A fixed concentration of *Af*UGM mutant protein (500 nM) was chosen so as to have less than 40% conversion to the product UDP-Gal*p*. Reactions were carried out with 0 – 300 µM of UDP-Gal*f* in a final volume of 100 µL 50 mM phosphate buffer pH 7.0 and 20 mM freshly prepared sodium dithionite. The incubations were carried out for 1 min at 37 °C then quenched with 100 µL *n*-butanol. The conversion of UDP-Gal*p* to UDP-Gal*f* was monitored at 262 nm using HPLC (Waters). The amount of conversion was determined by integration of the UDP-Gal*p* and UDP-Gal*f* peaks. The initial velocity was calculated from the substrate concentration and percentage UDP-Gal*p* conversion. Kinetic parameters were determined with GraphPad Prism software (GraphPad Software, San Diego, CA) using nonlinear regression analysis.

4.4.4 Mutagenesis and transformation

Strains used in this study are shown in Supplemental Table S1. The wild type (WT) and wild type complemented (WC) strains were compared with *Af*UgmA mutants R327K, R327A,

R182K, R182A, F66A and H63N, and with the An*ugmA*Δ strain. Af*ugmA* constructs for mutations in the *Af*UgmA active site and in *Af*UgmA loop III that had been used for structural studies (van Straaten et al., 2012) were used to generate An*ugmA* replacement constructs using fusion PCR (Figure S1) according to (Szewczyk et al., 2007). We used an Af*pyrG* selectable marker controlled by the α-tubulin promoter [*tubA*(p)-*pyrG*] to ensure a constitutive level of marker expression, whereas the wild type or mutated version of Af*ugmA* was controlled by their endogenous promoters (Figure S1). Constructs were transformed into wild type protoplasts (Szewczyk et al., 2007; Osmani and Oakley, 2006). Confirmation of the correct gene manipulations used genomic DNA (isolated as described in [Yang Y et al., 2008]) from putative transformant strains as a template for PCR (Figure S4) with combinations of primers as shown Suppl Table S1. Prior to phenotype analysis, genomic DNA from each *A. nidulans* strain was extracted. *ugmA* was amplified from these genomic DNA samples using PCR. Primers that we used to amplify *ugmA* target 100 bp upstream and 100 bp downstream (inside of *tubA* promoter) (Figure S1) of *ugmA*. PCR products were sequenced in order to confirm the expected construct generation and replacement. Fusion construction for replacement cassettes used primers that were ~50 bp inside of upstream and downstream primers from both sides. To confirm the correct insertion site, we used the outside pair of primers.

4.4.5 Colony growth, sporulation and surface adhesion

Colony characters were examined as in (El-Ganiny et al., 2008). Strains were streaked on CM and incubated for 3 d at 28 °C to give isolated colonies. The diameter of ten colonies/strain was measured to the nearest millimeter using a dissection microscope. The number of spores produced per colony was counted for four colonies/strain.

The hyphal surface adhesion assay was modified from (Lamarre et al., 2009). Fluorescent (excitation maximum 520 nm; emission maximum 540 nm) 0.5 μm diameter polystyrene beads (Sigma: aqueous suspension, 2.5 % solids content) were diluted 1:10 in sterile phosphate buffered saline (PBS). One hundred microliters of bead solution was added to CM liquid containing 20,000 spores and incubated for 8 h at 37 °C with 150 r.p.m. Images of germlings were collected using a Zeiss META510 confocal microscope with a 63x, 1.2

N.A. multi-immersion objective, a 514 nm excitation from Ar ion laser at 20 % power, and a 530–600 nm emission filter.

4.4.6 Cell wall preparation

Cell wall extraction was performed according to (Momany et al., 2004). Colonies were grown in shaken liquid at 37 ^{o}C for 48 h, filtered through Whatman #1 filter paper, washed with ultrapure water, and then with 0.5 M NaCl. Fungal hyphae were broken using 1 mm glass beads in buffer [20 mM Tris, 50 mM EDTA, pH 8.0]. Cell walls were separated from cytoplasmic debris by centrifugation at 3000 x *g* for 10 min. The pellet containing the cell wall fraction was washed with same buffer with stirring for 4 h at 4 ^{o}C, followed by a wash with ultrapure water. The pellet was frozen at -80 ^{o}C, then lyophilized overnight.

4.4.7 ELISA

Our ELISA protocol was adapted from (Momany et al., 2004). Isolated *A. nidulans* cell walls [0.5 mg/mL in PBS] were incubated in 96-well Immulon 2HB plates (Sigma) overnight at 4 ^{o}C. Subsequent steps were performed at room temperature using monoclonal antibodies to Gal*f* (L10; provided Prof. Frank Ebel, Univ Munich), α-1,3-glucan (MOPC-104E; Sigma), and β-glucan [(1-3)-β-glucan directed monoclonal antibody, Cat. No. 400-2, Biosupplies, Australia]. Primary antibodies were diluted 1:10 (Gal*f*), 1:30 (α-glucan), or 1:50 (β-glucan). Secondary antibodies (1:500) were alkaline phosphatase-conjugated goat anti-mouse IgM (Sigma) (for Gal*f* and α-glucan) and alkaline phosphatase-conjugated goat anti-mouse IgG (for β-glucan). At the final step, wells were incubated with alkaline phosphatase substrate (Sigma) (1 mg/mL) dissolved in substrate buffer (0.5 mM $MgCl_2.6H_2O$, 9.6 % diethanolamine, pH 9.6) for 30 min. Absorbance at 405 nm was recorded using ELISA reader. All ELISA experiments were performed at least twice with three replicates. We used PBS and cell wall extracts of wild type and deleted strains without primary antibody as a control.

4.4.8 Protein extraction and western blot

To extract total protein, *A. nidulans* conidia were grown in complex media (CM) for 20 h. Mycelia were then collected from liquid cultures by filtration through Miracloth paper,

washed with distilled water, dried on paper towels, and ground to a powder with mortar and pestle in liquid nitrogen (Efimov, 2003). The ground mycelium was resuspended and boiled in the urea/SDS buffer (Osherov, 1998): 1% SDS, 9 M urea, 25 mM Tris-HCl (pH 6.8), 1 mM EDTA, and 0.7 M 2 mercaptoethanol). The debris was removed by centrifugation at 13000 x *g*. Total protein concentration was determined by the Bio-Rad protein assay. UgmA-GFP fusions were detected on Western blots using purified mouse anti-GFP polyclonal antibody (eBioscience). IRDye 800-conjugated anti-mouse IgG was used as a secondary antibody. Bands were detected using the Odyssey Infrared Imaging System (LI-COR Biosciences). Images were processed by Odyssey 3.0.16 application software (LI-COR Bioscience).

4.4.9 Microscopy

Samples were prepared for confocal microscopy as described in (El-Ganiny et al., 2008). Gal*f*, α-glucan and β-glucan were immunolocalized using the same primary antibodies as described for ELISA. Primary antibodies were used at full strength for L10, at 1:50 dilutions for α-glucan and β-glucan. GFP was immunolocalized using anti-GFP primary antibody (eBioscience) at a dilution of 1:100. TRITC-conjugated goat-anti-mouse was used as secondary antibody at 1:100 dilutions. Immunofluorescence procedures followed (Alam et al., 2012). Samples were examined using confocal epifluorescence microscopy. The relative immunofluorescence intensity was quantified using Zeiss image browser software at 25 isolated cellular sites at hyphal wall where we had near-median confocal slices of subapical cells.

Scanning electron microscopy was used to examine conidiation following preparation as in (Alam et al., 2012). Strains were grown on dialysis tubing laid on CM for 3 d at 28 ºC. Colonies were fixed by immersion in 1 % glutaraldehyde, dehydrated in acetone, critical-point dried (Polaron E3000, Series II), and gold sputter coated (Edwards model S150B). Samples were imaged with a JEOL 840A scanning electron microscope.

4.4.10 Drug sensitivity testing

Sensitivity to Caspofungin, Itraconazole and Calcofluor White of wild type and engineered UgmA strains was measured using a disc-diffusion assay as described in (Afroz et

al., 2011, Alam et al., 2012). Stock solutions: itraconazole (1.6 mg/mL in DMSO), Calcofluor White (10 mg/mL in 25 mM KOH), and Caspofungin (20 mg/mL in sterile water) were stored at -80 ^{o}C. For this test, 1 x 10^{7} spores were mixed into 20 mL of 50 ºC CM agar and immediately poured in 9 cm Petri plates. Stock solutions were pipetted onto sterile 6 mm paper discs placed on the agar surface: 20 µL of CFW, 10 µL of itraconazole, and 20 µL of caspofungin. Solvent controls, DMSO and 50 % ethanol, showed no zone of inhibition. The plates were incubated at 30 ºC for 48 h, before measuring the zone of inhibition (Alam et al., 2012).

Drug sensitivity is presented as an index compared to wild type on the same medium, so that values greater than 1.0 indicate hypersensitivity. Statistical analysis of the raw data and comparison to sensitivity indices showed that a difference of >0.2 in index value correlated with statistical significance. Representative plates from the Caspofungin study are shown in Figure S3. Quantitative results are shown in Table 4.2.

Acknowledgements

We are pleased to acknowledge individual support from the Natural Science and Engineering Council of Canada Discovery Grant program (SGWK, DARS), and we thank the University of Saskatchewan UGS and GTF programs (MKA). We thank Prof. Frank Ebel (Univ Munich) for the L10 anti-Galf mAb, and Tom Bonli (Dept. Geological Sciences, University of Saskatchewan)

Table 4.1: Colony and hyphal characteristics[a] of wild type, and An*ugmA*Δ strains complemented with wild type AfUgmA, single residue AfUgmA mutants and deletion strains grown on CM.

Strains	Spores/colony ($\times 10^6$)[b]	Colony diameter (mm)[c]	Hyphal width (μm)[d]	Basal cell length (μm)[d]
Wild type (A1149)	109 ± 3.0^{e}	18 ± 0.5^{e}	2.5 ± 0.1^{e}	29 ± 1.7^{e}
An*ugmA*Δ:Af*ugmA*	99 ± 2.3^{f}	17 ± 0.6^{e}	2.5 ± 0.1^{e}	27 ± 1.7^{e}
F66A	90 ± 2.8^{g}	13 ± 0.3^{f}	2.6 ± 0.1^{e}	24 ± 0.9^{e}
H63N	6.4 ± 0.4^{h}	7.3 ± 0.4^{g}	3.3 ± 0.1^{f}	18 ± 0.8^{f}
R182K	3.2 ± 0.2^{i}	6.2 ± 0.3^{h}	3.4 ± 0.1^{fg}	17 ± 1.8^{f}
R182A	1.3 ± 0.1^{j}	5.0 ± 0.3^{i}	3.5 ± 0.1^{gh}	16 ± 0.7^{fg}
R327K	1.2 ± 0.1^{j}	5.1 ± 0.3^{i}	3.5 ± 0.1^{ghi}	15 ± 0.8^{g}
R327A	0.6 ± 0.1^{k}	4.6 ± 0.4^{i}	3.6 ± 0.2^{hi}	14 ± 0.8^{g}
An*ugmA*Δ	0.5 ± 0.4^{k}	5.2 ± 0.4^{i}	3.7 ± 0.1^{hi}	14 ± 0.8^{g}

a Values are presented as mean ± standard error. Statistical significance of the mean values was compared using a Kruskal–Wallis test, and shown for each characteristic to be significantly different at $P < 0.05$. For each column, values followed by different letters (e–k) are significantly different at $P < 0.05$.

b At least 4 colonies per strain were counted. Spores of wild type and mutated strains were streaked on CM and incubated for 3 d at 28 °C to give isolated colonies.

c The diameter of ten colonies/strain was measured using a dissection microscope.

d Hyphal width was measured at septa. Basal cell length was between adjacent septa for n=25 measurements per strain.

Table 4.2: *Aspergillus nidulans* wild type and chimaera cell wall carbohydrates[a], antifungal drug sensitivity[ac], and relative UGM activity[b].

Strains	Relative UgmA activity[b]	Gal*f* [a]	α-glucan [a]	β-glucan [a]	Antifungal drug sensitivity[a]		
					Casp[c]	Itra[c]	CFW[c]
Wild type	1	1	1	1	1	1	1
An*ugmA* :: Af*ugmA*	nd	0.96	1.05	0.96	1	1	1
F66A	0.16	0.78	1.18	0.87	1.2	1	1.1
H63N	na	0.52	1.46	0.74	1.5	1.1	1.1
R182K	0.10	0.43	1.58	0.69	1.7	1.2	1.2
R182A	6.0×10^{-6}	0.13	1.68	0.60	1.5	1.2	1.1
R327K	0.015	0.09	1.70	0.60	1.9	1.2	0.9
R327A	bd	0.04	1.79	0.58	1.7	1.2	1.1
An*ugmA*Δ	nd	0.00	1.84	0.57	1.9	1.2	1

[a] Absorbance at 405 nm was recorded using ELISA reader, Results are presented as an index of OD values with respect to wild type. Cell walls were isolated from *A. nidulans* strains after 48 h growth. Index sensitivity values are for each drug/strain combination compared to wild type. Index values > 1.0 were more sensitive than wild type. Index values that differed by > 0.2 were based on data that were significantly different: see Table S2

[b] Relative UGM activity *in vitro* with respect to wild type, derived from data in (33) and this study for F66A. nd, not determined; na, not available (low protein expression); bd, below detection.

[c] Caspofungin, Casp; Itraconazole, Itra; Calcofluor White, CFW. See Materials and Methods for drug dosage and medium formulation. Drug sensitivity was measured using a disc diffusion assay as described in methods (Figure S3). For Caspofungin, sensitivity was the radius (mm) of the clear zone with no visible growth. Mean ± SE of two measurements for each of four biological replicates were used for statistical analysis (Table S2).

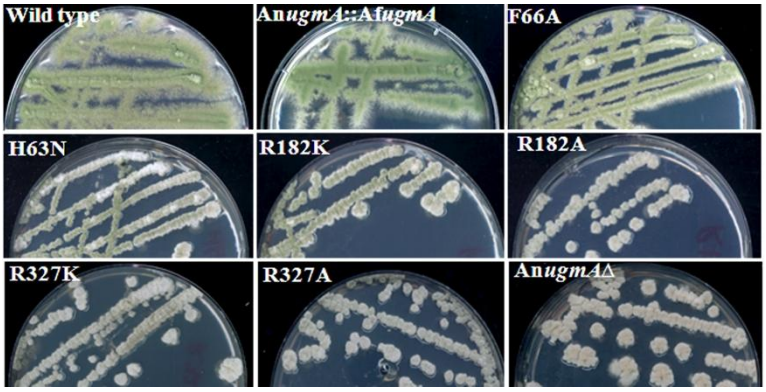

Figure 4.1. Colony morphology of *Aspergillus nidulans* wild type (WT) strain complemented with wild type *Af*UgmA (WC), single residue *Af*UgmA mutants (F66A, H63N, R182K, R182A, R327K, R327A) and An*ugmA*Δ strains, grown on complete medium at 30 °C for 3 d. The colour difference between WT and WC strains was due to slightly different ages of culture. See Figure S7 for a direct comparison of the spore colours of these two strains.

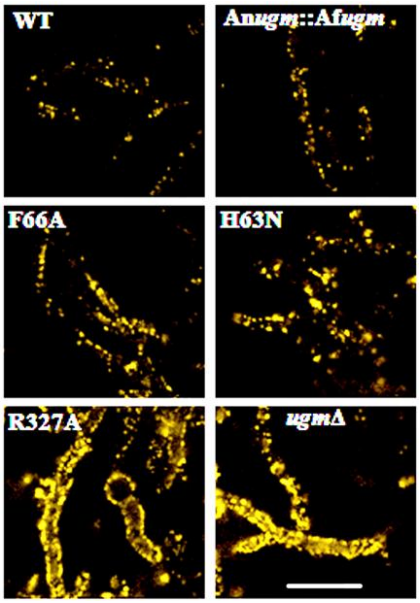

Figure 4.2. Surface adhesion of *Aspergillus nidulans* strains to fluorescent polysterene beads. Wild type (WT), strain complemented with wild type *Af*UgmA (WC), single residue *Af*UgmA mutants (F66A, H63N and R327A) and An*ugmA*Δ strains. Bar = 20 µm is for all images.

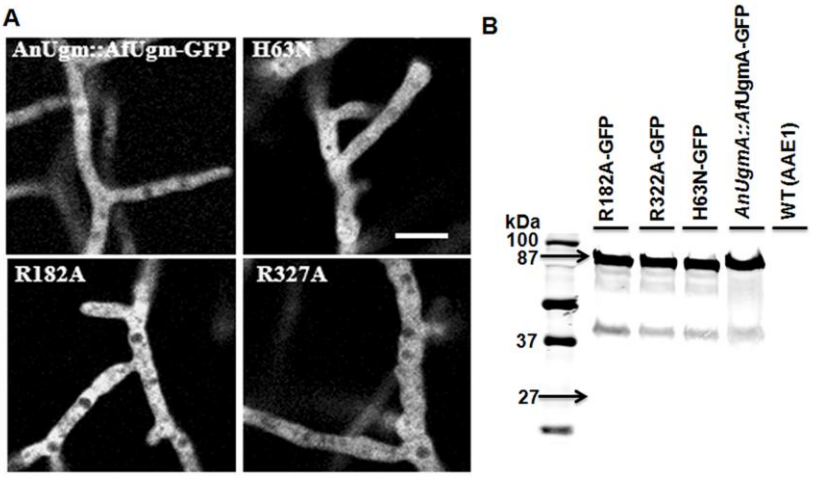

Figure 4.3. *In vivo* distribution of GFP-tagged *Af*UgmA in *Aspergillus nidulans*. A. Wild type complemented (WC) and single residue mutants (H63N, R182A and R327A) have comparable *Af*UgmA-GFP distribution. The single residue mutants have the *ugmA*Δ hyphal morphology. Bar = 20 µm for all images. **B.** Confirmation of *Af*UgmA-GFP fusion protein distribution by Western blot. Total protein was extracted from *A. nidulans* wild type (WT; AAE1) and GFP-tagged *Af*UgmA strains (R182A-GFP, R327A-GFP, H63N-GFP, *An*UgmA::*Af*Ugm-GFP). Total Proteins (15 µg/lane) were separated on 10% SDS-PAGE and immunoblotted with an anti-GFP antibody.

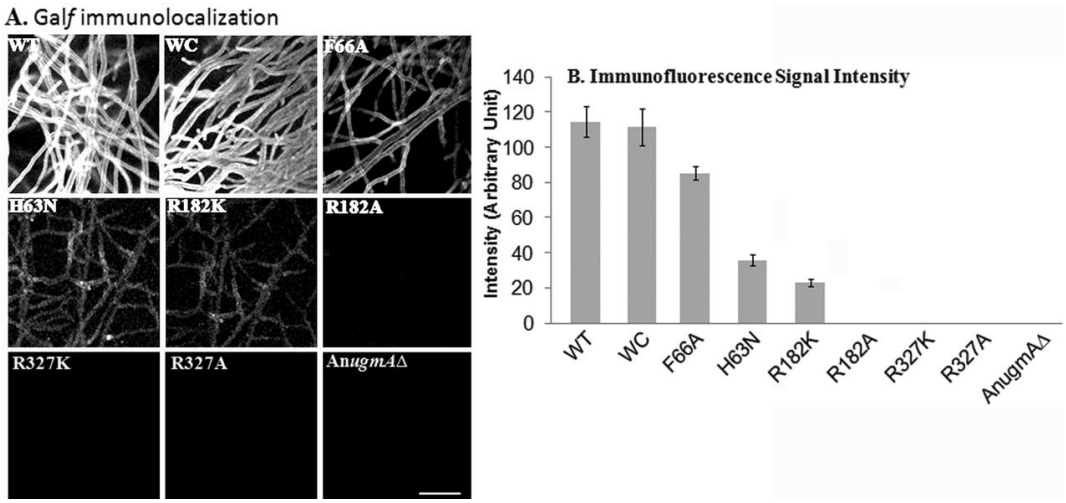

Figure 4.4. Galactofuranose immunolocalization (A) and immunofluorescence quantification (B) using confocal system software (see Methods). Error bar shows standard error. *Aspergillus nidulans* wild type (WT), wild type *Af*UgmA-complemented (WC), mutated *Af*UgmA (as listed), and An*ugmAΔ*. Bar = 10 µm for all images.

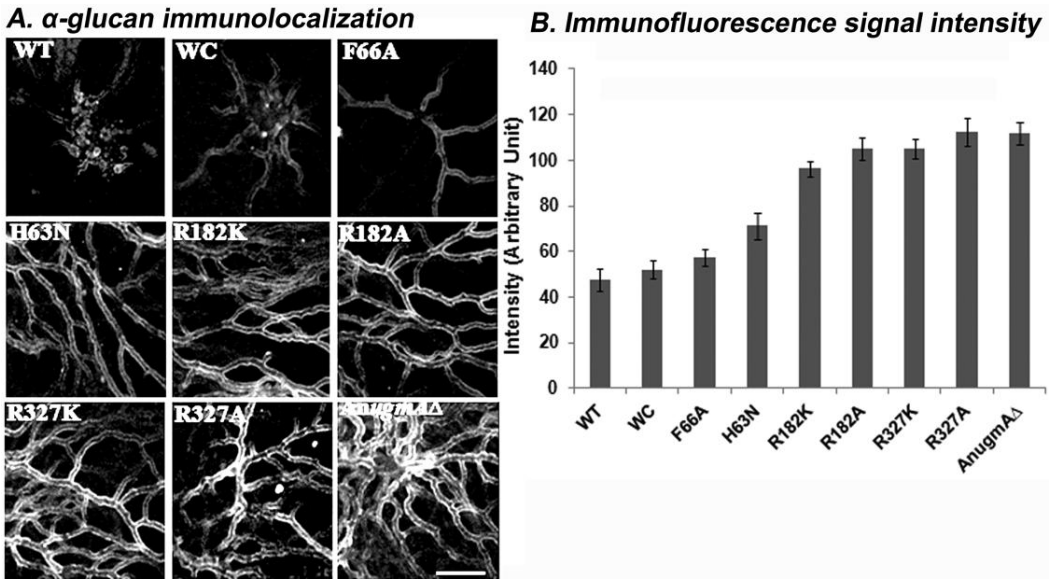

Figure 4.5. Alpha-glucan immunolocalization (A) and immunofluorescence quantification (B) using confocal system software (see Methods). Error bar shows standard error. *Aspergillus nidulans* wild type (WT), wild type *Af*UgmA-complemented (WC), mutated *Af*UgmA (as listed), and An*ugmAΔ*. Bar = 10 μm for all images.

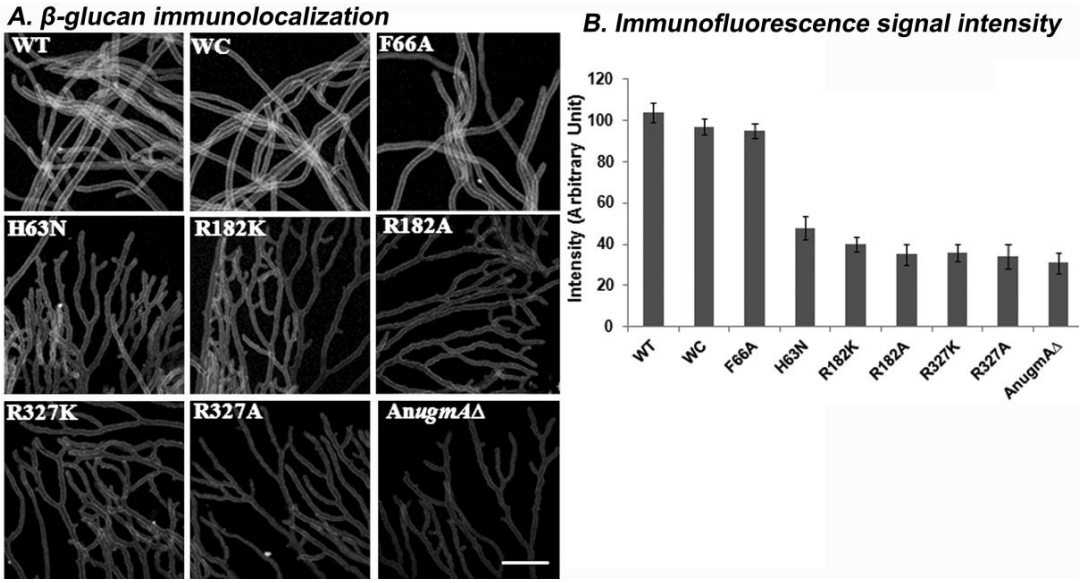

Figure 4.6. Beta-glucan immunolocalization (A) and immunofluorescence quantification (B) using confocal system software (see Methods). Error bar shows standard error. *Aspergillus nidulans* wild type (WT), wild type *Af*UgmA-complemented (WC), mutated *Af*UgmA (as listed), and An*ugmAΔ*. Bar = 10 μm for all images.

Supporting Information

Table S1: Strains and primers used in this study

Aspergillus

A1100 [a]	*Aspergillus fumigatus* wild type, AF293
A1149 [a]	*Aspergillus nidulans pyrG89*; *pyroA4*; *nkuA*::*argB*
AAE1	*Aspergillus nidulans pyrG89*:: Nc*pyr4+; pyroA4*; *nkuA*::*argB*
A. nidulans ugmAΔ [b]	AN3112::Af*pyrG*; *pyrG89*; *pyroA4*; *nkuA*::*argB*
An*ugmA*::Af*ugmA*[c]	AN3112::AfugmA:*tubA*p:Af*pyrG*; *pyrG89; pyroA4; nkuA::argB*
F66A[c]	AN3112::AfugmA-F66A:*tubA*p:Af*pyrG*;*pyrG89;pyroA4;nkuA::argB*
H63N[c]	AN3112::AfugmA-H63N:*tubA*p:Af*pyrG*;*pyrG89;pyroA4;nkuA::argB*
R182K[c]	AN3112::AfugmA-R182K:*tubA*p:Af*pyrG*;*pyrG89;pyroA4;nkuA::argB*
R182A[c]	AN3112::AfugmA-R182A:tubAp:Af*pyrG*;*pyrG89;pyroA4;nkuA::argB*
R327K[c]	AN3112::AfugmA-R327K:*tubA*p:Af*pyrG*;*pyrG89;pyroA4;nkuA::argB*
R327A[c]	AN3112::AfugmA-R327A:*tubA*p:Af*pyrG*;*pyrG89;pyroA4;nkuA::argB*
Af*ugmA*-GFP[c]	AN3112::AfugmA-GA5-GFP-*tubA*p-Af*pyrG*;*pyrG89;pyroA4; nkuA::argB*
H63N-GFP[c]	AN3112::Af*ugmA*-H63N-GA_5-GFP-*tubA*p-Af*pyrG*;*pyrG89*;*pyroA4*; *nkuA*::*argB*
R182A-GFP[c]	AN3112::Af*ugmA*-R182A-GA5-GFP-*tubA*p-Af*pyrG*;*pyrG89*;*pyroA4*; *nkuA*::*argB*
R327A-GFP[c]	AN3112::Af*ugmA*-R327A-GA5-GFP-*tubA*p-Af*pyrG*;*pyrG89*;*pyroA4*; *nkuA*::*argB*

Escherichia coli

BL21-gold (DE3) [d]

Plasmids

pAf*ugmA* [e]	pET22b, Af*ugmA*, amp^R
pAf*ugmA*-F66A [e]	pET22b, Af*ugmA*-F66A, amp^R
pAf*ugmA*-H63N [e]	pET22b, Af*ugmA*-H63N, amp^R
pAf*ugmA*-R182K [e]	pET22b, Af*ugmA*-R182K, amp^R
pAf*ugmA*-R182A [e]	pET22b, Af*ugmA*-R182A, amp^R
pAf*ugmA*-R327K [e]	pET22b, Af*ugmA*-R327K, amp^R
pAf*ugmA*-R327A [e]	pET22b, Af*ugmA*-R327A, amp^R
pFNO3 [a]	GA5-GFP, Af*pyrG*, Kan^R

Primers	Sequence 5' → 3'
Replacement of An*ugmA*	
P1, Up An*ugmA* F[c]	GACTCTTGAGATTTGCTTGGGT
P2, Up AnugmA R[c]	ACATATCGGGGTGGGTCATGAAGAGAGCGAAGCTGCAG
P3, Af*ugmA* F [c]	ATGACCCACCCCGATATGT
P4, Af*ugmA*(*tupA*p-tail) R[c]	AGTCACGTGCTGCATTTACTGGGCCTTGCTCTTG
P5, *tupA*p F [c]	ATGCAGCACGTGACTATT
P6, *tupA*p (*pyrG*-tail) R [c]	AATTGCGACTTGGACGACATCTTGTCTAGGTGGGTGGT
P7, Af*pyrG* F[c]	ATGTCGTCCAAGTCGCAATT
P8, Af*pyrG* R[c]	TCATGACTTGCCGCATACTC

P9, dn An*ugmA*(*pyrG*-T) F[c]	GAGTATGCGGCAAGTCATGAAACTCTTCTGCGTGGATGG
P10, dn An*ugmA* R[c]	GGACTGCAGGTTGAAGCAG

Fusion construct generation for replacement

P11, Fusion Up An*ugmA* F[c]	CCGTCCTTCGTAGAGTACTTGAG
P12, Fusion dnAn*ugmA* R[c]	GGTTGAACGATGTCAGCGTA

Replacement confirmation of An*ugmA*

P1, Up An*ugmA* F[c]	GACTCTTGAGATTTGCTTGGGT
P10, dn An*ugmA* R[c]	GGACTGCAGGTTGAAGCAG
Ame8, mid*PyrG* R[b]	CACATCCGACTGCACTTCC

Af*ugmA-gfp* tagging

P13, Af*ugmA*(GFP-tail) R [c]	CTCCAGCGCCTGCACCAGCTCCCTGGGCCTTGCTCTTGG
P14, Dn An*ugmA* R [c]	ATCAGTGCCTCCTCTCAGACAGAACTCTTCTGCGTGGATGG
Ame 27 5GA-GFPF[b]	GGAGCTGGTGCAGGC
Ame 28 5GA-GFPR[b]	TCATGACTTGCCGCATACT

Af*ugmA-gfp* tagging confirmation

P1, Up An*ugmA* F[c]	GACTCTTGAGATTTGCTTGGGT
P10, dn An*ugmA* R[c]	GGACTGCAGGTTGAAGCAG
Ame8, mid*PyrG* R[b]	CACATCCGACTGCACTTCC

Fusion constructs generation using fusion PCR for GFP tagging strains (same as replacement)

P11, Fusion Up An*ugmA* F[c]	CCGTCCTTCGTAGAGTACTTGAG
P12, Fusion dnAn*ugmA* R[c]	GGTTGAACGATGTCAGCGTA

H63N SDM

H63N forward	GTCGGTGGTCACGTCATCGCCTCCCACTACAAGTATTTC
H63N reverse	GAAATACTTGTAGTGGGAGGCGATGACGTGACCACCGAC

a Fungal Genetics Stock Center, www.fgsc.net
b El-Ganiny et al. (2008)
c This study
d Novagen (www.emdchemicals.com)
e van Straaten et al. (2012)

Table S2: Antifungal drug sensitivity[1] of wild type, deletion, and mutated Gal*f* biosynthesis strains.

Strains	Antifungal drug sensitivity[a]		
	Casp[c]	Itra[c]	CFW[c]
Wild type	4.25±0.3 [a]	5.25±0.2 [a]	2.0±0.1 [a]
An*ugmA* :: Af*ugmA*	4.38±0.2 [a]	5.25±0.1 [a]	2.0±0.2 [a]
F66A	4.75±0.1 [a]	5.5±0.1 [a]	2.25±0.3 [a]
H63N	6.13±0.1 [b]	6.0±0.1 [a]	2.5±0.3 [a]
R182K	7.13±0.1 [bc]	6.13±0.2 [a]	2.13±0.1 [a]
R182A	6.38±0.3 [bc]	6.25±0.3 [a]	2.13±0.1 [a]
R327K	7.38±0.2 [c]	6.25±0.1 [a]	1.89±0.[a]
R327A	8.00±0.2 [c]	6.5±0.2 [a]	2.25±0.2 [a]
An*ugmA*Δ	8.25±0.3 [c]	6.5±0.1 [a]	2.0±0.2 [a]

[1] Caspofungin, Casp; Itraconazole, Itra; Calcofluor White, CFW. See Materials and Methods for drug dosage and medium formulation. Drug sensitivity was measured using a disc diffusion assay as described in methods (Figure S3). For Caspofungin, sensitivity was the radius (mm) of the clear zone with no visible growth. Mean ± SE of two measurements for each of four biological replicates were used for statistical analysis (not shown). Statistical significance of the mean values was compared using a Kruskal–Wallis test, and shown for each characteristic to be significantly different at $P < 0.05$. For each column, values followed by different letters (a–c) are significantly different at $P < 0.05$. Data are presented as sensitivity index in Table 4.2.

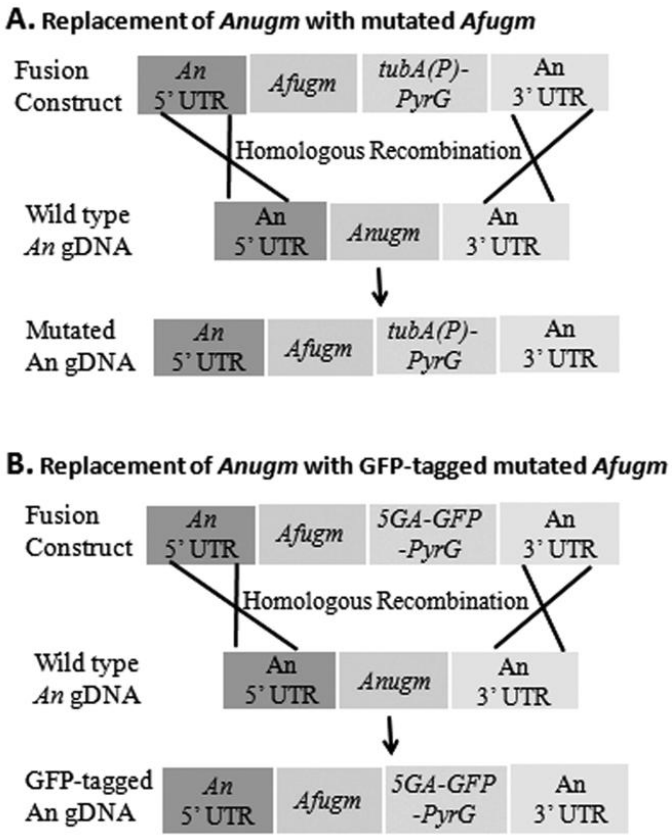

Figure S1. Strategy for generation of complemented, mutated and GFP tagged mutated strains in *A. nidulans*. A. Replacement of *A. nidulans ugmA* with wild type and mutated *A. fumigatus ugmA*. B. GFP-Tagging of *A. nidulans* UgmA with wild type and mutated *A. fumigatus* UgmA.

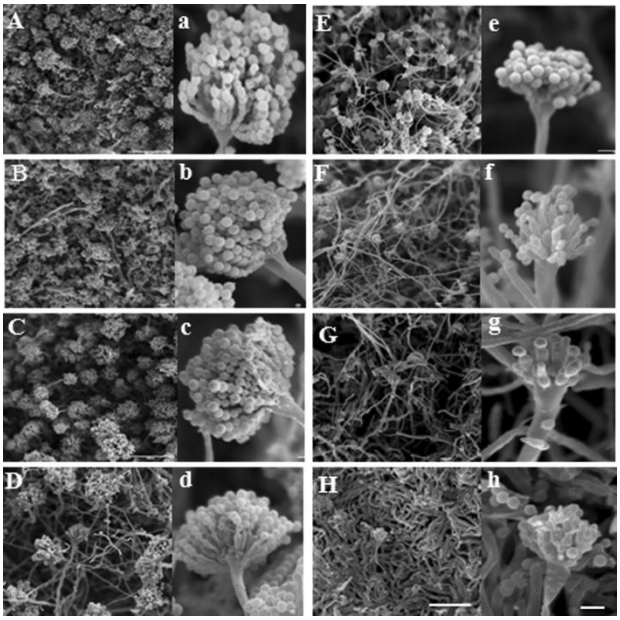

Figure S2. Scanning electron micrographs of *Aspergillus nidulans* showing: colony (A-H), and conidiophore (a-h) phenotype for wild type and mutated strains on complex media. Scale bar is 100 μm for A -H and 10 μm for a-h. A) wild type (AAE1), B) An*ugmA*::Af*ugmA*, C) An*ugmA*::Af*ugmA*-F66A, D) An*ugmA*::Af*ugmA*-H63N, E) An*ugmA*::Af*ugmA*-R182K, F) An*ugmA*::Af*ugmA*-R182A, G) An*ugmA*::Af*ugmA*-R327K, H) An*ugmA*::Af*ugmA*-R327A, I) An*ugmA*Δ.

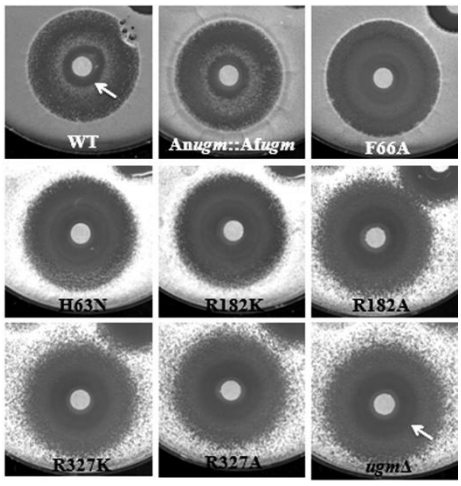

Figure S3: Response of wild type (WT), complemented, mutated and deleted strains to Caspofungin. Sensitivity is measured at the innermost clear zone (arrows). WT; wild type, An*ugmA*::Af*ugmA*, An*ugmA*::Af*ugmA*-F66A, An*ugmA*::Af*ugmA*-H63N, An*ugmA*::Af*ugmA*-R182K, An*ugmA*::Af*ugmA*-R182A, An*ugmA*::Af*ugmA*-R327K, An*ugmA*::Af*ugmA*-R327A, An*ugmA*Δ.

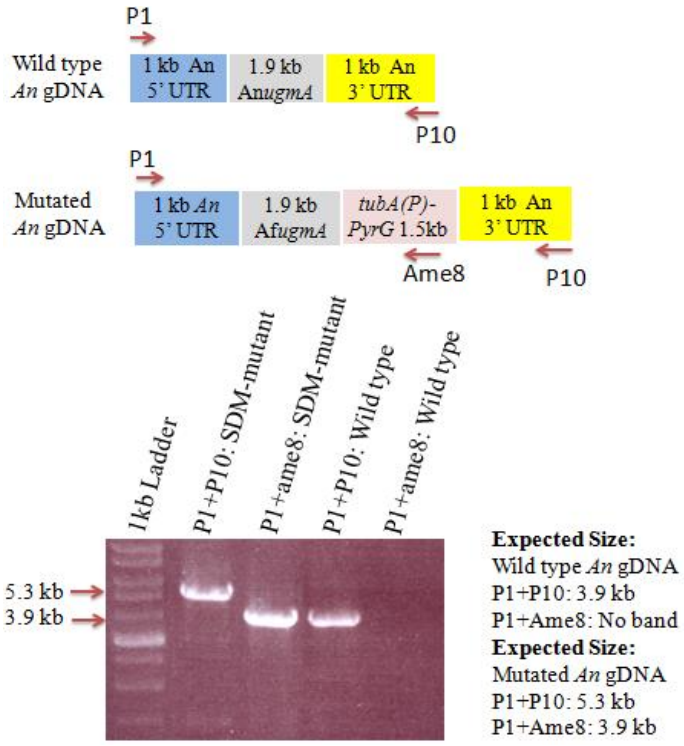

Figure S4. Confirmatory PCR for site directed mutated (SDM) replacement strain. This figure is for replacement of An*ugmA* by Af*ugmA*-R327A in *A. nidulans*. In addition to Confirmatory PCR, confirmation of all SDM strains was also done by DNA sequencing.

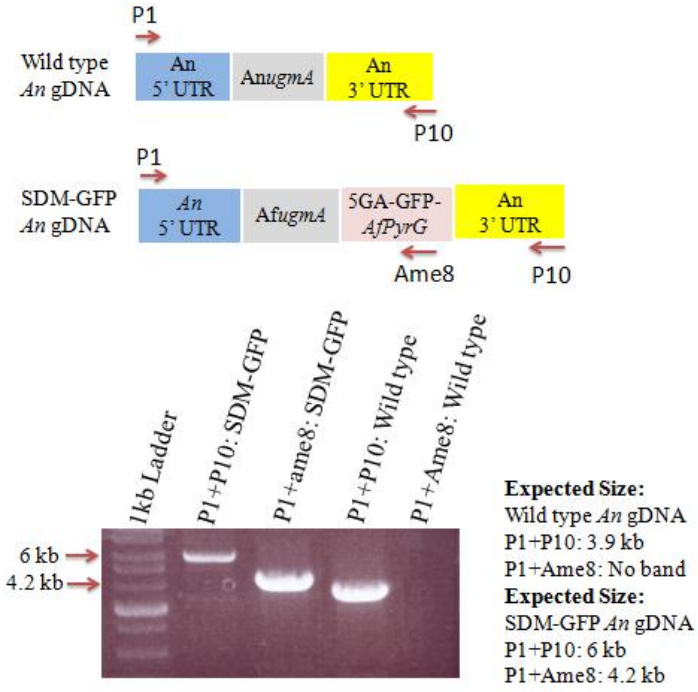

Figure S5. Confirmatory PCR for SDM-GFP tagging strains. This figure is for tagging Af*ugmA*-R327A with GFP and expressing in *A. nidulans***.** In addition to Confirmatory PCR, confirmation of all GFP tagged strains was also done by DNA sequencing.

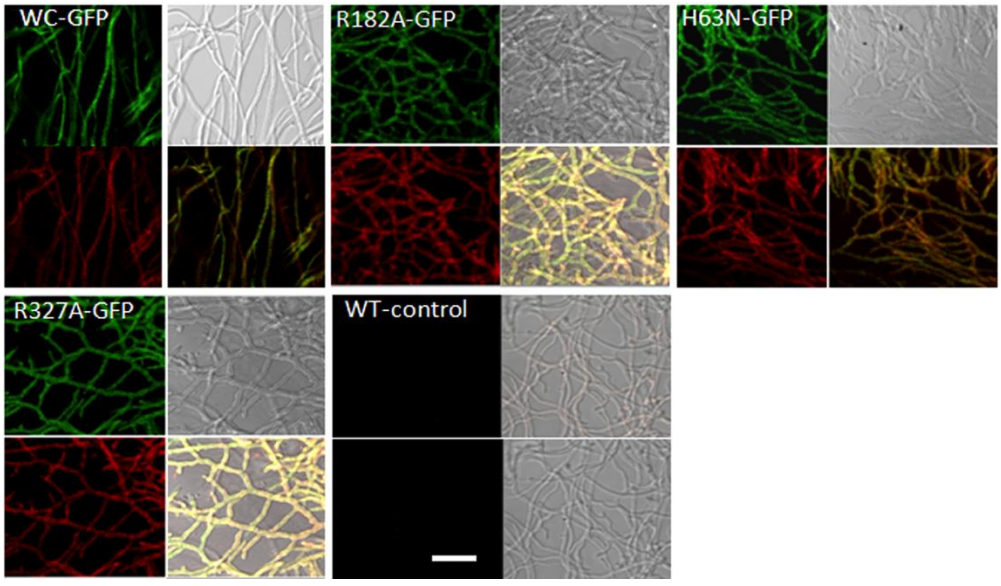

Figure S6. GFP immunolocalization in *Aspergillus nidulans* using anti-GFP antibody. Wild type complemented (WC) and single residue mutants (H63N, R182A and R327A) have GFP

localization comparable to *Af*UgmA-GFP distribution. Green channel: GFP distribution; Red channel: anti-GFP straining. Bar = 20 µm for all images.

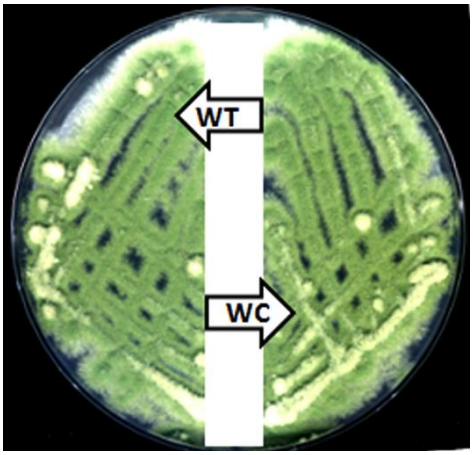

Figure S7: Colony morphology and spore colour of *Aspergillus nidulans* wild type (WT), complemented (WC) strains grown on complete medium at 30 °C for 3 d. Both WT and WC strains were grown on same plate. No difference in colony morphology was observed. Arrow indicates respective strains.

CHAPTER 5

Revealing the interacting partners of *Aspergillus nidulans* UDP-galactopyranose mutase using tandem affinity purification (TAP) and mass spectrometry.

This Chapter is based on the hypothesis that UgmA is part of a protein complex that likely includes UgeA, UgtA, and members of α-glucan and beta-glucan metabolism. This Chapter will be submitted in future with further study for publication as "**Revealing the interacting partners of *Aspergillus nidulans* UDP-galactopyranose mutase using tandem affinity purification (TAP) and mass-spectrometry analysis**"**.**

The objectives for this research are

1. To adopt the TAP tag strategy in our lab for studying protein interaction networks
2. To identify the interacting partners of UgmA

My contribution in this Chapter: I have generated C-terminal and N-terminal TAP tagged UgmA strains and confirmed the right insertions using DNA sequencing. I have purified UgmA from total proteins extract and pulled down UgmA with its interacting partners on polyacrylamide gel. I have sent the bands for Mass-spec analysis to NRC Mass-Spec facilities. Mass-Spec results will be confirmed by a future student using yeast two-hybrid system. I generated all the final figures and wrote the first draft, which was edited by Dr. Kaminskyj.

Revealing the interacting partners of *Aspergillus nidulans* UDP-galactopyranose mutase using tandem affinity purification (TAP) and mass-spectrometry analysis

Md. Kausar Alam and Susan GW Kaminskyj

Abstract

Galactofuranose (Gal*f*) is a nonessential component of the fungal cell wall, but its presence is important for *Aspergillus* growth, wall maturation and integrity. Previously, we showed that deletion or repression of any of three sequential-acting Gal*f* biosynthesis genes caused increased cell wall thickness in *A. nidulans*. In addition, we have recently shown that Gal*f*-repressed strains had increased alpha-glucan and decreased beta-glucan content in their cell walls. This suggested that the Gal*f* biosynthesis pathway might relate to other major cell wall synthesis pathways, particularly alpha-glucan and beta-glucan synthesis. Currently, how modification of Gal*f* biosynthesis leads to changes in cell wall composition is unknown. In addition, how Gal*f* is deposited in the cell wall is elusive. The cytosolic enzyme UDP-galactopyranose mutase (Ugm) is the first committed enzyme in the Gal*f* biosynthesis pathway. Revealing the interacting partners of UgmA using a proteomic approach might help us to elucidate the molecular mechanism behind wall Gal*f* deposition and its effect on the proportion of wall alpha-glucan and beta-glucan composition. Advanced biochemical methods combined with molecular biology and mass spectrometry are required to identify protein–protein interaction to understand the function of a given protein in its protein context. We used Tandem Affinity Purification (TAP) tagging combined with LC-MS/MS to study the interacting partners of UgmA. Tandem affinity purification and mass-spectrometry analysis we showed that UgmA has three major predicted interaction partners: AN6688, AN6010 and AN5327. These three proteins are involved in cytoskeleton generation, osmotic adaptation, and cell signalling pathway respectively. Unexpectedly, none are involved in galactose metabolism or Gal*f* transport. Further study is necessary to confirm these interactions using yeast two-hybrid screening and/or immunoprecipitation. Further study will help us to understand Gal*f* biosynthesis and dynamic coordination of Gal*f* biosynthesis pathway with other wall carbohydrate polymers for *Aspergillus* wall formation.

5.1. Introduction

The fungal cell wall is essential for the survival and growth of fungi and to establish fungus-environment and host-pathogen interactions (Latgé, 2007; Cummings and Doering, 2009). Fungal cell walls are mainly composed of glucans, chitin, galactomannan and mannoproteins (Free 2013). Polysaccharides and glycoconjugates have significant contributions to biological events including cell wall generation. In filamentous fungi, wall formation is also an integral part of hyphal extension (Read, 2011). Despite decades of effort to characterize the composition and architecture of fungal cell walls (Bartnicki-Garcia, 1968; Bowman et al 2006; de Groot et al 2009), many details still remain poorly understood. In particular, recent evidence shows that cell wall composition can be remodeled following environmental change (Levin, 2005; Fujioka et al 2007; Levin 2011), and altering certain minor wall components can cause major phenotype effects (Levin, 2005; Fujioka et al 2007; Levin 2011; Chapter 3 and references therein).

Galactofuranose (Gal*f*) is a minor but important cell wall component (Chapter 3&4) (Lamarre et al., 2009). Interestingly, the presence of Gal*f* is restricted to bacteria (Leone et al 2010), protozoa (Oppenheimer et al 2011), fungi (El-Ganiny et al., 2008; Latgé, 2009; Tefsen et al., 2012) as well as certain algae (Cordeiro et al 2008), archaea (Eichler and Adams, 2005), and lower invertebrates (Novelli et al 2009). Gal*f* is essential in *Mycobacterium tuberculosis*, making Gal*f* biosynthesis a drug target against mycobacteria (Scherman et al., 2003). In *A. fumigatus* walls, Gal*f* is said to account for about 5 % of the total wall dry weight (Lamarre et al., 2009; Free, 2013) and is reported to be part of galactomannans, glycoproteins, sphingolipids and lipophosphogalactomannans (Latgé, 2009). Although Gal*f* is not essential for fungal survival, its presence is important for cell wall growth, maturation and integrity (El-Ganiny et al 2008; Lamarre et al 2009; El-Ganiny et al, 2010; Afroz et al 2011; Paul et al, 2011).

The cytosolic enzyme UDP-galactopyranose mutase (Ugm) is the key enzyme in the Gal*f* biosynthesis pathway. Ugm is responsible for interconversion of UDP-galactopyranose (6-membered ring) and UDP-Gal*f* (5-membered ring). Deletion of *ugm* from *Mycobacterium tuberculosis* showed that it was essential for growth and survival (Pan et al., 2001). Targeted replacement of the orthologue *glf* in *L. major* (the causative agent of leishmaniasis) caused

attenuation of virulence (Kleczka et al., 2007). Deletion of *ugmA* in *A. fumigatus, A. nidulans*, and *A. niger* revealed that the corresponding knock-out strains were all completely lacking in Gal*f* and exhibited marked alterations to their cell wall and growth (Damveld et al. 2008; El-Ganiny et al 2008; Lamarre et al 2009; El-Ganiny et al 2010). Damveld et al. (2008) had shown that *A. niger* strains with defective *ugmA* homologues had impaired colony growth and increased wall α-glucan content. In our previous study, we showed that deletion or repression of *ugmA* caused increased cell wall thickness in *A. nidulans*. In addition, we have shown that *ugmA*-deleted strains had increased alpha-glucan and decreased beta-glucan in their cell walls. Therefore, our previous studies suggested that Gal*f* biosynthesis pathway might have relationships with other major cell wall synthesis pathway such as alpha-glucan and beta-glucan. Recent studies on Gal*f* biosynthesis indicated it is important for *Aspergillus* growth and cell maturation (El-Ganiny et al 2008 and 2010, Afroz et al 2011; Alam et al 2012). However, how Gal*f* is generated and deposited to the cell wall still remains elusive. In addition, how modification of UgmA expression leads to a change in cell wall composition (Chapter 4) is still unknown. Revealing the interacting partners of UgmA using a proteomic approach might help us to elucidate the molecular mechanism behind wall Gal*f* deposition and alteration of wall alpha-glucan and beta-glucan content.

Biochemical methods combined with molecular biology and mass spectrometry are required to efficiently identify protein–protein interaction in the absence of a specific antiserum. These methods can clarify the role of a given protein through understanding its interacting protein context. The tandem affinity purification (TAP) method represents an biochemical application that was first described for *Saccharomyces cerevisiae* (Rigaut et al., 1999; Puig et al., 2001) and was further applied to prokaryotes, plants, and mammalian cells, including humans, for *in vivo* studies (Rohila et al., 2004; Butland et al., 2006; Rohila et al., 2006; Gregan et al., 2007). TAP-tagging is based on a recombinant fusion tag containing two tags; two tandemly-repeated *Staphylococcus aureus* protein A epitopes that bind to IgG sepharose during the first purification step, and a calmodulin-binding peptide (CBP) that binds to calmodulin affinity resin in the second purification step. The protein A domain is connected to CBP by a tobacco etch virus (TEV) protease cleavage site. Purified and eluted protein is then separated by SDS-PAGE. Individual protein bands are sent for mass

spectrometry (MS) identification. The identification of putative interacting partners of the protein of interest should be confirmed by other methods, including the yeast two-hybrid, immunoprecipitation or bimolecular fluorescence complementation methods.

In this study, we describe the adaptation of the TAP purification protocol including all required steps (protein extract preparation, purification procedure, visualization of proteins in the SDS gels, and final mass spectrometry identification) to study the interaction network of *Aspergillus nidulans* UgmA. Using tandem affinity purification and mass-spectrometry analysis, we showed that UgmA interacted with proteins that are involved in cytoskeleton generation, osmotic adaptation, and cell signalling pathways. Further study will help us to understand Gal*f* biosynthesis and dynamic coordination of Gal*f* biosynthesis pathway with other wall carbohydrate polymers for *Aspergillus* wall formation.

5.2. Materials and methods

5.2.1 Strains, Plasmids and Cultures conditions

Strains, primers and plasmids are listed in Table S1. The *A. nidulans* strains were maintained on complete medium (0.5 % yeast extract, 1 % bacto-peptone, 0.1 % casamino acids, 1 % glucose, vitamins, and micronutrients) supplemented for nutritional markers as described in Kaminskyj (2001). Bacterial strains were grown on Luria Bertani (LB) medium with antibiotics as required (Table S1).

5.2.2 Construction of linear recombinant DNA for transformation and for generation of C-terminal and N-terminal TAP-tagged UgmA strains.

A codon optimized C-terminal TAP tag was amplified using primers cTAP1 and cTAP2 from plasmid pME3156 (a gift from Dr. Özgür Bayram, Germany). This was then fused with C-terminal of UgmA to generate UgmA::cTAP construct using fusion PCR as described in Szewczyk et al. (2007). The final module was generated using fusion PCR as US-UgmA::UgmA::cTAP::AfPyrG::DS-UgmA. This module was then transformed into A1149 protoplasts. Protoplasting and transformation followed procedures in Osmani et al. (2006) and Szewczyk et al. (2007). Primary transformants were grown on selective medium

containing 1 M sorbitol or 1 M sucrose as osmostabilizer. Confirmation of gene manipulation used genomic DNA from putative transformant strains as a template for PCR with combinations of primers, as shown in Supplementary Table S1. Primer binding sites used for confirmation were 50 bp outside the sites used for construction or were in the selectable marker. We used an *A. fumigatus* pyrimidine (Af*pyrG*) selectable marker controlled by the α-tubulin promoter [*tubA*(p)-*pyrG*] to ensure a constitutive level of marker expression, whereas the *ugmA*::*cTAP* was controlled by endogenous promoters (Figure 5.1). Prior to protein extraction, a genomic DNA sample from each *A. nidulans* strain was extracted. A *ugmA::cTAP* sequence was amplified from these genomic DNA samples using PCR. PCR products were sequenced in order to confirm the expected construct generation.

5.2.3 Culturing of the fungal strains and crude extract preparation

We inoculated 5× 800 mL liquid media with *A. nidulans ugmA::cTAP, nTAP::ugmA,* and wild-type control strains on CM (1×10^6 per 1 mL medium) and grew these cultures for 20 h at 37°C and 250 rpm. The TAP tag protocol was adopted from Bayram et al., 2012. Briefly, mycelia were filtered through a Miracloth filter using a vacuum flask connected to the air pump, then washed with harvest solution (0.96 % NaCl, 1 % dimethyl sulphoxide (DMSO), 1 mM phenylmethyl sulphonyl fluoride (PMSF)). Mycelia were ground in liquid nitrogen with a chilled mortar/pestle, and then transferred into 15 mL Falcon tubes and stored at −80°C. Approximately 40 g mycelia for each strain were transferred to three 50 mL Sorval centrifuge tubes. Five millilitres of collection buffer (100 mM Tris–HCl pH 7.5, 0.1 % NP-40, 1 mL PMSF, and 100 mL dithiothreitol) supplemented with EDTA-free protease inhibitor tablets (Roche), and phosphatase inhibitors (Merck) were added to the bottom of each Sorval tube containing frozen mycelia. Another 5 mL of collection buffer was l layered on the top of the tube and mixed until buffer was absorbed by the mycelium. Tubes were kept on ice for 5-10 min. Tubes were then centrifuged at 20,000 x *g* for 30 min at 4 °C. Supernatant was transferred to bovine serum albumin-treated 50 mL Falcon tubes containing washed (using collection buffer) IgG sepharose.

5.2.4 TAP purification and SDS PAGE

Crude extract/IgG sepharose mixture was incubated on a rotating platform at 4 °C for 2 h. This mixture was then passed through chromatography columns with gravity. IgG sepharose was accumulated at the bottom of the columns. Sepharose was then washed with 2 × 10 mL wash buffer 1 (250 mM NaCl, 40 mM Tris–HCl pH 8.0, 0.1 % NP-40, 1 mL PMSF, 100 mL DTT) supplemented with ethylene diamine tetra-acetate (EDTA)-free protease inhibitor tablets and phosphatase inhibitors, once with 10 mL wash buffer 2 (150 mM NaCl, 40 mM Tris–HCl pH 8.0, 0.1 % NP-40, 1 mM PMSF, 1 mM DTT) and once with TEV cleavage buffer (TCB) (150 mM NaCl, 40 mM Tris–HCl pH 8.0, 0.1 % NP-40, 0.5 mM EDTA, 1 mM PMSF, 1 mM DTT) supplemented with E-64. TEV protease cleavage was executed by adding 1 mL TCB and 20 µL of AcTEV™ enzyme (Invitrogen) and rotating the suspension overnight at 4 °C. TEV protease treated suspensions was then transferred to new column which had 300 µL of washed calmodulin affinity resin (Stratagene) and 6 mL of calmodulin-binding buffer (CBB). CBB columns were closed and rotated at 4 °C for 1 h. CBB columns were washed with 3 × 1 mL CBB. At the end, 2 x 500 µL elution buffer (EB) was added to the column and proteins were collected in 1.5 mL vials. Trichloroacetic acid (TCA)-precipitation was performed and then TCA-precipitated eluate was loaded onto a 10 % polyacrylamide gel, and then stained with Coomassie Brilliant Blue G (Sigma). Protein bands were cut out and sent to the NRC mass spectrometry facility for analysis.

5.2.5 In-gel digestion procedures

In-gel digestion was carried out at NRC mass spectrometry facility using the MassPrep II Proteomics Workstation (Micromass, UK). Briefly, Coomassie-stained protein gel bands were cut into pieces of ~1 mm^3 and placed into 96-well plates. Gel bands were de-stained twice (10 min incubations) with 100 µL of 1:1 (v/v) ammonium bicarbonate: acetonitrile. Protein reduction was performed with the addition of 10 mM DTT prepared in 0.1 M ammonium bicarbonate, for 30 min at 37 ºC. This step was followed by alkylation, achieved by adding 50 µL of 55 mM iodoacetamide (IAA) prepared in 0.1 M ammonium bicarbonate. The alkylation reaction was carried out for 20 minutes also at 37 ºC. Gels are washed and dehydrated before being saturated with 25 µL of 6 ng/µL trypsin prepared in

50 mM ammonium bicarbonate; digestion was carried out at 37 ºC for 5 h. Peptides were extracted with 30 µL 0.1% trifluoroacetic acid/3% acetonitrile for 30 min, and then twice with 24 µL, 0.1% trifluoroacetic acid/50% acetonitrile for 30 min. The combined extracts were dried in a speed vac (Labconco, Fishier Scientific). Samples were reconstituted in 40 µL of 0.1 % trifluoroacetic acid/3 % acetonitrile for LC-MS analysis.

5.2.6 LC-MS Spectra collection and Data analysis

For MS analysis we used commercial service of NRC MS facility. Briefly, tryptic peptides extracted from each gel slice were injected onto a liquid chromatographic column, then sample mass was analysed with a Quadrupole Time-Of-Flight (Q-TOF) Global Ultima mass spectrometer (Micromass, Manchester, UK) is equipped with a nano-electrospray (ESI) source and interfaced with a nanoACQUITY UPLC solvent delivery system (Waters, Milford, MA, USA).

Samples were analyzed using Data Dependant Acquisition (DDA), which consists of the detection of multiply charged positive ions (z = 2, 3, and 4 were used herein) from an MS survey scan. The mass scan range was set from m/z 400 to 1900 with a scan time of 1 s. Up to three MS/MS scans were triggered from each MS scan event (signal intensity threshold was 16 counts/second), with collision energy ranged from 20 to 80 eV depending on the charge state and precursor m/z. In MS/MS experiments, data was acquired in continuum mode with a scan time of 1.9 s, and dynamic exclusion of previously detected precursors was set at 2 min; peptides from trypsin and keratin were also excluded from MS/MS data collection.

The RAW mass spectra data files collected from each sample were processed with ProteinLynx Global Server 2.4 (PLGS 2.4, Waters), a PKL file was generated and subsequently submitted to Mascot (Matrix Science Ltd., London, UK) for peptide search against the NCBInr protein database hosted by National Research Council of Canada (NRC, Ottawa). In the database searching parameters, a maximum of one tryptin miscleavage was allowed. The mass tolerance for precursor peptide ions was ± 50 ppm and for fragment ions it was ± 0.2 Da. Peptides of identified proteins were individually blasted against a public *A. nidulans* genome-wide protein sequence database of the Broad Institute

(http://www.broad.mit.edu/annotation/genome/aspergillus_nidulans/Home.html) to ensure their unambiguous assignment to the Mascot-specified protein.

5.3. Results and discussion

To explore the coordination of the Gal*f* biosynthesis protein UgmA with that of other wall carbohydrate biosynthesis proteins, tandem affinity purification (TAP) and LC-MS were used.

5.3.1 Construction and validation of tagging strains

A linear fusion construct containing 1 kb upstream of *ugmA*, the whole *ugmA* expression sequence (genomic *ugmA* has 5 introns) except the stop codon, codon optimized TAP tag, nutritional marker Af*pyrG*, and 1 kb downstream of *ugmA* (Up-UgmA::UgmA::cTAP:: *tubA*(p)-::Af*pyrG*::DS-UgmA) was integrated into *A. nidulans* genomic DNA by homologous recombination (Fig. 5.1). Primary transformants were grown on CM containing 1 M sorbitol or 1 M sucrose as an osmotic stabilizer. Strain construction and confirmation is shown in Fig. 5.1. The nTAP::*ugmA* or *ugmA*::cTAP construct was controlled by the endogenous *ugmA* promoter, whereas the nutritional marker, Af*pyrG* was controlled by the α-tubulin promoter [*tubA*(p)-*pyrG*] to ensure a constitutive level of marker expression. The correct strain generation was confirmed by both PCR and sequencing analysis. Growth of *ugmA*::*cTAP*, *nTAP*::*ugmA* and wild-type were compared on CM. Growth of *ugmA*::*cTAP* was comparable to wild type strain (Fig. 5.2). However, *nTAP*::*ugmA* had substantially reduced sporulation, thereby resembling the *ugmA*Δ strain (Fig. 5.2).

5.3.2 Identification of interacting partners of UgmA using TAP tagging

We used tandem affinity purification (TAP) to identify UgmA-interacting proteins (a generalized TAP protocol is summarized in Fig. 5.3). Purified recombinant UgmA of *A. nidulans* carrying the functional UgmA tagged at its C-terminus by TAP tag (*ugmA*::ctap) were analyzed by mass spectrometry (Fig. 5.4). Analysis of the purified UgmA complex by SDS-PAGE showed several bands, which were absent from a control purification using extract from wild-type cells (Fig. 5.4). As judged from percent sequence coverage and number of peptides per protein, we identified AN6688 (Septin B; AspB), AN6010 (SgdE) and AN5327 (uncharacterized) as interacting partners of UgmA (Fig. 5.4 and Table1).

Septins are evolutionarily conserved GTP-binding proteins that form complexes and act as organizational cues, recruiting critical proteins to areas of new growth and cell division (Longtine *et al.*, 1996; Field and Kellogg, 1999; Gladfelter *et al.*, 2001; Hernandez-Rodriguez and Momany 2013). Septins are found in all eukaryotes except higher plants (Pan et al., 2007; Estey et al., 2011) and are involved in a variety of cellular processes including cytokinesis, vesicle trafficking, cytoskeleton organization, polarity (Lindsay and Momany, 2006; Hernández-Rodríguez et al. 2012). The filamentous fungus *Aspergillus nidulans* has five septins: AspA, AspB, AspC, AspD, and AspE (Hernández-Rodríguez et al. 2012). AspB is an essential gene (Momany and Hamer, 1997). However, other evidence showed that deletion of AspB caused aberrant morphology in several developmental stages and reduced conidiation (Momany and Hamer, 1997; Westfall and Momany, 2002). AspB localizes to sites of septation and branching and to emerging conidiophore layers, bars and filaments throughout vegetative growth and asexual reproduction (Westfall and Momany, 2002; Hernández-Rodríguez et al. 2012).

SgdE is an Hsp70-family protein required for conidial germination in *A. nidulans*. The *sgdE* gene is expressed at increased levels during osmoadaptation (Osherov and May, 2000). Single deletion of *sgdE* has not been performed in *A. nidulans*. In *Candida albicans*, SgdE is localized at yeast-form cell surface, but not the hyphal cell surface. It is also present in cytoplasmic extracts of *C. albicans* hyphae (Urban *et al.* 2003).

AN5327 is an uncharacterized protein in *A. nidulans*. It has high amino acid sequence identity with *S. cerevisiae* and *C. albicans* VPS1. VPS1 is a small GTPase that is important for biofilm formation and filamentous growth. In *C. albicans* VPS1 is induced upon adherence to polystyrene (Marchais *et al.* 2005). *Saccharomyces cerevisiae* VPS1 is involved in actin cytoskeleton organization and associates with Golgi membranes (Ekena and Stevens, 1995).

5.4. Conclusion and future work for this Chapter:

Using TAP tag and mass-spec analysis we showed that UmgA has at least three interacting partners. These are AN6688 (Septin B; AspB), AN6010 (SgdE) and AN5327

(uncharacterized) (Fig. 5.4). Without further investigation, it is too early to say whether UgmA really interacts with these proteins. It might be possible that these proteins bound nonspecifically to UgmA during purification. In order to confirm these interactions, we will have to study one-to-one interactions of UgmA with each of these proteins separately. One-to-one protein interaction can be confirmed by using different *in vivo* and *in vitro* techniques. These are bimolecular fluorescent complementation (split YFP), yeast two-hybrid system, and immunoprecipitation (IP). We will aso use reverse TAP to look for UgmA. Future work for this project might involve confirming these interactions of UgmA with AN6688, AN6010 and AN5327. Our future studies on these interactions will help to elucidate the molecular mechanisms underlying Gal*f* generation and deposition in cell wall. We expect that these will eventually lead to better understanding *Aspergillus* cell wall formation. In addition, AN6010 and AN5327 are not fully characterized in *A. nidulans*. Single deletion of each of these proteins will help us to understand their phenotypic roles in *A. nidulans* growth.

Acknowledgements

We are pleased to acknowledge individual support from the Natural Science and Engineering Council of Canada Discovery Grant program (SGWK), and we thank the University of Saskatchewan UGS and GTF programs (MKA). We thank Dr. Özgür-Bayram (Germany) for plasmid pME3156 which contains a codon optimized TAP.

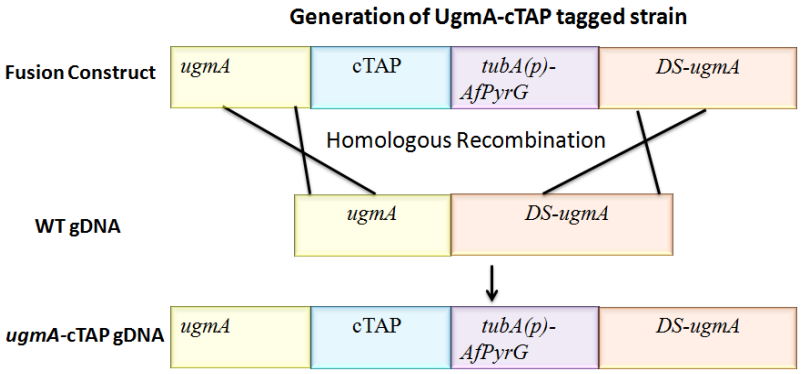

Figure 5.1. Strategy for generation of UgmA-cTAP tagged strain in *A. nidulans.* cTAP: C-terminus Tandem affinity purification, DS: downstream, WT: wild type, gDNA: genomic DNA.

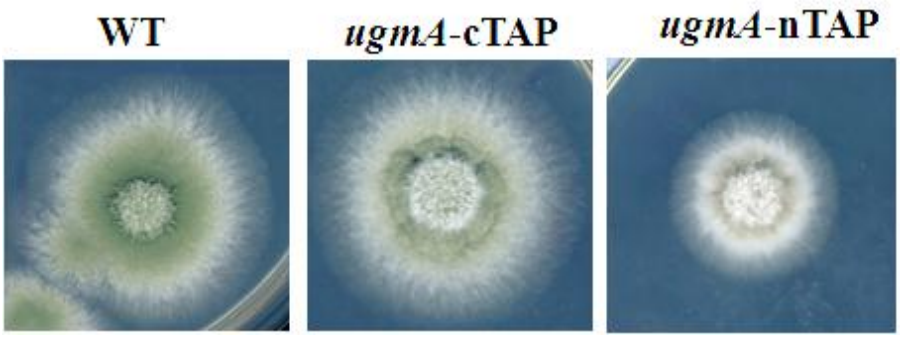

Figure 5.2: Colony morphology and spore colour of *Aspergillus nidulans* wild type (WT), *ugmA*-cTAP and *ugmA*-nTAP strains grown on complete medium at 30 °C for 3 d. *ugmA*-nTAP has lower spore production. However, no phenotypic difference in colony morphology was observed for wild type (WT) and *ugmA*-cTAP strains.

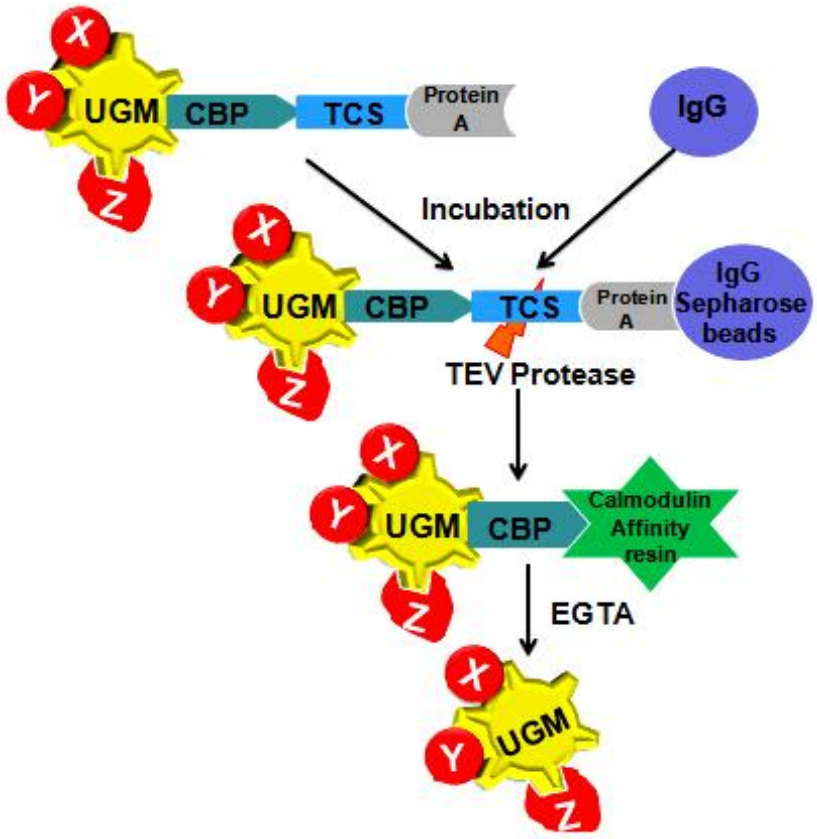

Figure 5.3: Work-flow of the tandem affinity protocol. UgmA is fused to C-TAP in the following order: (UgmA)-CBP-(TCS)-Protein A domain. Application steps of the protocol.

1st step: Binding of UgmA-TAP to the IgG sepharose.

2nd Step: TEV cleavage of the CBP domain and fusion protein from the IgG.

3rd Step: Binding of CBP to the calmodulin affinity resin.

4th Step: EGTA elution of the calmodulin affinity resin bound fusion protein and interaction partners.

5th Step: Elution of UgmA using EGTA.

TAP: tandem affinity purification, CBP: calmodulin-binding peptide, X-Y-Z: putative interacting partners, TCS: TEV cleavage buffer, TEV: tobacco etch virus.

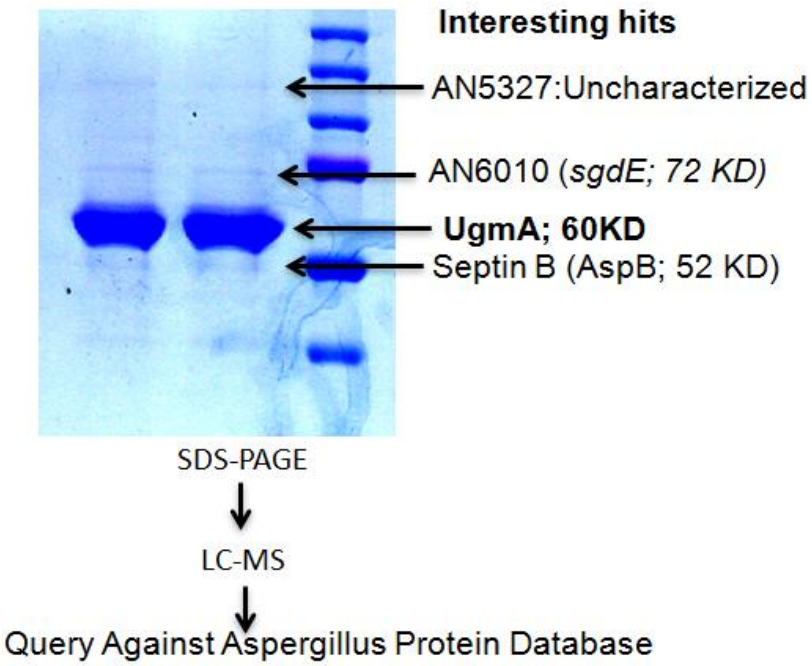

Figure 5.4: Identification of the interaction partners of the UgmA-TAP protein in *A. nidulans*. Strains were grown 20 h, total proteins were isolated and purified using TAP protocol. Purified UgmA was then run on 10% SDS-polyacrylamide gel and stained with Coomassie-blue. Individual bands were then sent for mass-spec analysis. Peptides of identified proteins were individually blasted against a public *A. nidulans* genome-wide protein sequence database of the Broad Institute (http://www.broadinstitute.org/scientific-community/science/projects/fungal-genome-initiative/fungal-genome-initiative) to ensure their unambiguous assignment to the Mascot-specified protein.

Table 5.1: Peptides identified from the bands using mass-spec belong to AN3112, AN6688, AN5327, and AN6010.

Protein Hits	Peptides Identified	Protein sequence coverage	Mass
AN3112.2 (UgmA)	R.VPSFQDILQGR.M K.YFDDCINEALPK.E K.EDDWYEHQR.I K.GQWVPYPFQNNISMLPK.E K.CIDGMIDAAIEHR.V K.DFDEWIVR.M R.MMGTGVADLFMRPYNYK.V K.VWAVPTTK.M K.MQCAWLGER.V K.AVTTNVILNK.T K.TAGNWGPNATFR.F R.DGTGGIWIAVANTLPK.E K.TVTLGDGTTVGYQK.L R.ATIFSNYSPYNQPDASK.K R.ATIFSNYSPYNQPDASKK.L K.KLPTLQLADGSKPK.N K.LPTLQLADGSKPK.N R.RFDHGYPTPSLER.E K.LQSMDIWSR.G R.RLVDGAQAFAK.N	41%	59764
AN6688 (Septin B;AspB)	R.YDAYLEAEN.V K.ADTLTDDEISMFK.K K.VPFAVVGANSEVATSDGR.K	10%	46826
AN5327 (uncharacterized)	K.TAGNWGPNATFR.F R.DGTGGIWIAVANTIPK.E K.QLFYSSTHVIGVGIR.G	8%	90000
AN6010 (SgdE)	R.AQLESLVEPLISR.T K.YSPAQIGGFVLGK.M	4%	72328

Supplemental Information

Table S1: Strains and primers used in this study

Aspergillus

AAE1[a]	*Aspergillus nidulans pyrG89*::Nc*pyr4+; pyroA4*; *nkuA*::*argB*
A. nidulans ugmA-cTAP[b]	AN3112::ugmA-cTAP:*tubA*p:Af*pyrG;pyrG89;pyroA4;nkuA::argB*
A. nidulans ugmA-cTAP[b]	AN3112::ugmA-cTAP:*tubA*p:Af*pyrG;pyrG89;pyroA4;nkuA::argB*

Escherichia coli

BL21-gold (DE3)[d]

Plasmids

pME3156[c]	pME3156, TAP, amp^R

Primers	Sequence 5' → 3'
cTAP tagging of *ugmA*	
P1 ugmA F	ATGCTTAGTCTAGCTCGCAAGACT
P2 ugmA (TAP-tail) R	CTTTTTCCATCTTCTCTTCTGCGCCTTATTCTTAGCA
P3 cTAP F	AAGAGAAGATGGAAAAAGAATTTCAT
P4 cTAP (*tubA*(p)-tail) R	AGTCACGTGCTGCATTCAGGTTGACTTCCCCGC
P5 *tupA*p F	ATGCAGCACGTGACTATT
P6 *tupA*p (*pyrG*-tail) R	AATTGCGACTTGGACGACATCTTGTCTAGGTGGGTGGT
P7 Af*pyrG* F	ATGTCGTCCAAGTCGCAATT
P8 Af*pyrG* R	TCATGACTTGCCGCATACTC
P9 dn An*ugmA*(*pyrG*-T) F	GAGTATGCGGCAAGTCATGAAACTCTTCTGCGTGGATGG
P10 dn An*ugmA* R	GGACTGCAGGTTGAAGCAG
Fusion construct generation	
P11 Fusion *ugmA* F	CCGTCCTTCGTAGAGTACTTGAG
P12 Fusion dn *ugmA* R	GGTTGAACGATGTCAGCGTA
Confirmation of *ugmA-cTAP*	
P1 *ugmA* F	ATGCTTAGTCTAGCTCGCAAGACT
P10 dn *ugmA* R	GGACTGCAGGTTGAAGCAG
Ame8 mid*PyrG* R	CACATCCGACTGCACTTCC
Sequence primers for Confirmation of *ugmA-cTAP*	
P13 mid ugmA F	ACATTGTCAACGGCGCTG
P14 mid *tupA(*p) R	CCATCCTTTCTGGGTCGC

a El-Ganiny et al. (2008)
b This study
c This study
d Novagen (www.emdchemicals.com)

CHAPTER 6

General Discussion

Galactose metabolism is conserved from prokaryotes to metazoans, consistent with its importance in catabolism for generation of ATP from sugars and its importance in anabolism for generation of extracellular carbohydrates and carbohydrate-conjugated proteins and lipids. Previous research by El-Ganiny and colleagues (2008, 2010) and Afroz et al. (2011) focussed on characterizing the function of three sequentially acting genes in the *Aspergillus nidulans* Leloir pathway: UgeA, UgmA, and UgtA. The research presented in this thesis focussed on placing the Leloir pathway genes, particularly *ugmA*, in their larger metabolic context. This included characterization of upstream genes GalD and GalE (Chapter 2), an analysis of the consequences of repression or overexpression of the Leloir genes including effects on alpha- and beta-glucan synthesis (Chapter 3), further characterization of the phenotypic consequences of particular amino acid residues in the UgmA active site (Chapter 4), and preliminary identification of protein interactors of UgmA (Chapter 5).

6.1. Galactose metabolism is more complex in *Aspergillus nidulans* than in *Saccharomyces cerevisiae*

The highly conserved Leloir pathway enzymes GalD and GalE are involved in galactose metabolism (Ross et al. 2004). In my first project (Chapter 2) characterization of phenotypes related to the roles of GalD and GalE revealed the complexity of galactose metabolism in *A. nidulans*. Previously Roberts (1963, 1970) described some roles of mutant alleles of these enzymes in galactose metabolism, and Fekete et al. (2004) explored the enzymatic role of galactokinase in *Aspergillus nidulans*. However, the biological function of galactokinase (GalE) and galactose-1-phosphate uridylyltransferase (GalD) had not previously been well characterized in *Aspergillus.*

Although GalD and GalE are essential for growth on D-galactose in many systems including *S. cerevisiae* (Dickson & Riley, 1989; Slepak et al. 2005, Seiboth et al 2007), my study showed that *A. nidulans* GalD and GalE play multiple but not essential roles in growth on galactose. Only GalD was essential for *A. nidulans* growth on galactose at pH 4.5, indicating that an alternative pathway of galactose metabolism might be available in *A. nidulans* at higher pH. By complementing respective *S. cerevisiae* genes, I showed that

A. nidulans GalD and GalE are functionally homologous to *S. cerevisiae* GAL7 and GAL1, respectively (Chapter 2). Thus, functional homology does not always ensure homologous function in different systems. As in *S. cerevisiae*, GalD and GalE gene expression was up-regulated when growing on galactose as a sole carbon source (Chapter 2). However, GAL7-GFP localization shows a clumped distribution in *S. cerevisiae* (Christacos et al. 2000), whereas GalD-GFP fluorescence distribution was even (Chapter 2). Together, this evidence strongly suggested that galactose metabolism is more complex and flexible in *A. nidulans* than in *S. cerevisiae*.

There are few existing hypotheses that might describe the disparity of galactose metabolism between yeast and filamentous fungi. First of all, the *S. cerevisiae* Leloir pathway enzymes have been proposed to form multi-enzyme complexes (Abadjieva et al. 2001; Kindzelskii et al. 2004). Unlike in *Saccharomyces*, pronounced galactose toxicity has not been reported in *Aspergillus* and their Leloir pathways genes are not clustered. Slot and Rokas (2010) suggested that gene clustering may correlate with Leloir pathway defects that produce toxic intermediates. GAL7 deficient cells had high accumulation of galactose-1-phosphate as an intermediate product, which has been shown to be toxic to both yeasts and mammals (Tsakiris et al., 2002; Slepak et al, 2005). Secondly, although the Leloir pathway appears to be the main D-galactose degrading route in *Aspergillus*, alternative or additional galactose metabolism pathways via galactitol, sorbitol and fructose (Elorza and Arst, 1971) and fructose-6-phosphate and sorbose-6-phosphate have been proposed in *A. nidulans* (Fekete *et al.* 2004). Flipphi *et al.* (2009) hypothesized that galactitol can also be epimerized to D-tagatose via L-sorbose, which might be catabolized via D-sorbitol and D-fructose to D-fructose-6-phosphate. Although an alternative pathway of galactose metabolism has not been reported in yeast, a non-phosphorolytic pathway for D-galactose utilization has been reported for *A. niger* (Elshafei & Abdel-Fatah 2001) but neither the genes nor the proteins have been identified. Similarly, a *Hypocrea jecorina* strain with deleted galE was able to grow on D-galactose (Seiboth et al. 2004). *Aspergillus* species, including *A. nidulans*, have approximately twice as many genes as *S. cerevisiae* and genomes approximately three times larger than that of *S. cerevisiae* (Goffeau et al 1996), indicating the difference in genomic organization between *Aspergillus* and *Saccharomyces*. Finally, although galactose metabolism

is conserved between yeast and filamentous fungi to the extent that many *S. cerevisiae* genes can fully complement *A. nidulans* gene deletion strains, the regulatory circuits achieving the cellular process appear to be distinct. Galactose metabolism genes in *S. cerevisiae* are regulated by the interplay of three proteins: a transcriptional activator, Gal4, a repressor, Gal80, and an inducer, Gal3 (Sellick et al 2008). However, the orthologues of GAL3 and GAL4 are absent in the genomes of *H. jecorina* and *A. nidulans* (Sellick et al 2008). Moreover, the genomic organization of the Leloir pathway genes in filamentous fungi reveals a major difference to yeasts, as they are not clustered (Slot and Rokas, 2010), indicating that galactose metabolism differs in filamentous fungi compared to yeast.

6.2. Gal*f* is nonessential, but is an important cell wall component

During my Ph.D. research, I studied the roles of Gal*f* in fungal growth, sporulation, wall maturation and hyphal surface adhesion in *A. nidulans* using two different approaches. In Chapter 3, I explored the roles of Gal*f* biosynthesis genes using strains whose endogenous promoter was replaced by the alcohol dehydrogenase promoter *alcA*(p) or the nitrogen regulated *niiA*(p) promoter. In Chapter 4, I showed how modification of *Af*UgmA leads to changes in cell wall α-glucan and β-glucan content, hyphal surface adhesion and response to antifungal drugs in *A. nidulans*. Previously, it was showed that deletion of any of three sequential-acting genes in the Gal*f* biosynthesis pathway causes similar defects in *A. nidulans* hyphal morphogenesis and colony development (El-Ganiny et al., 2008; El-Ganiny et al., 2010; Afroz et al., 2011) and in wall surface structure and force compliance (Paul et al., 2011). My work also showed that down-regulation of any of these genes, or *Af*UgmA site-directed mutagenesis in the enzyme active site, caused roughly comparably deficits in fungal growth, cell wall architecture, asexual sporulation, hyphal surface adhesion and response to antifungal drugs (Chapters 3 & 4).

Previous work by El-Ganiny et al (2008 & 2010) and Afroz et al (2011) showed that none of the Gal*f* biosynthesis enzymes is essential for viability of *A. nidulans*. Using a new anti-Gal*f* antibody called L10, I also showed that Gal*f* was absent in the cell wall of *ugeA*Δ, *ugmA*Δ, and *ugtA*Δ strains (Chapter 3). Although Gal*f* is nonessential for *Aspergillus* wall deposition, its presence is important for normal cell wall maturation, morphogenesis, hyphal

growth and surface integrity (Chapters 3 & 4). Schmalhorst et al. (2008) showed that an *A. fumigatus* strain deleted for its UgmA homologue had a similar phenotype to *ugeA*Δ, *ugmA*Δ, *ugtA*Δ strains. In addition, I showed that cell wall surface properties are severely compromised in *A. nidulans* strains that lacked Gal*f*. Previously Paul et al. (2011) showed that *ugmA*Δ *A. nidulans* had higher adhesion to AFM Si_3N_4 probe tips. Af*ugmA*Δ strains have been shown to be highly adherent to pulmonary epithelial cells, to glass or plastic surfaces compared to wild type (Lamarre et al., 2009). This change in adhesion properties was shown to be due to the unmasking of the cell wall mannan by removal of Gal*f* in *A. fumigatus* (Lamarre et al., 2009).

Gal*f* is also found as glycoconjugates on the cell surface of *Leishmania* and *Trypanosoma* and as such is important in parasite-cell interactions (Kleczka et al., 2007; MacRae et al., 2006). Gal*f* is essential in *Mycobacterium tuberculosis*, making Gal*f* biosynthesis as a drug target against mycobacteria (Scherman et al 2003). Unlike some bacteria and protozoa, Gal*f* contribution to *Aspergillus* pathogenicity has not been well established yet. Although Gal*f* lacking strains are highly adhesive, higher adhesion (Lamarre et al., 2009) has been correlated with both higher and lower pathogenicity (Schmalhorst et al., 2008; Lamarre et al., 2009) but there are few studies of this type and further research is needed. This disparity could be due to lower growth rates in *Af*UgmA mutants, thus potentially also to lower tissue penetration.

All together, these result and previous studies clearly show that Gal*f* is non essential but important *Aspergillus* wall component which contributes many aspects of fungal growth, sporulation, wall maturation and surface integrity. My study also indicated that Gal*f* lacking strains have severely compromised wall surfaces, which requires future study to explore its role in host-pathogen interaction or pathogenicity.

6.3. Loss or absence of Gal*f* contributes to increased sensitivity to antifungal drugs

In addition to having multiple roles in *Aspergillus* growth, sporulation and wall architecture (Chapters 3 and 4), the loss of Gal*f* is correlated with increased antifungal drug sensitivity. As Gal*f* deletion strains were structurally compromised (Paul et al., 2011), we

expected that wild type levels of Gal*f* biosynthesis would be important for Caspofungin (beta-glucan synthase inhibitor) resistance. To test this, we compared the drug sensitivity of gene deletion and wild type with regulated Gal*f*-biosynthesis strains and explore the role of Gal*f* biosynthesis proteins on drug sensitivity (Chapter 3). This study was initiated in 2010 by Dr. El-Ganiny, but required substantial additional work before publication. I also tested this hypothesis on *A. nidulans* strains that hosted mutated and wild type versions of the *A. fumigatus* homologue *Af*UgmA (Chapter 4).

As expected, we found increased echinocandin sensitivity for the deletion strains and repressed strains, but no significant change for compounds affecting ergosterol or its biosynthesis (Chapter 3). All the Af*ugmA* mutants in *A. nidulans* (Chapter 4) also showed significantly increased sensitivity towards Caspofungin. Consistent with this, Afroz et al (2011) showed that the *ugtA*Δ strain was hypersensitive to Caspofungin. None of the deletion, repression or *Af*UgmA mutations notably affected sensitivity to Calcofluor White that targets chitin microfibril crystallization or to Itraconazole that targets fungal membrane ergosterol biosynthesis. As a result, sensitivity to Itraconazole was typical of other membrane-targeting drugs, and was not related to Gal*f* biosynthesis gene presence or function. Calcofluor White (CFW) is a wall-targeting agent, which inhibits fungal growth, but is not clinically useful. Although my studies did not indicate a significant increase in CFW sensitivity, previously El-Ganiny et al. (2008) showed that the *A. nidulans ugmA*Δ strain was more sensitive to high concentrations of CFW (30 μg/mL or more) than the wild type strain. Consistently, the *A. niger ugmAΔ* strain was also more sensitive to high concentrations of CFW (30 μg/mL or more) than the wild type strains (Damveld et al., 2008). Interestingly, low levels of CFW (10 μg/mL) or growth on high osmolarity medium partially remediated the *ugmA*Δ strain phenotype defects (El-Ganiny et al. 2008), consistent with Gal*f* being important in cell wall structure and/or function.

Increased drug sensitivity of *ugmA*-deleted, -repressed, and -mutated strains to Caspofungin was consistent with our studies on the deletion and mutated strains that showed defects in wall architecture, wall surface integrity. An addition, previous AFM studies on the deletion strains showed defects in wall architecture and strength (Paul et al., 2011). Unexpectedly, colonies with over-expressed *alcA*(p)-*ugmA* were also significantly more

sensitive to Caspofungin than wild type. This is consistent with the abnormal width and branching of overexpressed *alcA*(p)-*ugmA* hyphae (Chapter 3), but the cause is not known. Consistent with this, increasing *Mycobacterium ugmA* expression was reported to increase resistance to isoniazid (a cytochrome P450 system inhibitor) (Richards and Lowary, 2009).

Gal*f* biosynthesis genes have both shared and divergent functions in cell wall metabolism. In sum we have shown that the *alcA*(p)- and *niiA*(p)-regulated control and site directed mutation of Gal*f* biosynthesis genes provide novel information about the role of this pathway in *A. nidulans*. Notably, deletion, mutation and repression phenotypes were significantly more sensitive to Caspofungin, suggesting that their walls are significantly less robust. We remain hopeful that an inhibitor of this pathway may be therapeutically beneficial. My results clearly indicated that Gal*f* lacking strains are hypersensitive to cell wall targeting drug, suggesting that Gal*f* biosynthesis could be a target for combination therapy.

6.4. Coordination of Gal*f* biosynthesis with other cell wall carbohydrate pathways

During my PhD. research I have shown that the deletion or repression or mutation of Gal*f* biosynthesis genes decreases *fksA* expression (Chapter 3) and wall beta-glucan content (Chapter 4). However, deletion or repression or mutation of Gal*f* biosynthesis genes increased *agsB* expression (Chapter 3) and wall alpha-glucan content (Chapter 4). The co-ordination of the Gal*f* pathway with beta-glucan and alpha-glucan pathways had never been reported previously in *A. nidulans* and *A. fumigatus*. Previously Damveld et al. 2008 showed that mutation of *ugm1* is associated with an increase in wall alpha-glucan content in *A. niger*. Decreased *fksA* expression and β-glucan content correlated with increased sensitivity to Caspofungin, which is mechanistically satisfying. This relationship has not been previously reported in fungi.

Not surprisingly, *A. nidulans* cell wall α-glucan and β-glucan content were found to be strongly correlated. This suggests that the cell is metabolically constrained as to where it apportions metabolites for wall synthesis, so that increases in abundance of one major polymer must limit the resources available for synthesis of the others. However, this does not directly explain why engineered changes in Gal*f* content are so strongly related to changes in α-glucan and β-glucan content. In an attempt to find how this relationship is maintained, I

used a tandem affinity purification (TAP) method combined with LC-MS/MS to study the interacting partners of UgmA (Chapter 5). My preliminary results suggested that UgmA has three predicted interaction partners (Chapter 5). Interestingly, none of them belong to alpha-glucan or beta-glucan biosynthesis pathways. This strongly suggested that there are no direct interactions among Gal*f*, alpha-glucan and beta-glucan biosynthesis proteins. The question how this dynamic co-ordination is maintained still remains open.

It is highly possible that Gal*f* co-ordinates with alpha-glucan and beta-glucan pathway via cell wall integrity pathway (CWI). CWI signaling pathway controls the remodeling of cell wall during growth and morphogenesis, and response to environmental challenges (Levin, 2005; Fujioka et al 2007; Fuchs and Mylonakis, 2009; Levin, 2011; Dichtl et al 2012). In fungi, the CWI signalling pathway regulates shape and biosynthesis of the cell wall (Smits et al 1999; Fujioka et al 2007; Dichtl et al 2012). CWI pathway transmits wall stress signals from the cell surface to the Rho1 GTPase, which proceeds via Pkc1p and a downstream mitogen-activated protein kinase (MAPK) cascade (Levin, 2005 & 2011; Dichtl et al 2012). CWI pathway is induced in response to several environmental stimuli such as osmotic stress, pH, and high temperature (Levin, 2005; Fujioka et al 2007; Levin, 2011), resulting in increased levels of expression of numerous genes, many of which encode integral cell wall proteins or enzymes involved in cell wall biogenesis. These include beta-1,3-glucan synthases (Fks1p and Fks2p) (Fujioka et al 2007; Levin, 2011), alpha-1-3 glucan (agsA and agsB) (Fujioka et al 2007) and chitin synthase (Chs3p) (Chant et al 1991; Birkaya et al 2009). In fungi, preventing the synthesis of one component of the cell wall is known to lead to a compensatory increase in another. For example, inhibition of beta-(1,3)-glucan synthesis by caspofungin resulted in a compensatory increase in chitin synthesis in *C. albicans* which was achieved through CWI signalling pathway (Walker et al., 2008). We did not look at the relationship Gal*f* with chitin synthesis pathway because of the involvement of many genes in chitin synthesis in *A. nidulans*. However, Nikkomycin Z (a chitin synthase inhibitor) caused morphological defects in wildtype *A. nidulans* hyphae, but was not able to inhibit the growth of either the wild type or the Gal*f*-defective strains, when assessed using disc diffusion method (Chapter 3). Taken all together, it might be possible that when Gal*f* is removed due to deletion or mutation of Gal*f* biosynthesis genes, CWI pathway becomes activated. This

activation might lead to changes in beta-glucan and alpha-glucan synthesis for *A. nidulans* survival.

My study clearly showed that there is a dynamic coordination between cell wall Gal*f*, with α-glucan, and β-glucan. This aspect of co-ordinations had never been reported previously in *Aspergillus*. This also suggests the possibility to use the Gal*f* biosynthesis pathway as model to study essential wall components, particularly beta-glucan.

6.5. Possibility for anti-Gal*f* as a part of a cocktail of anti-fungal treatments

Gal*f* appears to be both a structural and an antigenic component of important cell surface molecules in a variety of microbes, ranging from bacteria to parasites and fungi (Tsuji et al 2001; Latgé, 2009). Inability to synthesize Gal*f* compromises cell integrity in *Mycobacterium tuberculosis*, resulting in severely decreased viability and attenuated survival in the host (Pan et al 2001). Genetic deletion or chemical inhibition of UGM prevents mycobacterial growth (Pan et al 2001; Dykhuizen et al 2008). In *Leishmania*, loss of Gal*f* synthesis results in severe defects in the early stages of mammalian infection (Kleczka et al 2007; Madeira et al 2009). Gal*f* synthesis by Ugm is essential in *C. elegans* (Novelli et al 2009). As a consequence, a recent study suggested that Gal*f* biosynthesis pathway can also be a potential drug target in pathogenic nematodes (Wesener et al 2013).

Gal*f* is not essential for any fungi studied to date. However, its presence is important for cell wall growth, maturation and integrity. In addition, Gal*f* residues appear to form part of the secreted antigens in invasive aspergillosis infections (Leitao, 2003). Although the effects of Gal*f* observed vary with organism, generally Gal*f* deficient strains are hypersensitive to wall-targeting drugs and exhibit a constitutive osmotic stress phenotype (Afroz et al., 2011; El-Ganiny et al, 2008). Gauwerky et al. (2009) and Aimanianda & Latgé (2010) suggest that non-essential wall components as well as virulence factors have the potential to be useful anti-fungal drug targets.

Since none of the Gal*f* biosynthesis genes are essential for survival in fungi, inhibition of the Gal*f* biosynthesis pathway would not be fungicidal. However, substantial growth reduction might reduce the *Aspergillus* capacity to infect an immunocompromised host. Consistently, recent reviews of antifungal therapeutic strategies are no longer suggesting that

therapies need to be limited to killing fungi but rather to reduce their ability to cause disease (Gauwerky et al., 2009). For example, echinocandins including caspofungin do not kill *Aspergillus* (Denning, 2003) but in experimental animal studies these drugs induce morphological changes that decrease fungal pulmonary injury (Petraitiene et al., 2002) and so they are clinically effective. In addition, every step of the *Aspergillus* Gal*f* biosynthesis pathway is synthesised by single gene. Therefore, their enzymatic functions are less likely compensated by genetic redundancy, and thus have higher likelihood of being drug targets. For example, synthesis of *Aspergillus* β-1,3-glucan is catalyzed by only one enzyme that is encoded by single gene, *fksA* (Kelly et al., 1996). In contrast, at least eight genes with overlapping functions are involved in chitin synthesis (Mellado et al., 1995). Therefore, the echinocandins (β-1,3-glucan synthesis inhibitors) are clinically useful, whereas chitin synthase inhibitors (Nikkomycin Z) have not proven to be effective drugs in clinical use (Latgé, 2007).

All together, the pathogenic contribution of Gal*f* is not fully clarified. Gal*f* biosynthesis is not essential in *Aspergillus* species, unlike *Trypanosoma* (Roper et al., 2002) and several pathogenic bacteria (Pan et al., 2001), so selection pressure to overcome a future potential therapeutic compound might be reduced. However, considering Gal*f*-lacking strains had substantially reduced growth and hypersensitivity to caspofungin, anti-Gal*f* drugs (once created) may be useful in combination with existing antifungal drugs. Combination therapy is already in use to combat fungal infection (Baddley and Pappas, 2005; Mihu et al., 2010). For example, it has been shown that toxicity of amphotericin B can be reduced in combination with echinocandins (Mihu et al., 2010). Use of flucytosine in combination with many other drugs helps in preventing the rapid development of resistance (Johnson et al., 2004). Altogether, considering the emergence of resistance against antifungal drugs and the high rate of mortality from fungal infections, there is a pressing need for new therapeutic options. Use of combination therapy, especially anti-Gal*f* drugs (once created) in combination with echinocandins may overcome both emergence resistance and infection problems.

6.6. Future directions

The potential for Gal*f* to be a part of combination therapy, and its relationship with other major wall carbohydrate pathways, has not been previously explored. My Ph. D. research explored these two aspects of Gal*f*-biosynthesis pathway in *Aspergillus*, which may receive widespread research attention for future drug development and cell wall formation studies. Based on my Ph. D. research, the following experimental directions are possible.

1. From my first project (Chapter 2) we have shown that characterization of phenotypes related to the roles of GalD and GalE reveals the complexity of galactose metabolism in *A. nidulans*. Based on literature we also suggested that the complexity of galactose metabolism in *Aspergillus* might be due to availability of alternative pathway of galactose metabolism and the genomic organization of the Leloir pathway genes in filamentous fungi. Alternative pathways of galactose metabolism (Fekete *et al.* 2004; Flipphi *et al.* 2009) are not well characterized in filamentous fungi. Exploring these putative alternative pathways might help us to better understand the growing environment of medically and industrially important *Aspergillus* species.
2. My study showed that Gal*f* is important for *Aspergillus* growth, sporulation, cell wall maturation and integrity. However, the pathogenic contribution of Gal*f* is still debatable, and this needs to be resolved. The pathogenicity of different Gal*f*-defective strains can be tested in tissue culture or animal model systems. Preliminary results, through collaboration with our group, showed that *ugmAΔ* strains cannot grow in tissue culture plates although the wild type can, suggesting that *ugmAΔ* strains will be less able to cause disease. I also attempted to use Zebra fish larvae as an alternative model to study *Aspergillus* infection. My preliminary results indicated that *Aspergillus* spores were unable to form colonies on zebra fish larvae if we exposed them through water. To further continue this study we needed a microinjection facility. Unfortunately, we did not find any microinjection facilities at level-2 lab. This is why I could not continue this experiment. Future developments in this area will include development of zebra fish larvae as a new animal pathogenicity model system for *Aspergillus* infection study.

3. Crystal structure of *Af*Ugm is solved (van Straaten et al 2012) and our study showed that R327 is essential for *Af*Ugm function (Chapter 4). Based on structural and functional information, it might be possible to develop an inhibitor against UgmA in collaboration with Dr. David Sanders who has expertise on drug development. Once an anti-Gal*f* drug is developed, disc diffusion assay can be adapted to screen and compare the effect of candidate compounds in combination with Caspofungin for their effect against *Aspergillus* strains. An inhibitor against prokaryotic UGM was developed to prevent mycobacterial growth (Dykhuizen et al 2008). Although inhibitor against eukaryotic UGM has not been developed yet, a prokaryotic inhibitor can partially inhibit UGM function (Wesener et al 2013). Prokaryotic UGM inhibitors have not been tested against *Aspergillus*, likely because there is insufficient material available for this study, but possibly also due to the relatively low sequence conservation outside the enzyme active site. However, we remain hopeful that the use of combination therapy, especially anti-Gal*f* drugs in combination with echinocandins may overcome both emergence resistance and infection problems.
4. Using TAP tag and mass-spec analysis we showed that UmgA appears to have at least three interacting partners including AN6688 (Septin B; AspB), AN6010 (SgdE) and AN5327 (uncharacterized) (Fig. 5.4). However, it is too early to say whether UgmA actually interacts with these proteins. In order to confirm these potential interactions, we have to study one-to-one interactions between UgmA with each of these proteins separately. One-to-one protein interaction can be assessed by using *in vivo* as well as *in vitro* techniques. These include bimolecular fluorescent complementation (split YFP), yeast two hybrid system, co-immunoprecipitation (Co-IP; using an epitope tagged strain plus available antibody), and TAP tagging the genes of interest to determine if they interact with UgmA. Our future studies on these interactions are expected to help elucidate the molecular mechanisms underlying Gal*f* generation and deposition in cell wall, which eventually should lead to better understanding *Aspergillus* cell wall formation. In addition, AN6010 and AN5327 are not fully characterized in *A.*

nidulans. Single deletion analysis of each of these proteins should help us to understand their phenotypic roles in *A. nidulans* growth.

5. My study also showed that cell wall Gal*f*, α-glucan, and β-glucan content are correlated *in A. nidulans* hyphal walls, suggesting a dynamic coordination between cell wall synthesis and cell wall integrity. However, how modification of Gal*f* biosynthesis leads to change in cell wall compositions is still unknown. Interestingly, tandem affinity purification combined with LC-MS/MS suggested that there are no direct interactions among Gal*f*, alpha-glucan and beta-glucan biosynthesis proteins. The question how is this dynamic co-ordination maintained remains open. In fungi, preventing the synthesis of one component of the cell wall is known to lead to a compensatory increase in another, which is achieved via the cell wall integrity pathway (CWI). Future studies might include study the co-ordination of Gal*f* pathway with α-glucan, and β-glucan pathway via targeting CWI pathway members.

In summary, my thesis has presented a comprehensive study on the roles of Gal*f* biosynthesis in the model experimental fungal system *Aspergillus nidulans*. My results clearly show that Gal*f* plays important roles in *Aspergillus* growth, sporulation, hyphal wall architecture, wall maturation, wall surface integrity and also in responses to currently available antifungal drugs. The co-ordination of the Gal*f* pathway with alpha-glucan and beta-glucan synthesis is also presented in this thesis. To begin to explore how coordination might occur, my research studied interacting partners of UgmA. Although compounds that could inhibit Gal*f* biosynthesis have yet to be generated, there are considerable reasons for continuing to work in this area. In particular, pathogenic contribution of Gal*f* in *Aspergillus* needs to be resolved. Future study also needs to explore the co-ordination of the Gal*f* pathway with α-glucan, and β-glucan pathways. Besides potentially being part of combination therapy, Gal*f* can also serve a model sugar to study essential wall components, particularly beta-glucan. Future study on UgmA interactions may also elucidate the molecular mechanisms underlying Gal*f* generation and deposition in cell wall which eventually lead to better understand the *Aspergillus* cell wall formation. Finally, the details of fungal cell wall composition and structure are still a very complicated puzzle; each element plays a role on its

own as well as in concert with the others in the functioning of this structure. Therefore, the more we study the fungal wall, the better we will understand its formation, host interaction, and pathogenic contribution which will eventually allow us to find a better therapeutic approach.

Appendix A: Zebra fish larvae as an experimental model system for vertebrate pathogenesis

Aspergillosis is the second most common human systemic fungal disease. Zebrafish are vertebrates and their larvae are transparent, so they have the potential to be a superior model for *Aspergillus* infection in a vertebrate system. The only alternative non-vertebrate model that is occasionally utilized is the silkworm larva. However, this model does not allow for proper determination of pathogenicity since *Aspergillus* spores are injected into the larvae directly.

The hypothesis to be tested was that zebrafish larvae could serve as an effective model for studying *Aspergillus* infection. Specific research objectives were aimed at assessing colonization of zebrafish larvae by fungal spores, assessing the potential impact of colonization on larvae, and examining changes in pathogenicity following colonization by *Aspergillus* wild type and mutants. For assessing pathogenicity and infection, newly hatched larvae were exposed to *Aspergillus* spores that express green fluorescent protein through water. It was expected that this would allow us to monitor the progress of *Aspergillus* growth in the transparent zebrafish larvae at real time using fluorescence microscopy. The experiment was conducted at 9 CM Petri dish where 25 larvae (newly hatched to 2 d old) were put into sea water. Then larvae were exposed to *Aspergillus* spores at different concentration (10^5 -10^9 spores/dish) through water. Several trials were carried out until 7 d post-fertilization using standard protocol. Unfortunately, we did not see any growth of *Aspergillus* on larvae. We did not even observe any mortality or abnormalities in larval development. Therefore, this experiment clearly indicates that *Aspergillus* spores are unable to form colonies on zebra fish larvae if we exposed them through water. For this study we included *A. fumigatus*, *A. flavus, A. nidulans* strains. *A. flavus* is one of the major causes of farm fish disease (Olufemi & Roberts, 1986, Hashem, 2011). Therefore, we included *A. flavus* for our infection study. But in all cases our results turned out to be negative.

For studying *Candida* infection in Zebrafish larvae, microinjection was used to inject spores directly into the hindbrain region or peritoneal cavity of 1-3 d old larvae (Chao et al., 2010). Therefore, we decided to inject *Aspergillus* spores directly into the hindbrain region or peritoneal cavity of larvae. Unfortunately, we did not find any microinjection facilities in a

Biosafety level-2 lab. This is why I could not continue this experiment. But we are still looking for such as microinjection facilities.

Appendix B: Molecular biology, microscopic and microbiological techniques used in the thesis

1. Protein extraction and purification

1. 1. Total Protein Extraction

1. Grow *A. nidulans* conidia in liquid complex media (CM) for 20 h.
2. Collect mycelia from liquid cultures by filtration through Miracloth paper
3. Wash mycelia with distilled water, dry on paper towels and ground to a powder with mortar and pestle in liquid nitrogen.
4. Resuspend the ground mycelium and boil in the urea/SDS buffer (1% SDS, 9 M urea, 25 mM Tris-HCl (pH 6.8), 1 mM EDTA, and 0.7 M 2 mercaptoethanol).
5. Remove the debris by centrifugation at 13000 x *g*.
6. Determine the total protein concentration.

1.2 SDS and Western blotting

The acrylamide percentage in SDS PAGE gel depends on the size of the target protein in the sample. (Details shown below)

Acrylamide %	**M.W. Range**
7%	50 kDa - 500 kDa
10%	20 kDa - 300 kDa
12%	10 kDa - 200 kDa
15%	3 kDa - 100 kDa

- **For a 5 ml stacking gel:**

H_2O	2.975 ml
0.5 M Tris-HCl, pH 6.8	1.25 ml
10% (w/v) SDS	0.05 ml

Acrylamide/Bis-acrylamide (30%/0.8% w/v)	0.67 ml
10% (w/v) ammonium persulfate (AP)	0.05 ml
TEMED	0.005 ml

- **For a 10ml separating gel:**

Acylamide percentage	6%	8%	10%	12%	15%
H_2O	5.2ml	4.6ml	3.8ml	3.2ml	2.2ml
Acrylamide/Bis-acrylamide (30%/0.8% w/v)	2ml	2.6ml	3.4ml	4ml	5ml
1.5M Tris(pH=8.8)	2.6ml	2.6ml	2.6ml	2.6ml	2.6ml
10% (w/v)SDS	0.1ml	0.1ml	0.1ml	0.1ml	0.1ml
10% (w/v) ammonium persulfate (AP)	100µl	100µl	100µl	100µl	100µl
TEMED	10µl	10µl	10µl	10µl	10µl

Note: AP and TEMED must be added right before each use.

- **5X Sample buffer (loading buffer):**

10% w/v	SDS
10 mM	Dithiothreitol, or beta-mercapto-ethanol
20 % v/v	Glycerol
0.2 M	Tris-HCl, pH 6.8
0.05% w/v	Bromophenolblue

- **1x Running Buffer:**

25 mM	Tris-HCl
200 mM	Glycine
0.1% (w/v)	SDS

1.2 SDS PAGE Protocol:

1**. Make the separating gel:**

1. Set the casting frames (clamp two glass plates in the casting frames) on the casting stands.
2. Prepare the gel solution (as described above) in a separate small beaker.
3. Swirl the solution gently but thoroughly.
4. Pipet appropriate amount of separating gel solution (listed above) into the gap between the glass plates.
5. To make the top of the separating gel be horizontal, fill in water (either isopropanol) into the gap until a overflow.
6. Wait for 20-30min to let it gelate.

2. Make the stacking gel:

1. Discard the water and you can see separating gel left.
2. Pipet in stacking gel until an overflow. Insert the well-forming comb without trapping air under the teeth. Wait for 20-30 min to let it solidifies.

3. Prepare the samples:

1. Mix your samples with sample buffer (loading buffer).
2. Heat them in boiling water for 5-10 min.
3. Load prepared samples into wells and make sure not to overflow. Don't forget loading protein marker into the first lane. Then cover the top and connect the anodes.
4. Set an appropriate volt and run the electrophoresis when everything is done, generally, about 1 hour for a 120 V voltage and a 12 % separating gel.

PAGE Staining Methods

Coomassie blue staining:

Staining solution:

0.3 % Coomassie Brilliant Blue R-250 (w/v)

45 % methanol (v/v)

10 % glacial acetic acid (v/v)

45 % ultrapure water

Destaining solution:

20% methanol (v/v)

10% glacial acetic acid (v/v)

70 % ultrapure water

Procedure:

1. Immerse the gel with staining solution, and slowly shake it on horizontal rotator for about 20 30 min.
2. Immerse the gel in destaining solution and put it on the same shaker for about 20-30min.

Western Blotting:

1. Soak 2 pads, nitrocellulose membrane and 6 x 3 Whatman paper in 1 x transfer buffer for 5-10 min.
2. Prepare transfer sandwich in the following order: black-face of plastic holder, pre-soaked pad, pre-soaked 3 x 3 mm Whatman papers, gel, pre-soaked nitrocellulose membare, pre-soaked 3 x 3 mm Whatman papers, presoaked pad, white-face of plastic holder.
3. Place the cassette, along with the ice pack, into the electrophoretic cell. The black face of the cassette must face the negative electrode (black panel of the transfer container).
4. Fill the transfer apparatus to the top with the ice-cold 1X transfer buffer. Transfer the gel at 80 V for 1. 5 h
5. Rinse your blot in wash buffer after blotting, add blocking buffer, incubate with gentle agitation for 30-60 min at room temperature or overnight at 4 °C, on a shaker.
6. Pour out the blocking buffer (can be reused), add washing buffer, agitate on a shaker for 10 min. Remove washing buffer, repeat two more times. (Can be done with four steps of 5 min each)
7. Add primary antibody solution to blot. Incubate for 2 h to overnight with gentle agitation. Pour off primary antibody solution (Can be reused).
8. Wash 3 x 5 min with TBST
9. Add secondary antibody solution. Incubate for 1/2 to 1.5 hours with gentle agitation. Pour off secondary antibody solution (Can be reused).

10. wash 3 x 5 min with TBST

11. Scan the membrane with the appropriate scanner.

1.3. TAP protocol

1. Collect total protein from *A. nidulans* strains

2. Incubate crude extract/IgG sepharose mixture on a rotating platform at 4 °C for 2 h.

3. Pass the mixture through chromatography columns with gravity. IgG sepharose will be accumulated at the bottom of the columns.

4. Wash Sepharose with 2 × 10 mL wash buffer 1 (250 mM NaCl, 40 mM Tris–HCl pH 8.0, 0.1 % NP-40, 1 mL PMSF, 100 mL DTT) supplemented with ethylene diamine tetra-acetate (EDTA)-free protease inhibitor tablets and phosphatase inhibitors, once with 10 mL wash buffer 2 (150 mM NaCl, 40 mM Tris–HCl pH 8.0, 0.1 % NP-40, 1 mM PMSF, 1 mM DTT) and once with TEV cleavage buffer (TCB) (150 mM NaCl, 40 mM Tris–HCl pH 8.0, 0.1 % NP-40, 0.5 mM EDTA, 1 mM PMSF, 1 mM DTT) supplemented with E-64.

5. Execute TEV protease cleavage reaction by adding 1 mL TCB and 20 µL of AcTEV™ enzyme (Invitrogen) and rotating the suspension overnight at 4 °C.

6. Transfer TEV protease treated suspensions to new column with 300 µL of washed calmodulin affinity resin (Stratagene) and 6 mL of calmodulin-binding buffer (CBB).

7. Close CBB columns and rotate at 4°C for 1 h.

8. Wash CBB columns with 3× 1 mL CBB.

9. Add 2 x 500 µL elution buffer (EB) to the column and collect proteins in 1.5 mL vials.

10. Perform Trichloroacetic acid (TCA)-precipitation and then load TCA-precipitated proteins onto a 10 % polyacrylamide gel, and then stain with Coomassie Brilliant Blue G (Sigma).

11. Cut the Protein bands and send to the PBI mass spectrometry facility for analysis.

2. DNA extraction, manipulation and PCR

2.1. Genomic DNA extraction protocol

1. Inoculate 20 mL liquid CM media in Petri plates with *A. nidulans* spores; incubate overnight at 37ºC.

2. Harvest mycelia by filtration through sterile paper towel, squeeze between several layers of paper towel to move extra water

3. Transfer into sterile microfuge tube, freeze in -80 ºC for 30 min then lyophilize overnight.

4. Break the lyophilized mycelia into fine powder using round toothpick

5. Transfer 100 µL of fine powder into fresh microfuge tube

6. Prepare fresh extraction buffer (pH 7.5-8) immediately before use as follow:

For 1 mL solution:

500 mM EDTA	100 µL
10% SDS	20 µL
Ultrapure water	880 µL

7. Add 500 µL extraction buffer per tube, Mix vigorously and transfer immediately to preheated 68ºC water bath.

8. Incubate at 68ºC for 10 min meanwhile chill KOAc solution on ice (60 mL 5M potassium acetate, 11.5 mL glacial acetic acid, 28.5 mL ultrapure water).

9. Vortex microfuge tubes briefly, centrifuge 5 min at maximum speed

10. Transfer supernatant to fresh microfuge tube (using micropipette)

11. Add 30 µL chilled KOAc solution, leave on ice for 5 min the centrifuge for 5 min

12. Transfer supernatant into fresh microfuge tube

13. Add equal volume of phenol:chloroform:isoamyl alcohol using Pasteur pipette

14. Vortex 30s then microfuge for 2 min.

15. Transfer the upper layer to a fresh microfuge tube (do not transfer the material at the interface).

16. Add equal volume of chloroform to the partially clean supernatant, vortex for 30s the centrifuge for 2 min

17. Transfer the upper layer to a fresh microfuge tube (do not disturb the interface).

18. Add 600 µL isopropanol, vortex well, centrifuge for 5 min.

19. Pour off isopropanol then add 500 µL of 70% ethanol, vortex till the DNA pellet is not stuck, centrifuge for 5 min then decant supernatant and let the pellet dry.

20. Resuspended in 100 µL (containing 5 µl RNAse). May require heating to dissolve

21. Run agarose gel to check quality of DNA (sharp band) before proceeding into other steps.

22. Finally, DNA is cleaned using Qiagen columns before using it in PCR.

2.2. Fusion PCR and Transformation:

Fusion PCR is widely used to fuse multiple DNA sequences together to generate one construct that can be used for gene targeting (gene deletion, replacement, tagging and promoter exchange).

Recipe for fusion PCR

DNA	1x3 µL
Primers (10µm)	1x2 µL
Taq polymerase	0.2 µL
Buffer (10x)	5 µL
H_2O	39.8 µL
Total	50 µL

Fusion products were then transformed into *A. nidulans* protoplast to target genes by homologous recombination.

3. RNA manipulation and qRT-PCR

3.1. RNA extraction

1. Inoculate *A. nidulans* spores in liquid CM media (2x 10^5 spores/ mL media), incubate at 37°C with shaking for 16 h

2. Collect mycelia by centrifugation, remove supernatant and flash froze the pellet in liquid nitrogen. Lyophilize the mycelia overnight

3. Transfer the lyophilized hyphae to RNase free centrifuge tube (start with a similar weight for all samples).

4. Break the mycelia completely into fine powder using a small pestle.

5. Add 450 µl RLC buffer (to which β-mercaptoethanol was added), vortex vigourously

6. Transfer the lysate to QIAshredder spin column and centrifuge for 2 min at maximum speed.

7. Transfer the supernatant to a new micro-centrifuge tube without disrupting the pellet

8. Add 0.5 volume 100% ethanol and mix immediately by pipetting, transfer directly to RNeasy spin column, centrifuge for 15s at 8000 x *g*, discard the flow-through

9. Add 700 µl buffer RW1 to the column, close the lid gently and centrifuge for 15 s at 8000 x *g*, discard the flow-through.

10. Add 500 µL buffer RPE to the column, centrifuge for 15s at 8000 x *g*, and discard the flow through.

11. Add 500 µL buffer RPE to the column, centrifuge for 2 min at 8000 x *g*, and discard the flow through.

12. Place the column in a new 2 mL collection tube, centrifuge for 1 min at maximum speed

13. Place the RNeasy column in a new 1.5 micro-centrifuge tube, add 50 µL RNase-free water directly to the membrane, centrifuge for 1 min at 8000 x *g*

14. The eluted solution contains total RNA, measure the RNA concentration with Nanodrop and dilute to the appropriate concentration, aliquot and store in -20 °C.

3.2. gDNA elimination and cDNA synthesis

Quantitect reverse transcription kit (Qiagen) was used to remove gDNA contamination and synthesize DNA first strand. This protocol is optimized to be used for up to 1 µg RNA. RNA should be diluted up to 500 ng / µL.

For gDNA elimination follow the following steps

1. Thaw template RNA, gDNA Wipeout buffer and RNase-free water on ice

2. Prepare genomic DNA elimination reaction on ice as follow gDNA Wipeout buffer 7x 2 µL

Template RNA (500 ng/µl)	2 µL
RNase-free water	10µL
Total	14 µL

3. Incubate for 2-3 min at 42°C, then place immediately on ice

For reverse transcription (cDNA synthesis) follow the following steps

4. Thaw Quantiscript Reverse Transcriptase, Quantiscript RT buffer and RT primer Mix on ice.

5. Prepare the reverse-transcription master mix as follow

Quantiscript Reverse Transcriptase	1 µL

Quantiscript RT buffer 5x	4 µL
RT primer Mix	1 µL
RNA from step 3	14 µL
Total	20 µL

6. Incubate for 15-30 min at 42 °C.

7. Incubate at 95 °C for 3 min to inactivate the reverse transcriptase.

8. Measure the cDNA concentration, dilute as required (e.g. 1:10), aliquot and store in -20 °C, this cDNA can be used for qRT-PCR or cloning.

3.3. qRT-PCR procedure

QuantiTect SYBR Green kit (Qiagen) and IQ cycler (BioRad) were used for performing qRT-PCR. We determined the relative expression of targeted genes using actin as a reference gene and ΔΔct to calculate the fold change in gene expression.

Procedure

1) Thaw QuantiTect SYBR Green PCR Master Mix, template cDNA, primers and nuclease-free water on ice.

2) The following recipe is used for 1 reaction

QuantiTect SYBR Green PCR Master Mix (2X)	10 µL
Primers (10 µm)	2x0.3 µL
cDNA	3 µL
Nuclease free-water	6.4 µL
Total	20 µL

3) For each gene (Actin or *ugmA*) multiply the above recipe by 10 to make a cocktail for 10 reactions (3 technical replicates, 3 No template control).

4) Mix all the ingredients (except cDNA) and divide equally into 3 tubes (A, B, C).

5) Add 10 µL cDNA to tube A (wild type) and B (mutant) and 10 µL water to tube C.

6) Mix and dispense 20 µL in the bottom of each well (of the 96-well plate).

7) Place the plastic film over the plate and carefully seal firmly, clean the surface with Kim wipes before putting in the IQ cycler.

4. DNA cloning, bacterial transformation, site directed mutagenesis

4.1. Cloning using restriction digest and ligation

1) The DNA fragment (insert) and the cloning plasmid (vector) should be cut using the same restriction enzymes to generate compatible ends.

2) Set up the following reaction mixtures

	Test	Negative control
Vector	DNA 5 µL	ultrapure water 5 µL
Insert DNA	5 µL	-
5X ligase buffer	4 µL	4 µL
Water	5 µL	10 µL
T4DNA ligase	1 µL	1 µL

3) Leave at room temperature at least for 2 hours or ligate overnight

4) Transform 10 µl of the rection mix into *E. coli* comptent cells; shake at 37 °C for 1 hr

5) Spread 50-100 µl on LB plates + suitable antibiotics; incubate overnight at 37°C

6) Colonies on test plates can be used for plasmid extraction, negative control plates should have no colonies.

4.2. Site directed mutagenesis

Site-directed mutagenesis is performed using the GENEARTR^{R} site-directed mutagenesis kit (life technologies) according to the manufacturer's protocol. An over-expression vector pET22b harboring the Af*ugm* gene was used as the template DNA.

Procedure:

1. Create the following reaction mixture:

Component	**Volume**
10X AccuPrime™ *Pfx* Reaction mix	5 µL
10X Enhancer	5 µL
Primer mix (10 µM each)	1.5 µL
Plasmid DNA (20 ng/µL)	1 µL
DNA Methylase (4 U/µL)	1 µL
25X SAM	2 µL

AccuPrime™ *Pfx* (2.5 U/μL)	0.4 μL
PCR water to	50 μL

2. Perform PCR using the following parameters.*****

Temperature	Duration	Number of Cycles
37 °C	20 min	1
94 °C	2 min	
94 °C	20 s	
57 °C	30 s	18 cycles******
68 °C	30 s/kb of plasmid	
68 °C	5 min	1
4 °C	forever	1

3. Set up the recombination reaction:

Component	**Volume**
5X Reaction Buffer	4 μL
PCR water	10 μL
PCR sample	4 μL
10X Enzyme mix	2 μL

4. Mix well and incubate at room temperature for 10 minutes.
5. Stop the reaction by adding 1 μL 0.5 M EDTA. Mix well and place the tubes on ice.
6. Place the tubes on ice and immediately proceed to transformation.
7. Select Ampicillin-resistant colonies from the LB plates and the specific mutation can be verified by DNA sequencing.

4.3. DNA sequencing protocol

Protocol for sequencing in Dr. Andres Lab

You can use your plasmid or PCR product for sequencing. It is better to start with the PCR product.

Step One: Cleaning the PCR product (Not needed for extracted plasmid)

Add following things to a new PCR tube:

PCR product	8 μL
PCR buffer 10x	1 μL
SAP	0.5 μL
EXOT	0.05 μL

*one drop of mineral oil to seal the tube

Put the tube into PCR machine, run the following PCR program:

37 ^{0}C	40 min
80 ^{0}C	15 min
l5 ^{0}C	hold

Step Two: Sequencing Reaction:

Template DNA	1 μL
ABI 5 x Buffer	0.5 μL
Primers (only one)	0.1 μL
RR	0.75 μL
ultrapure water	up to 5 μL

*Add one drop of mineral oil to seal the tube.

It is better to make master mix with RR, primer, ABI -5x buffer and H_2O first. Then add 4 μL of master mix to 1 μL template DNA.

Put the tube into PCR machine, run the following program:

94 ^{0}C	2 min
95 ^{0}C	50 s
Annealing Temperature	30 s
60 ^{0}C	4 min
15 ^{0}C	hold

Step Three: Cleaning the Sequencing Reaction tube

Follow the ABI cleaning process:

1. Shake the Agencourt Clean SEQ to fully resuspend the magnetic beads before using

2, Add 8 ul of Agencourt Clean SEQ to each sample.

3, Add 31 ul 85% ethanol to each sample, and mix 7 times by pipette. (Or until it becomes homogenous)

4. Place the tube onto an Agencourt SPIRPlate 96R (magnet) for 3-5 min, until the solution become clear.

5. Aspirate the cleared solution (supernatant) from the plate and discard (don't touch the brown beads on the tube wall by your tip)

6. Dispense 100 μL 85% ethanol into each well. Wait at least 30s and completed remove the ethanol and discard, repeat once (don't touch the beads on the tube wall by your tip)

7. Repeat 6 twice

8. Let the sample air-dry for l0 min (usually 5min is enough in Andres lab)

10. Transfer 35 ul of solution from each well to a new 96 direct inject plate, use A1-H1 column first and then A2-H2 (do not touch the beads on the wall and don't bring any bead to the 96 well plates).

11. ***lf your sample number is less than 16. You should fill up other wells in the first two columns by water. Because the machine will load l6 samples at one time)

l2. Put your plate into a cassette; make sure the wells with samples face to the front (the side without the notch).

Step Four: Loading the sample

l. Turn on the Computer

2. Turn on the machine; wait for the green light to switch on.

3. Run the program "3130" on the desktop

(A panel with 4 items will show on the screen. When all items become green, the panel will disappear and a new control panel will show up)

4. Select "ga3130XL", and then select "plate manager", then at the bottom of the panel to build a "New" program.

5. *wear a glove to touch the machine

Push "tray" button on the machine. When the tray stop at the front of the machine, open the door and put your cassette on the left position.

6. **check if there is any bubble in the circular system (at the left hand side of machine, start from a bottle and end in a glass jar)

7. Click "3l30XL", choose "Run Schedule" and "plate view". Find the file with your name and choose it. Then click panel A on the screen, the color will turn to green at the panel A place Then choose "run view" to see if it shows the right place of your sample on panel A
8. Click "  " symbol to run the machine.

5. **Immunofluorescence**

Protocol:

1. Grow *Aspergillus nidulans* spores on dialysis tubing over night
2. Cut the dialysis tubing into pieces and transfer into Petri dish
3. Fix 30-60 min at room temperature in formaldehyde/MBS/P+BS.
4. Dilute the 10x wash solution P+BS/PIPES into 1x.
5. Wash the samples 3x 5 min with 1x washing solution.
6. Block the nonspecific binding with freshly prepared 5 % non-fat milk in P+BS solution for 20-30 min.
7. Dilute the 5 % non-fat milk in P+BS solution into o.5 % non-fat milk in P+BS solution.
8. Dilute the primary antibody at 1:100 dilution in 0.5 % non-fat milk solution
9. Incubate the sample in dissolved primary antibody for 30-90 min
10. Wash the samples 3x 5 min with 1x washing solution.
11. Dissolve the secondary antibody in 0.5 % non-fat milk solution
12. Incubate the sample with 100 µL fluorescent labelled secondary antibody for 30-90 min in dark place.
13. Final wash the samples 3 x 5 min with 1x washing solution.
14. Then mount the sample on the cover slip and on the slide to see under confocal microscope on the same day.

6. Cell wall extracts preparation protocol.

1. Grow *Aspergillus nidulans* strains at 30 ^{o}C for 24-48 h on CM + amp.
2. Inoculate about 10^5 Spores in 200 mL CM + amp for 48 hours with shaking at 160 rpm.

3. Filter through a #1 Whatman filter
4. Wash with ddH2O followed by washing with 0.5 M NaCl.
5. Store at -80 ^{o}C for 2-4 hours
6. Thaw mycelia and wash once with ddH2O followed by washing with 0.5 M NaCl.
7. Fungal hyphae are broken in Disruption Buffer (DB; 20 mM Tris, 50 mM EDTA, pH 8.0) using glass beads and vortex until microscopic examination shows hyphal ghosts.
8. Cell walls are separated by centrifugation at 3000 x *g* for 10 min.
9. The pellet containing the cell wall fraction are washed with chilled DB with stirring for 4 h at 4 ^{o}C
10. Collect the Cell walls by centrifugation at 3000 g for 10 min.
11. The pellet containing the cell wall fraction are washed with ultrapure water with stirring for 4 h at 4 ^{o}C
12. Collect the pellet by vaccum filtration on filter paper.
13. Place the filter paper, which contains the cell wall material in 50 mL conical flask, freeze at -80 for 20 min and then lyophilize overnight.

Disruption Buffer (DB) for 250 ml;

20 mM Tris	0.61 g
50 mM EDTA, pH 8.0)	4.8 g
H2O upto	250 mL

O.5M NaCl buffer:

NaCl	7.3 g
H2O upto	250 mL

7. ELISA protocol for *Aspergillus nidulans* cell wall galactofuranose quantification

1. Add 100-150 ul of cell wall preparation (Isolated cell walls at 0.5 mg/ml in EPBS (8.2 mM Na_2HPO_4, 1.8 mM $NaH_2PO_4.H_2O$, 140 mM NaCl, pH 7.4) are incubated in 96-well Immulon 2HB plates) and incubate overnight at 4 ^{o}C.
2. Wells are washed three times with ELISA wash buffer (10 mM Tris, 0.05% Tween 20, 3.1 mM sodium azide, pH 8.0) at room temperature

3. Block with ELISA blocking solution (10 mg BSA /ml, 0.02% sodium azide in EPBS) for 30 min at room temperature
4. Wells are washed three times with ELISA wash buffer at room temperature
5. Incubate L10 (Mouse IgM) antibody for 1 to 2 h. L10 antibodies are diluted 1: 10 with ELISA diluent (0.05% Tween 20, 0.02% sodium azide, 10 mg BSA /ml in EPBS) at room temperature.
6. Wells are washed three times with ELISA wash buffer at room temperature
7. Incubate with alkaline phosphatase-conjugated goat antimouse IgM antibody (Sigma) for 1–2 h (diluted 1: 500 in ELISA diluent) at room temperature.
8. Wells are washed three times with ELISA wash buffer at room temperature
9. Incubate with phosphatase substrate tablets (Sigma) dissolved in 8.33 ml alkaline phosphatase substrate buffer (0.5 mM MgCl2.6H2O, 9.6% diethanolamine, pH 9.6) for 30 min at room temperature.
10. Read absorbance at 405 nm.

ELISA experiment needs to be performed at least two times.

8. **Sample preparation and critical point drying for scanning electron microscope (SEM)**
    a. Grow on dialysis tube for 3 days at 30 ^{o}C.
    b. Soak sample in 8% glutaraldehyde for 1 h
    c. Fix in 8% glutaraldehyde vapour for 1 h
    d. Place samples in -80 ^{o}C acetone and place them in -80 ^{o}C freezer for 1 h
    e. Put all samples in -20 ^{o}C for 1 h
    f. Put all samples in 4 ^{o}C for 1 h
    g. Put all samples at room temperature for 1 h
    h. Put sample in critical point dryer in acetone
    i. Let liquid CO_2 into chamber
    j. CO_2 replace acetone
    k. Raise the temperature to over 31.5 ^{o}C
    l. CO_2 vaporise and leaves samples
    m. Remove samples from critical point dryer.

n. Gold coat the samples and observe under SEM.

o.

9. Protocol for transmission electron microscope (TEM)

Day 1—Preparation

Grow conidia on sterile dialysis tubing on CM+ medium overnight

Day 2: Fixation-done in the fume hood

1. Make 5% glutaraldehyde in 50mM buffer (from 100 mM NaKPO4 pH7.5)
2. Cut dialysis tubing into ~mm squares
3. Fix dialysis tubing in glutaraldehyde in 50mM buffer for 1 hour.
4. Wash 3X15 min 50 mM buffer
5. Fix 1 hour in 1 % OsO_4 in buffer (2O drops of 100 mM NaKPO4 buffer, 16 drops ultrapure water, 10 drops 1% OsO4)
6. Wash in graded ethanol series-10 min each in 20 %, 40 %, 60 %, 80 %, and 100 % ethanol
7. Transition to dry 100 % acetone
8. 2X30 min washes in 100 % acetone

Day 2: Embedding- done in the fume hood

9. Transition to 1:1 acetone:resin for 1 h. Open the top slightly and leave acetone to evaporate slowly overnight.
10. Transfer to fresh resin on a coated glass slide, topped with a second slide for 4-5 h in a dessicator.

Polymerisation:

11. Polymerize resin at 60 ^{o}C for 2 d.

Staining EM sections:

Wash and rinse the staining dishes (NO grease) and shake off excess ultrapure water.

Have two pairs of clean fine-tipped forceps.

Have 500 mL ultrapure water (ddHOH) for washing and a beaker to collect used wash water
Have filter paper triangles for drying

Uranyl acetate staining - 20 min at room temperature

1. Fill part of one groove in a staining dish with uranyl acetate (UrAc). The solution should have a slightly convex top, so that it will be easy to submerge the grids.
2. Pick up each grid by its border, holding by the wide part of the edge, and place it into the staining solution so it is fully submerged, then release to leave it there. Wipe the forceps dry before picking up the next grid.
3. After 20 min staining in uranyl acetate (precise timing is not critical) transfer each grid to water, then rinse each individually for 20-30 s with a gentle stream of dHOH and put in fresh ddHOH.
4. When all grids are rinsed after UrAc, fill the lead citrate channel with lead citrate stain. Do not disturb any crystals on the sides of the PbCit container - take stain from the middle of the solution, and transfer gently into the lead citrate channel.

References

Abadjieva, A., Pauwels, K., Hilven, P., and Crabeel, M. (2001). A new yeast metabolon involving at least the two first enzymes of arginine biosynthesis: acetylglutamate synthase activity requires complex formation with acetylglutamate kinase. J. Biol. Chem. 276, 42869-42880.

Afroz, S., El-Ganiny, A.M., Sanders, D.A.R., Kaminskyj, S.G.W. (2011). Roles of the *Aspergillus nidulans* UDP-galactofuranose transporter, UgtA in hyphal morphogenesis, cell wall architecture, conidiation, and drug sensitivity. Fungal Genet Biol. 48, 896–903.

Aimanianda, V., Latgé, J.P. (2010). Problems and hopes in the development of drugs targeting the fungal cell wall. Expert Review of Anti-infective Therapy 8, 359-364.

Alam, M.K., El-Ganiny, A.M., Sanders, D.A.R., Liu, J., Kaminskyj, S.G.W. (2012). *Aspergillus nidulans* galactofuranose biosynthesis affects antifungal drug sensitivity. Fungal Genetics and Biology 49, 1033–1043.

Arendrup, M.C., Garcia-Effron, G., Lass-Flörl, C. et al. (2010). Susceptibility testing of *Candida* species to echinocandins: comparison of EUCAST EDef 7.1, CLSI M27-A3, Etest, disk diffusion and agar-dilution using RPMI and IsoSensitest medium. Antimicrob Agents Chemother. 54, 426–39.

Arnaud, M.B., Chibucos, M.C., Costanzo, M.C., Crabtree, J., Inglis, D.O., Lotia, A., Orvis, J., Shah, P., Skrzypek, M.S., Binkley, G., Miyasato, S.R., Wortman, J.R., Sherlock, G. (2010). The *Aspergillus* Genome Database, a curated comparative genomics resource for gene, protein and sequence information for the *Aspergillus* research community. Nucleic Acids Res. 38, D420-427.

Baddley, J. W., and Pappas, P. G. (2005). Antifungal combination therapy: clinical potential. Drugs, 65(11),1461-80.

Barchiesi, F., Arzeni, D., Caselli, F., Scalise, G. (2000). Primary resistance to flucytosine among clinical isolates of *Candida* spp. J. Antimicrob. Chemother. 45, 408-409.

Bartnicki-Garcia, S. (1968). Cell wall chemistry, morphogenesis, and taxonomy of fungi. Annu. Rev. Microbiol. 22, 87-108.

Barr, D.P., Aust, S.D. (1994). Pollutant degradation by white rot fungi. Rev. Environ. Contam. Toxicol. 138, 49-72.

Barr, K., Laine, R.A., Lester, R.L. (1984). Carbohydrate structures of three novel phosphoinositol-containing sphingolipids from the yeast *Histoplasma capsulatum*. Biochemistry 23, 5589-5596.

Bayram, O., Bayram, O. S., Valerius, O., Jöhnk, B., Braus, G.H. (2012). Identification of protein complexes from filamentous fungi with tandem affinity purification. Methods Mol Biol. 944, 191-205.

Beauvais, A., Bruneau, J.M., Mol, P.C., Buitrago, M.J., Legrand, R., Latgé, J.P. (2001). Glucan synthase complex of *Aspergillus fumigatus*. J. Bacteriology 183, 2273–2279.

Beis, K., Srikannathasan, V., Liu, H., Fullerton, S.W., Bamford, V.A., Sanders, D.A.R., Whitfield, C., McNeil, M.R., Naismith, J.H. (2005). Crystal structures of *Mycobacterium tuberculosis* and *Klebsiella pneumoniae* UDP-galactopyranose mutase in the oxidised state and *Klebsiella pneumoniae* UDP-galactopyranose mutase in the (active) reduced state. J. Mol. Biol. 348, 971-982.

Belanova, M., Dianiskova, P., Brennan, P.J., Completo, G.C., Rose, N.L., Lowary, T.L., Mikusova, K. (2008). Galactosyl transferases in mycobacterial cell wall synthesis. J. Bacteriol. 190, 1141-1145.

Bennett, J.W. (1998). Mycotechnology: the role of fungi in biotechnology. J. Biotechnol. 66, 101-107.

Bennett, J. E., Bhattacharjee, A. K., Glaudemans, C. P. (1985). Galactofuranosyl groups are immunodominant in *Aspergillus fumigatus* galactomannan. Molec Immunol. 22, 251-254

Bernard, M., and Latgé, J.P. (2001). *Aspergillus fumigatus* cell wall: composition and biosynthesis. *Medical Mycology*. 39, 9-17.

Beverley, S.M., Owens, K.L., Showalter, M., Griffith, C.L., Doering, T.L., Jones, V.C., McNeil, M.R. (2005). Eukaryotic UDP-galactopyranose mutase (*GLF* gene) in microbial and metazoal pathogens. Eukaryot. Cell. 4, 1147-1154.

Bhat, P.J., Murthym, T.V. (2001). Transcriptional control of the GAL/MEL regulon of yeast *Saccharomyces cerevisiae*: mechanism of galactose-mediated signal transduction. Molecular Microbiology 40, 1059–1066.

Bhushan, B., Halasz, A., Spain, J., Thiboutot, S., Ampleman, G., and Hawari, J. (2002). Biotransformation of hexahydro-1,3,5-trinitro-1,3,5-tiazine catalyzed by a

NAD(P)H:nitrate oxidoreductase from *Aspergillus niger*. Environ. Sci. Technol. 36, 3104–3108

Binder, U., Oberparleiter, C., Meyer, V., Marx, F. (2010). The antifungal protein PAF interferes with PKC/MPK and cAMP/PKA signalling of *Aspergillus nidulans*. Molec Microbiol. 75, 294-307.

Birkaya, B., Maddi, A., Joshi, A., Free, S. J., and Cullen, P. J. (2009). Role of the cell wall integrity and filamentous growth mitogen-activated protein kinase pathways in cell wall remodeling during filamentous growth. Eukaryotic Cell, 8 (8), 1118–1133.

Blackwell, M. (2011). The Fungi: 1, 2, 3 … 5.1 million species? Am. J. Bot. 98:426–438.

Bolard, J. (1986). How do the polyene macrolide antibiotics affect the cellular membrane properties? Biochim. Biophys. Acta. 864, 257-304.

Bossche, H.V., Marichal, P., Odds, F.C. (1994). Molecular mechanisms of drug resistance in fungi. Trends in Microbiology 2, 393-400.

Bowman, J.C., Hicks, P.S., Kurtz, M.B., Rosen, H., Schmatz, D.M., Liberator, P.A., and Douglas, C.M. (2002). The antifungal echinocandin caspofungin acetate kills growing cells of *Aspergillus fumigatus* in vitro. Antimicrob. Agents Chemother. 46, 3001–3012.

Bowman, S.M., Free, S.J. (2006). The structure and synthesis of the fungal cell wall. BioEssays, 28, 799-808.

Bohle, K., Jungebloud, A., Göcke, Y., Dalpiaz, A., Cordes, C., Horn, H., Hempel, D. C. (2007). Selection of reference genes for normalisation of specific gene quantification data of *Aspergillus niger*. J Biotechnol. 132, 353-358.

Bradsher, R.W. (1996). Histoplasmosis and blastomycosis. Clin Infect Dis. Suppl 2, S102-11.

Brenner, C., Bieganowski, P., Pace, H.C., and Huebner, K. (1999). The histidine triad superfamily of nucleotide-binding proteins. J. Cell. Physiol. 181, 179-187.

Broach, J.R. (1979). Galactose regulation in *Saccharomyces cerevisiae*: the enzymes encoded by the *GAL7, 10, 1* cluster are co-ordinately controlled and separately translated. J. Mol. Biol. 131, 41-53.

Butland, G., Zhang, J.W., Yang, W., Sheung, A., Wong, P., Greenblatt, J.F., Emili, A., Zamble, D.B. (2006). Interactions of the *Escherichia coli* hydrogenase biosynthetic proteins: HybG complex formation. FEBS Lett. 580, 677–681.

Cabib, E., Roh, D.H., Schmidt, M., Crotti, L.B., Varma, A. (2001). The yeast cell wall and septum as paradigms of cell growth and morphogenesis. The J. of Biol. Chem., 276, 19679–19682.

Cannon, R.D., Lamping, E., Holmes, A.R., Niimi, K., Baret, P.V., Keniya, M.V., Tanabe, K., Niimi, M., Goffeau, A., Monk, B.C. (2009). Efflux-mediated antifungal drug resistance. Clin. Microbiol. Rev. 22, 291-321.

Carrillo-Muñoz, AJ., Giusiano, G., Ezkurra, PA., Quindós, G., 2006. Antifungal agents: mode of action in yeast cells. Rev. Esp. Quimioter. 19, 130-139.

Carrillo-Munoz, A.J., Quindos, G., Tur, C., Ruesga, M.T., Miranda, Y., del Valle, O., Cossum, P.A., Wallace, T.L. (1999). *In-vitro* antifungal activity of liposomal nystatin in comparison with nystatin, amphotericin B cholesteryl sulphate, liposomal amphotericin B, amphotericin B lipid complex, amphotericin B desoxycholate, fluconazole and itraconazole. J. Antimicrob. Chemother. 44, 397-401.

Chant, J., Corrado, K., Pringle, J. R., and Herskowitz, I. (1991). Yeast BUD5, encoding a putative GDP-GTP exchange factor, is necessary for bud site selection and interacts with bud formation gene BEM1. Cell, 65, 1213–1224.

Chao, C. C., Hsu, P. C., Jen, C. F., Chen, I. H., Wang, C. H., Chan, H. C., Tsai, P. W., Tung, K. C., Wang, C. H., Lan, C. Y., and Chuang, Y. J. (2010). Zebrafish as a Model Host for *Candida albicans* Infection. Infection and Immunity, 2512–2521.

Chapman, S.W., Sullivan, D.C., Cleary, J.D. (2008). In search of the holy grail of antifungal therapy. Trans. Am. Clin. Climatol. Assoc. 119, 197-216.

Chau, A.S., Gurnani, M., Hawkinson, R., Laverdiere, M., Cacciapuoti, A., and McNicholas, P. M. (2005). Inactivation of sterol Delta (5,6)-desaturase attenuates virulence in *Candida albicans*. Antimicrob. Agents Chemother. 49, 3646–3651.

Chen, C.A., Okayama, H. (1988). Calcium phosphate-mediated gene transfer: a highly efficient transfection system for stably transforming cells with plasmid DNA. BioTechniques 6, 632-638.

Cheng, J. (2011). Protein glycosylation in *Aspergillus fumigatus* is essential for cell wall synthesis and serves as a promising model of multicellular eukaryotic development. *International Journal of Microbiology*, 2012, 1-21.

Christacos, N.C., Marson, M.J., Wells, L., Riehman, K., and Fridovich-Keil, J.L. (2000). Subcellular localization of galactose-1-phosphate uridylyltransferase in the yeast *Saccharomyces cerevisiae*. Mol. Genet. Metab. **7**0, 272-280.

Claverie-Martin, F., Diaz-Torres, M. R., Geoghegan, M. J. (1988). Chemical composition and ultrastructure of wild-type and white mutant *Aspergillus nidulans* conidial walls. Curr. Microbiol. 16, 281-287.

Cordeiro, L.M., de Oliveira, S.M., Buchi, D.F., and Iacomini, M. (2008). Galactofuranose-rich heteropolysaccharide from *Trebouxia* sp., photobiont of the lichen *Ramalina gracilis* and its effect on macrophage activation. Int. J. Biol. Macromol. 42, 436–440.

Cortés, J.C., Sato, M., Munoz, J., Moreno, M.B., Clemente-Ramos, J.A., Ramos, M. *et al.* (2012). Fission yeast Ags1 confers the essential septum strength needed for safe gradual cell abscission. J Cell Biol. 198**,** 637-656.

Costachel, C., Coddeville, B., Latgé, J.P., & Fontaine, T. (2005). Glycosylphosphatidylinositol-anchored fungal polysaccharide in *Aspergillus fumigatus*. The J. of Biol. Chem., 280, 39835–39842.

Cuero, R., Ouellet, T., Yu, J., Mogongwa, N. (2003). Metal ion enhancement of fungal growth, gene expression and aflatoxin synthesis in *Aspergillus flavus*: RT-PCR characterization. Appl Microbiol. 953-956.

Cummings, R.D. and Doering, T.L. (2009). Essentials of Glycobiology. 2nd edition. Varki, A. *et al.*, editors. Cold Spring Harbor (NY): *Cold Spring Harbor Laboratory Press*. Ch 21.

Dagenais, T.R.T., Keller, N.P. (2009). Pathogenesis of *Aspergillus fumigatus* in invasive aspergillosis. Clin. Microbiol. Reviews 22: 447-465.

Damveld, R.A., Franken, A., Arentshorst, M., Punt, P.J., Klis, F.M., van den Hondel, C.A.M.J.J., Ram, A.F.J. (2008). A novel screening method for cell wall mutants in *Aspergillus niger* identifies UDP-galactopyranose mutase as an important protein in fungal cell wall biosynthesis. Genetics 178, 873–881.

Deacon, J.W. (1997). Modern Mycology. Blackwell Scientific, London, p 303

de Aguirre, L., Hurst, S.F., Choi, J.S., Shin, J.H., Hinrikson, H.P., Morrison, C.J. (2004). Rapid differentiation of *Aspergillus species* from other medically important opportunistic molds and yeasts by PCR-enzyme immunoassay. J. Clin. Microbiol. 42, 3495-3504.

de Groot, P.J.W., Brandt, B.W., Horiuchi, H., Ram, A.F.J., de Koster, C.G., Klis, F.M. (2009). Comprehensive genomic analysis of cell wall genes in *Aspergillus nidulans*. Fungal Genetics and Biology, 46, S72-S81.

Denning, D.W., 2003. Echinocandin antifungal drugs. The Lancet. 362, 1142-1151.

Denning, D.W. (1998). Invasive aspergillosis. Clinical Infectious Diseases 1998; 26:781–805.

Deshpande, N., Wilkins, MR., Packer, N., Nevalainen, H. (2008). Protein glycosylation pathways in filamentous fungi. Glycobiology 18, 626-637.

Dichtl, K., Helmschrott, C., Dirr, F. and Wagener, J. (2012). Deciphering cell wall integrity signalling in *Aspergillus fumigatus*: identification and functional characterization of cell wall stress sensors and relevant Rho GTPases. Mol Microbiol. 83, 506-19.

Dickson, R.C., Riley, M.I. (1989). The lactose-galactose regulon of *Kluyveromyces lactis*. Biotechnology; 13:19-40.

Dykhuizen, E. C., May, J.F., Tongpenyai, A., Kiessling, L.L. (2008). Inhibitors of UDPgalactopyranose mutase thwart mycobacterial growth. J. Am. Chem. Soc. 130, 6706-6707.

Efimov PV (2003) Roles of NUDE and NUDF Proteins of *Aspergillus nidulans*: insights from intracellular localization and overexpression effects. Molec Biol Cell 14: 871–888.

Eichler, J., and Adams, M.W. (2005). Posttranslational protein modification in Archaea. Microbiol. Mol. Biol. Rev. 69, 393–425.

Ekena, K., Stevens, T. H. (1995). The *Saccharomyces cerevisiae* MVP1 gene interacts with VPS1 and is required for vacuolar protein sorting. Mol Cell Biol. 15(3), 1671–1678.

El-Ganiny, A.M., Sanders, D.A.R., and Kaminskyj, S.G.W. (2008). *Aspergillus nidulans* UDP-galactopyranose mutase, encoded by *ugmA* plays key roles in colony growth, hyphal morphogensis, and conidiation. Fungal Genet Biol. 45, 629–635.

El-Ganiny, A.M., Sheoran, I., Sanders, D.A.R., and Kaminskyj, S.G.W. (2010). *Aspergillus nidulans* UDP-glucose-4-epimerase UgeA has multiple roles in wall architecture, hyphal morphogenesis, and asexual development. Fungal Genet. Biol. 47, 1533–1542.

Elorza, V., and Arst, H.N. Jr. (1971). Sorbose resistant mutants of *Aspergillus nidulans*. Molec. Gen. Genet. 111, 185-193.

Elsas, L. J., and Lai, K. (1998). The molecular biology of galactosemia. Genetics in Medicine **1**: 40-48.

Elshafei, A.M., Abdel-Fatah, O.M. (2001). Evidence for a nonphosphorylated route of galactose breakdown in cell-free extracts of *Aspergillus niger*. Enzyme and Microbial Technology. 29: 76–83.

Engel, J., Schmalhorst, P.S., Dork-Bousset, T., Ferrieres, V., Routier, F.H. (2009). A single UDPgalactofuranose transporter is required for galactofuranosylation in *Aspergillus fumigatus*. J. Biol. Chem. 284, 33859-33868.

Erjavec, Z., Kluin-Nelemans, H., Verweij, P.E. (2009). Trends in invasive fungal infections, with emphasis on invasive aspergillosis. Clin. Microbiol. Infect. 15, 625–633

Espinel-Ingroff, A. (2009). Novel antifungal agents, targets or therapeutic strategies for the treatment of invasive fungal diseases: a review of the literature (2005-2009). Rev Ibero De Micologia. 26:15-22.

Estey, M.P., Kim, M.S., Trimble, W.S. (2011). Septins. Curr. Biol. 21, R384–R387.

Fang, W., Ding, W., Wang, B., Zhou, H., Ouyang, H., Ming, J., Jin, C. (2010). Reduced expression of the O-mannosyltransferase 2 (AfPmt2) leads to deficient cell wall and abnormal polarity in *Aspergillus fumigatus*. Glycobiology. 2010, 542-552.

Fedorova, N.D., Khaldi, N., Joardar, V.S., Maiti, R., Amedeo, P. et al. (2008). Genomic islands in the pathogenic filamentous fungus *Aspergillus fumigatus*. PLoS Genetics 4(4): e1000046.

Fekete, E., Karaffa, L., Sándor, E., I. Bányai, B., Seiboth, G., Gyémánt, Sepsi, A., Szentirmai, A., and Kubicek, C.P. (2004). The alternative D-galactose degrading pathway of *Aspergillus nidulans* proceeds via L-sorbose. Arch. Microbiol. 181, 35-44.

Field, C., and Kellogg, D. (1999). Septins: cytoskeletal polymers or signaling GTPases? Trends Cell Biol. 9, 387–394.

Fisher, M. C., Henk, D. A., Briggs, C. J., Bronstein, J. S., Madoff, L. C., McCraw, S. L., Gurr, S. J. (2012). Emerging fungal threats to animal, plant, and ecosystem health. Nature 484, 186-194.

Flipphi, M., Sun, J., Robellet, X., Karaffad, L., Fekete, E., Zeng, A.P., and Kubicek, C.P. (2009). Biodiversity and evolution of primary carbon metabolism in *Aspergillus nidulans*

and other *Aspergillus* spp. Fung. Genet. Biol. 46, S19-S44.

Fontaine, T., Simenel, C., Dubreucq, G., Adam, O., Delepierre, M., Lemoine, J. et al. (2000). Molecular organization of the alkali-insoluble fraction of the *Aspergillus fumigatus* cell wall. The J. of Biol. Chem., 275, 27594–27607.

Fortwendel, J., Juvvadi, P. R., Pinchai, N., Perfect, B. Z., Alspaugh, J. A., Perfect, J. R., Steinbach, W. J. (2009). Differential effects of inhibiting chitin and 1,3-beta-D-glucan synthesis in Ras and calcineurin mutants of *Aspergillus fumigatus*. Antimicrob Agents Chemother. 53, 476-482.

Free, S.J. (2013). Fungal cell wall organization and biosynthesis. Advances in Genetics, 81, 33–82.

Fuchs, B. B., and Mylonakis, E. (2009). Our paths might cross: the role of the fungal cell wall integrity pathway in stress response and cross talk with other stress response pathways. Eukaryotic Cell, 1616–1625

Fujikawa, T., Sakaguchi, A., Nishizawa, Y., Kouzai, Y., Minami, E., Yano, S. *et al.* (2012). Surface alpha-1,3-glucan facilitates fungal stealth infection by interfering with innate immunity in plants. PLoS Pathog. 8, e1002882.

Fujioka, T., Mizutani, O., Furukawa, K., Sato, N., Yoshimi, A., Yamagata, Y. *et al.* (2007). MpkA-dependent and -independent cell wall integrity signaling in *Aspergillus nidulans*. Eukaryot Cell, 6, 1497-1510.

Futagami, T., Nakao, S., Kido,Y., Oka, T., Kajiwara, Y., Takashita, H., Omori, T., Furukawa, K., Goto, T. (2011). Putative stress sensors WscA and WscB are involved in hypo-osmoticand acidic pH stress tolerance in *Aspergillus nidulans.* Eukaryotic Cell, 11, 1504-1515.

Galagan, J.E., Calvo, S.E. *et al*. (2005). Sequencing of *Aspergillus nidulans* and comparative analysis with *A. fumigatus* and *A. oryzae*. Nature 438, 1105-1115.

Gallis, H.A., Drew, R.H., Pickard, W.W. (1990). Amphotericin B: 30 Years of Clinical Experience. Rev. of Infect. Dis., 12, 308-329.

Gardiner, R.E., Souteropoulos, P., Park, S., Perlin, D.S. (2005). Characterization of *Aspergillus fumigatus* mutants with reduced susceptibility to caspofungin. Med Mycol. 43, Suppl 1:S299–305.

Garcia-Contreras, R., Vos, P., Westerhoff, H.V., Boogerd, F.C. (2012). Why *in vivo* may not equal *in vitro* – new effectors revealed by measurement of enzymatic activities under the same *in vivo*-like assay conditions. Fed.of Euro. Biochem. Soci. J., 279, 4145–4159.

Gastebois, A., Clavaud, D., Aimanianda, V., Latgé, J.P. (2009). *Aspergillus funigatus*: Cell wall polysaccharides, their biosynthesis and organization. Future Microbiology, 4, 583–595.

Gauwerky, K., Borelli, C., Korting, H.C. (2009). Targeting virulence: a new paradigm for antifungals. Drug Discov. Today 14, 214-222.

Gladfelter, A.S., Pringle, J.R., and Lew, D.J. (2001). The septin cortex at the yeast mother-bud neck. Curr. Opin. Microbiol. 4(6), 681-9.

Goffeau, A., Barrell, B. G. et al. (1996). Life with 6000 genes. Science, 274, 546:563–567

Gough, K. M., Kaminskyj, S. G. W. (2010). sFTIR, Raman and surface enhanced Raman spectroscopic imaging of fungal cells. *In Vibrational Spectroscopic Imaging for Biomedical Applications*. *Edited* by G. Srinivasan. McGraw-Hill, U.S.A. pp125-156.

Goswami, S., Rani, A., Priyadarshini, R., Bhunia, B., Mandal, T. (2012). A review on production of echinocandins by *Aspergillus sp.* J Biochem Tech. 4(1): 568-575.

Gould, D. (2011). Diagnosis, prevention and treatment of fungal infections. Nursing Standard. 25, 38-47.

Gregan, J., Riedel, C.G., Petronczki, M., Cipak, L., Rumpf, C., Poser, I., Buchholz, F., Mechtler, K., Nasmyth, K. (2007). Tandem affinity purification of functional TAP-tagged proteins from human cells. Nat Protoc. 2, 1145–1151.

Guan, S., Clarke, A.J., Whitfield, C. (2001). Functional analysis of the galactosyltransferases required for biosynthesis of D-galactan I, a component of the lipopolysaccharide O1 antigen of *Klebsiella pneumoniae*. J. Bacteriol. 183, 3318-3327

Guest, G.M., Momany, M. (2000). Analysis of cell wall sugars in the pathogen *Aspergillus fumigatus* and the saprophyte *Aspergillus nidulans*. Mycologia 92, 1047–1050.

Handford, M., Rodriguez-Furlan, C., Orellana, A. (2006). Nucleotide-sugar transporters: structure, function and roles *in vivo*. Braz. J. Med. Biol. Res. 39, 1149-1158.

Hartl, L., Kubicek, C. P., and Seiboth, B. (2007). Induction of the *gal* pathway and cellulase genes involves no transcriptional inducer function of the galactokinase in *Hypocrea jecorina*. J. Biol. Chem. 282, 18654–18659.

Hashem, M. (2011). Isolation of mycotoxin-producing fungi from fishes growing in aquacultures. Research journal of microbiology. (6)12, 862-872.

He, X. S ., Li, S. J., Kaminskyj, S. G. W. (2014). Characterization of *Aspergillus nidulans* α-glucan synthesis: roles for two synthases and two amylases. Molecular Microbiology 91: 579-595.

Heinemann, S., Symoens, F., Gordts, B., Jannes, H., Nolard, N. (2004). Environmental investigations and molecular typing of *Aspergillus flavus* during an outbreak of postoperative infections. J. Hosp. Infect. 57(2):149-55.

Henry, C., Latgé, J. P., Beauvais, A. (2011). 1,3 glucans are dispensable in *Aspergillus fumigatus*. Eukaryotic Cell, 11, 26-29.

Hernández-Rodríguez, Y., Hastings, S., Momany, M. (2012). The septin AspB in *Aspergillus nidulans* forms bars and filaments and plays roles in growth emergence and conidiation. Eukaryotic Cell, 11(3), 311.

Hernández-Rodríguez, Y., Momany, M. (2012). Posttranslational modifications and assembly of septin heteropolymers and higher-order structures. Curr Opin Microbiol 15, 660-668.

Hernandez, R., Nombela, C., Diez-Orejas, R., Gil, C. (2004). Two-dimensional reference map of *Candida albicans* hyphal forms. *Proteomics* 4(2), 374-82

Hessemann, L., Kotz, A., Echtenacher, B., Broniszewska, M., Routier, F., Hoffmann, P., and Ebel, F. (2011). Studies on galactofuranose-containing microstructures of the pathogenic mold *Aspergillus fumigatus*. Int. J. Med. Microbiol. 301, 523-530

Hibbett, D.S., Binder, M., Bischoff, J.F., Blackwell, M., Cannon, P.F., Eriksson, O.E., Huhndorf, S., James, T., Kirk, P.M., Lucking, R. *et al.* (2007). A higher-level phylogenetic classification of the Fungi. *Mycol Res* 111, 509-47.

Hill, T.W., Loprete, D.M., Momany, M., Ha, Y., Harsch, L.M., Livesay, J.A., Mirchandani, A., Murdock, J.J., Vaughan, M.J., and Watt, M.B. (2006). Isolation of cell wall mutants in *Aspergillus nidulans* by screening for hypersensitivity to Calcofluor White. Mycologia 98, 399-409.

Horiuchi, H. (2009). Functional diversity of chitin synthases of *Aspergillus nidulans* in hyphal growth, conidiophore development and septum formation. Medical Mycology, 47 (Supplement 1), S47-S52.

Ho, K. and Cheng, T. (2010). Common superficial fungal infections – a short review. Hong Kong Medical Diary. Medical Bulletin. 15:11.

Hochstenbach, F., Klis, F. M., van den Ende, H., van Donselaar, E., Peters, P. J., and Klausner, R. D. (1998). Identification of a putative alpha-glucan synthase essential for cell wall construction and morphogenesis in fission yeast. Proc. Natl. Acad. Sci. 95, 9161–9166.

Holden, H.M., Rayment, I., Thoden, J.B. (2003). Structure and function of enzymes of the Leloir pathway for galactose metabolism. J. Biol. Chem. 278, 43885-43888.

Hu, W., Sillaots, S., Lemieux, S., Davison, J., Kauffman, S., Breton, A., Linteau, A., Xin, C., Bowman, J., Becker, J., Jiang, B., Roemer, T. (2007). Essential gene identification and drug target prioritization in *Aspergillus fumigatus*. PLoS Pathol. 3, e24.

Ichinomiya, M., Motoyama, T., Fujiwara, M., Takagi, M., Horuichi, H., Ohta, A. (2002). Repression of *chsB* expression reveals the functional importance of class IV chitin synthase gene *chsD* in hyphal growth and conidiation of *Aspergillus nidulans*. Microbiology (Reading). 148, 1335-1347.

Jiang, H., Ouyang, H., Zhou, H., Jin. C. (2008). GDP-mannose pyrophosphorylase is essential for cell wall integrity, morphogenesis and viability of *Aspergillus fumigatus*. Microbiology (Reading). 154, 2730-2739.

Johnson, M.D., MacDougall, C., Ostrosky-Zeichner, L., Perfect, J.R., Rex, J.H. (2004). Combination Antifungal Therapy. Antimicrob. Agents Chemother. 48, 693-715.

Kaminskyj, S.G.W., and Heath, I.B. (1995). Integrin and spectrin homologues, and cytoplasm-wall adhesion in tip growth. J. Cell Sci. 108, 849–85

Kaminskyj, S.G.W., Heath, I.B. (1996). Studies on *Saprolegnia ferax* suggest the importance of the cytoplasm in determining hyphal morphology. Mycologia, 88, 20-37

Kaminskyj, S.G.W. (2000). Septum position is marked at the tip of *Aspergillus nidulans* hyphae. Fung. Genet. Biol. 31, 105-113.

Kaminskyj, S.G.W. (2001). Fundamentals of growth, storage, genetics and microscopy of *Aspergillus nidulans*. Fung. Genet. Newsl. 48, 25-31.

Kapoor, A., Viraraghavan, T., Cullimore, D.R. (1999). Removal of heavy metals using the fungus *Aspergillus niger*. Bioresour. Technol. 70, 95-104.

Kauffman, C.A., Carver, P.L. (2008). Update on echinocandin antifungals. Semin. Respir. Crit. Care. Med. 29, 211-219.

Kelly, R., Register, E., Hsu, M., Kurtz, M., Nielsen, J., 1996. Isolation of a gene involved in 1, 3-β-glucan synthesis in *Aspergillus nidulans* and purification of the corresponding protein. J. Bacteriol. 178, 4381-4391.

Keshet, Y., Seger, R. (2010). The MAP kinase signaling cascades: a system of hundreds of components regulates a diverse array of physiological functions. Meth Molec Biol. 661, 3-38.

Kindzelskii, A. L., Ueki, T., Michibata, H., Chaiworapongsa, T., Romero, R., and Petty, H. R. (2004). 6-phosphogluconate dehydrogenase and glucose-6-phosphate dehydrogenase form a supramolecular complex in human neutrophils that undergoes retrograde trafficking during pregnancy. J. Immunol. 172, 6373-6381.

Kirk , P. M. , Cannon, P.F., Minter, D.W., and Stalpers, J. A. (2008). Dictionary of the Fungi, 10th ed. CABI, Wallingford, UK.

Kiraz, N., Dag, I., Yamac, M., Kiremitci, A., Kasifoglu, N., and Akgun, Y. (2009). Antifungal activity of Caspofungin in combination with Amphotericin B against *Candida glabrata*: comparison of disk diffusion, Etest, and time-kill methods. Antimicrob Agents Chemother. 53, 788-790.

Kleczka, B., Lamerz, A.C., van Zandbergen, G., Wenzel, A., Gerardy-Schahn, R., Wiese, M., Routier, F.H. (2007). Targeted gene deletion of *Leishmania major* UDP-galactopyranose mutase leads to attenuated virulence. J. Biol. Chem. 282, 10498-10505.

Klis, F.M., Boorsma, A., de Groot, P.W.J. (2006). Cell wall construction in *Saccharomyces cerevisiae*. Yeast, 23, 185–202.

Klutts, J.S., Yoneda, A., Reilly, M.C., Bose, I., Doering, T.L. (2006). Glycosyltransferases and their products: cryptococcal variations on fungal themes. FEMS Yeast Res. 6, 499-512.

Komachi, Y., Hatakeyama, S., Motomatsu, H., Futagami, T., Kizjakina, K., Sobrado, P., Ekino, K., Takegawa, K., Goto, M., Nomura, Y., Oka, T. (2013). *gfsA* encodes a novel galactofuranosyltransferase involved in biosynthesis of galactofuranose antigen of

O-glycan in *Aspergillus nidulans* and *Aspergillus fumigatus*. Molecular Microbiology, 90(5), 1054–1073.

Kontoyiannis, D. P., Lewis, R. E., Osherov, N., Albert, N. D., and May, G. S. (2003). Combination of caspofungin with inhibitors of the calcineurin pathway attenuates growth *in vitro* in *Aspergillus* species. J. Antimicrob. Chemother. 51, 313-316.

Kovács, Z., Szarka, M., Kovács, S., Boczonádi, I., Emri, T., Abe, K., Pócsi, I., Pusztahelyi, T. (2013). Effect of cell wall integrity stress and RlmA transcription factor on asexual development and autolysis in *Aspergillus nidulans*. Fungal Genetics and Biology, 54, 1–14.

Köplin, R., Brisson, J.R., and Whitfield, C. (1997). UDP-galactofuranose precursor required for formation of the lipopolysaccharide O antigen of *Klebsiella pneumoniae* serotype O1 is synthesized by the product of the *rfbD*KPO1 gene. J. Biol. Chem. 272, 4121–4128

Lamarre, C., Beau, R., Balloy, V., Fontaine, T., Sak Hoi, J.W., Guadagnini, S., Berkova, N., Chignard, M., Beauvais, A., and Latgé, J.P. (2009). Galactofuranose attenuates cellular adhesion of *Aspergillus fumigatus*. Cell Microbiol. 11, 1612-1623.

Lass-Florl, C. (2009). The changing face of epidemiology of invasive fungal disease in Europe. Mycoses. 52, 197-205.

Latgé, J.P., Kobayashi, H., Debeaupuis, J.P., Diaquin, M., Sarfati, J., Wieruszeski, J.M., Parra, E., Bouchara, J.P., Fournet, B. (1994). Chemical and immunological characterization of the extracellular galactomannan of *Aspergillus fumigatus.* Infect Immun. 62:5424-5433.

Latgé, J.P. (1999). *Aspergillus fumigatus* and aspergillosis. Clinical Microbiology Reviews. 310–350.

Latgé, J.P. (2001). The pathobiology of *Aspergillus fumigatus*, Trends Microbiol. 9: 382–389.

Latgé, J.P. (2007). The cell wall: a carbohydrate armour for the fungal cell. Molecular Microbiology, 66 (2): 279–290.

Latgé, J.P. (2009). Galactofuranose containing molecules in *Aspergillus fumigatus*. Med. Mycol. 47, S104-S109

Latgé, J.P. (2010). Tasting the fungal cell wall. Cellular Microbiology. 12, 863–872.

Lee, K. K., MacCallum, D. M., Jacobsen, M. D., Walker, L. A., Odds, F. C. Gow, N. R. A. and Munro, C. A. (2012). Elevated cell wall chitin in *Candida albicans* confers echinocandin

resistance *in vivo*. Antimicrob Agents Chemother. 56, 208–217.

Leone, M. R., Lackner, G., Silipo, A., Lanzetta, R., Molinaro, A., and Hertweck, C. (2010). An unusual galactofuranose lipopolysaccharide that ensures the intracellular survival of toxin-producing bacteria in their fungal host. Angew. Chem. Int. Ed. Engl. 49, 7476–7480

Lesage, G., Bussey, H. (2006). Cell wall assembly in *Saccharomyces cerevisiae*. Microbiology and Molecular Biology Reviews, 70, 317–343.

Levin, D. E. (2005). Cell wall integrity signaling in *Saccharomyces cerevisiae*. Microbiol Mol Biol Rev. 69, 262–291.

Levin, D. E. (2011). Regulation of cell wall biogenesis in *Saccharomyces cerevisiae*: the cell wall integrity signaling pathway. Genetics, 189, 1145-75.

Lindsay, R., Momany, M. (2006). Septin localization across kingdoms: three themes with variations. Curr Opin Microbiol. 9, 559-565

Livak, K. J., Schmittgen, T. D. (2001). Analysis of relative gene expression data using real-time quantitative PCR and the 2-ΔΔCT method. Methods. 25, 402-408.

Lohr, D., Venkov, P., Zlatanova, J. 1995. Transcriptional regulation in the yeast GAL gene family: a complex genetic network. FASEB J. **9**: 777-787.

Longtine, M.S., DeMarini, D.J., Valencik, M.L., Al-Awar, O.S., Fares, H., De Virgilio, C., and Pringle, J.R. (1996). The septins: roles in cytokinesis and other processes. Curr. Opin. Cell Biol. 8, 106–119.

Ma, N., Tang, H.F., Qiu, F., Lin, H.W., Tian, X.R., and Yao, M.N. (2010). Polyhydroxysteroidal glycosides from the starfish *Anthenea chinensis*. J. Nat. Prod. 73, 590–597

MacRae, J.I., Obado, S.O., Turnock, D.C., Roper, J.R., Kierans, M., Kelly, J.M. and Ferguson, MAJ. (2006). The suppression of galactose metabolism in *Trypanosoma cruzi* epimastigotes causes changes in cell surface molecular architecture and cell morphology. Molec. Biochem. Parasitol. 147, 126-136.

Madeira da Silva, L., Owens, K. L., Murta, S. M., and Beverley, S. M. (2009). Regulated expression of the *Leishmania major* surface virulence factor lipophosphoglycan using conditionally destabilized fusion proteins. Proc. Natl. Acad. Sci. 106, 7583–7588

Manavathu, E.K., Cutright, J.L., Chandrasekar, P.H. (1998). Organism dependent fungicidal

activities of azoles. Antimicrob Agents Chemother. 42, 3018–21.

Martel, C.M., Parker, J.E., Bader, O., Weig, M., Gross, U., Warrilow, A., Kelly, D.E. and Kelly, S.L. (2010). A clinical isolate of *Candida albicans* with mutations in *ERG11* (Encoding Sterol 14α-Demethylase) and *ERG5* (Encoding C22 Desaturase) is cross resistant to azoles and amphotericin B. Antimicrob. Agents Chemother. 54(9), 3578–3583.

Martinelli, S., and Clutterbuck, A.J. (1971). A quantitative survey of conidiation mutants in *Aspergillus nidulans*. J. Gen. Microbiol. 69, 261-268.

Marchais, V., Kempf, M., Licznar, P., Lefrançois, C., Bouchara, J. P., Robert, R., Cottin, J. (2005). DNA array analysis of *Candida albicans* gene expression in response to adherence to polystyrene. *FEMS Microbiol Lett* 245, 25-32

Mellado, E., Aufauvre-Brown, A., Specht, C.A., Robbins, P.W., Holden, D.W., 1995. A multigene family related to chitin synthase genes of yeast in the opportunistic pathogen *Aspergillus fumigatus*. Mol. Gen. Genet. 246, 353-359.

Mihu, C.N., Kassis, C., Ramos, E.R., Jiang, Y., Hachem, R.Y., Raad, I.I. (2010). Does combination of lipid formulation of amphotericin B and echinocandins improve outcome of invasive aspergillosis in hematological malignancy patients? Cancer, 116, 5290-5296.

Milewski, S., Gabriel, I., and Olchowy, J. (2006). Enzymes of UDP-GlcNAc biosynthesis in yeast. Yeast 23, 1–14.

Mikusova, K., Belanova, M., Kordulakova, J., Honda, K., McNeil, M.R., Mahapatra, S., Crick, D.C., Brennan, P.J. (2006). Identification of a novel galactosyl transferase involved in biosynthesis of the mycobacterial cell wall. J. Bacteriol. 188, 6592-6598.

Mircus, G., Hagag, S., Levdansky, E., Sharon, H., Shadkchan, Y., Shalit, I. and Osherov, N. (2009). Identification of novel cell wall destabilizing antifungal compounds using a conditional *Aspergillus nidulans* protein kinase C mutant. J Antimicrob Chemother. 64, 755-763.

Momany, M. (2002). Polarity in filamentous fungi: establishment, maintenance and new axes. Curr. Opin. Microbiol. 5, 580–585.

Momany, M., Lindsey, R., Hill, T.W., Richardson, E.A., Momany, C., Pedreira, M., Guest, G.M., Fisher, G.F., Hessler, R.B., Roberts, K.A. (2004). The *Aspergillus fumigatus* cell wall is organized in domains that are remodelled during polarity establishment. Microbiology,

150, 3261–3268.

Momany, M., Hamer, J.E. (1997). The *Aspergillus nidulans* septin encoding gene, aspB, is essential for growth. Fungal Genet. Biol. 21, 92–100.

Monk, B.C., Goffeau, A. (2008). Outwitting multidrug resistance to antifungals. Science, 321, 367-369.

Monteiro, M. C., DeLucas, J. R. (2010). Study of the essentiality of the *Aspergillus fumigatus triA* gene, encoding RNA triphosphatase, using the heterokaryon rescue technique and the conditional gene expression driven by the *alcA* and *niiA* promoters. Fung Genet Biol. 47, 66-79.

Moyrand, F., Lafontaine, I., Fontaine, T. and Janbon, G. (2008). UGE1 and UGE2 regulate the UDP-glucose/UDP-galactose equilibrium in *Cryptococcus neoformans*. Euk. Cell, 7, 2069-2077.

Munro, C.A., Whitton, R.K., Hughes, H.B., Rella, M., Selvaggini, S., Gow, N.A.R. (2003). CHS8—A fourth chitin synthase gene of *Candida albicans* contributes to the in vitro chitin synthase activity, but is dispensable for growth. Fung. Geneti. Biol. 40, 146–158.

Nayak, T., Szewczyk, E., Oakley, C.E., Osmani, A., Ukil, L., Murray, S.L., Hynes, M.J., Osmani, S.A., and Oakley, B.R. (2006). A versatile and efficient gene-targeting system for *Aspergillus nidulans*. Genetics 172, 1557-1566.

Newbound, M., Mccarthy, M.A., Lebel, T. (2010). Fungi and the urban environment: A review. Landscape Urban Plann. 96, 138-145.

Novelli, J.F., Chaudhary, K., Canovas, J., Benner, J.S., Madinger, C.L., Kelly, P., Hodgkin, J., Carlow, C.K.S. (2009). Characterization of the *Caenorhabditis elegans* UDP-galactopyranose mutase homolog *glf-1* reveals an essential role for galactofuranose metabolism in nematode surface coat synthesis. Dev. Biol. 335, 340-355.

Novozhilova, N.M., Bovin, N.V. (2010). Structure, functions, and biosynthesis of glycoconjugates of *Leishmania* spp cell surface. Biochemistry 75, 686-694.

O'Brien , B.L., Parrent, J.L., Jackson, J.A., Moncalvo, J.M., and Vilgalys, R. (2005). Fungal community analysis by large-scale sequencing of enviromental samples. Applied and Environmental Microbiology, 71, 5544 – 5550.

Olufemi, B. E. and Roberts, R. J. (1986). Induction of clinical aspergillomycosis by feeding

contaminated diet to tilapia, *Oreochromis niloticus.* Journal of Fish Diseases, 9, 123-128

Onnis, V., De Logu, A., Cocco, M.T., Fadda, R., Meleddu, R., Congiu, C. (2009). 2-Acylhydrazino-5-arylpyrrole derivatives: synthesis and antifungal activity evaluation. Eur. J. Med. Chem. 44, 1288-95.

Openo, K.K., Schulz, J.M., Vargas, C.A., Orton, C.S., Epstein, M.P., Schnur, RE., Scaglia, F., Berry, G.T., Gottesman, G.S., Ficicioglu, C., Slonim, A.E., Schroer, RJ., Yu, C., Rangel, V.E., Keenan, J., Lamance, K., Fridovich-Keil, J.L. (2006). Epimerase-deficiency galactosemia is not a binary condition. American Journal of Human Genetics, 78, 89-102.

Oppenheimer, M., Valenciano, A.L., and Sobrado, P. (2011). Biosynthesis of galactofuranose in kinetoplastids: novel therapeutic targets for treating leishmaniasis and Chagas' disease. Enzyme Res. 2011, 415976

Osherov, N., May, G. (2000). Conidial germination in *Aspergillus nidulans* requires RAS signaling and protein synthesis. Genetics, 155(2), 647-56

Osherov, N., and May, G.S. (1998). Optimization of protein extraction from *Aspergillus nidulans* for gel electrophoresis. Fungal Genet. Newsl. 45, 38–40.

Osiewacz, H.D. (2002). Genes, mitochondria and aging in filamentous fungi. Ageing Res. Rev. 1, 425-442.

Osmani, A.H., Oakley, B.R., 137: 4934-42 Osmani, S.A. (2006). Identification and analysis of essential *Aspergillus nidulans* genes using the heterokaryon rescue technique. Nat Protocols. 1, 2517-2526.

Osmani, S.A., Engle, D.B., Doonan, J.H., Morris, N.R. (1988). Spindle formation and chromatin condensation in cells blocked at interphase by mutation of a negative cell cycle control gene. Cell, 52, 241–251.

Pan, F., Jackson, M., Ma, Y., McNeil, M. (2001). Cell wall core galactofuran is essential for growth of *Mycobacteria*. J. Bacteriol. 183, 3991–3998.

Pan, F., Malmberg, R.L., Momany, M. (2007). Analysis of septins across kingdoms reveals orthology and new motifs. BMC Evol. Biol. 7, 103.

Partha, S.K., van Straaten, K.E., Sanders, D.A.R. (2009). Structural basis of substrate binding to UDP-galactopyranose mutase. Crystal structures in the reduced and oxidized state complexed with UDP-galactopyranose and UDP. Journal of Molecular Biology, 394,

864-877.

Paul, B.C., El-Ganiny, A.M., Abbas, M., Kaminskyj, S.G.W., Dahms, T.E.S. (2011). Quantifying the importance of galactofuranose in *Aspergillus nidulans* hyphal wall surface organization by atomic force microscopy. Eukaryotic Cell, 10, 646–653.

Pedersen, L.L., Turco, S.J. (2003). Galactofuranose metabolism: a potential target for antimicrobial chemotherapy. Cellular and Molecular Life Sciences, 60, 259-266.

Peltier, P., Belanova, M., Dianiskova, P., Zhou, R., Zheng, R.B., Pearcey, J.A., Joe, M., Brennan, P.J., Nugier-Chauvin, C., Ferrieres, V., Lowary, T.L., Daniellou, R., Mikusova, K. (2010). Synthetic UDP-furanoses as potent inhibitors of mycobacterial galactan biogenesis. Chem. Biol. 17, 1356-1366.

Perfect, J.R. and Casadevall, A. (2006). Fungal molecular pathogenesis: what can it do and why do we need it? *In Molecular principles of fungal pathogenesis*. Heitman J, Filler SG, Edwards JE Jr, Mitchell AP, eds, pp 3–11. ASM Press, Washington DC.

Petraitiene, R., Petraitis, V., Groll, A.H., Sein, T., Schaufele, R.L., Francesconi, A., Bacher, J., Avila, N.A., Walsh, T.J., 2002. Antifungal efficacy of caspofungin (MK-0991) in experimental pulmonary aspergillosis in persistently neutropenic rabbits: pharmacokinetics, drug disposition, and relationship to galactomannan antigenemia. Antimicrob. Agents Chemother. 46, 12-23.

Petranyi, G., Meingassner, J.G., Mieth, H. (1987). Antifungal activity of the allylamine derivative terbinafine *in vitro*. Antimicrob. Agents Chemother. 31, 1365-1368.

Prusinkiewicz, M.A., Farazkhorasani, F., Dynes, J.J., Wang, J., Gough, K.M., Kaminskyj, S.G.W. (2012). Proof-of-principle for SERS imaging of *Aspergillus nidulans* hyphae via *in vivo* synthesis of gold nanoparticles. The Analyst 137, 4934-4942

Puig, O., Caspary, F., Rigaut, G., Rutz, B., Bouveret, E., Bragado-Nilsson, E., Wilm, M., Seraphin, B. (2001). The tandem affinity purification (TAP) method: a general procedure of protein complex purification. Methods, 24, 218–229.

Rambold, G., Stadler, M., Begerow, D. (2013). Mycology should be recognized as a field in biology at eye level with other major disciplines – a memorandum. Mycological Progress, 12, 455-463.

Rappleye, C.A., Eissenberg, L.G., and Goldman, W.E. (2007). *Histoplasma capsulatum*

α-(1,3)-glucan blocks innate immune recognition by the β-glucan receptor. Proc. Natl. Acad. Sci. U.S.A, 104, 1366–1370.

Read, N., D. (2011). Exocytosis and growth do not occur only at hyphal tips. Molecular Microbiology, 81(1), 4–7

Reese, A.J., Yoneda, A., Breger, J.A., Beauvais, A., Liu, H., Griffith, C.L. *et al.* (2007). Loss of cell wall alpha(1,3)glucan affects *Cryptococcus neoformans* from ultrastructure to virulence. Molecular Microbiology, 63, 1385–1398.

Reese, A.J., and Doering, T.L. (2003). Cell wall alpha-1,3-glucan is required to anchor the C*ryptococcus neoformans* capsule. Mol Microbiol. 50, 1401-1409.

Reyes, F., Orellana, A. (2008). Golgi transporters: opening the gate to cell wall polysaccharide biosynthesis. Curr. Opin. Plant Biol. 11, 244-251.

Richards, M.R., Lowary, T.L. (2009). Chemistry and biology of galactofuranose-containing polysaccharides. Chembiochem. 10, 1920-1938.

Rigaut, G., Shevchenko, A., Rutz, B., Wilm, M., Mann, M., Seraphin, B. (1999). A generic protein purification method for protein complex characterization and proteome exploration. Nat Biotechnol. 17, 1030–1032

Roberts, C. F. (1963). The genetic analysis of carbohydrate utilization in *Aspergillus nidulans.* J Gen Microbiol. 31, 45-58.

Roberts, C.F. (1970). Enzyme lesions in galactose non-utilising mutants of *Aspergillus nidulans.* Biochim. Biophys. Acta. 201, 267–283.

Rocha, E.M., Garcia-Effron, G., Park, S., Perlin, D.S. (2007). A Ser678Pro substitution in *FKS1P* confers resistance to echinocandin drugs in *Aspergillus fumigatus*. Antimicrob Agents Chemother. 51, 4174–6.

Rodriguez, R., Redman, R. (2008). More than 400 million years of evolution and some plants still can't make it on their own: plant stress tolerance via fungal symbiosis. J. Exp. Bot. 59, 1109-1114.

Rodriguez-Tudela. J.L., Arendrup, M.C., Arikan, S., Barchiesi, F., Bille, J., Chryssanthou, E., Cuenca-Estrella, M., Dannaoui, E., Denning, D.W., Donnelly, J.P., Fegeler, W., Lass-Flörl, C., Moore, C., Richardson, M., Gaustad, P., Schmalreck, A., Velegraki, A., and Verweij, P. (2008). Method for the determination of broth dilution minimum

inhibitory concentrations of antifungal agents for conidia forming moulds. EUCAST Definitive Document E. DEF 9.1.

Rohila, J.S., Chen, M., Cerny, R., Fromm, M.E. (2004). Improved tandem affinity purification tag and methods for isolation of protein heterocomplexes from plants. Plant J 38, 172–181

Rohila, J.S., Chen, M., Chen, S., Chen, J., Cerny, R., Dardick, C., Canlas, P., Xu, X., Gribskov, M., Kanrar, S., Zhu, J.K., Ronald, P., Fromm, M.E. (2006). Protein-protein interactions of tandem affinity purification-tagged protein kinases in rice. Plant J. 46,1–13.

Rokas, A., Payne, G., Fedorova, N.D., Baker, S.E., Machida, M., Yu, J., Georgianna, D.R., Dean, R.A., Bhatnagar, D., Cleveland, T.E., Wortman, J.R., Maiti, R., Joardar, V., Amedeo, P., Denning, D.W., Nierman, W.C. (2007). What can comparative genomics tell us about species concepts in the genus *Aspergillus*? Stud. Mycol. 59, 11-17.

Romero, B., Turner, G., Olivas, I., Laborda, F., and Lucas, J.R. (2003). The *Aspergillus nidulans alcA* promoter drives tightly regulated conditional gene expression in *Aspergillus fumigatus* permitting validation of essential genes in this human pathogen. Fung. Genet. Biol. 40, 103–114.

Ronen, R., Sharon, H., Levdansky, E., Romano, J., Shadkchan, Y., Osherov, N. (2007). The *Aspergillus nidulans pkcA* gene is involved in polarized growth, morphogenesis and maintenance of cell wall integrity. Curr Genet. 51, 321-329.

Roper, J.R., Guther, M.L., MacRae, J.L., Prescott, A.R., Hallyburton, I., Acosta-Serrano, A. and Ferguson, M.A.J. (2005). The suppression of galactose metabolism in procyclic form *Trypanosoma brucei* causes cessation of cell growth and alters procycloin glycoprotein structure and copy number. J. Biol. Chem. 280, 19728-19736.

Ross, K.L., Davis, C.N., and Fridovich-Keil, J.L. (2004). Differential roles of the Leloir pathway enzymes and metabolites in defining galactose sensitivity in yeast. Molec. Gen. Metab. 83, 103-116.

Rubio-Texeira, M. (2005). A comparative analysis of the GAL genetic switch between not-so-distant cousins: *Saccharomyces cerevisiae* versus *Kluyveromyces lactis*. FEMS Yeast Research. 5, 1115–1128.

Sanglard, D. (2011). Resistance to antifungal drugs. Essentials of Clinical Mycology. 2011, pp 135-151

Sanders, D.A.R., Staines, A.G., McMahon, S.A., McNeil, M.R., Whitfield, C., Naismith, J.H. (2001). UDP-galactopyranose mutase has a novel structure and mechanism. Nat. Struct. Biol. 8, 858–863.

Scherman, M.S., Winans, K.A., Stern, R.J., Jones, V., Bertozzi, C.R., McNeil, M.R. (2003). Drug targeting *Mycobacterium tuberculosis* cell wall synthesis: development of a microtiter plate-based screen for UDP-galactopyranose mutase and identification of an inhibitor from a uridine-based library. Antimicrob. Agents Chemother. 47, 378-382.

Schmalhorst, P.S., Krappmann, S., Vervecken, W., Rohde, M., Muller, M., Braus, G.H., Contreras, R., Braun, A., Bakker, H., Routier, F.H. (2008). Contribution of galactofuranose to the virulence of the opportunistic pathogen *Aspergillus fumigatus*. Eukaryot. Cell. 7, 1268-1277.

Seiboth, B., Pakdaman, B.S., Hartl, L., Kubicek, C.P. (2007). Lactose metabolism in filamentous fungi: how to deal with an unknown substrate source. Fung. Biol. Reviews. 21(1), 42-48.

Seiboth, B., Hartl, L., Pail, M., Fekete, E., Karaffa, L., Kubicek, C.P. (2004). The galactokinase of *Hypocrea jecorina* is essential for cellulose induction by lactose but dispensable for growth on D-galactose. Molec. Microbiol. 51, 1015–1025.

Sellick, A.C., Campbell, R.N., and Reece, R.J. (2008). Galactose metabolism in yeast structure and regulation of the Leloir pathway enzymes and the genes encoding them. Intl. Rev. Cell Molec. Biol. 269, 111–150

Sheehan, D.J., Hitchcock, C.A., Sibley, C.M. (1999). Current and emerging azole antifungal agents. Clin. Microbiol. Rev. 12, 40-79.

Sheppard, D.C., Rieg, G., Chiang, L. Y., Filler, S. G., Edwards, J.E. Jr., Ibrahim, A. S. (2004). Novel inhalational murine model of invasive pulmonary aspergillosis. Antimicrob. Agents Chemother. 48, 1908–1911

Shibata, N., Okawa, Y. (2011). Chemical structure of β-galactofuranosecontaining polysaccharide and O-linked oligosaccharides obtained from the cell wall of pathogenic dematiaceous fungus *Fonsecaea pedrosoi*. Glycobiology 21, 69–81.

Shibata, N., Saitoh, T., Tadokoro, Y., Okawa, Y. (2009). The cell wall galactomannan antigen from *Malassezia furfur* and *Malassezia pachydermatis* contains β-1,6-linked linear

galactofuranosyl residues and its detection has diagnostic potential. Microbiology 155, 3420-3429.

Singh, V., Satheesh, S.V., Raghavendra, M.L., Sadhale, P.P. (2007). The key enzyme in galactose metabolism, UDP-galactose-4-epimerase, affects cell-wall integrity and morphology in *Candida albicans* even in the absence of galactose. Fungal Genet. Biol. 44, 563-574.

Slepak, T., Tang, M., Addo, F., and Lai, K. (2005). Intracellular galactose-1-phosphate accumulation leads to environmental stress response in yeast model. Molec. Genet. Metab. 86, 360-371.

Slot, J.C., and Rokas, A. (2010). Multiple *GAL* pathway gene clusters evolved independently and by different mechanisms in fungi. Proc. Natl. Acad. Sci. U.S.A. 107, 10136–10141.

Smits, G. J., Kapteyn, J. C., van den Ende, H., and Klis, F. M. (1999). Cell wall dynamics in yeast. Curr. Opin. Microbiol. 2, 348–352.

Spanakis, E.K., Aperis, G., Mylonakis, E. (2006). New agents for the treatment of fungal infections: clinical efficacy and gaps in coverage. Clin. Infect. Dis. 43, 1060-1068.

Stynen, D., Sarafati, J., Goris, A., Prevost, A. M., Lesourd, M., Kamphuis, H., Darras, V., Latgé, J. P. (1992). Rat monoclonal antibodies against *Aspergillus* galactomannan. Infect Immun. 60, 2237-2245.

Suzuki, S., Matsuzawa, T., Nukigi, Y., Takegawa, K., Tanaka, N. (2009). Characterization of two different types of UDP-glucose/-galactose 4-epimerase involved in galactosylation in fission yeast. Microbiology. 156, 708-718.

Szewczyk, E., Nayak, T., Oakley, C.E., Edgerton, H., Xiong, Y., Taheri-Talesh, N., Osmani, S.A., and Oakley, B.R. (2007). Fusion PCR and gene targeting in *Aspergillus nidulans*. Nat Protocols. 1, 3111-3120.

Szczepina, M.G., Zheng, R.B., Completo, G.C., Lowary, T.L., Pinto, B.M. (2010). STD-NMR studies of two acceptor substrates of GlfT2, a galactofuranosyltransferase from *Mycobacterium tuberculosis*: epitope mapping studies. Bioorg. Med. Chem. 18, 5123-5128.

Taylor, D.L., Herriott, I.C., Stone, K.E., McFarland, J.W., Booth, M.G., and Leigh, M.B. (2010). Structure and resilience of fungal communities in Alaskan boreal forest soils.

Canadian Journal of Forest Research. 40, 1288–1301.

Tefsen, B., Ram, A.F., van Die, I., and Routier, F.H. (2012). Galactofuranose in eukaryotes: aspects of biosynthesis and functional impact. Glycobiology, 22, 456–469

Tekaia, F., and Latgé, J.P. (2005). *Aspergillus fumigatus*: saprophyte or pathogen? Curr Opin Microbiol 8:385–392.

Thompson, J.R., Douglas, C.M., Li, W., Jue, C.K., Pramanik, B., Yuan, X. *et al.* (1999). A glucan synthase FKS1 homolog in *Cryptococcus neoformans* is single copy and encodes an essential function. Journal of Bacteriology, 181, 444–453.

Timberlake, W.E. (1990). Molecular genetics of *Aspergillus* development. Annu. Rev. Genet. 24, 5–36.

Timson, D.J. (2005). Functional analysis of disease-causing mutations in human UDP-galactose 4-epimerase. FEBS J. 272, 6170-6177.

Timson, D.J. (2007). Galactose metabolism in *Saccharomyces cerevisiae*. Dynamic Biochemistry, Process Biotechnology and Molecular Biology 1, 63-73.

Todd, R.B., Davis, M.A., Hynes, M.J. (2007a). Genetic manipulation of *Aspergillus nidulans*: meiotic progeny for genetic analysis and strain construction. Nat. Protoc. 2, 811-821.

Todd, R.B., Davis, M.A., Hynes, M.J. (2007b). Genetic manipulation of *Aspergillus nidulans*: heterokaryons and diploids for dominance, complementation and haploidization analyses. Nat. Protocols, 2(4), 822-30.

Tribus, M., Bauer, I., Galehr, J., Rieser, G., Trojer, P., Brosch, G., Loidl, P., Haas, H., Graessle, S. (2010). A novel motif in fungal class 1 histone deacetylases is essential for growth and development of *Aspergillus*. Mol Biol Cell. 21, 345-353.

Tsakiris, S., Marinou, K., and Schulpis, K. H. (2002). The in vitro effects of galactose and its derivatives on rat brain Mg2þ ATPase activity. Pharmacol. Toxicol. 91, 254–257.

Upadhyay, S., and Shaw, B.D. (2008). The role of actin, fimbrin and endocytosis in growth of hyphae in *Aspergillus nidulans*. Molec. Microbiol. 68, 690-705.

Urban, C., Sohn, K., Lottspeich, F., Brunner, H., Rupp, S. (2003) Identification of cell surface determinants in *Candida albicans* reveals Tsa1p, a protein differentially localized in the cell. *FEBS Lett* 544, 228-35

Urbaniak, M.D., Tabudravu, J.N., Msaki, A., Matera, K.M., Brenk, R., Jaspars, M., Ferguson,

MAJ. (2006). Identification of novel inhibitors of UDP-Glc 4′-epimerase, a validated drug target for African sleeping sickness. Bioorg. Med. Chem. Lett. 16, 5744-5747.

Vaishnav, V.V., Bacon, B.E., O'Neill, M., Cherniak, R. (1998). Structural characterization of the galactoxylomannan of *Crytococcus neoformans*. Carbohydr Res. 306, 315-330.

van der Klei, I.J., Veenhuis, M. (2006). Yeast and filamentous fungi as model organisms in microbody research. Biochimica Biophysica Acta. 1763(12), 1364-73

van der Woude, H.J., Boorsma, M., Bergqvist, P.B.F. *et al.* (2004). Budesonide/formoterol in a single inhaler rapidly relieves methacholine-induced moderate-to-severe bronchoconstriction. Pulm Pharmacol Ther. 17, 89–95.

van Straaten, K.E., Routier, F.H., Sanders, D.A.R. (2012). Structural insight into the unique substrate binding mechanism and flavin redox state of UDP-galactopyranose mutase from *Aspergillus fumigatus*. The J. of Biol. Chem., 287, 10780–10790.

van Straaten, K.E., Routier, F.H., Sanders, D.A.R. (2012a). Towards the crystal structure elucidation of eukaryotic UDP-galactopyranose mutase. Acta Crystallographica F. 68, 455-459

Verweij, P.E., Snelders, E., Kema, G.H., Mellado, E., Melchers, W.J. (2009). Azole resistance in *Aspergillus fumigatus*: a side-effect of environmental fungicide use? The Lancet Infectious Diseases, 9, 789-795.

Walker, L.A., Gow, N.A.R. Munro, CA. 2010. Fungal echinocandin resistance. Fung. Gene. and Biol., 47, 117–126.

Walker, L. A., Munro, C. A., de Bruijn, I., Lenardon, M. D., McKinnon, A., Gow, N. A. (2008). Stimulation of chitin synthesis rescues *Candida albicans* from echinocandins. PLoS Pathog. 4(4), e1000040.

Wallis, G.L.F., Hemming, F. W., and Peberdy, J.F. (2001). β-Galactofuranoside glycoconjygate on the conidia and conidiophores of *Aspergillus niger*. FEMS Microbiol. Lett. 201, 21–27.

Waring, R. B., May, G. S., Morris, N. R. (1989). Characterization of an inducible expression system in *Aspergillus nidulans* using *alcA* and tubulin-coding genes. Gene. 79, 119-130.

Wasilenko, J., Fridovich-Keil, J.L. (2006). Relationship between UDP-galactose 4'-epimerase activity and galactose sensitivity in yeast. J. Biol. Chem. 281, 8443-8449.

Wearing, J. (2010). *Fungi : Mushrooms, Toadstools, Molds, Yeasts, and Other Fungi*. Crabtree Pub., St. Catharines, Ont.; New York.

Wedekind, J.E., Frey, P.A., and Rayment, I. (1996). The structure of nucleotidylated histidine-166 of galactose-1-phosphate uridylyltransferase provides insight into phosphoryl group transfer. Biochemistry 35, 11560-11569.

Welsh, O., Vera-Cabrera, L., Rendon, A., Gonzalez, G., Bonifaz, A. (2012). Coccidioidomycosis. Clinics in Dermatology, 30, 573–591.

Wesener, D. A., May, F. J., Huffman, E. M., Kiessling, L. L. (2013). UDP-galactopyranose mutase in nematodes. Biochemistry, 52, 4391−4398.

Weston, A., Stern, R.J., Lee, R.E., Nassau, P.M., Monsey, D., Martin, S.L., Scherman, M.S., Besra, G.S., Duncan, K., McNeil, M.R. (1998). Biosynthetic origin of mycobacterial cell wall galactofuranosyl residues. Tubercle Lung Dis. 78, 123-131.

Westfall, P.J., Momany, M. (2002). *Aspergillus nidulans* septin AspB plays pre- and postmitotic roles in septum, branch, and conidiophore development. Mol. Biol. Cell, 13, 110 –118.

Wing, C., Errey, J.C., Mukhopadhyay, B., Blanchard, J.S., Field, R.A. (2006). Expression and initial characterization of WbbI, a putative D-Galf:alpha-D-Glc beta-1,6-galactofuranosyltransferase from *Escherichia coli* K-12. Org. Biomol. Chem. 4, 3945-3950.

Wortman, J.R., Gilsenan, J.M. *et al.* (2009). The 2008 update of the *Aspergillus nidulans* genome annotation: a community effort. Fungal Genet. Biol. 46 Suppl 1, S2-13.

Yang, Y., El-Ganiny, A.M., Bray, G.E., Sanders, D.A.R., Kaminskyj, S.G.W. (2008). *Aspergillus nidulans hypB* encodes a Sec7-domain protein important for hyphal morphogenesis. Fungal Genetics and Biology, 45, 749–759.

Yoshimi, A., Sano, M., Inaba, A., Kokubun, Y., Fujioka, T., Mizutani, O. *et al.* (2013). Functional analysis of the alpha-1,3-glucan synthase genes *agsA* and *agsB* in *Aspergillus nidulans*: AgsB is the major alpha-1,3-glucan synthase in this fungus. PLoS One, 8: e54893.

Yu, J.H., Keller, N. (2005). Regulation of secondary metabolism in filamentous fungi. Annu. Rev. Phytopathol. 43, 437–458.

Zhang, A.Y., Camp, W.L., Elewski, B.E. (2007). Advances in topical and systemic antifungals. Dermatol. Clin. 25, 165,183.

Zarrin, M., Leeder, A. C., Turner, G. (2005). A rapid method for promoter exchange in *Aspergillus nidulans* using recombinant PCR. Fung Genet Biol. 42, 1-8.